REPUBLIC OF THE UNION OF MYANMAR
MINISTRY OF CONSTRUCTION
DEPARTMENT OF BRIDGE

DETAILED DESIGN STUDY ON THE BAGO RIVER BRIDGE CONSTRUCTION PROJECT

FINAL REPORT ATTACHMENTS

VOLUME VI WIND TUNNEL REPORT

DECEMBER 2017

JAPAN INTERNATIONAL COOPERATION AGENCY (JICA)

NIPPON KOEI CO., LTD.
ORIENTAL CONSULTANTS GLOBAL CO., LTD.
METROPOLITAN EXPRESSWAY COMPANY LIMITED.
CHODAI CO., LTD.
NIPPON ENGINEERING CONSULTANTS CO., LTD.

EI
CR(3)
17-136

REPUBLIC OF THE UNION OF MYANMAR
MINISTRY OF CONSTRUCTION
DEPARTMENT OF BRIDGE

DETAILED DESIGN STUDY ON THE BAGO RIVER BRIDGE CONSTRUCTION PROJECT

FINAL REPORT ATTACHMENTS

VOLUME VI WIND TUNNEL REPORT

DECEMBER 2017

JAPAN INTERNATIONAL COOPERATION AGENCY (JICA)

NIPPON KOEI CO., LTD.
ORIENTAL CONSULTANTS GLOBAL CO., LTD.
METROPOLITAN EXPRESSWAY COMPANY LIMITED.
CHODAI CO., LTD.
NIPPON ENGINEERING CONSULTANTS CO., LTD.

Contents

1. Overview of Bago Cable-Stayed Bridge

1.1 General

This report is to summarize the wind tunnel test condition and measurement items to estimate the wind-resistant characteristics of the main girder of Bago Cable-Stayed Bridge in under construction and after completion stages conducted by Bridge Engineering Laboratory and Structural Dynamics Laboratory, Department of Civil and Earth Resources Engineering, Kyoto University, Japan.

The Bridge (see Fig. 1.1.1) is a 3-span steel cable-stayed bridge (112.0m+224.0m+112.0m) to cross Bago river in the city of Yangon. The pylon with a rectangular cross section of 3.0m (along bridge axis) x 2.5m has 58.0m high above the upper deck level. 10 stay cables are installed in single plane at the center of the girder. The elevation of the main girder being taken from the average water level (M.W.L.) to the upper surface level of the main girder is 13.01+1.935(=14.945)+2.70=17.645m.

The cross section of the main girder has 22.9m in width (B) and the fairing with 0.80m in horizontal width is installed at both ends. The fairing is partially installed in under construction stage. Therefore, the overall width of girder is defined as 0.8+22.9+0.8=24.7m. The height of the girder (D) is chosen as 2.70m which is the distance between the lower surface of bottom flange of box girder and the upper deck surface at the center of the main girder.

SUPERSTRUCTURE STRUCTURAL DRAWING

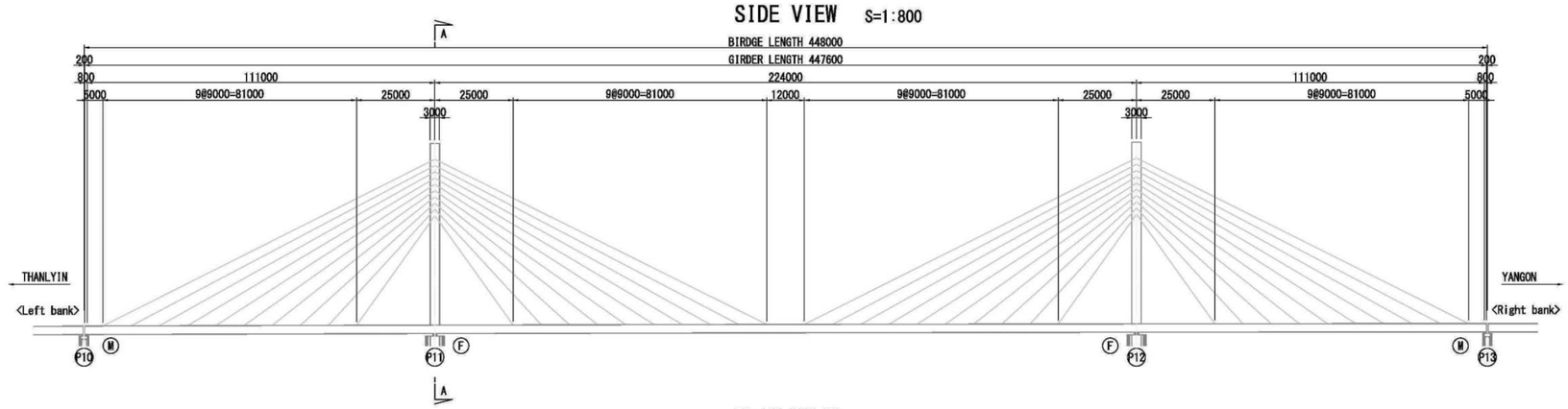

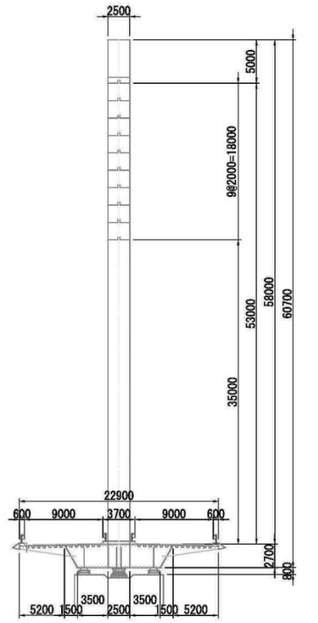

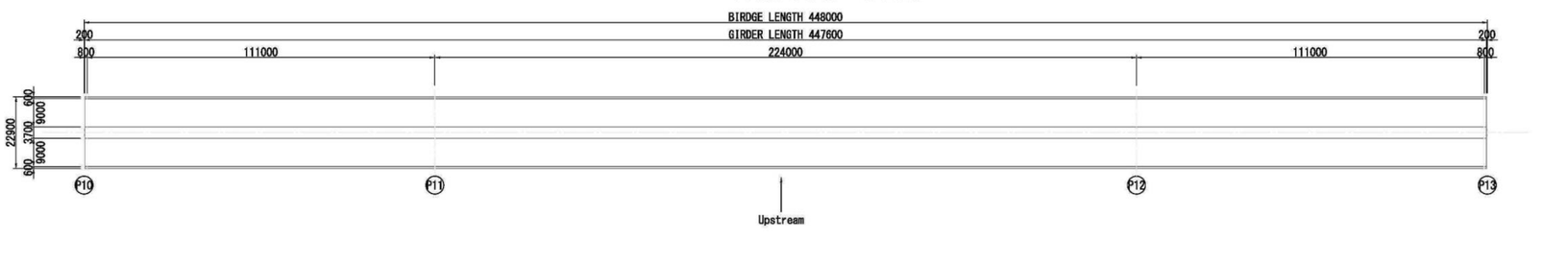

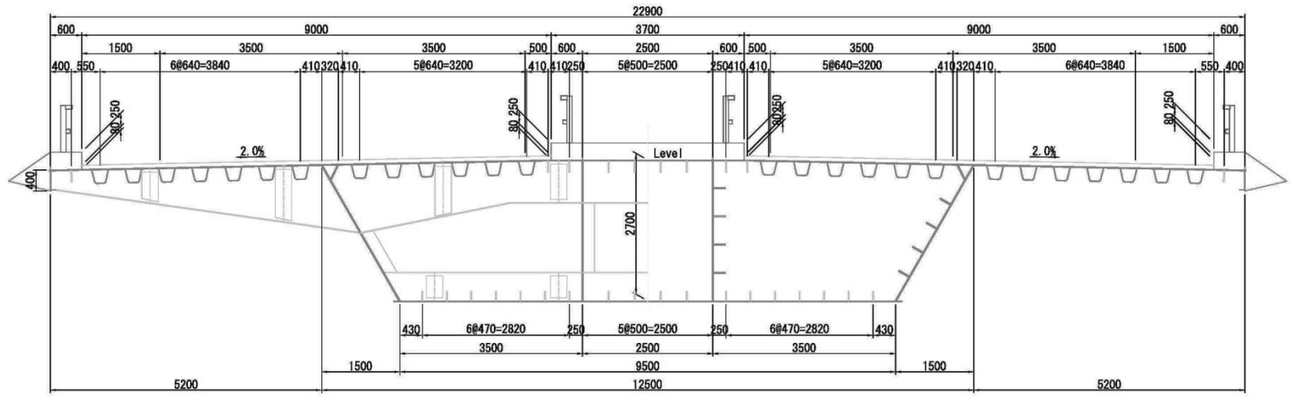

Fig. 1.1.1 General view of Bago Bridge

1.2 Basic Condition to Evaluate Aerodynamic Stability

The wind tunnel test is to be conducted based on the following conditions [1]:

Elevation of main girder **17.663 m**
Girder width (B) **22.9 m**
Girder depth (D) **2.70 m** (B/D = 8.48)
Category of surface roughness: **II**
Power exponent of vertical profile of wind speed **0.16**
(Longitudinal) intensity of turbulence: **17 %**
At the elevation of the main girder

<u>For after completion stage</u>

Basic wind speed (U_{10}) **30 m/s**
10 minute mean wind speed at 10m elevation
Design wind speed (U_d) **32.7 m/s**
At the girder elevation, the design wind speed U_d is
$U_d = U_{10} \times E_1 = 30 \times 1.09 = 32.7$
(E_1: a factor based on surface roughness and elevation)
Reference wind speed for flutter (U_{rf}) **45.1 m/s**
$U_{rf} = 1.2 \times E_{r1} \times U_d = 1.2 \times 1.15 \times 32.7 = 45.1$
(E_{r1}: a factor based on the variation of wind speed and natural period of the target bridge)
The safety for flutter requires that the critical wind speed for flutter measured in wind tunnel test in smooth flow is higher than U_{rf}.
Reference wind speed for VIV (U_{rv}) **32.7 m/s**
$U_{rv} = U_d$ for heaving and torsional
The safety for VIV requires that the onset wind speed at which the maximum amplitude is measured in wind tunnel test in smooth flow is higher than U_{rv}.
Allowable amplitude for VIV (h_{rvh}, $h_{rv\theta}$) **0.09 m** for heaving
0.39 deg. for torsional
$h_{rvh} = h_a$ (for heaving), $h_{rv\theta} = \theta_a$ (for torsional)
If the onset wind speed is lower than U_{rv}, the safety for VIV requires that the maximum amplitude being measured in wind tunnel test in smooth flow is lower than the allowable amplitude h_a, θ_a.

The allowable amplitude h_a, θ_a are evaluated by the following formulae:

$h_a = 0.04/f_h$ (for heaving), $\theta_a = 2.28/(b \cdot f_\theta)$

where, h_a: allowable heaving amplitude (m),

θ_a: allowable torsional amplitude (deg.),

f_h: heaving natural frequency (Hz),

f_θ: torsional natural frequency (Hz),

b: distance between the center of most outer road traffic or pedestrian lane to the girder center.

$h_a = 0.04/0.446 = 0.09$ m (for heaving), $\theta_a = 2.28/(6.5 \times 0.895) = 0.39$ deg.

<u>For under construction stage</u>

Basic wind speed (U_{10E}) **22.1 m/s**

The estimation method is to be explained later.

Design wind speed (U_{dE}) **24.1 m/s**

At the girder elevation ($22.1 \times E_1 = 24.1$).

Reference wind speed for flutter (U_{rf}) **33.3 m/s**

$U_{rfE} = 1.2 \times E_{r1} \times U_{dE} = 1.2 \times 1.15 \times 24.1 = 33.3$

Reference wind speed for VIV (U_{rfE}) **24.1 m/s**

$U_{rfE} = U_{dE}$ for heaving and torsional

Allowable amplitude for VIV (h_{rvhE}, $h_{rv\theta E}$) **0.01 m** for heaving

0.14 deg. for torsional

$h_a = 0.04/3.977 = 0.01$ m (for heaving), $\theta_a = 2.28/(6.5 \times 2.594) = 0.14$ deg.

Determination of the design wind speed for under construction stage is based on the following idea [1]:

Basic design wind speed in under construction stage is normally lower than that for after completion stage because construction period is much shorter than its design lifetime. The following formula for design wind speed for under construction stage is provided in te reference:

$$U_{10E} = U_{10} \cdot \frac{0.61 - 0.10\left(\ln\left(\ln\left(\frac{R}{R-1}\right)\right)\right)}{1.07} \tag{1.1}$$

where, U_{10E} : basic wind speed for under construction stage (*m*/*s*),

U_{10} : basic wind speed for after completion stage (*m*/*s*),

R : return period for under construction stage (*year*).

Note: U_{10E} and U_{10} are 10 minutes mean wind speed at 10m elevation.

The return period R can be determined by the following formula:

$$P = \left(1 - \frac{1}{R}\right)^N \tag{1.2}$$

where, P : non-exceeding probability of annual maximum wind speed,

N : Construction duration (*year*).

The non-exceeding probability P should be determined taking social importance of the bridge, meteorological condition at the site, etc. into account. Table 1.1 compares return period R, service lifetime T, and the non-exceeding probability P for ordinary road bridges with span length being less than 200m [2] and for major long-span bridges in Honshu-Shikoku connecting route [3]. For Bago Bridge, if P and its construction duration N are assumed to be 0.6 and at most 3 years (Aug. 2018 to Mar. 2021), respectively, then R becomes 6.39 (*years*) and $U_{10E} = 0.74 \cdot U_{10}$ according to eqs.(1) and (2). The basic wind speed for under construction stage U_{10E} will be, therefore, 30.0×0.74=22.1 (*m*/*s*).

Then, the wind tunnel test for under construction stage will be conducted so as to cover the reference wind speed for flutter and for vortex-induced vibration (VIV). With referring to the margin after completion stage, the measurement in wind tunnel test will be conducted up to 40.0(*m/s*) for under construction stage. For after completion stage, the measurement will be conducted up to 50.0(*m*/*s*).

Table 1.1 Comparison of return period R, service lifetime T, and non-exceeding probability P.

			Return period R (years)	Service life T (years)	Non-exceeding prob. P
Design code for road bridge [2]			100	50	0.6
Dynamic wind resistant design handbook [1]					
Wind resistant design Standard for Honshu-Shikoku Bridges [3]	After completion		150	100	0.5
			150	75	0.6
	Construction stage	Akashi	22.9	5	0.8
		Kurushima	18.4	4	0.8
		Tatara	18.4	4	0.8

1.3 Aerodynamic phenomena to be examined

By taking the geometry of the girder into account, the dynamic stability of the following phenomena should be checked mainly in smooth and in turbulent flow:

- Vortex-induced vibration (VIV)
- Flutter
- Buffeting

Galloping is considered as one of the most destructive aerodynamic phenomena. The occurrence of galloping is not so much expected since the side ratio B/D (B: width, D: height) of the girder cross section is relatively large. Heaving response should be also measured carefully.

The above aerodynamic phenomena are to be measured by the free vibration test in wind tunnel, mainly. Stability for flutter is to be also examined by the forced vibration test.

Target modes for heaving/torsional dof will be determined by mode shape and equivalent mass for two phases in under construction stage and for after completion stage. (See chapter 6)

Wind tunnel test will be conducted for under construction stage in which and for after completion stage.

2. Wind Tunnel and Models

2.1 Wind tunnel

The wind tunnel facility used for the test is the Eiffel type wind tunnel in Department of Civil and Earth Resources Engineering, Kyoto University, Japan (see Figs. 2.1.1 and 2.1.2). Width and height of working section is 1.0m and 1.8m for section model test. Wind velocity in the working section can be adjusted up to about 25m/s. Turbulent intensity in the empty working section is less than 0.5(%). (See also Table 2.1.1)

The list of equipment to be used in a series of wind tunnel test is shown in Table 2.1.2.

Fig. 2.1.1 Wind tunnel in Department of Civil and Earth Resources Engineering, Kyoto University

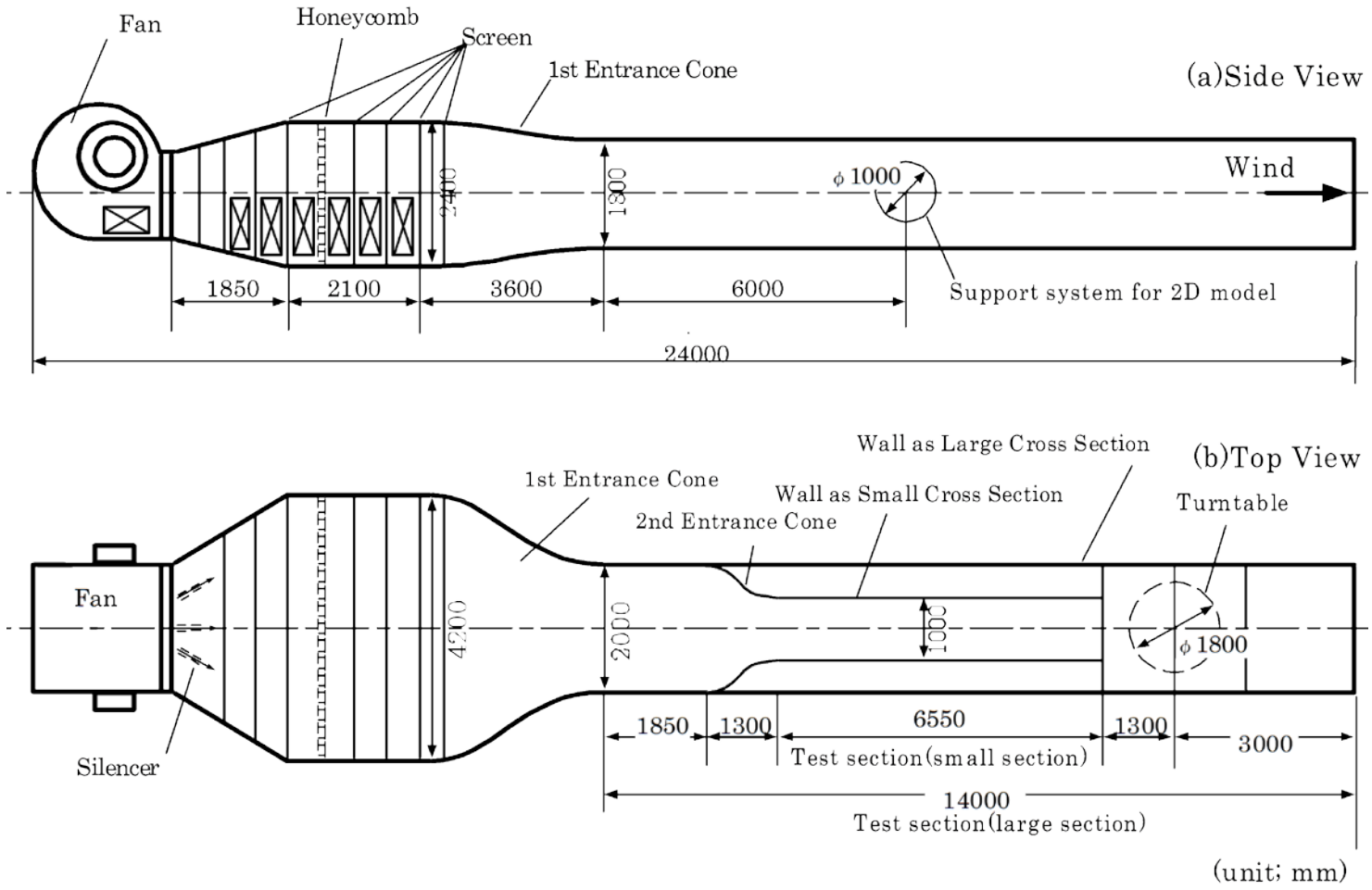

Fig.2.1.2 Wind tunnel

Table 2.1.1 Specification of wind tunnel

Subject	Direction	Value
Wind Tunnel Type	-	Eoiffel Type
Section Size	Width	1,000 (mm)
	Height	1,800 (mm)
	Length	6,550 (mm)
Wind Speed	Streamwise	0 ～ 25 (m/s)
Turbulence Intensity (in smooth flow)	Streamwise	< 0.5 (%)

Table 2.1.2 List of equipment

Device Name	Manufacturer	Model Number	Unit
Multi component load cell	Nissho Electric Works Co., Ltd.	LMC3501-20N	2
Laser displacement meter	Keyence Co., Ltd.	LB-300, LB-1200	3
A/D converter	Graphtec Co., Ltd.	GL7000	1
Hot wire anemometer	KANOMAX Co., Ltd.	Model, 1011, 1013	2
Hot wire anemometer probe	KANOMAX Co., Ltd.	Model 0252R-T5	1
Dynamic strain meter	Kyowa Dengyo Co., Ltd.	MCD-8A	1

2.2 Models

2.2.1 Section model of main girder

The cross section of the model realizes the representative outer configuration of the main girder. Between the under construction stage and the after completion, main difference of the model is:

- ✓ Fairing: Installed in discrete manner for the under construction stage and installed continuously for after completion stage.
- ✓ Handrails and pavement layer: Installed only in after completion stage.

Scale ratio of the model was determined as 1/70 by taking the wind tunnel facility condition into account. The detail of the section model is shown in Fig.2.2.1 to Fig.2.2.8.

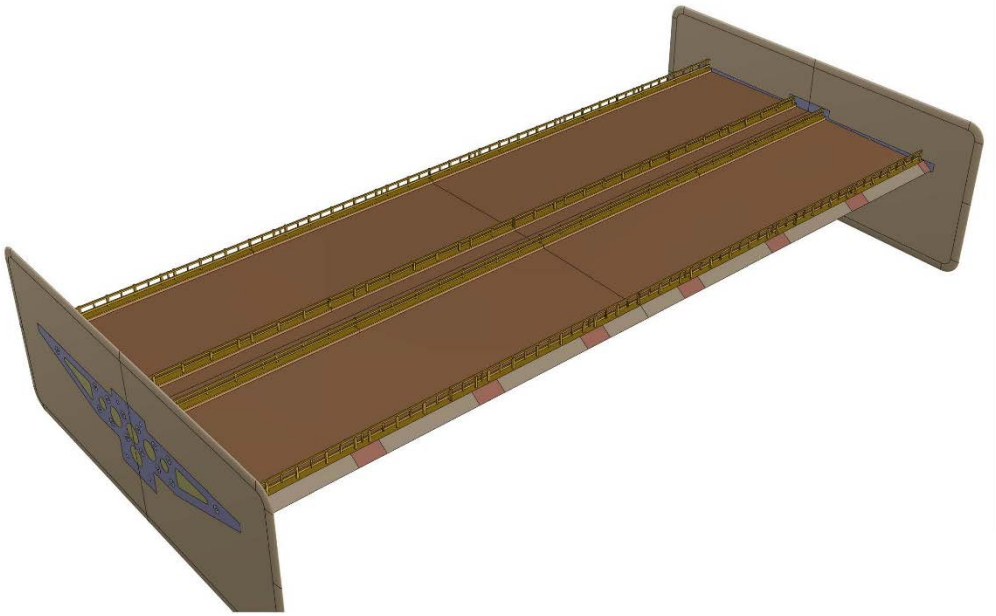

Fig. 2.2.1　3-D image of section model (for after completion stage)

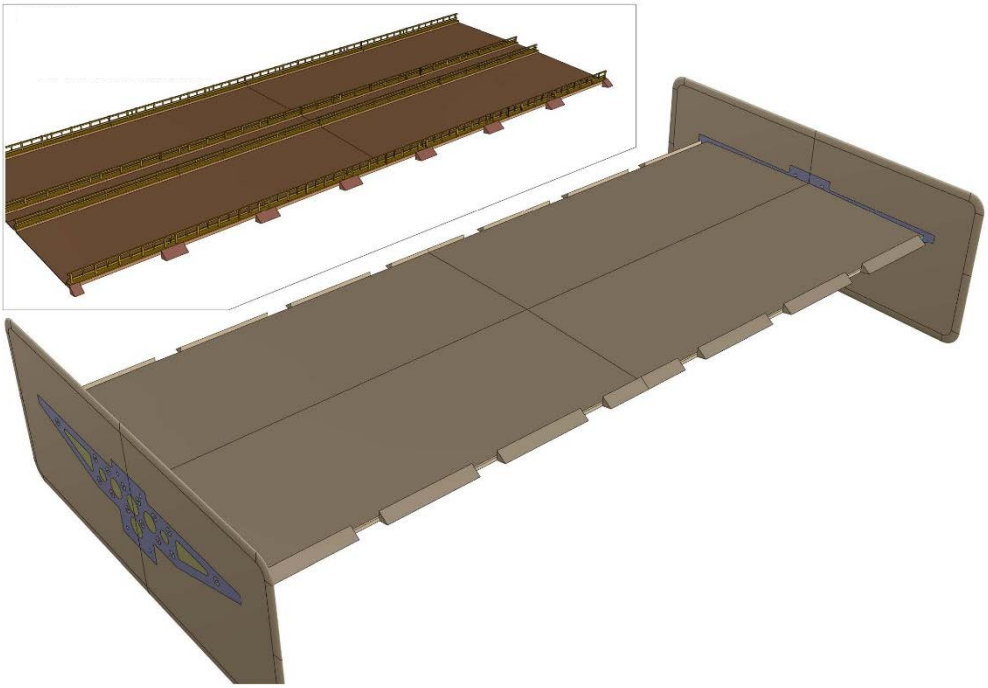

Fig. 2.2.2　3-D image of section model (for under construction stage)
(The configuration is reproduced by taking out the top left piece from the section model.)

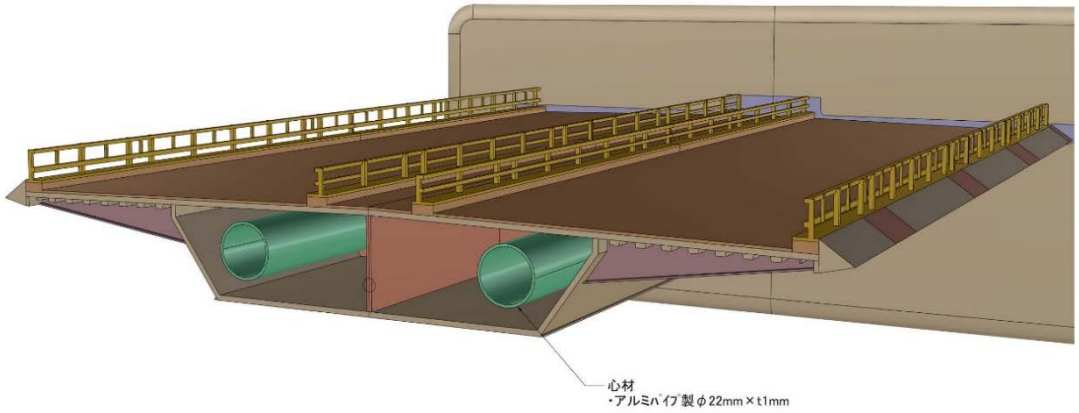

Fig.2.2.3　Inner image of the section model
(two aluminum pipes are installed to keep enough rigidity)

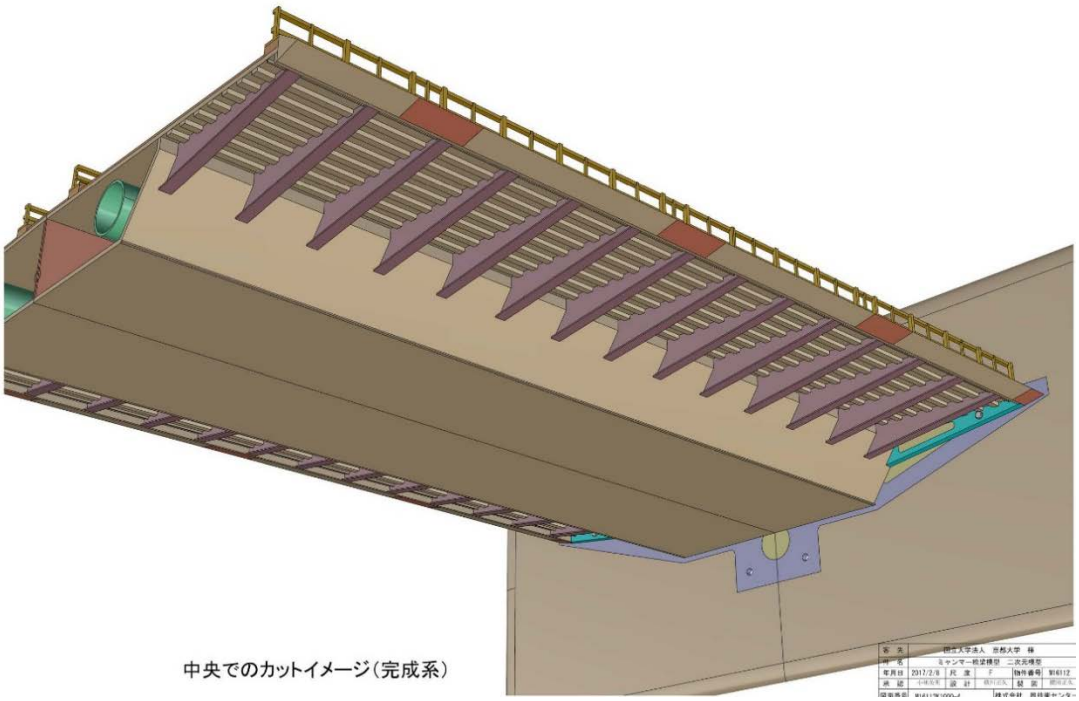

Fig. 2.2.4　Image of lower side of the section model

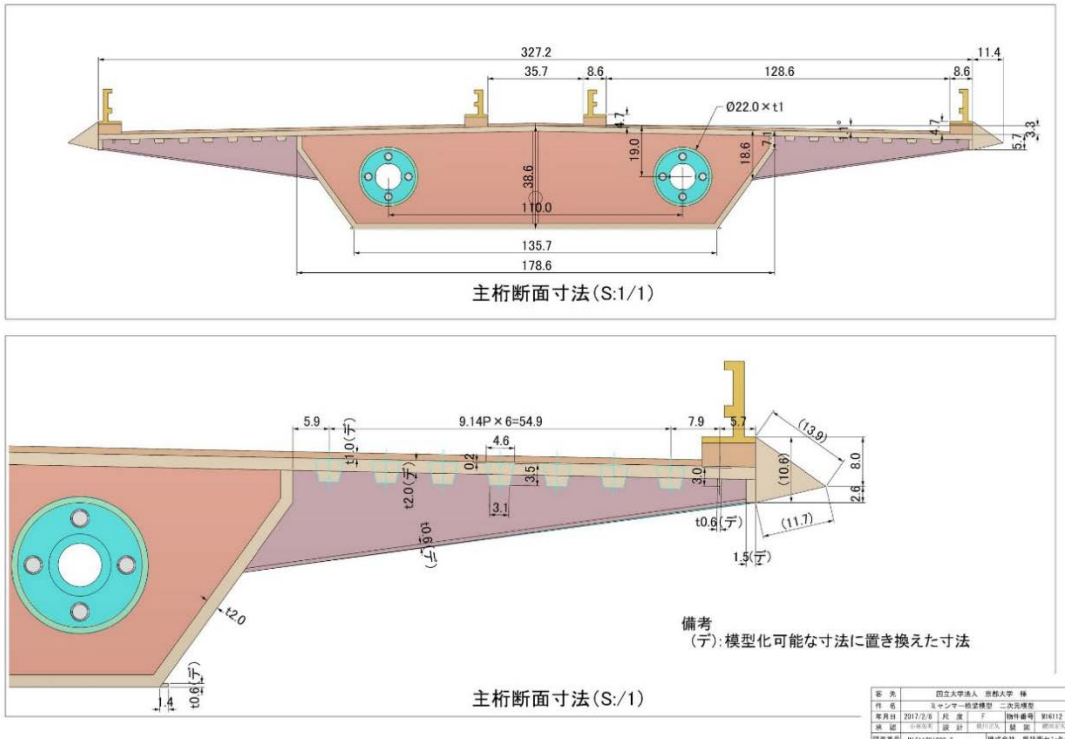

Fig.2.2.5　Cross section of the section model (unit in mm)

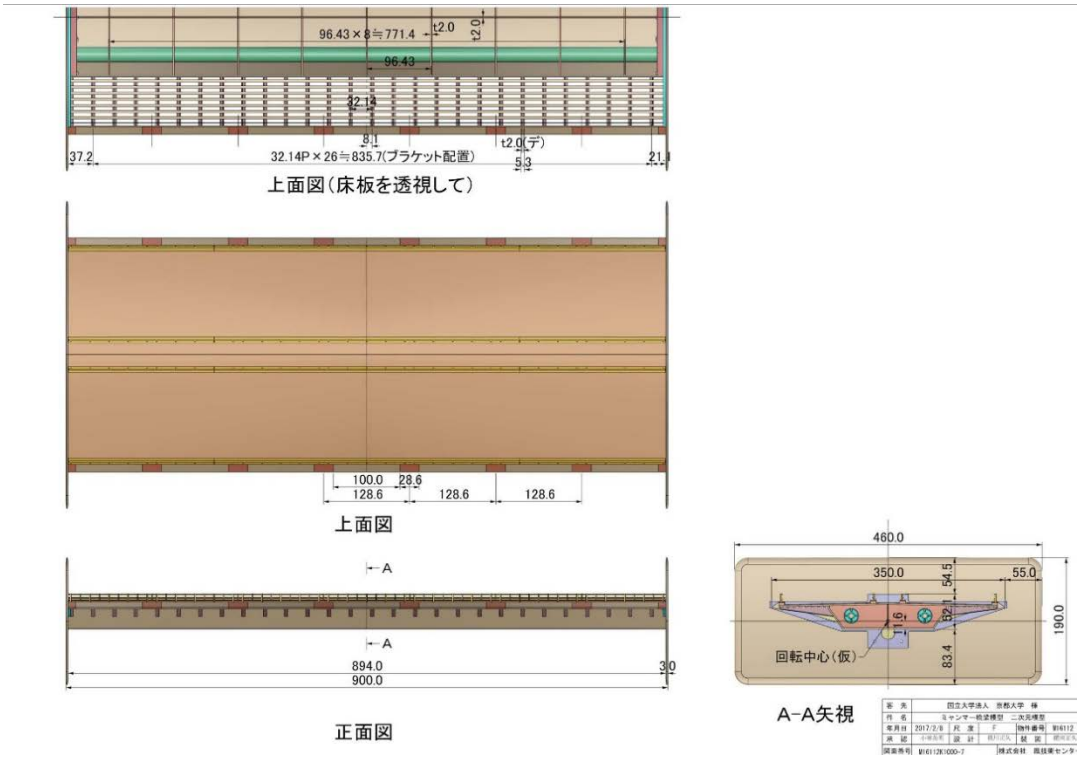

Fig.2.2.6　Plan view of the section model (unit in mm)

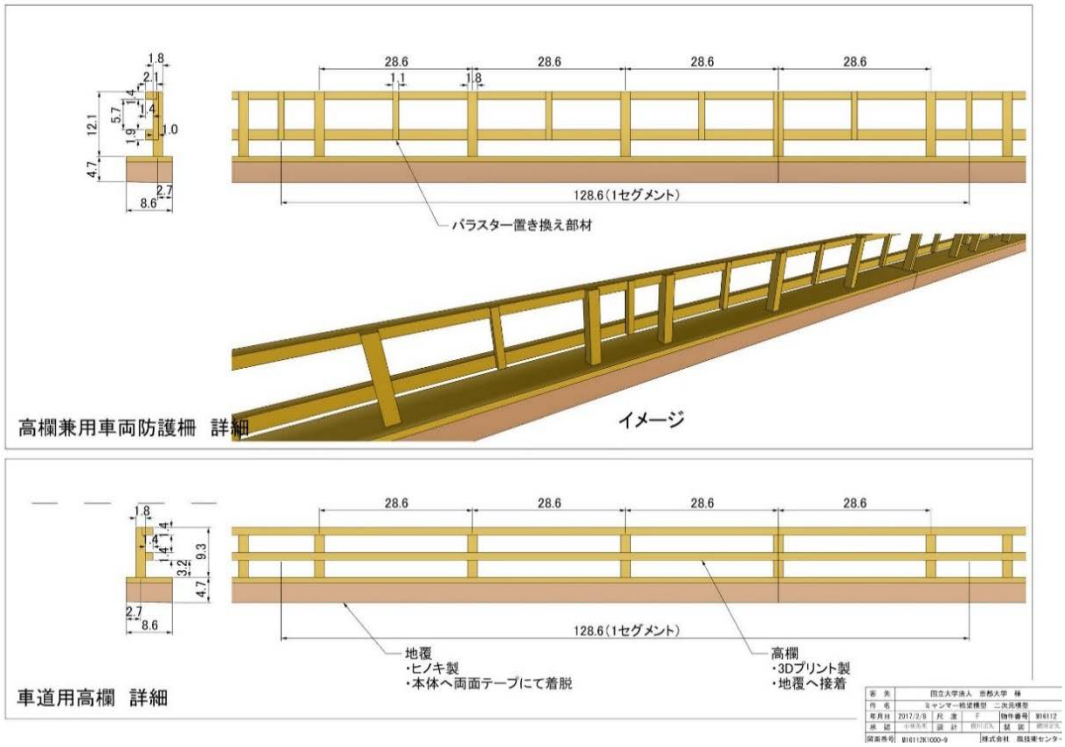

Fig.2.2.7　The parapets (upper: to be installed at both edge of the girder deck, lower: to be installed at the center, unit in mm)

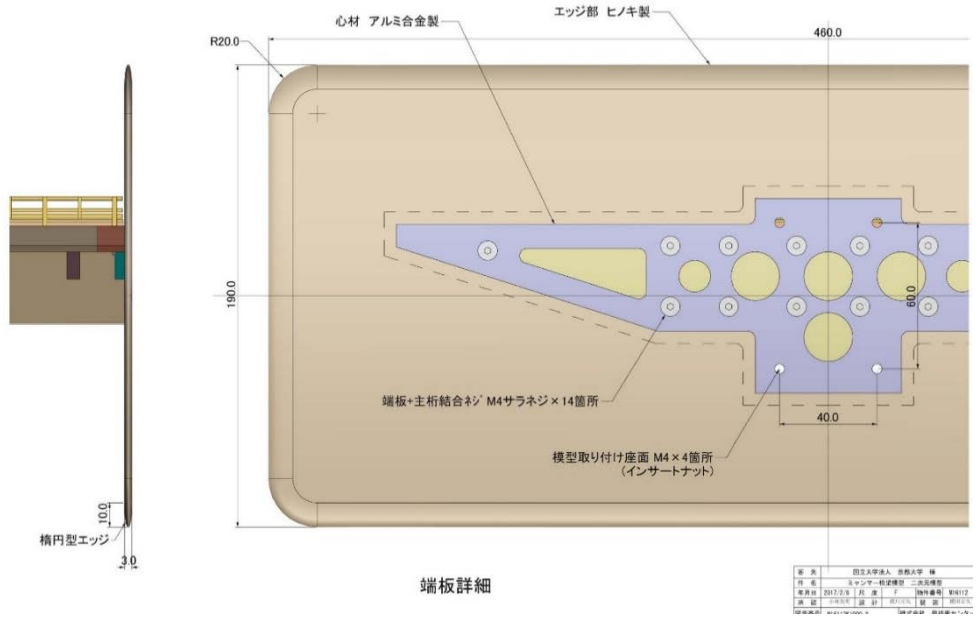

Fig.2.2.8　End plate (consists of aluminum part (grey colored), which is rigidly connected with the two aluminum pipes, and wooden part (brown colored), unit in mm)

2.2.2 3-D elastic model of tower

The 3-D elastic model is to be manufactured in order to measure the aerodynamic response of the tower. This model consists of the fully elastic tower part and the rigid girder part. The bent during the early period of the under construction stage is also realized. Girder length is changeable and the cable can be installed when necessary. The cable is realized by steel wires which the diameter is determined so as to simulate the drag force. Tensile force in each cable is given by using a weight before fixing.

Scale ratio of the model was determined as 1/120. The detail of the section model is shown in Fig.2.2.9 to Fig.2.2.16.

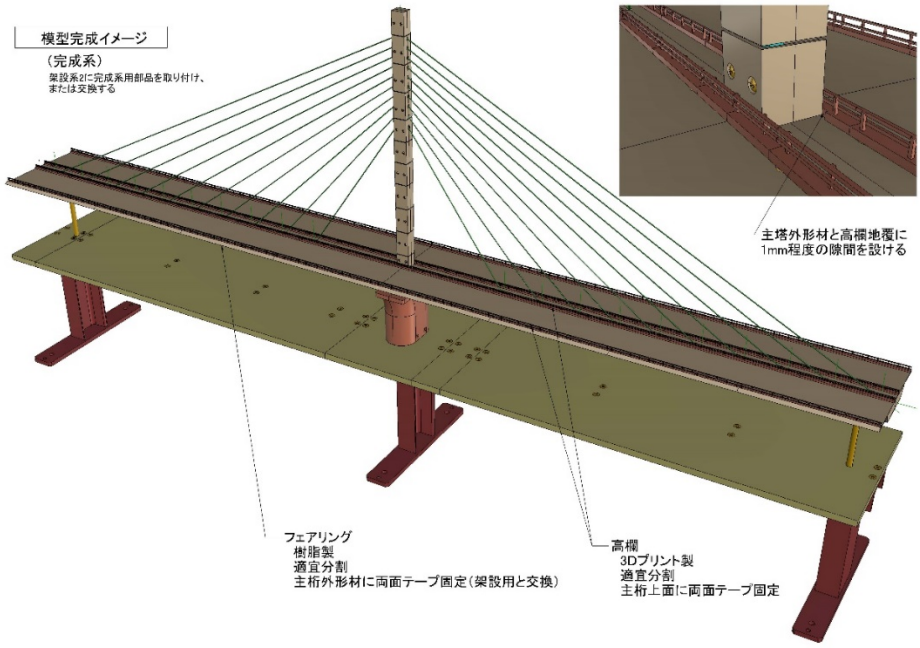

Fig.2.2.9　3-D image of the elastic model (for after completion stage)
(The min girder part is a rigid model.)

Fig.2.2.10　3-D image of elastic bar for the tower and rigid bar for the main girder
(The supports at both ends of the model are to keep the girder as rigid.)

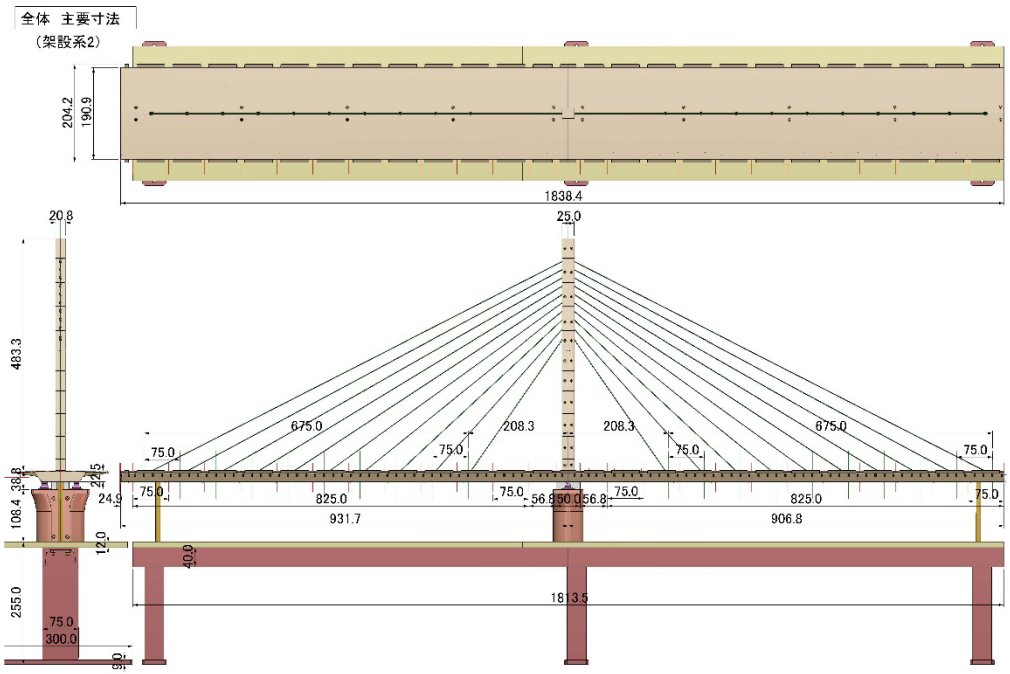

Fig.2.2.11　The elastic model (for after completion stage, unit in mm)

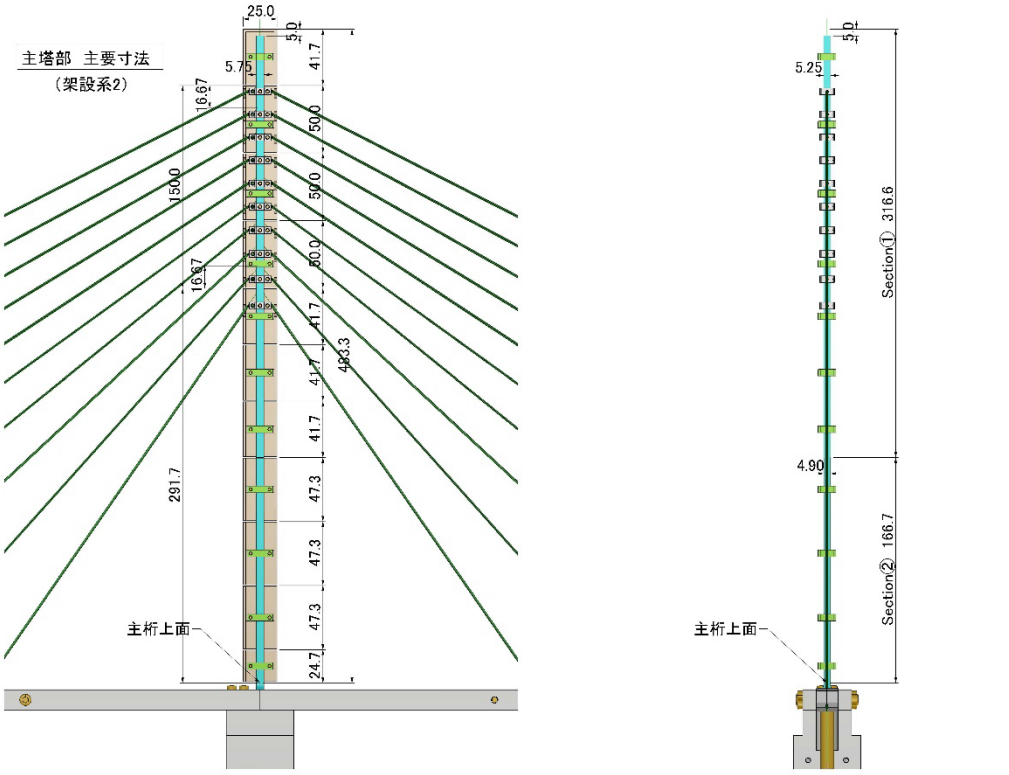

Fig.2.2.12　The tower and elastic bar with additional mass arrangement (unit in mm)

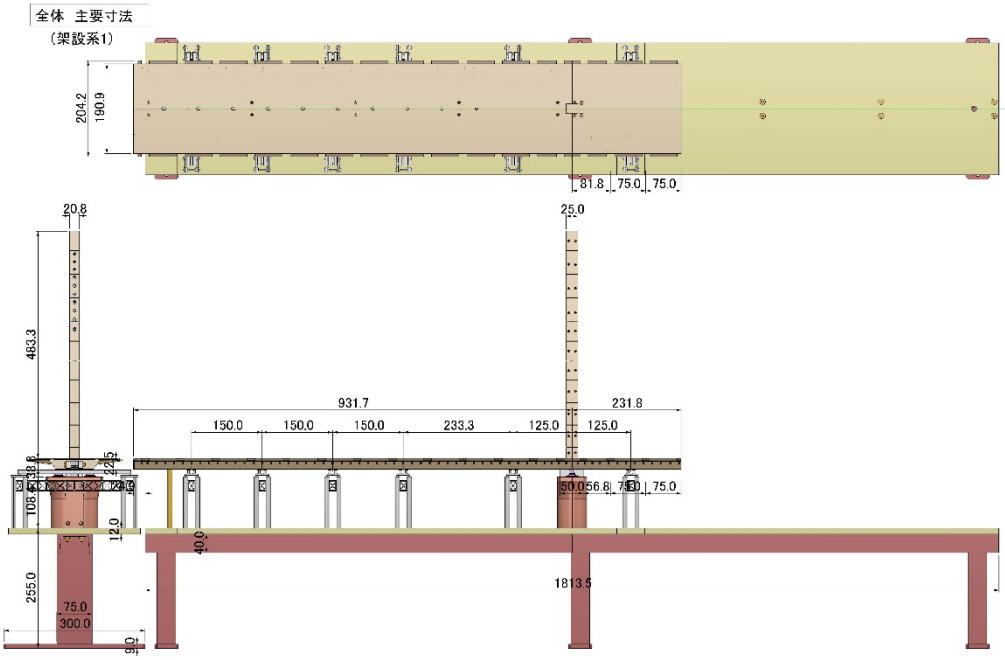

Fig.2.2.13　The elastic model (for under construction stage before the lowest cable being installed and just after the first segment of the main girder was installed), unit in mm)

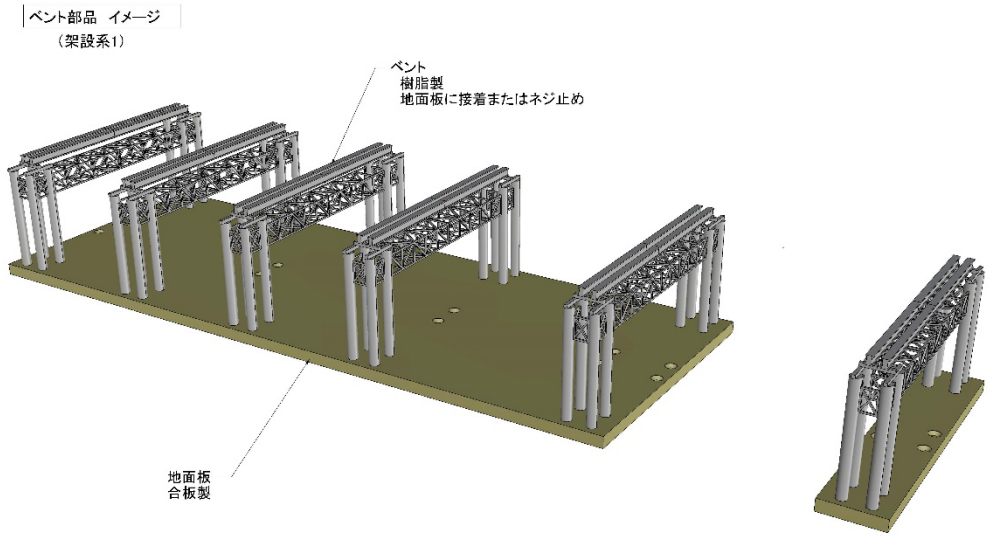

Fig.2.2.14　3-D image of the bents (The bents are installed to reproduce the under construction stage before the lowest cable being installed and just after the first segment of the main girder was installed.)

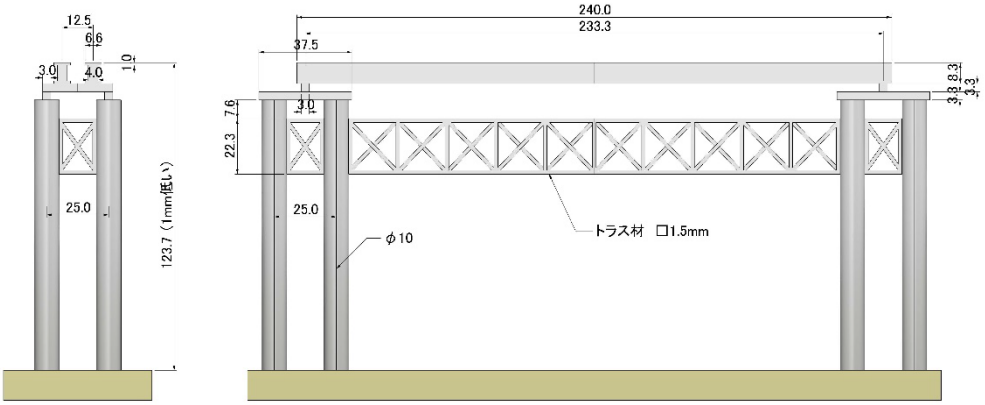

Fig.2.2.15　The bent (unit in mm)

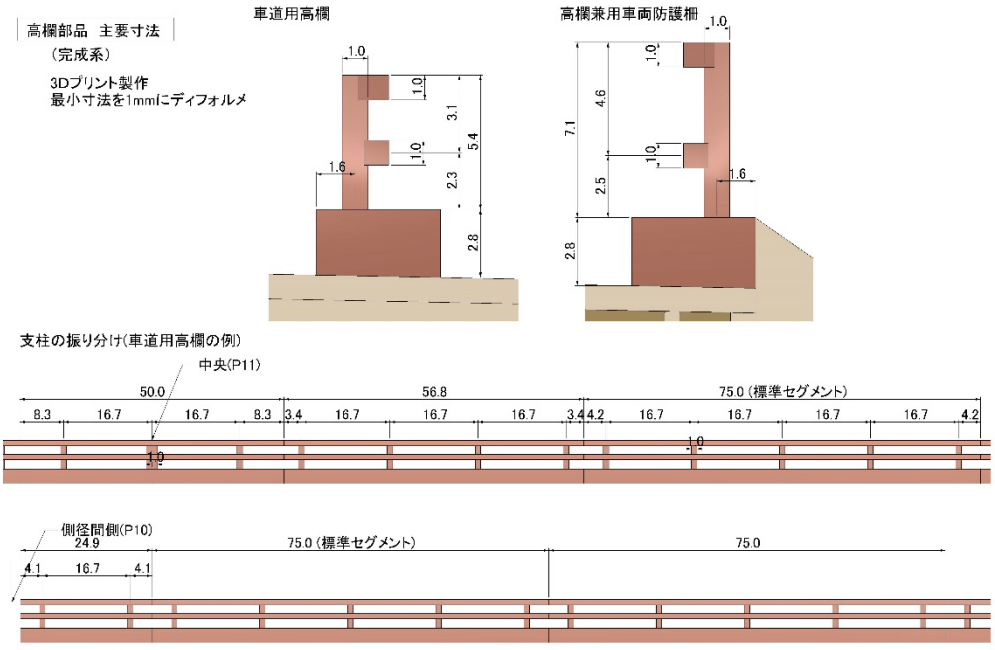

Fig.2.2.16　The parapets (Top left: to be installed at the center, Top right: to be installed at both edge of the girder deck), unit in mm)

3. Similarity Rules

The similarity rules for wind tunnel test can be summarized as follows:

1) Wind velocity:
$$\frac{U_p}{f_p L_p} = \frac{U_m}{f_m L_m} \tag{3.1}$$

2) Dynamic sensitivity (Scruton number):
$$\frac{2m_p\delta_p}{\rho L_p^{\,2}} = \frac{2m_m\delta_m}{\rho L_m^{\,2}} \tag{3.2}$$

$$\frac{2I_p\delta_p}{\rho L_p^{\,4}} = \frac{2I_m\delta_m}{\rho L_m^{\,4}} \tag{3.3}$$

where, U : wind velocity (*m*/*s*),
f : natural frequency (*Hz*),
L : reference length (*m*),
m : mass per unit span length for heaving mode (*kg*/*m*),
I : moment of inertia per unit span length for torsional mode ($kg \cdot m^2/m$),
δ : logarithmic decrement of structural damping (-),
ρ : air density (kg/m^3) ,
$(\ )_p$: for real structure,
$(\ )_m$: for model

Note: Since the wind tunnel test was conducted in air, $\rho_p = \rho_m$.

For the forced vibration test in order to measure aerodynamic forces, only eq.(3.1) should be satisfied. Whereas, for free vibration test in order to measure dynamic response using spring supported model, eqs.(3.1) to (3.3) has to be satisfied.

The similarity conditions in Table 3.1 are required to be satisfied:

Table 3.1 Similarity conditions (*n*: scale ratio of a section model, *n*=70)

item	unit	symbol		scale ratio	note
		real structure	model		
length	*m*	L_p	L_m	*n*	$L_p = nL_m$
time	*sec*	t_p	t_m	-	$\frac{U_p t_p}{L_p} = \frac{U_m t_m}{L_m}, \quad (t_p = t_m)$
wind velocity	*m*/*sec*	U_p	U_m	-	$\frac{U_p}{f_p L_p} = \frac{U_m}{f_m L_m}$
mass per unit span length	*kg*/*m*	m_p	m_m	n^2	$\frac{2m_p\delta_p}{\rho {L_p}^2} = \frac{2m_m\delta_m}{\rho {L_m}^2}$
moment of inertia per unit span length	kgm^2/m	I_p	I_m	n^4	$\frac{2I_p\delta_p}{\rho {L_p}^4} = \frac{2I_m\delta_m}{\rho {L_m}^4}$
natural frequency	*Hz*	f_p	f_m	-	-
logarithmic decrement of structural damping	-	δ_p	δ_m	1	$\delta_p = \delta_m$

4. Equivalent mass

If the overall 3-dimensional aerodynamic vibration response is examined by using spring supported 2-dimensional section model of the main girder, the equivalent mass will be one of the important requirement which the spring system has to satisfy through similarity condition. The idea of equivalent mass is described as follows:

The equivalent mass m_{eqz} for heaving and the equivalent moment of inertia I_{eqx} for torsional (rotation around bridge axis) of the girder are evaluated by the following equations (6) and (7):

$$m_{eqz} = \frac{\int_{str} \left\{ m(s)\left[\phi_x{}^2(s) + \phi_y{}^2(s) + \phi_z{}^2(s)\right] + I_{rx}(s)\phi_{rx}{}^2(s) + I_{ry}(s)\phi_{ry}{}^2(s) + I_{rz}(s)\phi_{rz}{}^2(s) \right\} ds}{\int_{girder} \phi_z{}^2(x) dx} \tag{4.1}$$

$$I_{eqx} = \frac{\int_{str} \left\{ m(s)\left[\phi_x{}^2(s) + \phi_y{}^2(s) + \phi_z{}^2(s)\right] + I_{rx}(s)\phi_{rx}{}^2(s) + I_{ry}(s)\phi_{ry}{}^2(s) + I_{rz}(s)\phi_{rz}{}^2(s) \right\} ds}{\int_{girder} \phi_{rx}{}^2(x) dx} \tag{4.2}$$

where, $\int_{str}\{\ \}ds$: integral along each structural member axis (s),

$\int_{girder}\{\ \}dx$: integral along girder axis (x),

$m(s)$: mass per unit span length (kg/m),

$I_{rx}(s)$, $I_{ry}(s)$, $I_{rz}(s)$: moment of inertia per unit span length around local x, y, z coordinates (kgm^2/m),

$\phi_x(s)$, $\phi_y(s)$, $\phi_z(s)$: displacement component of mode vector for local x, y, z coordinates,

$\phi_{rx}(s)$, $\phi_{ry}(s)$, $\phi_{rz}(s)$: rotational displacement component of mode vector for local x, y, z coordinates

As for the equivalent mass for the tower, eq. (4.1) can be applied after replacing the

denominator with $\int_{tower} \phi_x^{\,2}(s)ds$ for bending along bridge axis, and with $\int_{tower} \phi_y^{\,2}(s)ds$ for bending normal to bridge axis. That is,

For bending along bridge axis (along cable plane):

$$m_{eqx} = \frac{\int_{str} \left\{ m(s)\left[\phi_x^{\,2}(s) + \phi_y^{\,2}(s) + \phi_z^{\,2}(s)\right] + I_{rx}(s)\phi_{rx}^{\,2}(s) + I_{ry}(s)\phi_{ry}^{\,2}(s) + I_{rz}(s)\phi_{rz}^{\,2}(s) \right\} ds}{\int_{tower} \phi_x^{\,2}(s)ds} \tag{4.3}$$

For bending normal to bridge axis (normal to cable plane):

$$m_{eqy} = \frac{\int_{str} \left\{ m(s)\left[\phi_x^{\,2}(s) + \phi_y^{\,2}(s) + \phi_z^{\,2}(s)\right] + I_{rx}(s)\phi_{rx}^{\,2}(s) + I_{ry}(s)\phi_{ry}^{\,2}(s) + I_{rz}(s)\phi_{rz}^{\,2}(s) \right\} ds}{\int_{tower} \phi_y^{\,2}(s)ds} \tag{4.4}$$

5. Items of wind tunnel tests

5.1 Target modes for the main girder

The wind tunnel test is to be conducted in or der to measure the aerodynamic response of the main girder during under construction stage and after completion stage.

For the under construction stage, the following 2 stages were focused:

- Before the lowest cable being installed and just after the first segment of the main girder was installed. (Heaving 1 DOF, This condition was abbreviated as **UC1**, hereafter.)
- Just before the last segment of the main girder in the main span is installed. (Heaving and torsional 2 DOF, **UC2**)

For after completion stage, the following modes combination was set to the model:

- (Heaving and torsional 2 DOF, **AC**)

The items of the wind tunnel test are as follows:

(1) Measurement of vibration response (Free vibration test)
Incidence angle of wind: 0, +3 and -3 [deg.]
Air flow: Smooth flow, Grid turbulence (Turbulence intensity: 11%)
For Heaving 1 DOF (Under construction stage, UC1, 7^{th} mode)
For Heaving/Torsional 2 DOF (Under construction stage, UC2, 1^{st} and 7^{th} mode)
For Heaving/Torsional 2 DOF (After completion stage, AC, 1^{st} and 5^{th} mode)
This measurement is to measure vibration amplitude in each wind speed up to the maximum test wind speed* for the target vibration mode.
* The maximum test wind speed should cover the design wind speed with enough margin

(2) Measurement of aerostatic forces, steady lift and pitching moment
Incidence angle of wind: -10 [deg.] to +10 [deg.] with 1 [deg.] pitch
Air flow: Sooth flow, Grid turbulence (Turbulence intensity: 11%)
For Under construction stage, UC1* / After completion stage (AC)
* Configuration of cross section of the main girder for UC2 is identical to that for UC1.

(3) Measurement of aerodynamic forces, unsteady lift force and unsteady pitching moment. (Forced vibration test)
Incidence angle of wind: 0, +3 and -3 [deg.]
Air flow: Sooth flow, Grid turbulence (Turbulence intensity: 11%)

For Under construction stage, UC1* / After completion stage (AC)

* Configuration of cross section of the main girder for UC2 is identical to that for UC1.

The equivalent masses of the main girder and their natural frequencies for the target modes are shown in Table 5.1.1 to Table 5.1.3 and the corresponding mode shapes in Fig.5.1.1 to Fig.5.1.3. For UC1, torsional deformation in the side span is restricted since the it is supported by temporal bents. Therefore, the 5th and 6th modes will not be tested.

Table 5.1.1 Dynamic properties of each mode (UC1, For main girder).

mode	natural frequency	equivalent mass m_{eqz}	equivalent moment of inertia I_{eqx}	mode shape
unit	Hz	kg/m	kg・m^2/m	-
1 and 2	0.655			tower bending (normal to cable plane) 1st
3 and 4	0.754			tower bending (along cable plane) 1st
5 and 6	2.594		5.875E+05	torsional (side span) 1st
7 and 8	3.977	1.171E+04		heaving (main span) 1st
9 and 10	4.199			tower bending (normal to cable plane) 2nd
11 and 12	4.810			tower bending (along cable plane) 2nd
13 and 14	5.197			torsional (side span) 2nd
15 and 16	5.826			torsional (main span) 1st
17 and 18	7.594			torsional (side span) 3rd
19 and 20	9.837			torsional (side span) 4th

Note: m_{eqz} is given by eq. (4.1) and I_{eqx} by eq. (4.2)

The shaded mode is the target mode.

Table 5.1.2 Dynamic properties of each mode (UC2, For main girder).

mode	natural frequency	equivalent mass m_{eqz}	equivalent moment of inertia I_{eqx}	mode shape
	Hz	kg/m	kg・m^2/m	
1 and 2	0.439	2.065E+04		heaving 1st
3 and 4	0.509			tower bending (normal to cable plane) 1st
5 and 6	0.822			heaving ?
7 and 8	0.944		8.855E+05	torsional (main span) 1st
9 and 10	1.000			heaving 2nd
11	1.137			torsional (side span) 1st
12 and 13	1.421			heaving 3rd
14	1.841			torsional (side span) 2nd
15 and 16	2.374			heaving 4th
17 and 18	2.816			torsional (main span) 2nd
19 and 20	2.859			heaving 5th

Note: m_{eqz} is given by eq. (4.1) and I_{eqx} by eq. (4.2)

The shaded mode is the target mode.

Table 5.1.3 Dynamic properties of each mode (AC, For main girder).

mode	natural frequency	equivalent mass m_{eqz}	equivalent moment of inertia I_{eqx}	mode shape
	Hz	kg/m	kg・m^2/m	
1	0.446	2.044E+04		heaving 1st
2	0.509			tower bending (normal to cable plane) 1st (in-phase)
3	0.509			tower bending (normal to cable lane) 1st (out-phase)
4	0.740			heaving 2nd
5	0.895		8.749E+05	torsional (main span) 1st
6	0.984			sway 1st
7	1.014			heaving 3rd
8	1.137			torsional (side span) 1st
9	1.177			heaving 4th
10	1.583			heaving 5th

Note: m_{eqz} is given by eq. (4.1) and I_{eqx} by eq. (4.2)

The shaded mode is the target mode.

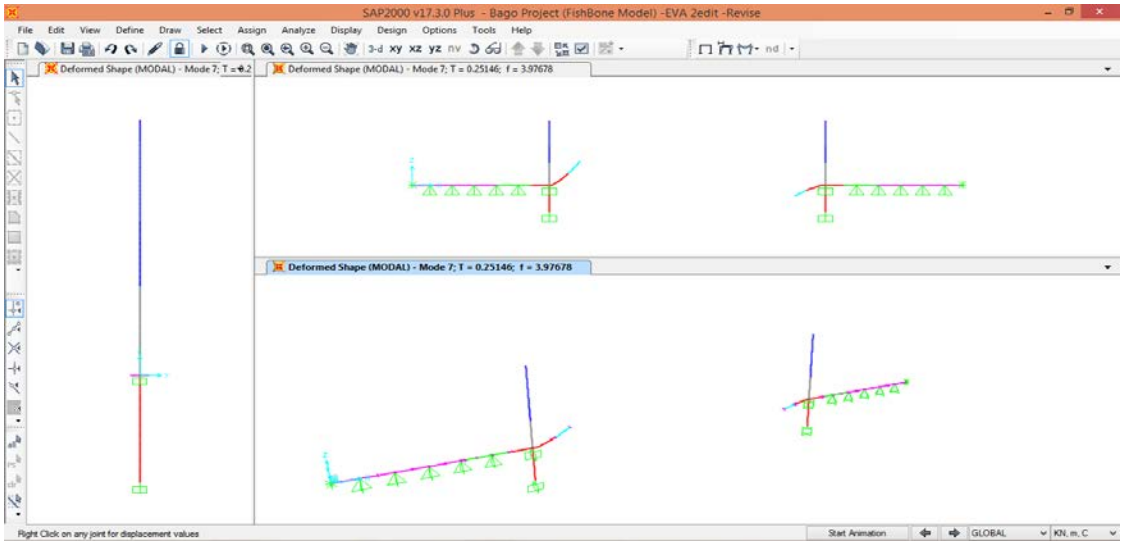

Fig. 5.1.1 Target mode shape (7th, UC1)

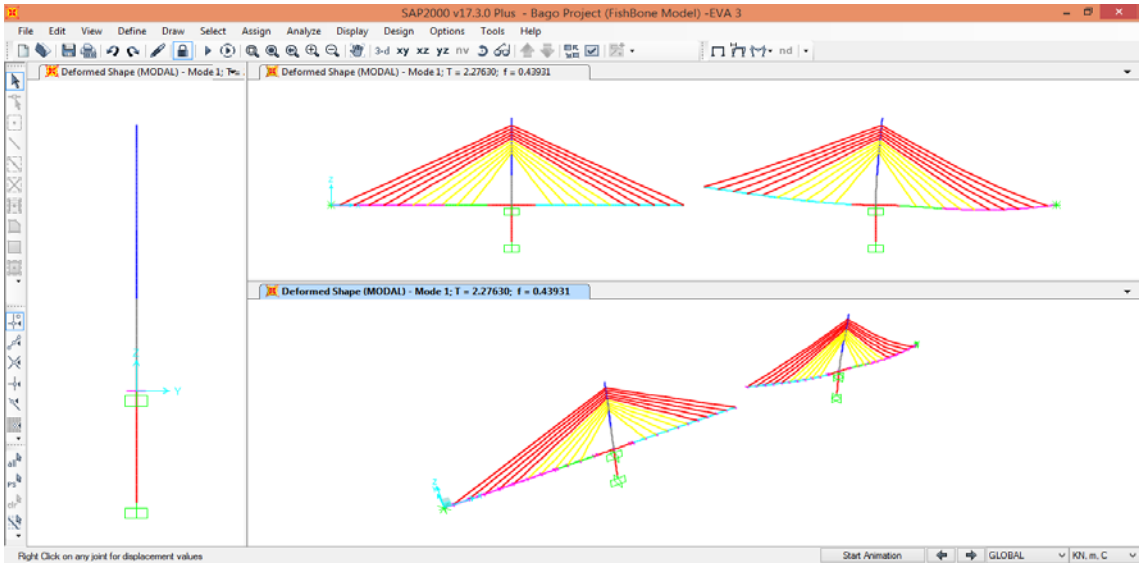

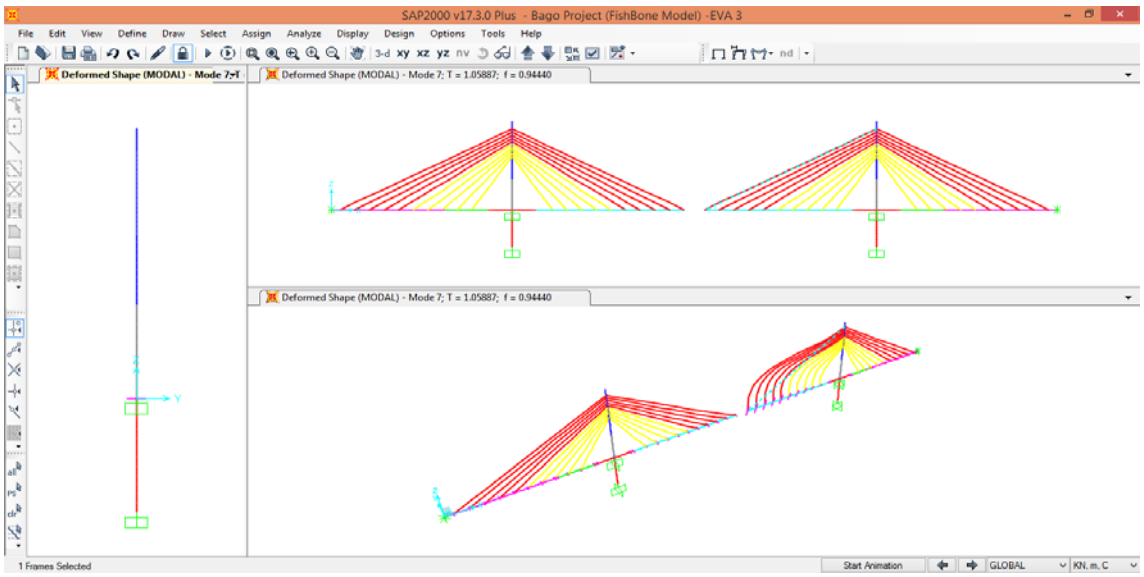

Fig. 5.1.2 Target mode shape (1st (upper) and 7th (lower), UC2)

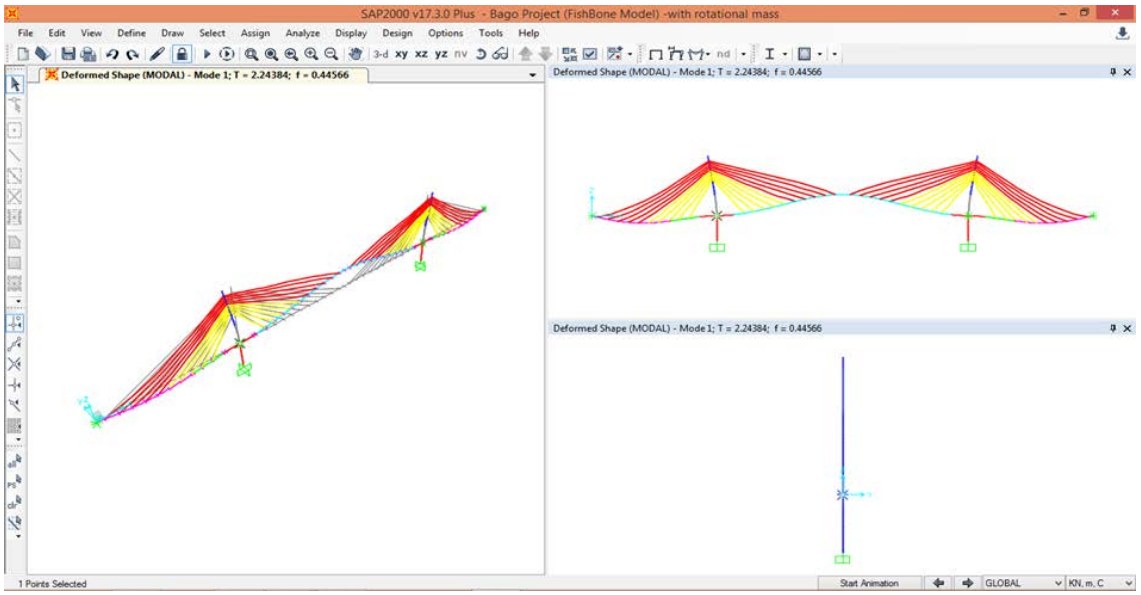

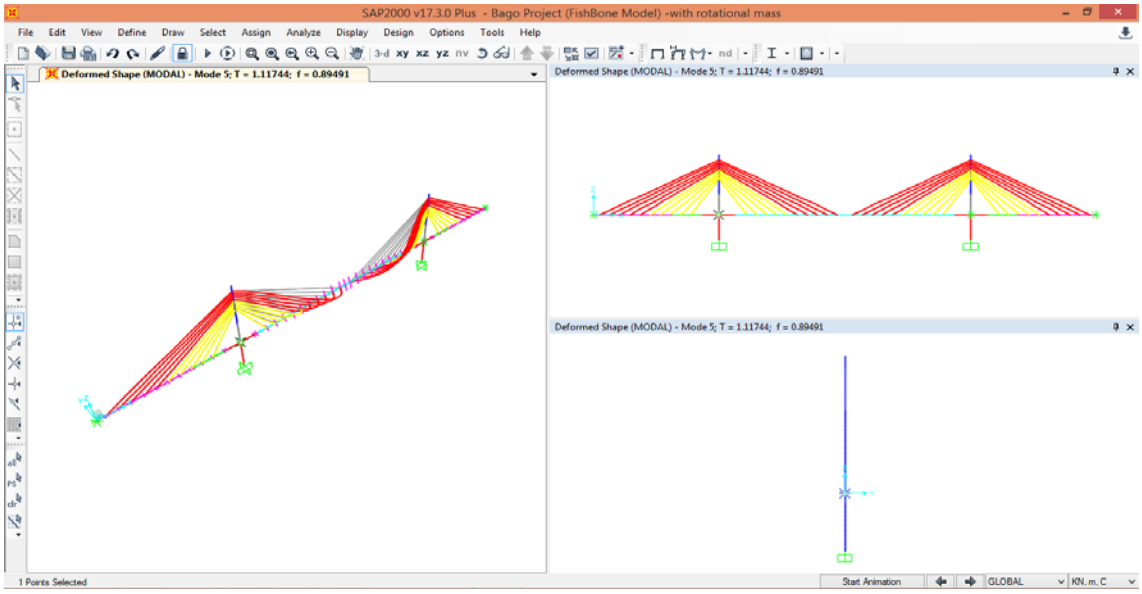

Fig. 5.1.3 Target mode shape (1st (upper) and 5th (lower), AC)

5.2 Target modes for the tower

The aerodynamic response of the tower was measured in wind tunnel during under construction stage and after completion stage. Each stage is identical to that for the test of the main girder.

- Before the lowest cable being installed and just after the first segment of the main girder was installed. (**UC1**)
- Just before the last segment of the main girder in the main span is installed. (**UC2**)
- After completion (**AC**)

The condition of wind and target modes for the measurement are as follows:

- ✓ Wind direction: 0, 5, 22.5, 45, 67.5, 80, 85, 90 and 180 [deg.]*
- ✓ Air flow: Smooth flow, Turbulent boundary layer (Turbulence intensity at the upper deck surface: 11%)
- ✓ Bending in x-direction (along bridge axis) and in y-direction (normal to bridge axis) (UC1, 3rd and 7th mode)
- ✓ Bending in y-direction (UC2 and AC, 2nd mode)

* The origin of the wind direction is chosen as wind comes from the side span along bridge axis.

** The maximum test wind speed should cover the design wind speed with enough margin

For UC2, since the bending displacement of the tower along bridge axis will be significantly restricted by the cables and the suspended girder, the target modes are assumed to be identical to those for AC. The bending vibration in y-direction (along cable plane) for both stages will be out of target mode by the same reason.

The equivalent masses of the main girder and their natural frequencies for the target modes are shown in Table 5.2.1 and Table 5.2.2 and the corresponding mode shapes in Fig.5.2.1 and Fig.5.2.2.

Table 5.2.1 Dynamic properties of each mode (UC1, For tower).

mode	natural frequency	equivalent mass m_{eqx}	equivalent mass m_{eqy}	mode shape
unit	Hz	kg/m	kg/m	-
1	0.234			
2	0.634			
3 and 4	0.655		1.224E+04	tower bending (normal to cable plane) 1st
5 and 6	0.680			girder heaving (side span) 1st
7 and 8	0.754	6.217E+03		tower bending (along cable plane) 1st

Note: m_{eqx} and m_{eqy} are given by eq. (4.3) and eq. (4.4), respectively.

The shaded mode is the target mode for measurement.

Table 5.2.2 Dynamic properties of each mode (AC, For tower).

mode	natural frequency	equivalent mass m_{eqx}	equivalent mass m_{eqy}	mode shape
unit	Hz	kg/m	kg/m	-
1	0.446	7.393E+05		tower bending and girder heaving (along cable plane) 1st
2	0.509		1.949E+04	tower bending (normal to cable plane) 1st (in-phase)
3	0.509		1.949E+04	tower bending (normal to cable plane) 1st (out-phase)
4	0.740			tower bending and girder heaving (along cable plane) 2nd
5	0.895			girder torsional 1st
6	0.984			girder sway 1st
7	1.014			tower bending and girder heaving (along cable plane) 3rd
8	1.137			girder torsional (side span) 1st
9	1.177			girder heaving 4th
10	1.583			tower bending and girder heaving (along cable plane) 5th

Note: m_{eqx} and m_{eqy} are given by eq. (4.3) and eq. (4.4), respectively.

The shaded mode is the target mode for measurement.

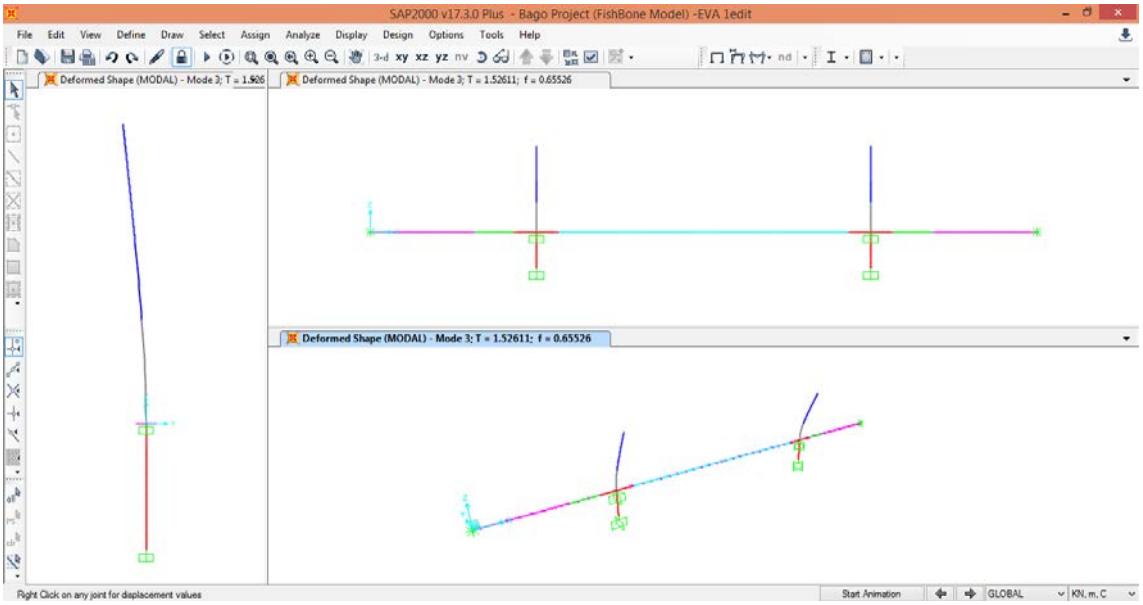

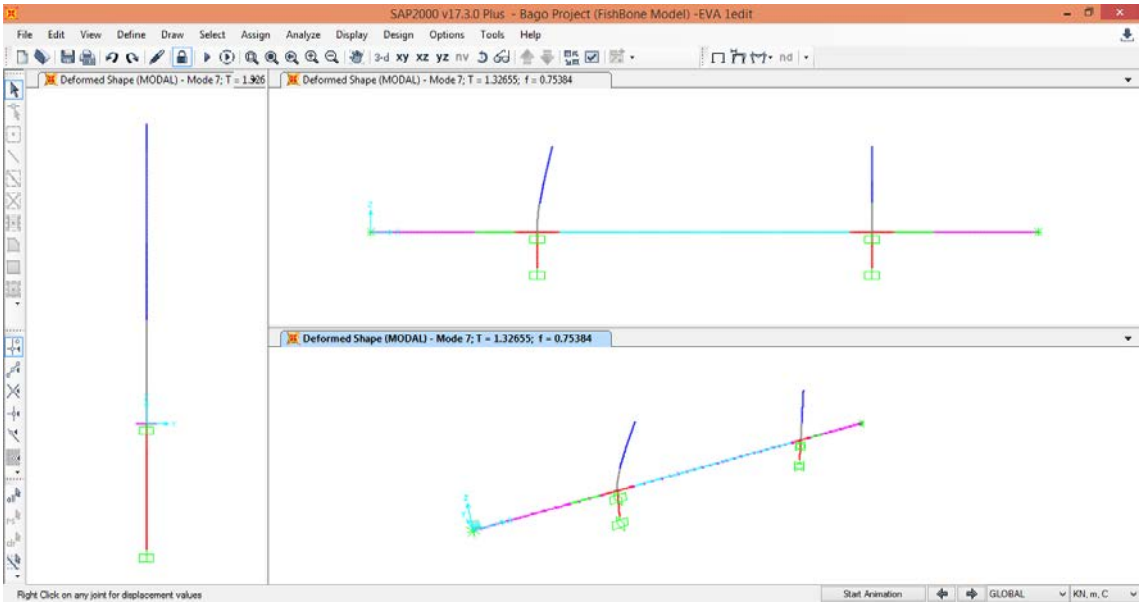

Fig. 5.2.1 Target mode shape (3rd (upper) and 7th (lower), UC1)

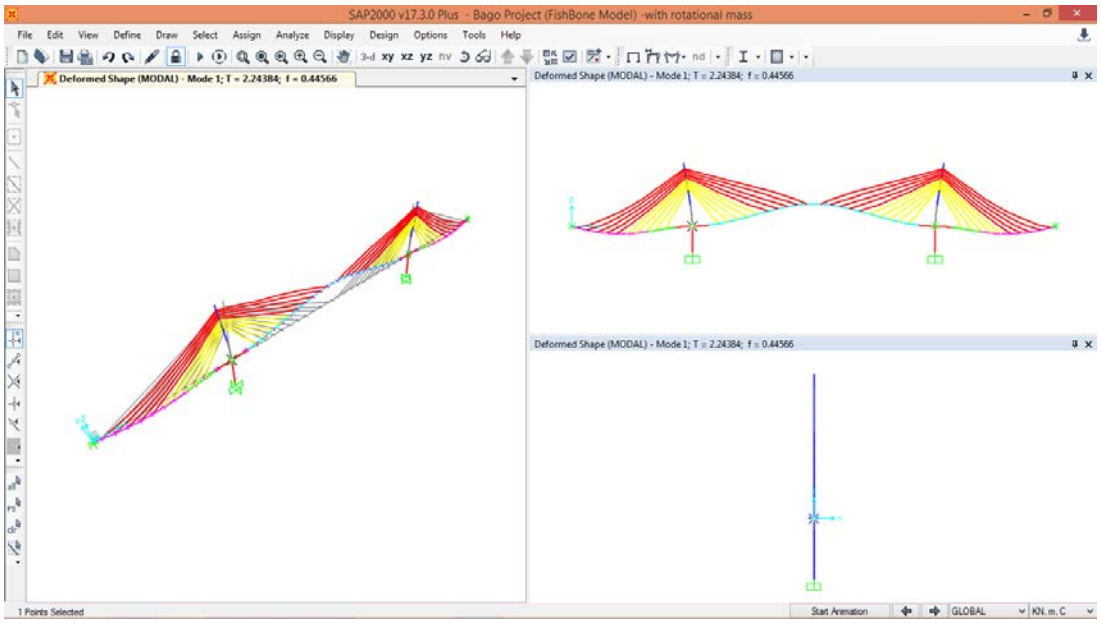

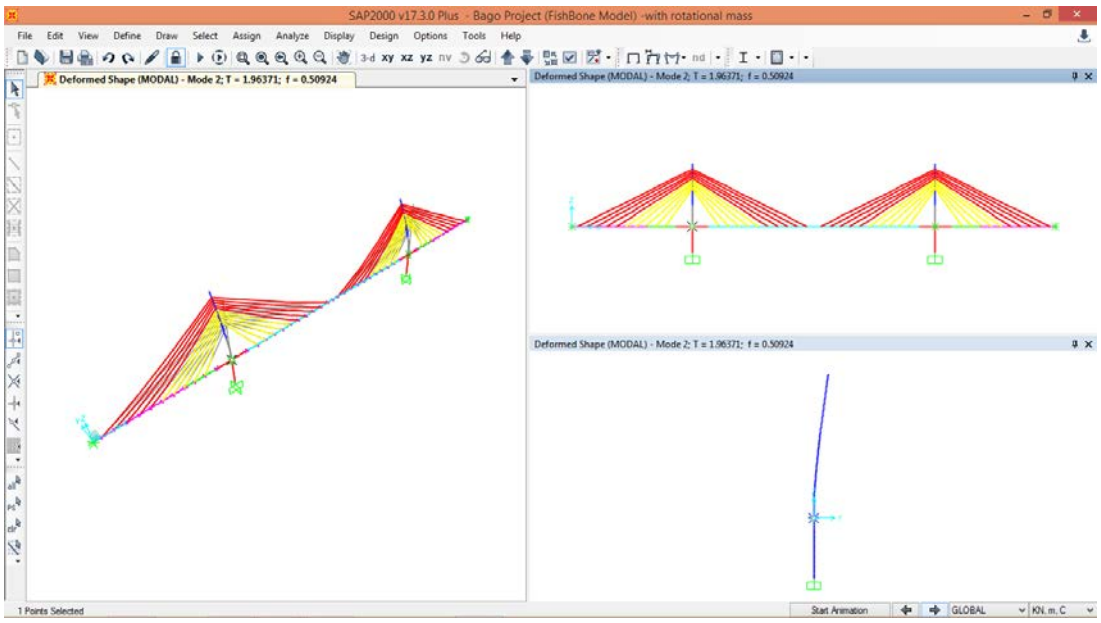

Fig. 5.2.2 Target mode shape (1st (upper) and 2nd (lower), AC)

5.3 Experimental conditions

5.3.1 Flow condition

The turbulence intensity *Iu* along wind direction in wind tunnel at the model position was kept being less than 0.5% in smooth flow condition in the measurement of aerodynamic response of the girder. While, those for the tower at the level of the main girder, *Iu* was less than 2% at the girder elevation and less than 0.5% where the elevation is higher than 300 [mm] (= 36.0 [m] for real bridge). The vertical profile of longitudinal wind speed and turbulent intensity is shown in Fig.5.3.1.

Turbulent flow for the measurement of the girder was produced by the grid as shown in Fig. 5.3.2. The turbulent intensity *Iu* along wind direction in wind tunnel at the model position is 11%. This intensity level is lower than the required condition of 17% which exceeds the limit to keep the uniformity of approaching turbulence at the model position. In general, the aerodynamic vibration response under the condition of *Iu*=11% provides safer judgement to the aerodynamic stability.

In the measurement in turbulent flow condition for the tower, turbulent boundary layer was created in wind tunnel by installing the grid and chains on the artificial floor which is to be simulated the surface of the average water level (M.W.L.). The vertical profile of wind speed and turbulence intensity are shown in Fig. 5.3.3. The distribution along the horizontal direction normal to the main wind direction in wind tunnel is confirmed along $0.8 < y/W < 0.8$ (y: horizontal coordinate normal to wind in wind tunnel [m], W: half width of the width of the working section in wind tunnel (2W=2.0 [m]) as shown in Fig. 5.3.4.

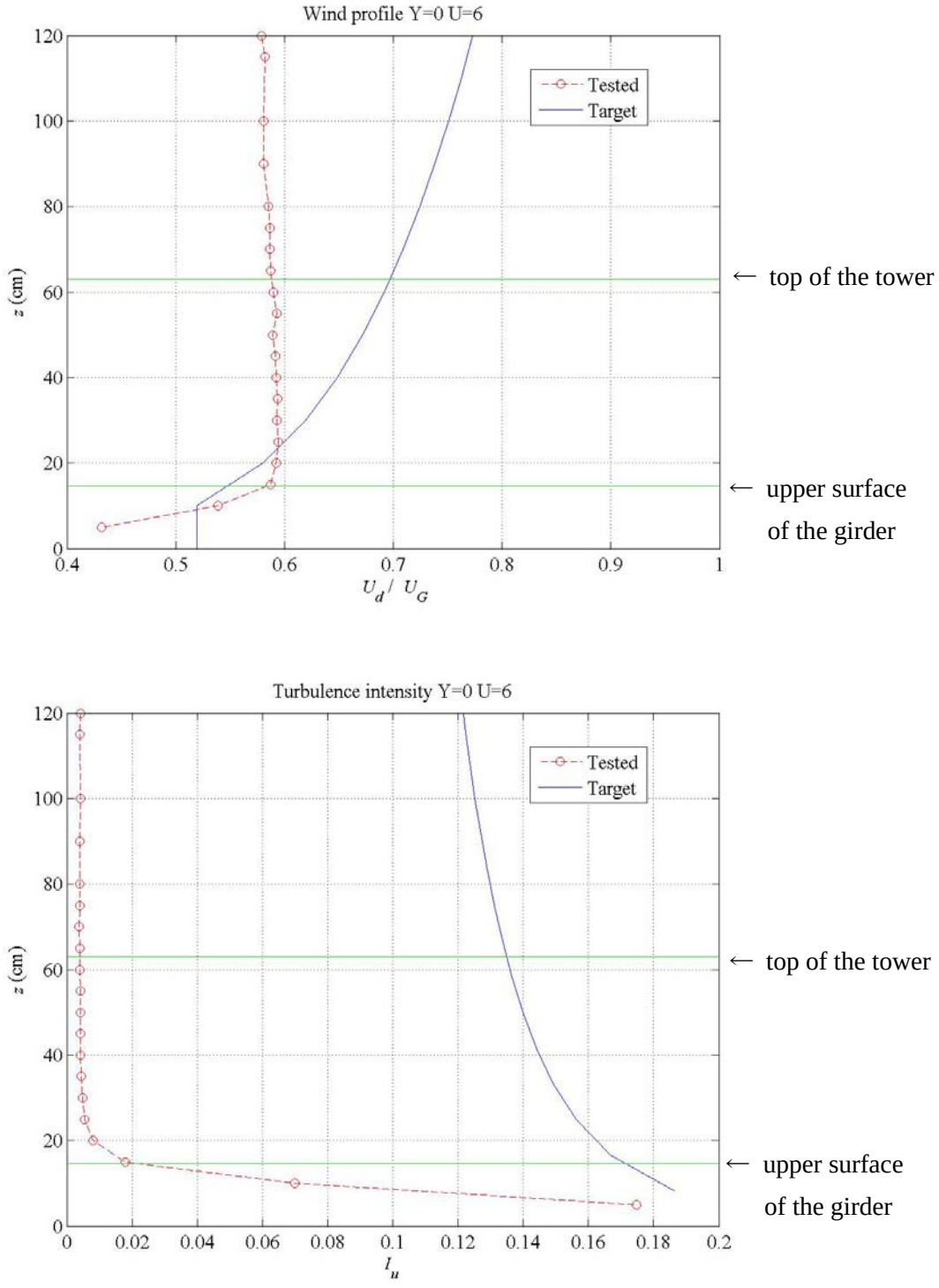

Fig.5.3.1 Vertical profile of turbulence intensity *Iu* at the model position in smooth flow condition for the measurement of the tower model
(upper: longitudinal wind speed, lower: turbulence intensity)

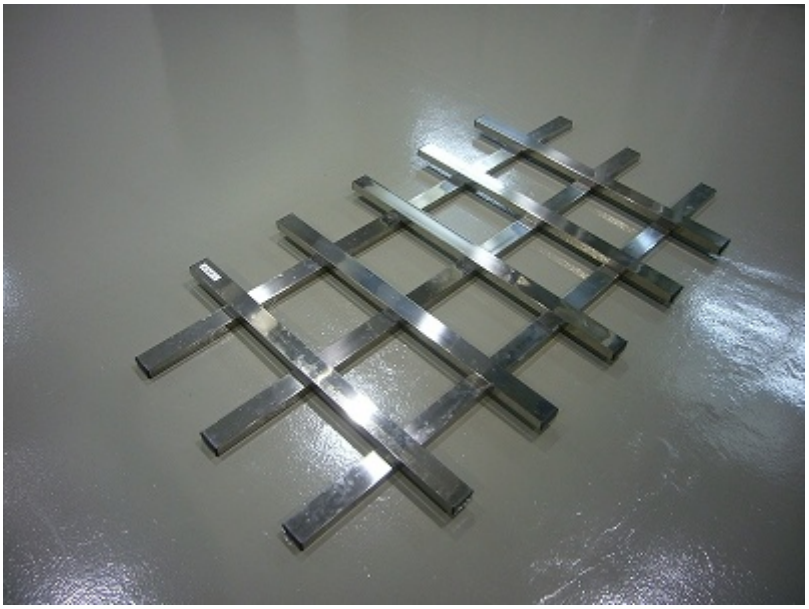

Fig.5.3.2 Grid to produce turbulence in wind tunnel.

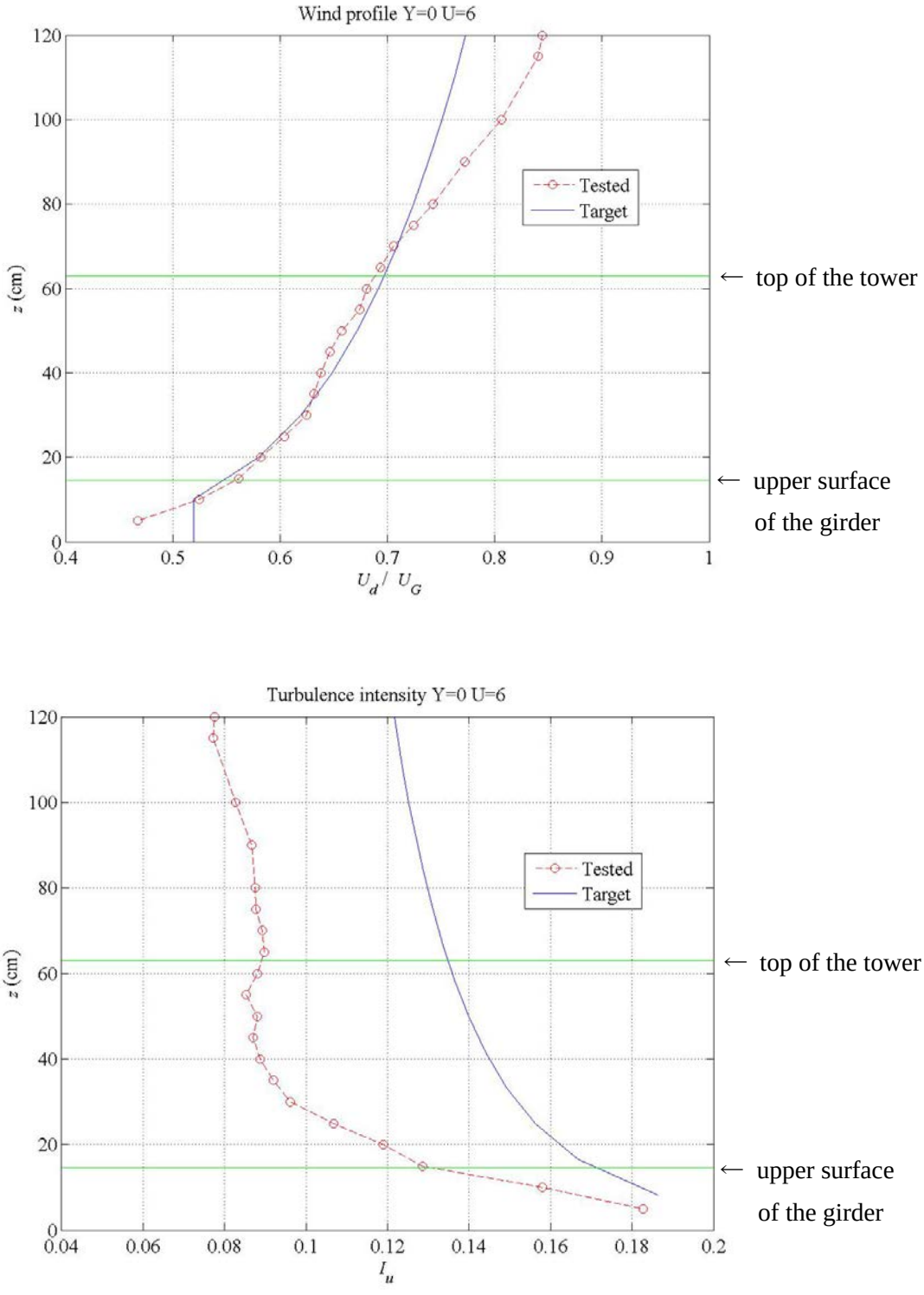

Fig.5.3.3 Vertical profile of turbulence intensity *Iu* at the model position in turbulent flow condition for the measurement of the tower model
(upper: longitudinal wind speed, lower: turbulence intensity)

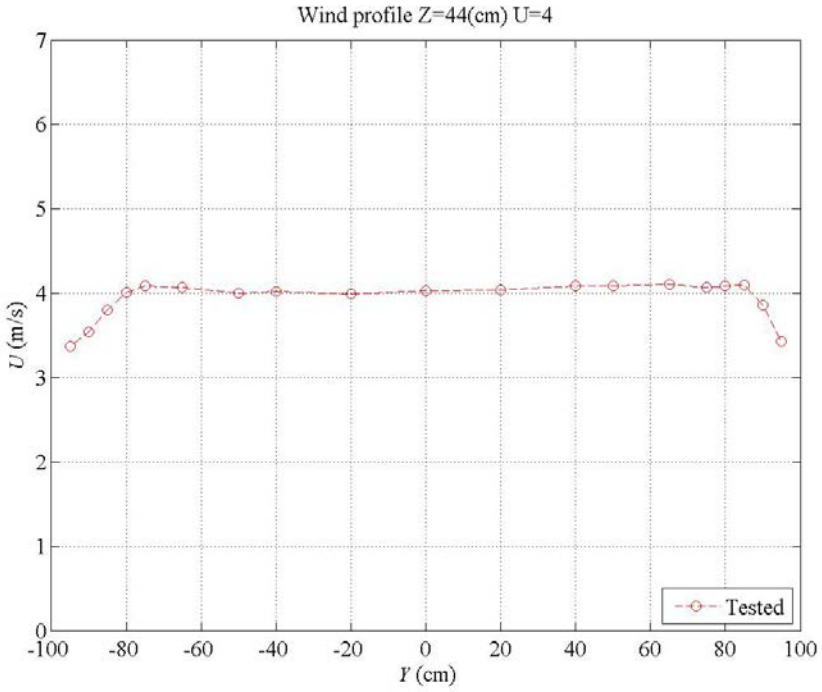

Fig.5.3.4 Horizontal profile of wind speed at the model position in turbulent flow condition for the measurement of the tower model (at the top of the tower)

5.3.2 Test condition

The test condition in each measurement of the main girder are summarized in Table 5.3.1 for UC1, Table 5.3.2 for UC2 and in Table 5.3.3 for AC, respectively.

The experimental conditions in each measurement of the tower are summarized in Table 5.3.4 and Table 5.3.5 for UC1, in Table 5.3.6 for UC2, and in Table 5.3.7 to Table 5.3.9 for AC, respectively.

Table 5.3.1 Experimental conditions for the main girder (UC1)

No.	Stage	Flow condition	Attack angle	m (kg/m)	f_h(Hz)	δ_h					
						2A =2.5mm	**2A =5.0mm**	2A =7.5mm	2A =10.0mm	2A =15.0mm	2A =20.0mm
1	Under construction (UC1)	Smooth	0º	3.102E+00	5.736E+00	1.405E-02	1.748E-02	2.091E-02	2.357E-02	2.744E-02	3.020E-02
2			+3º	3.085E+00	5.742E+00	1.224E-02	1.637E-02	2.045E-02	2.351E-02	2.785E-02	3.090E-02
3			-3º	3.055E+00	5.744E+00	1.504E-02	1.814E-02	2.162E-02	2.439E-02	2.845E-02	3.136E-02
4		Turbulence	0º	3.102E+00	5.736E+00	1.405E-02	1.748E-02	2.091E-02	2.357E-02	2.744E-02	3.020E-02
5			+3º	3.082E+00	5.740E+00	1.403E-02	1.784E-02	2.160E-02	2.449E-02	2.866E-02	3.161E-02
6			-3º	3.100E+00	5.731E+00	1.292E-02	1.719E-02	2.131E-02	2.440E-02	2.880E-02	3.189E-02

Table 5.3.2 Experimental conditions for the main girder (UC2)

No.	Stage	Flow condition	Attack angle	m(kg/m)	f_h(Hz)	δ_h					
						2A =2.5mm	**2A =5.0mm**	2A =7.5mm	2A =10.0mm	2A =15.0mm	2A =20.0mm
				I (kg*m^2/m)	f_t(Hz)	δt					
						2A =0.4deg	2A =0.6deg	2A =0.8deg	2A =1.0deg	2A =1.4deg	2A =1.8deg
1	Under construction (UC2)	Smooth	0º	4.186E+00	4.940E+00	1.935E-02	2.177E-02	2.428E-02	2.635E-02	2.951E-02	3.186E-02
				3.709E-02	1.074E+01	0.000E+00	1.605E-02	1.626E-02	1.671E-02	1.782E-02	1.892E-02
2			+3º	4.267E+00	4.857E+00	1.992E-02	2.108E-02	2.344E-02	2.560E-02	2.905E-02	3.166E-02
				3.656E-02	1.082E+01	2.065E-02	2.361E-02	2.392E-02	2.326E-02	2.050E-02	1.623E-02
3			-3º	4.234E+00	4.929E+00	1.986E-02	2.078E-02	2.323E-02	2.551E-02	2.916E-02	3.192E-02
				3.745E-02	1.050E+01	1.992E-02	1.939E-02	1.964E-02	2.017E-02	2.146E-02	2.272E-02
4		Turbulence	0º	4.234E+00	4.929E+00	1.885E-02	2.137E-02	2.380E-02	2.577E-02	2.876E-02	3.097E-02
				3.614E-02	1.075E+01	1.693E-02	1.535E-02	1.526E-02	1.560E-02	1.658E-02	1.758E-02
5			+3º	4.199E+00	4.923E+00	2.064E-02	2.115E-02	2.332E-02	2.544E-02	2.892E-02	3.159E-02
				3.633E-02	1.079E+01	1.987E-02	2.433E-02	2.463E-02	2.392E-02	2.115E-02	1.647E-02
6			-3º	4.209E+00	4.927E+00	1.803E-02	1.949E-02	2.206E-02	2.432E-02	2.786E-02	3.050E-02
				3.745E-02	1.049E+01	1.837E-02	1.887E-02	1.930E-02	1.967E-02	2.030E-02	2.081E-02

Table 5.3.3 Experimental conditions for the main girder (AC)

No.	Stage	Flow condition	Attack angle	m(kg/m)	f_h(Hz)	δ_h(average)					
						2A =2.5mm	**2A =5.0mm**	2A =7.5mm	2A =10.0mm	2A =15.0mm	2A =20.0mm
				I (kg*m^2/m)	f_t(Hz)	δt (average)					
						2A =0.4deg	2A =0.6deg	2A =0.8deg	2A =1.0deg	2A =1.4deg	2A =1.8deg
1	After completion (AC)	Smooth	0º	4.105E+00	4.973E+00	1.996E-02	1.892E-02	1.980E-02	2.101E-02	2.332E-02	2.526E-02
				3.624E-02	1.015E+01	2.516E-02	2.136E-02	1.908E-02	1.772E-02	1.664E-02	1.676E-02
2			+3º	4.121E+00	4.984E+00	2.069E-02	2.080E-02	2.172E-02	2.268E-02	2.441E-02	2.583E-02
				3.637E-02	1.018E+01	2.808E-02	2.575E-02	2.215E-02	1.989E-02	1.772E-02	1.732E-02
3			-3º	4.145E+00	4.977E+00	2.091E-02	2.043E-02	2.111E-02	2.199E-02	2.366E-02	2.510E-02
				3.618E-02	1.016E+01	2.839E-02	2.408E-02	2.130E-02	1.946E-02	1.752E-02	1.700E-02
4		Turbulence	0º	4.118E+00	4.974E+00	1.986E-02	1.929E-02	2.016E-02	2.123E-02	2.324E-02	2.493E-02
				3.632E-02	1.016E+01	2.810E-02	2.399E-02	2.140E-02	1.973E-02	1.805E-02	1.767E-02
5			+3º	4.122E+00	4.969E+00	2.090E-02	2.053E-02	2.148E-02	2.260E-02	2.465E-02	2.636E-02
				3.611E-02	1.016E+01	2.590E-02	2.173E-02	1.916E-02	1.757E-02	1.624E-02	1.630E-02
6			-3º	4.099E+00	4.976E+00	2.041E-02	2.041E-02	2.132E-02	2.231E-02	2.408E-02	2.555E-02
				3.615E-02	1.016E+01	2.725E-02	2.296E-02	2.030E-02	1.865E-02	1.721E-02	1.719E-02

Table 5.3.4 Experimental conditions for the tower (UC1, without aerodynamic device)

No.	Flow condition	Wind direction [deg.]	Model		Prototype	U_m	V	U_p	δ (2A=5mm)
			f_x(Hz)	s_m (m)	f_x(Hz)				δ_x
			f_y(Hz)	w_m (m)	f_y(Hz)				δ_y
1	Smooth flow	0	8.93	0.0250	0.754	7	31.35	70.91	7.44E-03
			7.62	0.0208	0.655	7	44.11	72.23	1.14E-02
2		5	8.93	0.0250	0.754	7	31.37	70.95	7.36E-03
			7.60	0.0208	0.655	7	44.21	72.40	1.14E-02
3		22.5	8.93	0.0250	0.754	7	31.36	70.93	7.45E-03
			7.60	0.0208	0.655	7	44.20	72.37	1.17E-02
4		45	8.93	0.0250	0.754	7	31.36	70.94	7.51E-03
			7.60	0.0208	0.655	7	44.19	72.37	1.14E-02
5		67.5	8.93	0.0250	0.754	7	31.34	70.90	7.51E-03
			7.60	0.0208	0.655	7	44.20	72.37	1.11E-02
6		80	8.94	0.0250	0.754	7	31.33	70.87	7.79E-03
			7.60	0.0208	0.655	7	44.20	72.38	1.12E-02
7		85	8.93	0.0250	0.754	7	31.34	70.90	7.85E-03
			7.60	0.0208	0.655	7	44.19	72.37	1.14E-02
8		90	8.93	0.0250	0.754	7	31.36	70.94	7.52E-03
			7.60	0.0208	0.655	7	44.21	72.40	1.12E-02

Table 5.3.5 Experimental conditions for the tower
(UC1, with aerodynamic device (length = 2P*))

No.	Flow condition	Wind direction [deg.]	Model		Prototype	U_m	V	U_p	δ (2A=5mm)
			f_x(Hz)	s_m (m)	f_x(Hz)				δ_x
			f_y(Hz)	w_m (m)	f_y(Hz)				δ_y
9	Smooth flow	0	8.80	0.0250	0.754	7	31.81	71.95	7.49E-03
			7.50	0.0208	0.655	7	44.81	73.38	1.16E-02
10		90	8.80	0.0250	0.754	7	31.83	71.99	7.93E-03
			7.49	0.0208	0.655	7	44.88	73.49	1.12E-02
11	Turbulence	80	8.80	0.0250	0.754	7	31.83	72.01	7.85E-03
			7.48	0.0208	0.655	7	44.92	73.55	1.13E-02
12		85	8.80	0.0250	0.754	7	31.83	72.00	7.84E-03
			7.49	0.0208	0.655	7	44.86	73.47	1.08E-02
13		90	8.80	0.0250	0.754	7	31.83	72.00	7.84E-03
			7.48	0.0208	0.655	7	44.90	73.53	1.10E-02
14		180	8.79	0.0250	0.754	7	31.84	72.02	7.52E-03
			7.48	0.0208	0.655	7	44.90	73.52	1.14E-02

*Length of aerodynamic device: 91.7mm (= 11.0m for real bridge) from the top of the tower)

Table 5.3.6 Experimental conditions for the tower

(UC2, with aerodynamic device (length = 2P*))

No.	Flow condition	Wind direction [deg.]	Model		Prototype	U_m	V	U_p	δ (2A=5mm)
			f_y(Hz)	w_m (m)	f_y(Hz)				δ_y
1	Smooth flow	0	6.62	0.0208	0.509	7	50.79	64.63	1.25E-02
2		5	6.62	0.0208	0.509	7	50.79	64.63	1.31E-02
3	Turbulence	0	6.62	0.0208	0.509	7	50.76	64.59	1.23E-02
4		5	6.77	0.0208	0.509	7	49.61	63.13	1.19E-02

*Length of aerodynamic device: 91.7mm (= 11.0m for real bridge) from the top of the tower)

Table 5.3.7 Experimental conditions for the tower (AC, without aerodynamic device)

No.	Flow condition	Wind direction [deg.]	Model		Prototype	U_m	V	U_p	δ (2A=5mm)
			f_y(Hz)	w_m (m)	f_y(Hz)				δ_y
1	Smooth flow	0	6.82	0.0208	0.509	6	42.23	53.74	1.19E-02
2		5	6.82	0.0208	0.509	6	42.23	53.74	1.19E-02
3		10	6.82	0.0208	0.509	6	42.23	53.74	1.19E-02
4		22.5	6.82	0.0208	0.509	6	42.23	53.74	1.19E-02
5		45	6.82	0.0208	0.509	6	42.23	53.74	1.19E-02
6		67.5	6.82	0.0208	0.509	6	42.23	53.74	1.19E-02
7		90	6.82	0.0208	0.509	6	42.23	53.74	1.19E-02
8	Turbulence	0	6.82	0.0208	0.509	6	42.23	53.74	1.19E-02
9		5	6.82	0.0208	0.509	6	42.23	53.74	1.19E-02
10		10	6.82	0.0208	0.509	6	42.23	53.74	1.19E-02
11		22.5	6.82	0.0208	0.509	6	42.23	53.74	1.19E-02
12		45	6.82	0.0208	0.509	6	42.23	53.74	1.19E-02
13		67.5	6.82	0.0208	0.509	6	42.23	53.74	1.19E-02
14		90	6.82	0.0208	0.509	6	42.23	53.74	1.19E-02

Table 5.3.8 Experimental conditions for the tower
(AC, with aerodynamic device (length = 2P*))

No.	Flow condition	Wind direction [deg.]	Model		Prototype	U_m	V	U_p	δ (2A=5mm)
			f_y(Hz)	w_m (m)	f_y(Hz)				δ_y
15	Smooth flow	0	6.62	0.0208	0.509	7	50.76	64.59	1.27E-02
16		5	6.62	0.0208	0.509	7	50.76	64.59	1.27E-02
17	Turbulence	0	6.62	0.0208	0.509	6	43.53	55.40	1.20E-02
18		5	6.62	0.0208	0.509	6	43.53	55.40	1.24E-02

*Length of aerodynamic device: 91.7mm (= 11.0m for real bridge) from the top of the tower)

Table 5.3.9 Experimental conditions for the tower
(AC, with various device (length = “Pieces” in the table*))

No.	Flow condition	Wind direction [deg.] / Pieces	Model		Prototype	U_m	V	U_p	δ (2A=5mm)
			f_y(Hz)	w_m (m)	f_y(Hz)				δ_y
19	Smooth flow	0/ 3P	6.59	0.0208	0.509	7	51.02	64.92	1.25E-02
20		5/ 3P	6.59	0.0208	0.509	7	51.02	64.92	1.27E-02
21		0/ 2P	6.62	0.0208	0.509	7	50.76	64.59	1.27E-02
22		5/ 2P	6.62	0.0208	0.509	7	50.76	64.59	1.27E-02
23	Turbulence	0 /5P	6.67	0.0208	0.509	6	43.18	54.94	1.25E-02
24		5 /5P	6.67	0.0208	0.509	6	43.18	54.94	1.25E-02
25		0 /4P	6.65	0.0208	0.509	6	43.31	55.11	1.24E-02
26		5 /4P	6.65	0.0208	0.509	6	43.31	55.11	1.20E-02
27		0 /3P	6.60	0.0208	0.509	6	43.62	55.51	1.24E-02
28		5 /3P	6.60	0.0208	0.509	6	43.62	55.51	1.23E-02
29		0 /2P	6.62	0.0208	0.509	6	43.53	55.40	1.20E-02
30		5 /2P	6.62	0.0208	0.509	6	43.53	55.40	1.24E-02
31		0 /1P	6.52	0.0208	0.509	6	44.16	56.19	1.27E-02
32		5 /1P	6.52	0.0208	0.509	6	44.16	56.19	1.28E-02

*Length of aerodynamic device from top of the tower:

5P: 233.4mm (= 28.0m for real bridge)

4P: 191.7mm (23.0m)

3P: 141.7mm (17.0m)

1P: 41.7mm (5.0m)

5.4 Experimental setup

5.4.1 Free vibration test

The section model is supported horizontally by 8 coil springs in the wind tunnel working section. (see Fig.5.4.1 and Fig.5.4.2) Heaving and torsional displacements were detected by the laser displacement meters (LB-300, LB-1200, Keyence) fixed on a rigid frame of the working section. Small targets made of hard polystyrene plate to reflect the laser beam were attached at the ends of the model supporting rods. The electric signal from each displacement meter is led to the A/D converter (GL7000, Graphtec) with sampling rate of 1.0 [kHz]. The record length of each data is 120 [sec.]. Heaving and torsional displacements are obtained by adding or subtracting these digital data with each other.

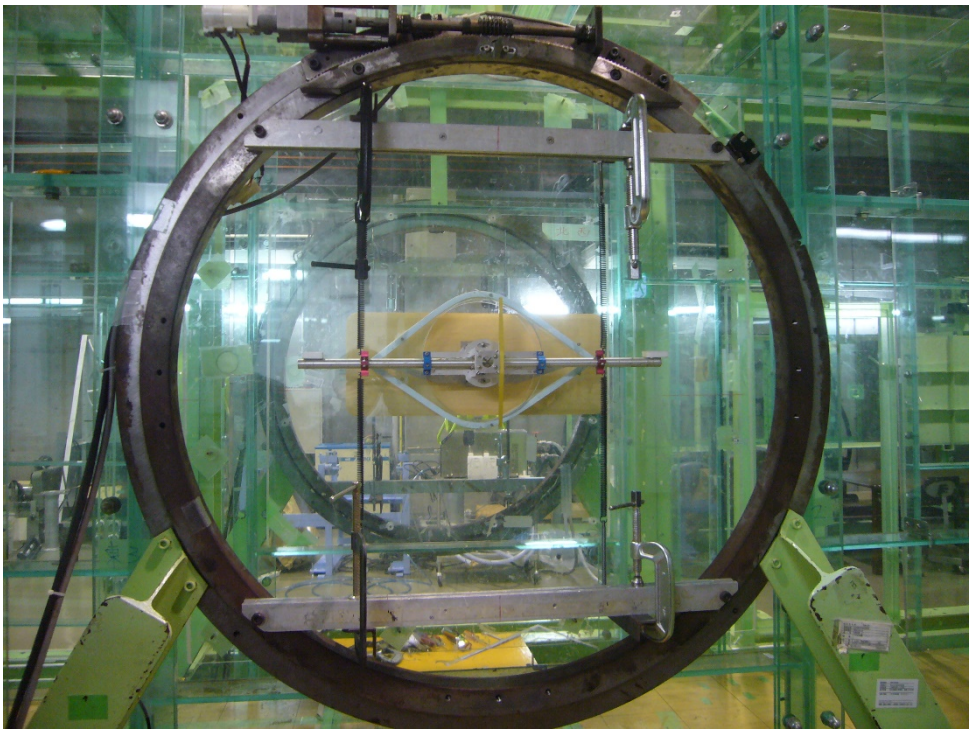

Fig.5.4.1 setup of the free vibration test of the section model

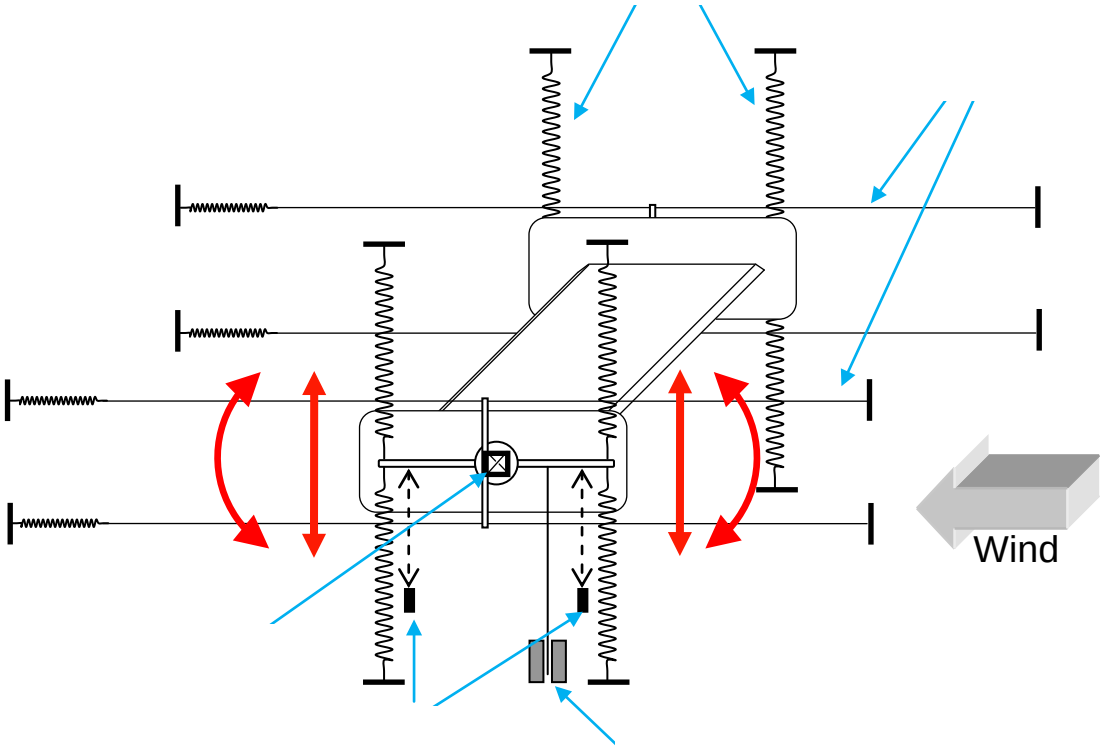

Fig.5.4.2 Experimental setup for free vibration test

5.4.2 Forced vibration test and Aero-static force components test

The section model is supported by the three-component load cells (LMC3501-20, Nissho Electric Works) at both sides and set horizontally in the working section. The signals from the load cells are led to the A/D converter via the dynamic strain meter. (MCD-8A, Kyowa Dengyo).

In case of the forced vibration test, heaving 1DOF or torsional 1DOF harmonic motion is applied to the section model of the main girder by the motor and link structure. The amplitude of the harmonic motion is set 10 [mm] for heaving and 2 [deg] for torsional. Two load cells are connected rigidly with the end plates at both sides of the model. In wind condition, the signal from the load cell consists of the aerodynamic force and the inertia force due to the motion. The inertia force can be measured in no wind condition.

In case of the aero-static force components test, drag, lift and pitching moment, on the section model are measured in wind tunnel for -10 [deg] to +10 [deg] of the incidence angle of wind (a) in smooth and in turbulent flow conditions. The section model is supported by the three-component load cells as mentioned above. Aerodynamic forces are measure in every α with 1 [deg] pitch. The aerodynamic force coefficient is determined by the time averaged level of each force component. (see Fig.5.4.3)

Fig.5.4.3　Experimental setup for forced vibration test

6. Wind tunnel tests of Bago Cable-stayed Bridge

6.1. Introduction

The aerodynamic response of Bago Cable-Stayed Bridge was measured in wind tunnel. In this chapter, the results of wind tunnel tests for the aerodynamic response of the main girder as well as for the tower are summarized.

6.2 Free vibration test of main girder (scale ratio 1/70)

The test was conducted in or der to measure the aerodynamic response of the main girder during under construction stage and after completion stage.

For the under construction stage, the following 2 stages were focused:

- Before the lowest cable being installed and just after the first segment of the main girder was installed. (Heaving 1 DOF, This condition was abbreviated as UC1, hereafter.)
- Just before the last segment of the main girder in the main span is installed. (Heaving and torsional 2 DOF, UC2)

For after completion stage, the following modes combination was set to the model:

- (Heaving and torsional 2 DOF, AC)

Note: The condition to choose the focused modes was described in Chapter 5.

In the following tables, ‘o’ means the corresponding response was not observed, and ‘×’ means the corresponding response occurred. The corresponding prototype wind speed interval *Up* [m/s] is shown for the vortex-induced vibration (VIV), while the prototype onset wind speed is shown for flutter and galloping.

6.2.1 Under construction (UC1, Before the lowest cable being installed)

In the case of UC1, the free vibration test was conducted under 3 incidence angles of wind (0, +3, and -3 [deg]) in smooth and in turbulent flow, respectively. Displacement of the model was allowed only 1 DOF along heaving (across-wind) direction, and an initial heaving vibration (disturbance) was applied to the model at several wind speed conditions in the test. The response was recorded after the response amplitude became stable.

For all of the cases in UC1, neither vortex-induced vibration (VIV) nor flutter was observed. The results are summarized in Table 6.2.1. The response of each case is shown in Fig 6.2.1-Fig. 6.2.6.

Table 6.2.1 Aerodynamic response of the main girder in UC1 (Heaving 1 DOF)

Flow condition	Vertical incidence angle of wind [deg]	Vortex-induced vibration	Flutter	Corresponding figure
Smooth	0	o	o	Fig.6.2.1
	+3	o	o	Fig.6.2.2
	-3	o	o	Fig.6.2.3
Turbulent	0	o	o	Fig.6.2.4
	+3	o	o	Fig.6.2.5
	-3	o	o	Fig.6.2.6

“o” : The corresponding response was not observed.

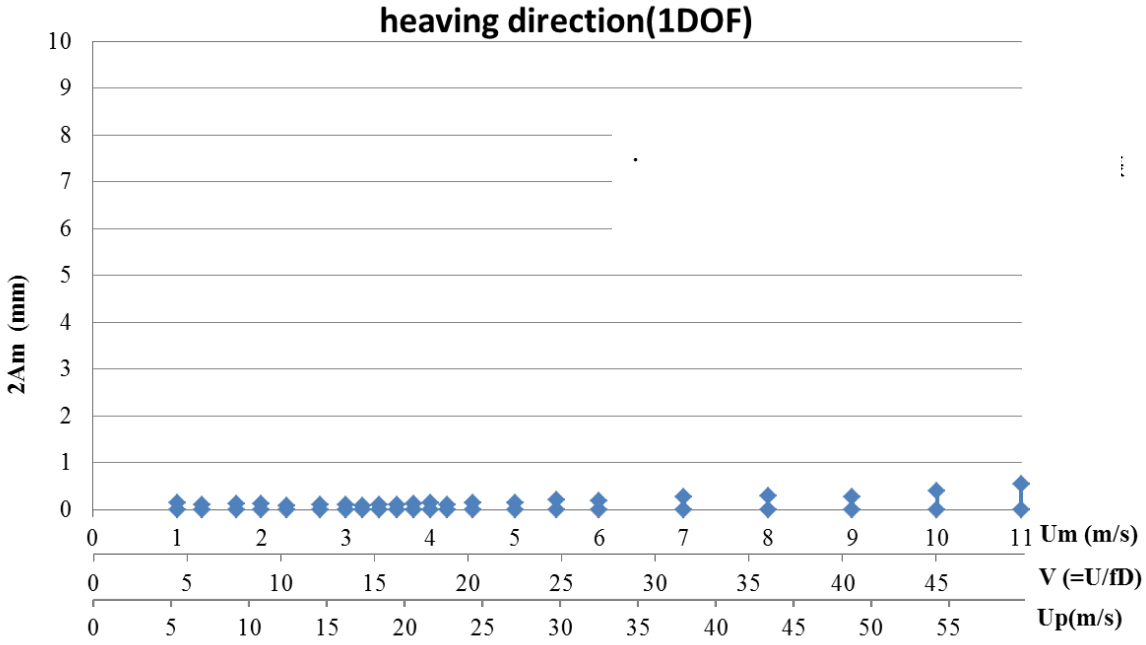

Fig. 6.2.1 Heaving response (UC1, incidence angle = 0 [deg], in smooth flow)

(Stable response amplitude was measured after providing initial disturbance to the model.)

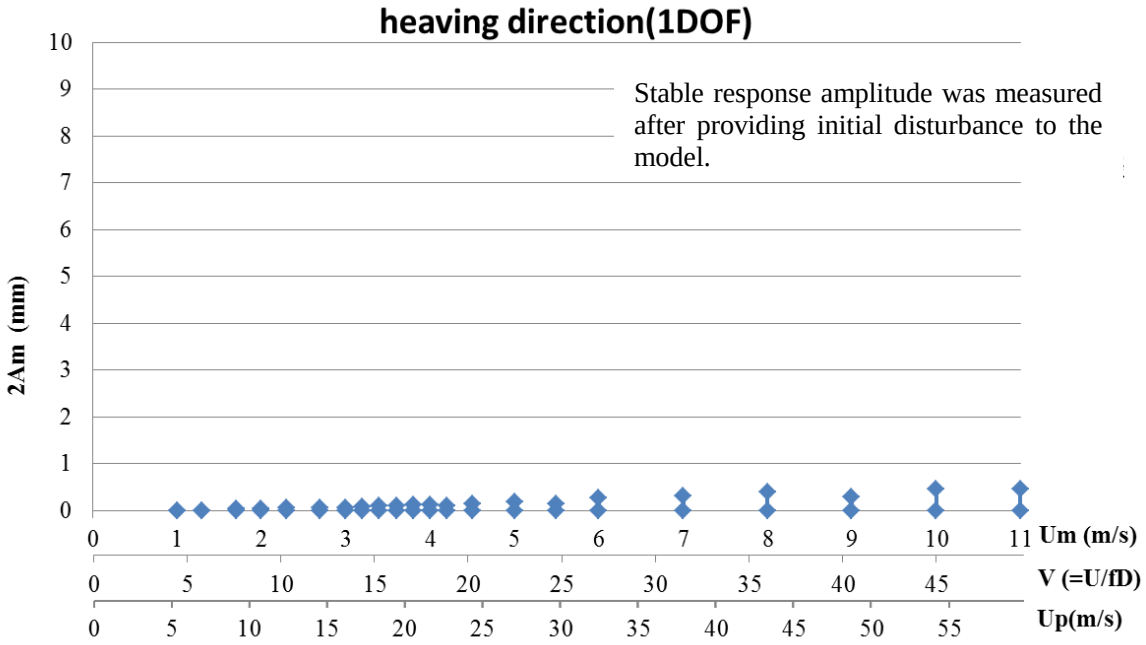

Fig. 6.2.2 Heaving response (UC1, incidence angle = +3 [deg], in smooth flow)

(Stable response amplitude was measured after providing initial disturbance to the model.)

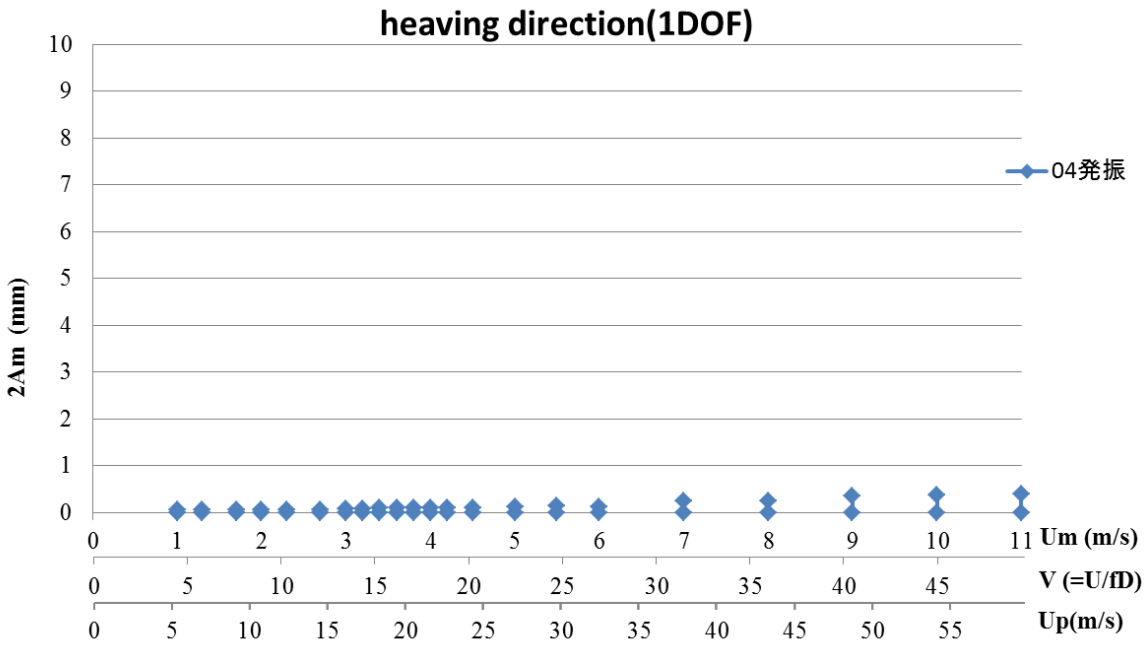

Fig. 6.2.3 Heaving response (UC1, incidence angle = -3 [deg], in smooth flow)

(Stable response amplitude was measured after providing initial disturbance to the model.)

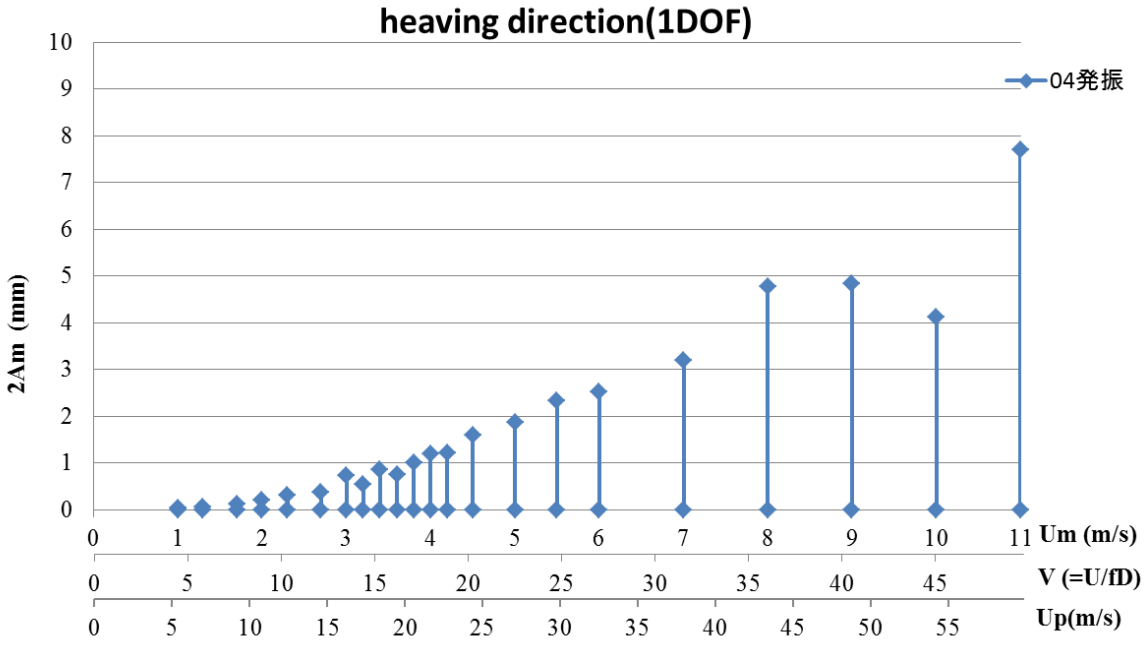

Fig. 6.2.4 Heaving response (UC1, incidence angle = 0 [deg], in turbulent flow)

(Stable response amplitude was measured after providing initial disturbance to the model.)

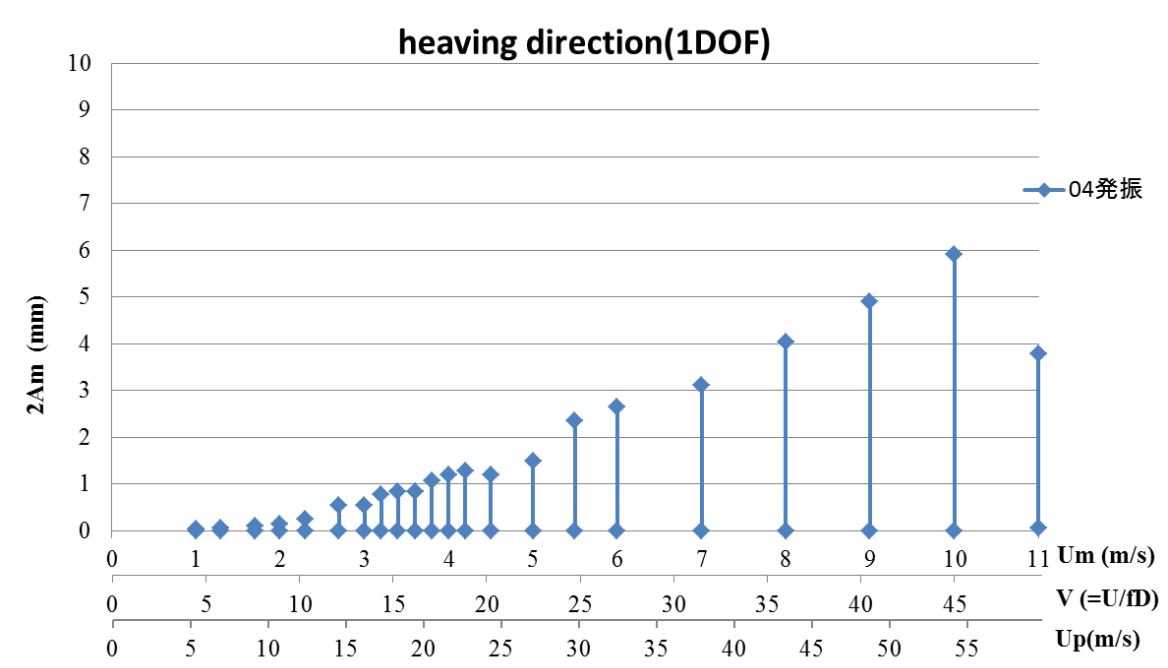

Fig. 6.2.5 Heaving response (UC1, incidence angle = +3 [deg], in turbulent flow)

(Stable response amplitude was measured after providing initial disturbance to the model.)

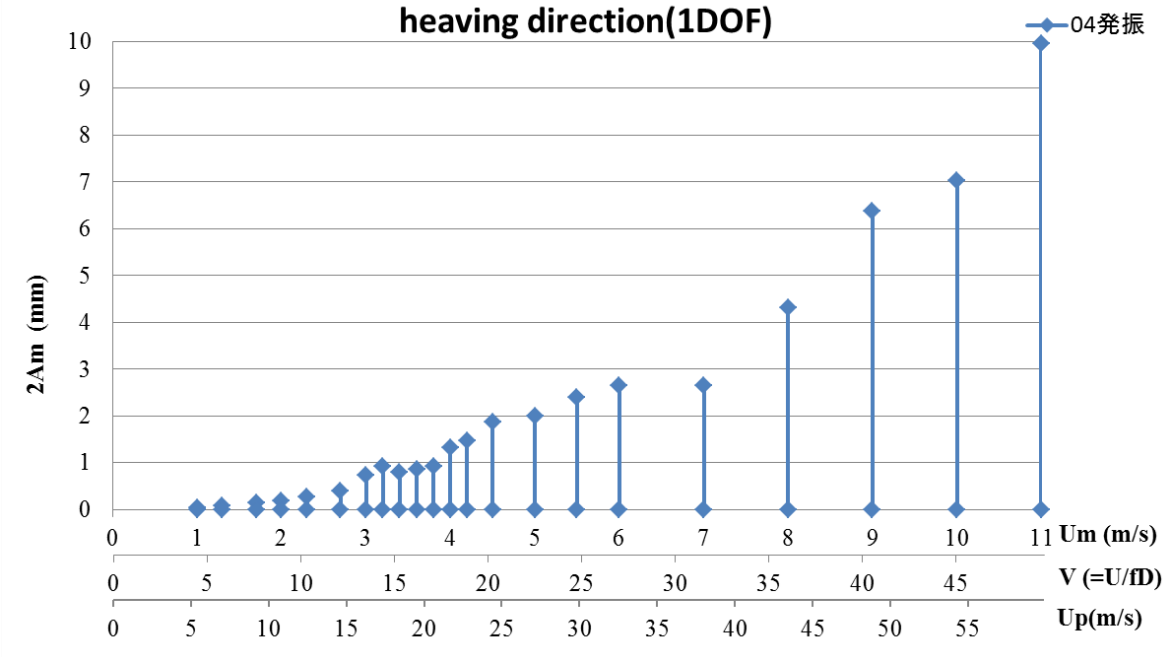

Fig. 6.2.6 Heaving response (UC1, incidence angle = -3 [deg], in turbulent flow)

(Stable response amplitude was measured after providing initial disturbance to the model.)

6.2.2 Under construction (UC2, Just before the last segment of the main girder in the main span is installed)

In the case of UC2, the free vibration test was conducted under 3 incidence angles of wind (0, +3, and -3 [deg]) in smooth and in turbulent flow, respectively. Displacements being allowed in the model was 2 DOF along heaving and torsional direction. An initial heaving or torsional disturbance was applied to the model separately at several wind speed conditions in the test. The response was recorded after the response amplitude became stable.

For all of the tests, neither VIV nor flutter was observed. The results are summarized in Table 2. The response of each case is shown in Fig 6.2.7-Fig. 6.2.12.

Table 6.2.2 Aerodynamic response of the main girder in UC2 (Heaving/torsional 2 DOF)

Flow condition	Vertical incidence angle of wind [deg]	Vortex-induced vibration	Flutter	Corresponding figure
Smooth	0	o	o	Fig.6.2.7
	+3	o	o	Fig.6.2.8
	-3	o	o	Fig.6.2.9
Turbulent	0	o	o	Fig.6.2.10
	+3	o	o	Fig.6.2.11
	-3	o	o	Fig.6.2.12

“o” : The corresponding response was not observed.

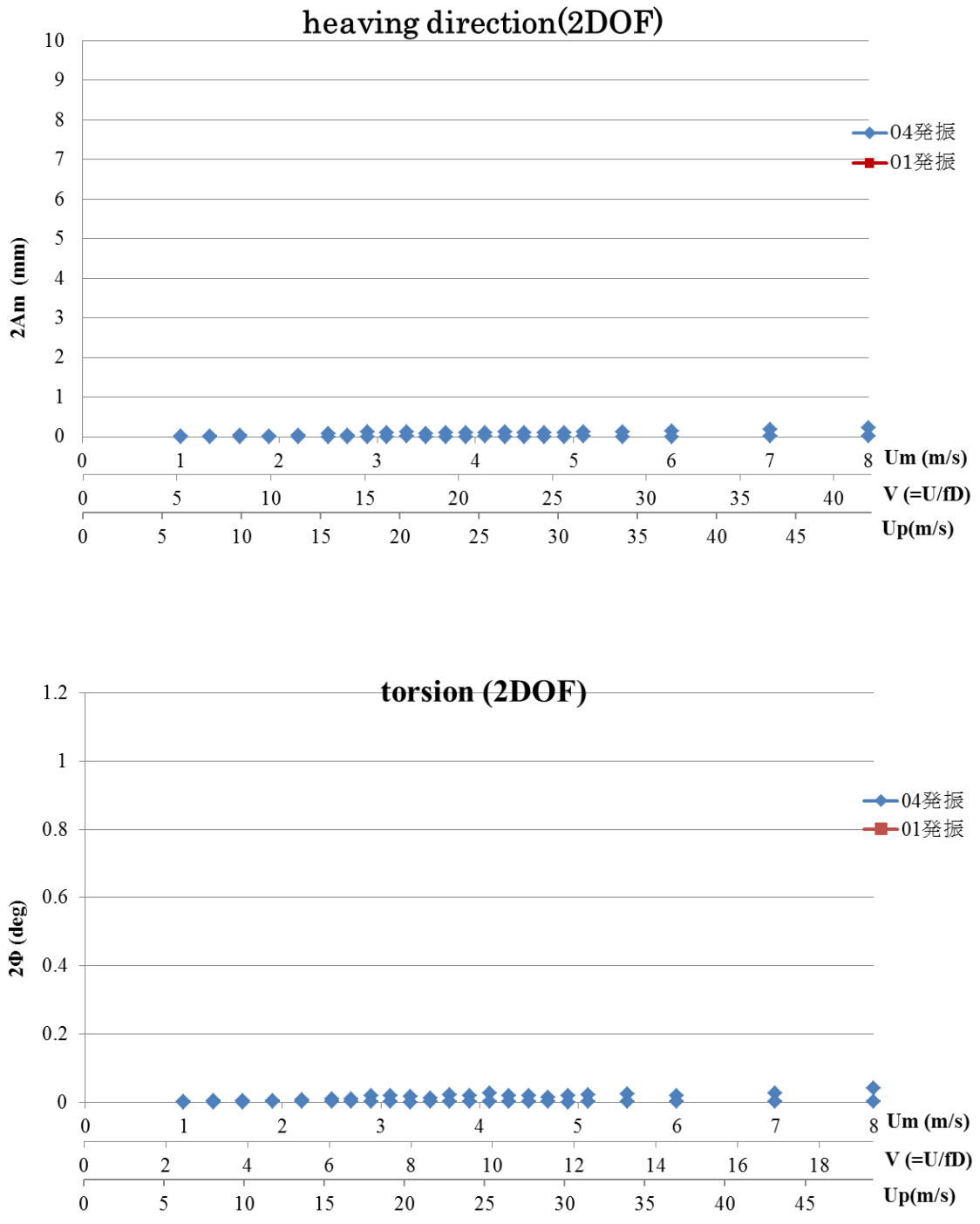

Fig 6.2.7 Heaving and torsional response (UC2, incidence angle = 0 [deg], in smooth flow)
(Stable response amplitude was measured after providing relevant initial disturbance to the model.)

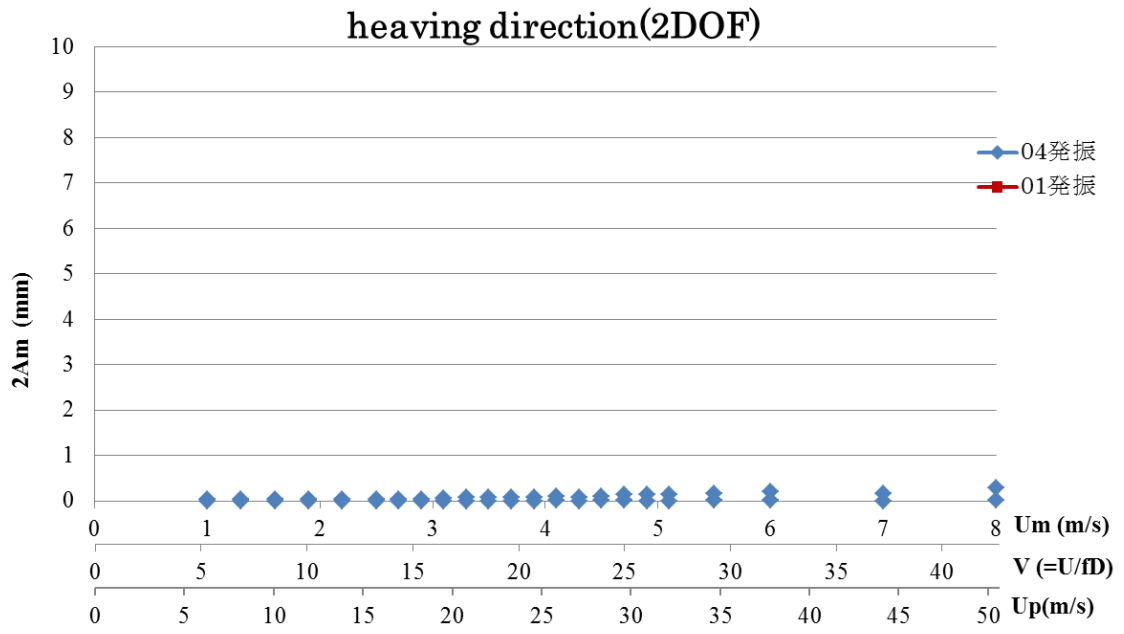

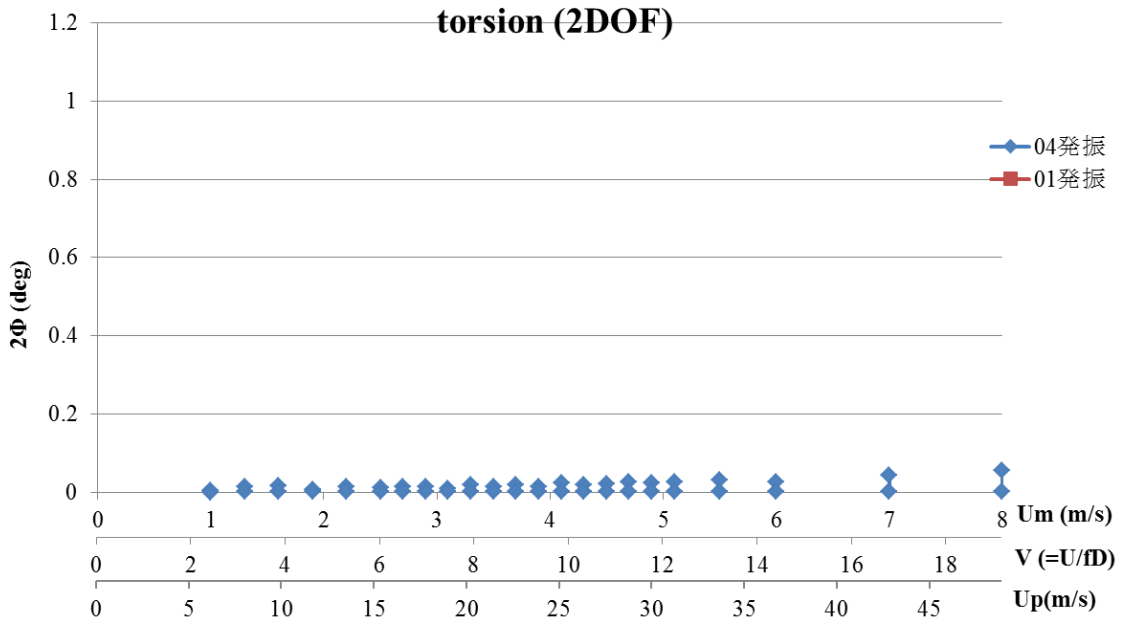

Fig. 6.2.8 Heaving and torsional response (UC2, incidence angle = +3 [deg], in smooth flow)
(Stable response amplitude was measured after providing relevant initial disturbance to the model.)

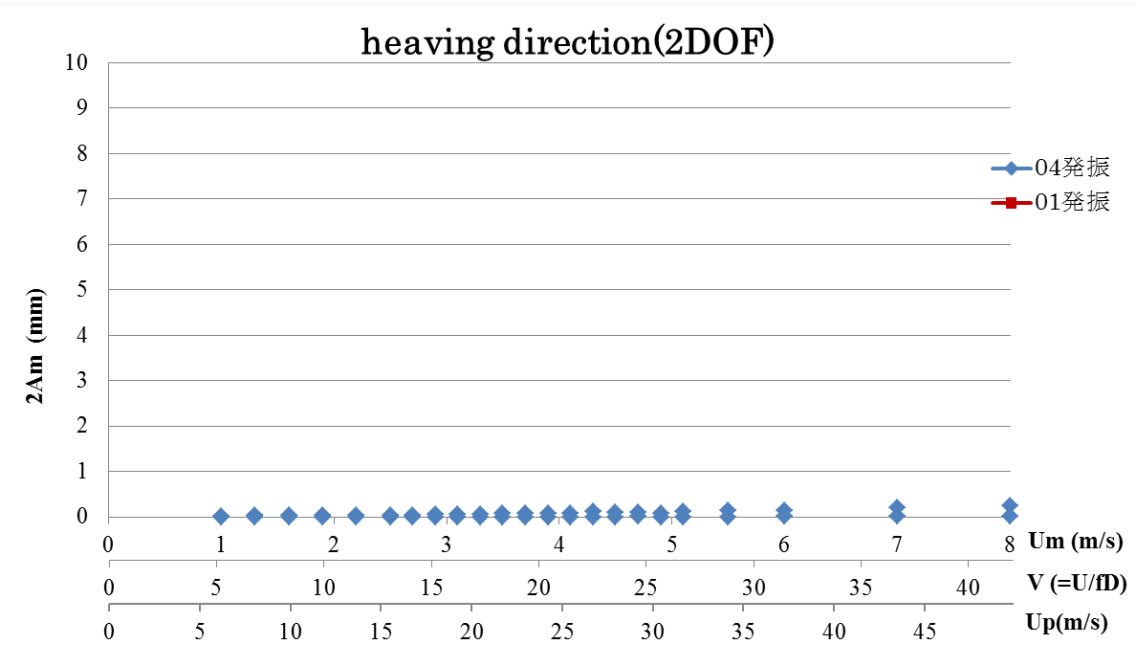

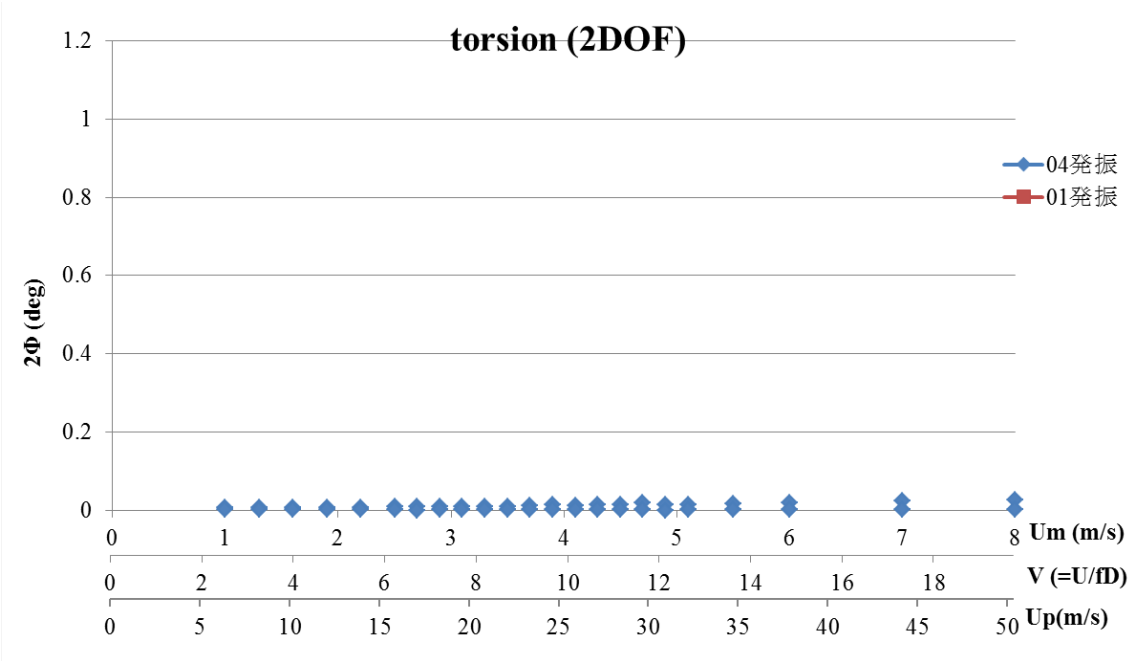

Fig. 6.2.9 Heaving and torsional response (UC2, incidence angle = -3 [deg], in smooth flow) (Stable response amplitude was measured after providing relevant initial disturbance to the model.)

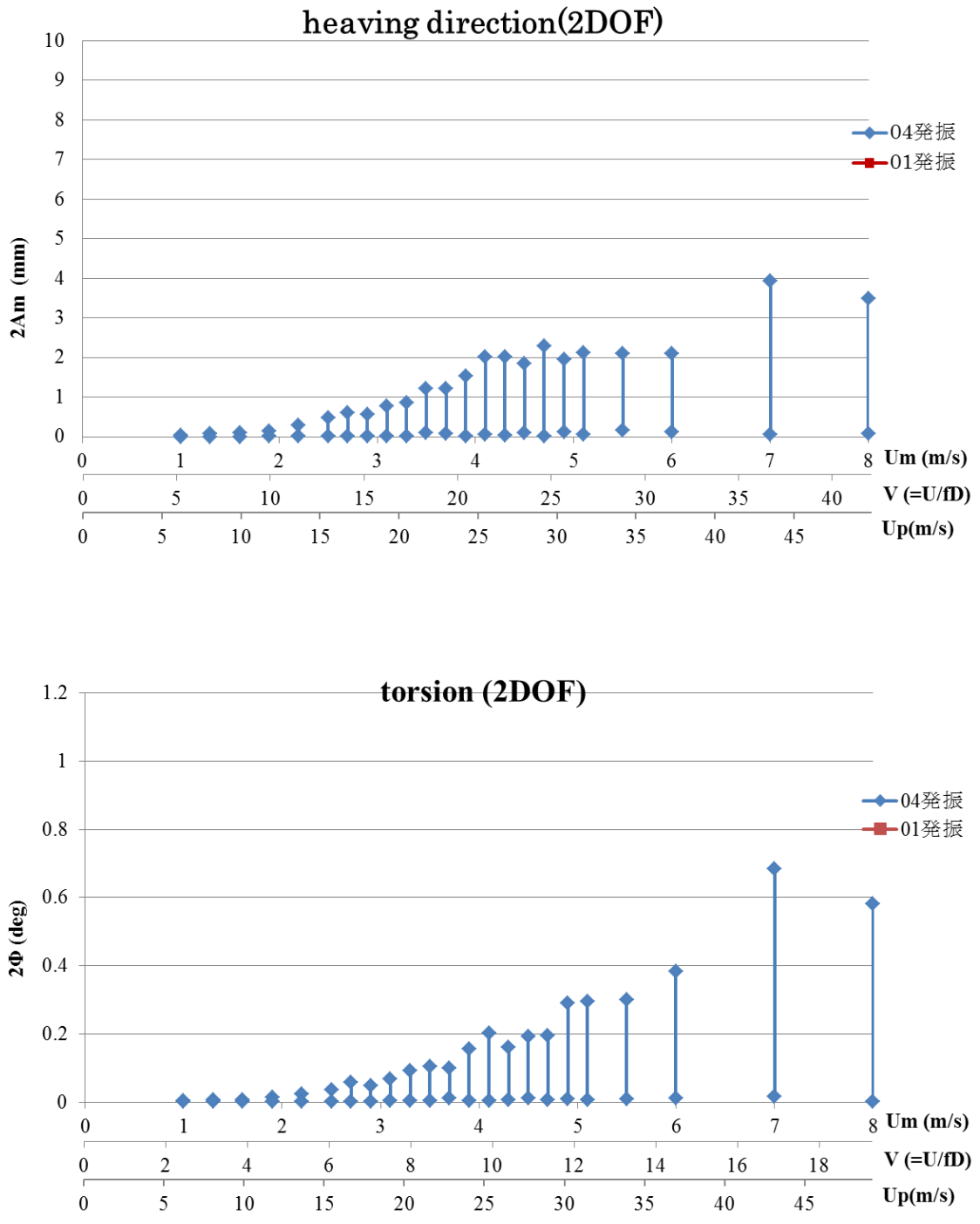

Fig. 6.2.10 Heaving and torsional response (UC2, incidence angle = 0 [deg], in turbulent flow) (Stable response amplitude was measured after providing relevant initial disturbance to the model.)

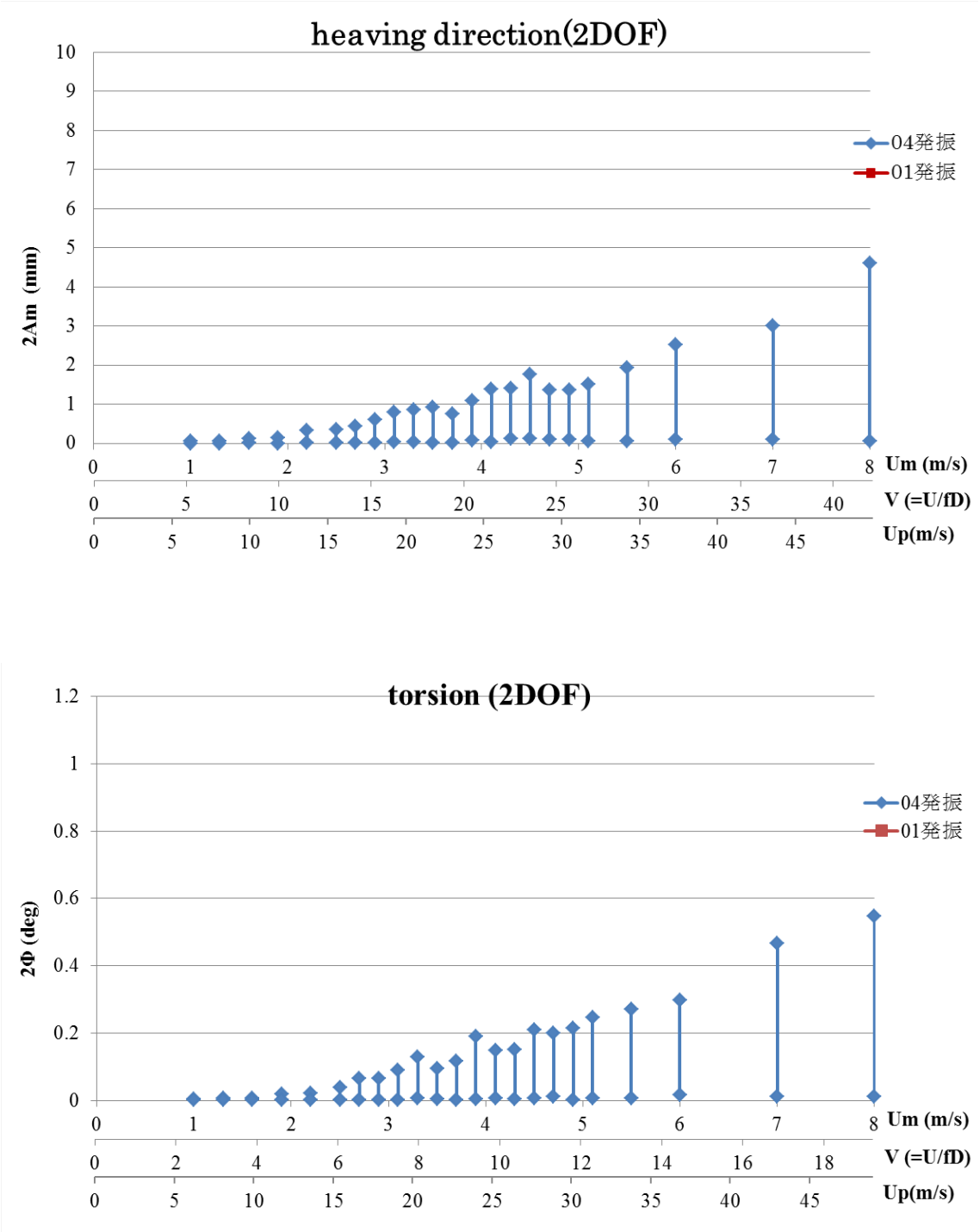

Fig. 6.2.11 Heaving and torsional response (UC2, incidence angle = +3 [deg], in turbulent flow) (Stable response amplitude was measured after providing relevant initial disturbance to the model.)

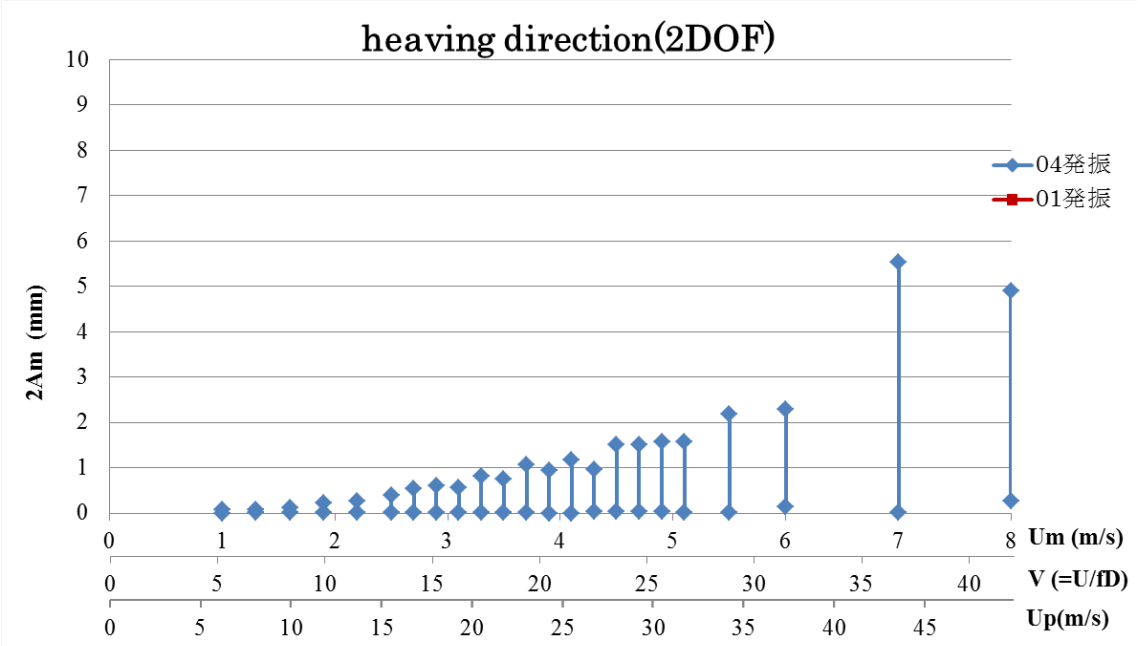

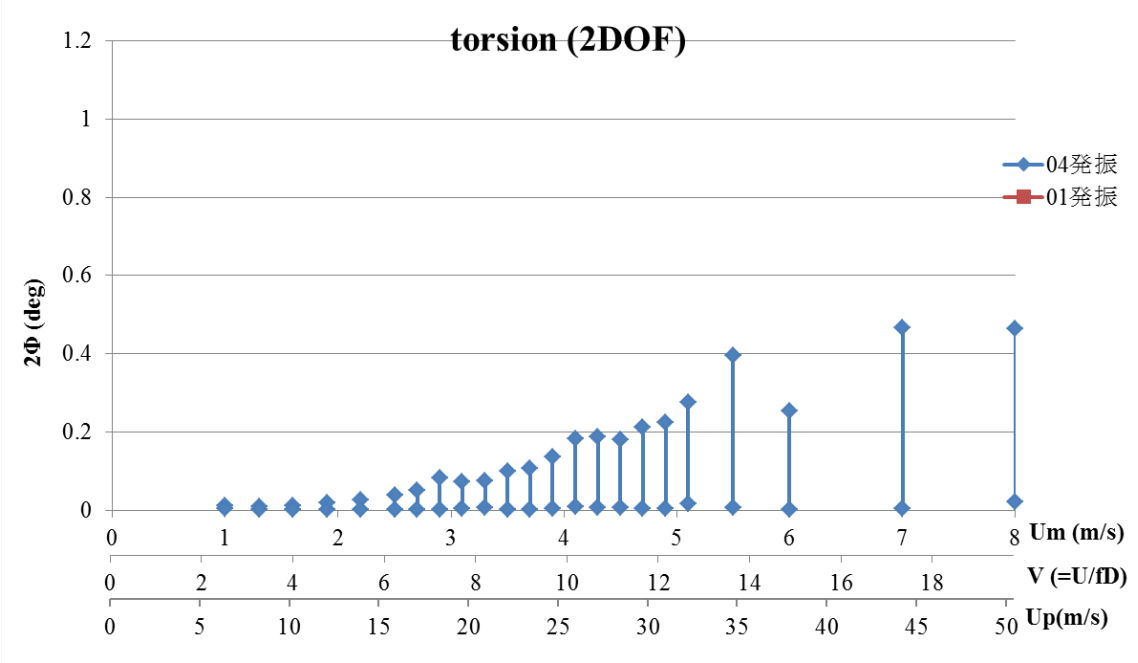

Fig. 6.2.12 Heaving and torsional response (UC2, incidence angle = -3 [deg], in turbulent flow) (Stable response amplitude was measured after providing relevant initial disturbance to the model.)

6.2.3 After completion (AC, Heaving and torsional 2 DOF)

In the case of AC, the free vibration test was conducted under 3 incidence angles of wind (0, +3, and -3 [deg]) in smooth and in turbulent flow, respectively. Displacement being allowed in the model was 2 DOF along heaving and torsional direction. An initial heaving or torsional disturbance was applied to the model separately at several wind speed conditions in the test. The response was recorded after the response amplitude became stable. The results are summarized in Table 6.2.3. The response of each case is shown in Fig 6.2.13-Fig. 6.2.18.

In smooth flow condition, the torsional VIV was observed for all of the three incidence angles (0, +3, and -3 [deg]), while no heaving VIV was observed. The prototype wind speed *Up* of torsional VIV was at around 21.6 [m/s] for the incidence angle of 0 [deg] (see Fig.), 15.4 - 17.9 [m/s] and 22.8 - 25.2 [m/s] (see Fig.) for +3 [deg], and 15.4 - 17.9 [m/s] and 20.3 - 24.0 [m/s] for -3 [deg] (see Fig.).

In turbulent flow, no VIV was observed for both heaving and torsional direction.

For all of the tests conducted in smooth flow and in turbulent flow, no flutter was observed.

Table 6.2.3 Aerodynamic response of the main girder in AC (Heaving/torsional 2 DOF)

Flow condition	Vertical incidence angle of wind [deg]	Vortex-induced vibration	Flutter	Corresponding figure
Smooth	0	× Torsional (at around 21.6 [m/s])	o	Fig.6.2.13
	+3	× Torsional (15.4 - 17.9 [m/s]) (22.8 - 25.2 [m/s])	o	Fig.6.2.14
	-3	× Torsional (15.4 - 17.9 [m/s]) (20.3 - 24.0 [m/s])	o	Fig.6.2.15
Turbulent	0	o	o	Fig.6.2.16
	+3	o	o	Fig.6.2.17
	-3	o	o	Fig.6.2.18

"o" : The corresponding response was not observed.

"×" : The corresponding response occurred.

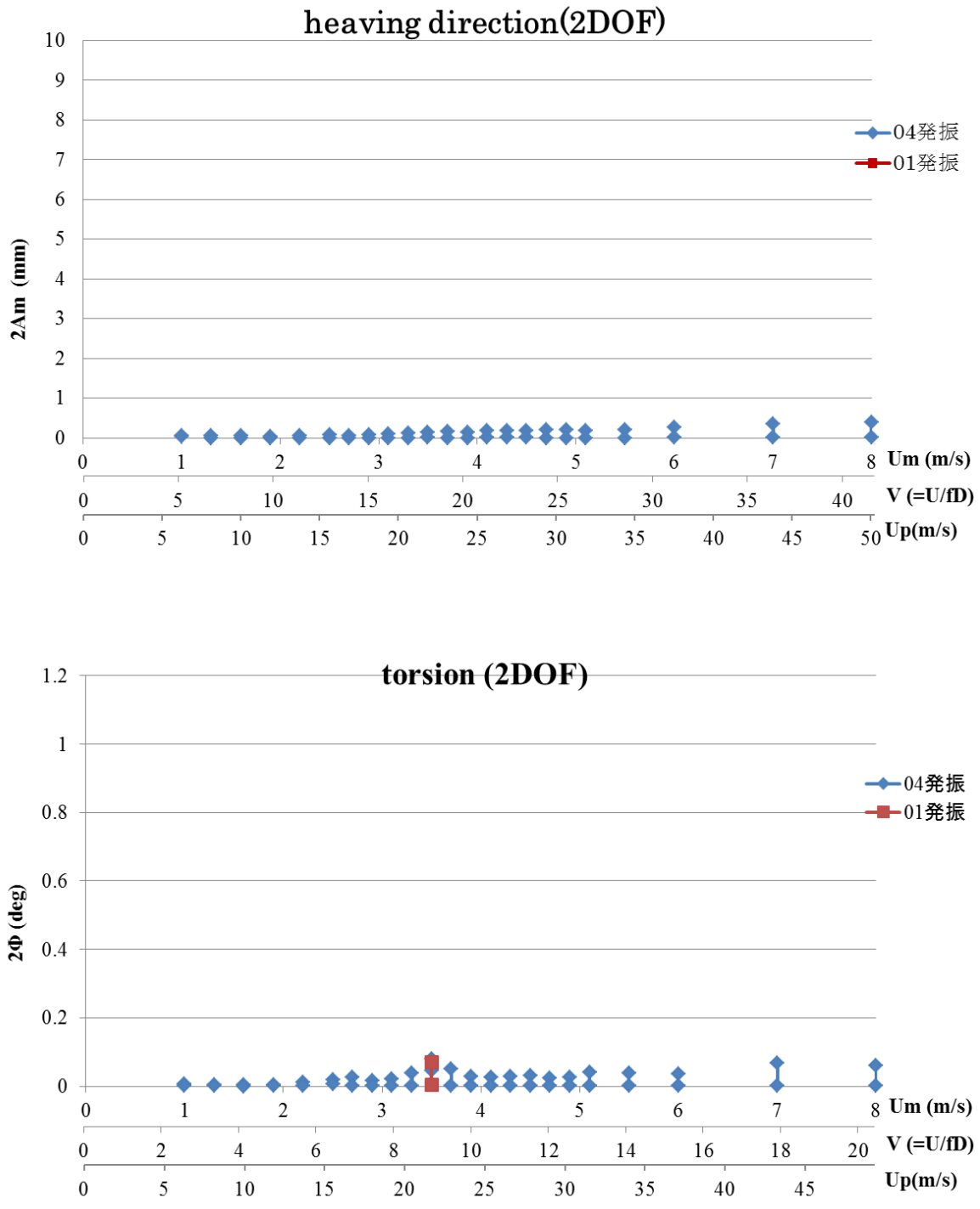

Fig. 6.4.13 Heaving and torsional response (AC, incidence angle = 0 [deg], in smooth flow)
(Stable response amplitude was measured after providing relevant initial disturbance to the model.)

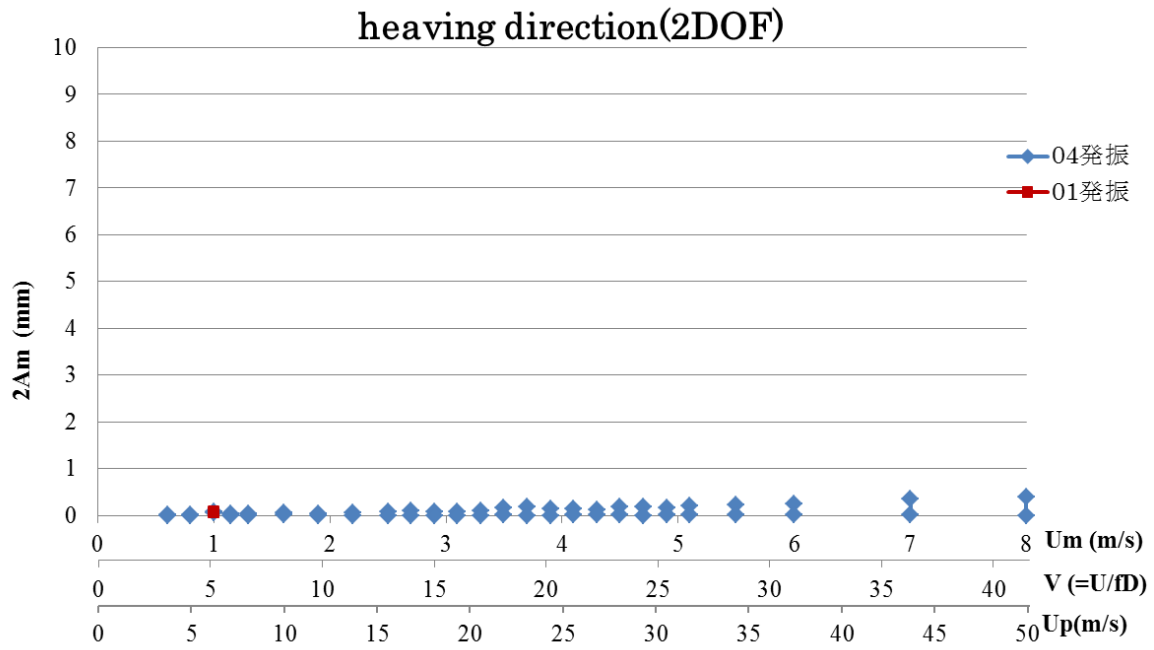

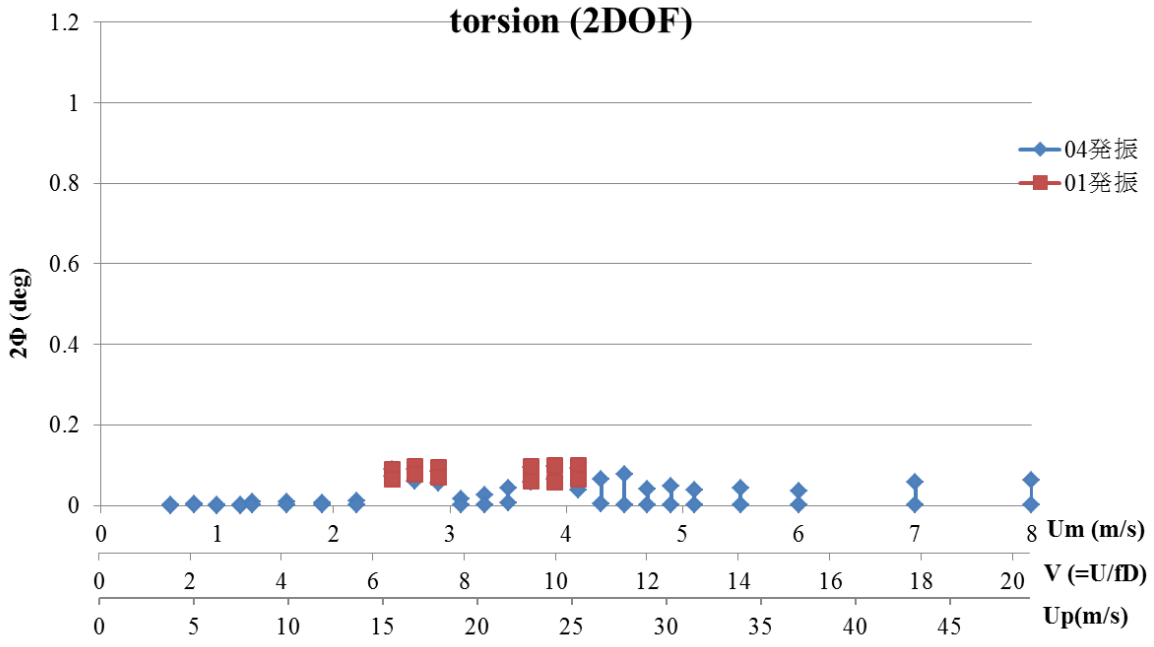

Fig. 6.4.14 Heaving and torsional response (AC, incidence angle = +3 [deg], in smooth flow)
(Stable response amplitude was measured after providing relevant initial disturbance to the model.)

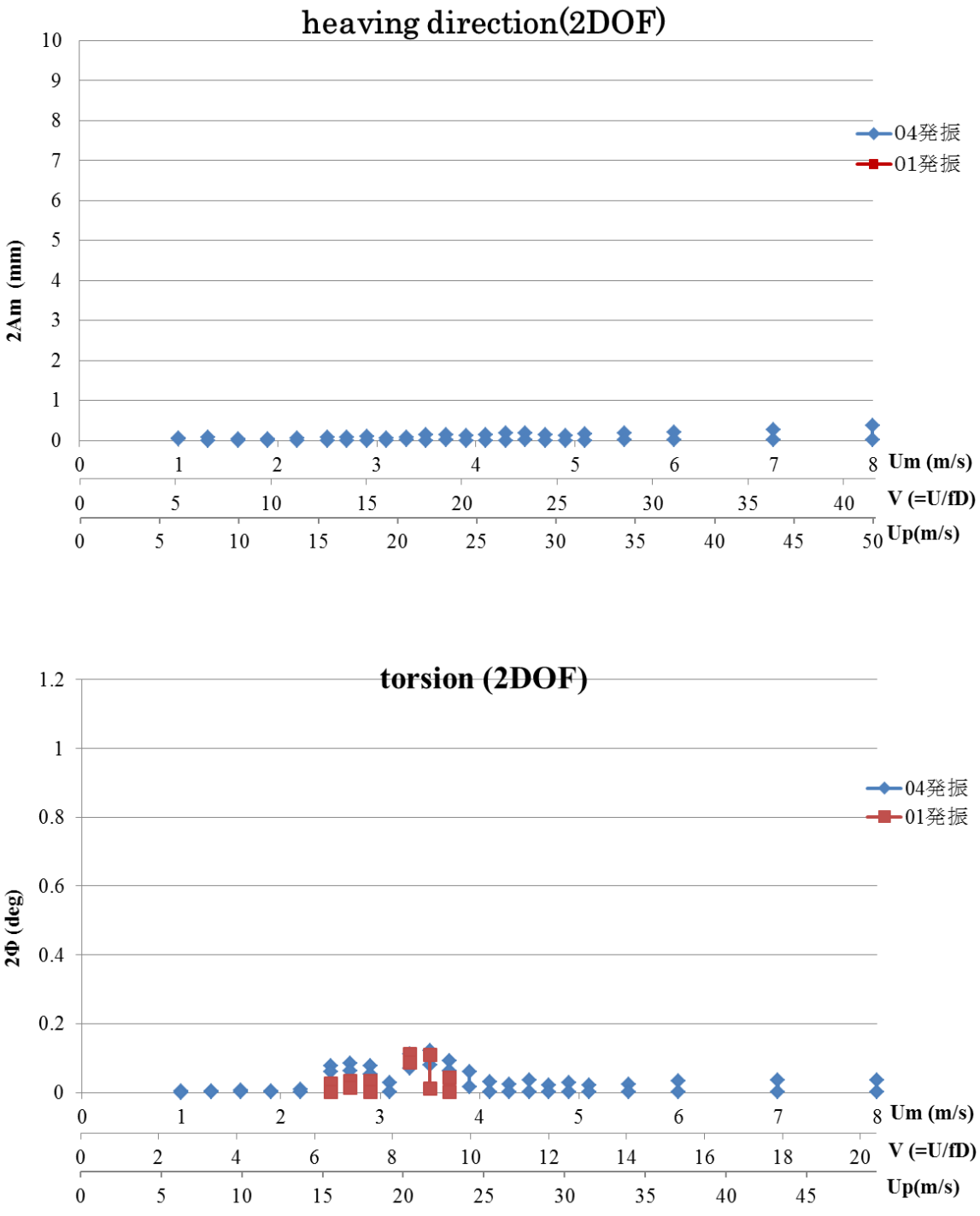

Fig. 6.4.15 Heaving and torsional response (AC, incidence angle = -3 [deg], in smooth flow) (Stable response amplitude was measured after providing relevant initial disturbance to the model.)

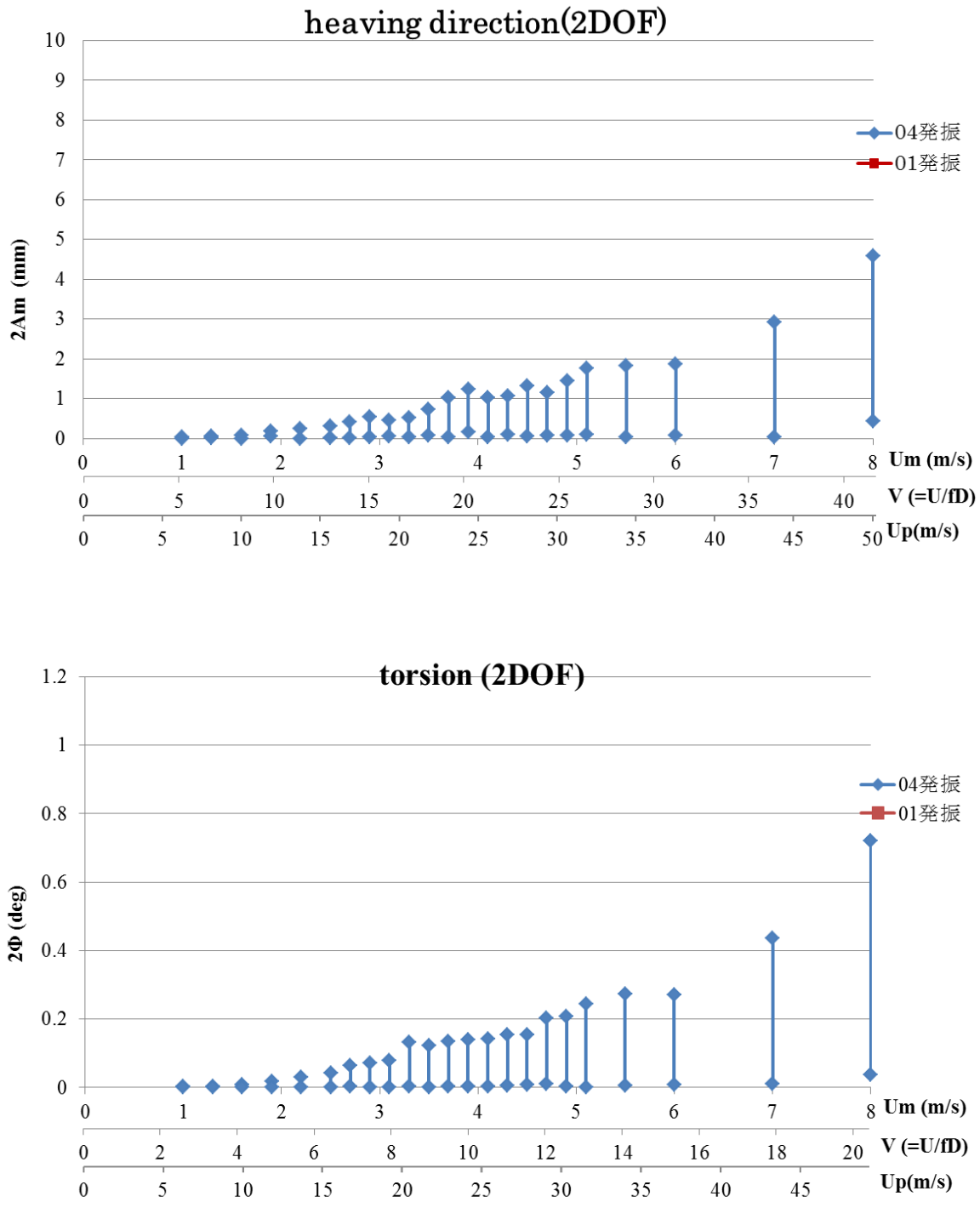

Fig. 6.4.16 Heaving and torsional response (AC, incidence angle = 0 [deg], in turbulent flow) (Stable response amplitude was measured after providing relevant initial disturbance to the model.)

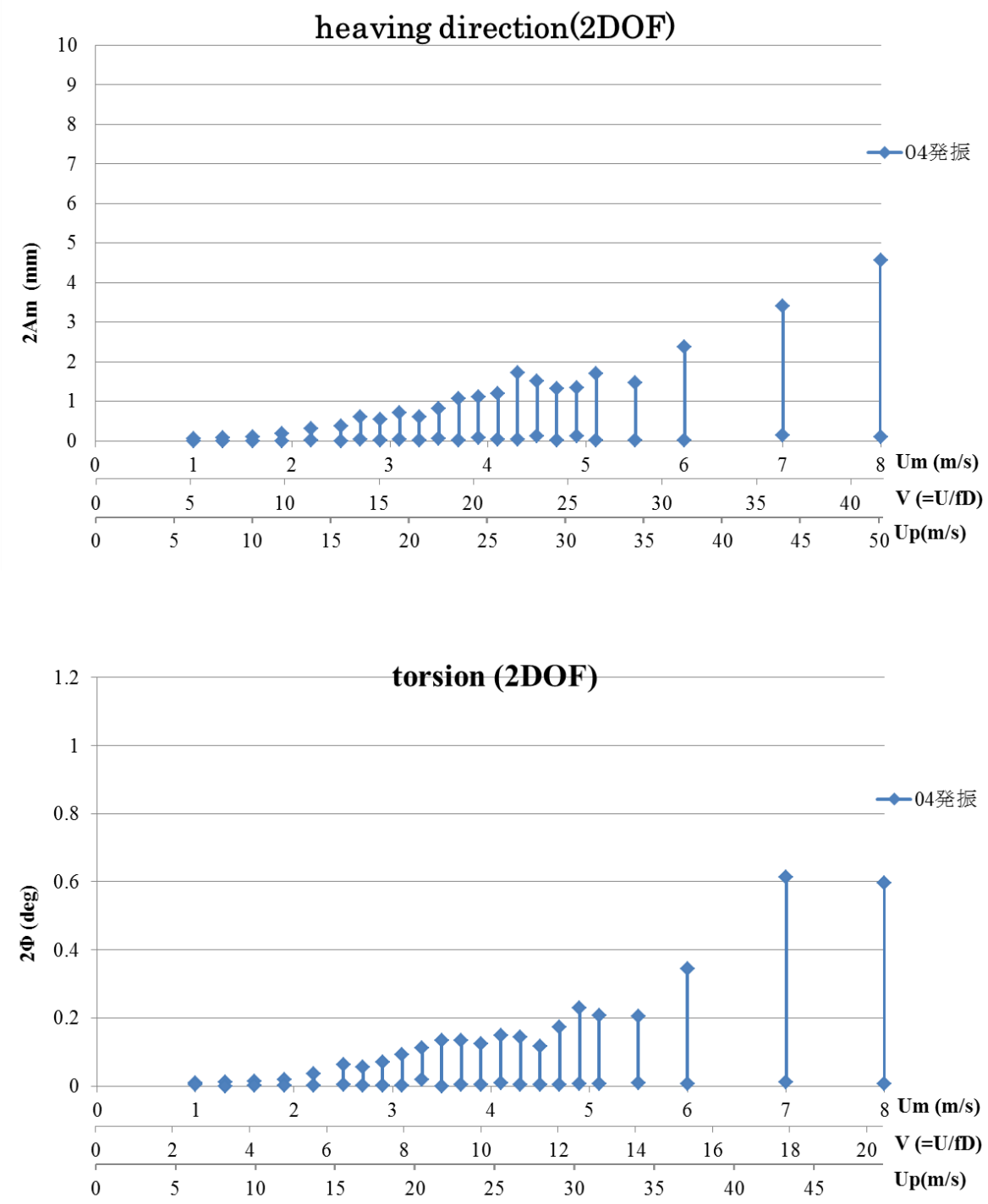

Fig. 6.4.17 Heaving and torsional response (AC, incidence angle = +3 [deg], in turbulent flow) (Stable response amplitude was measured after providing relevant initial disturbance to the model.)

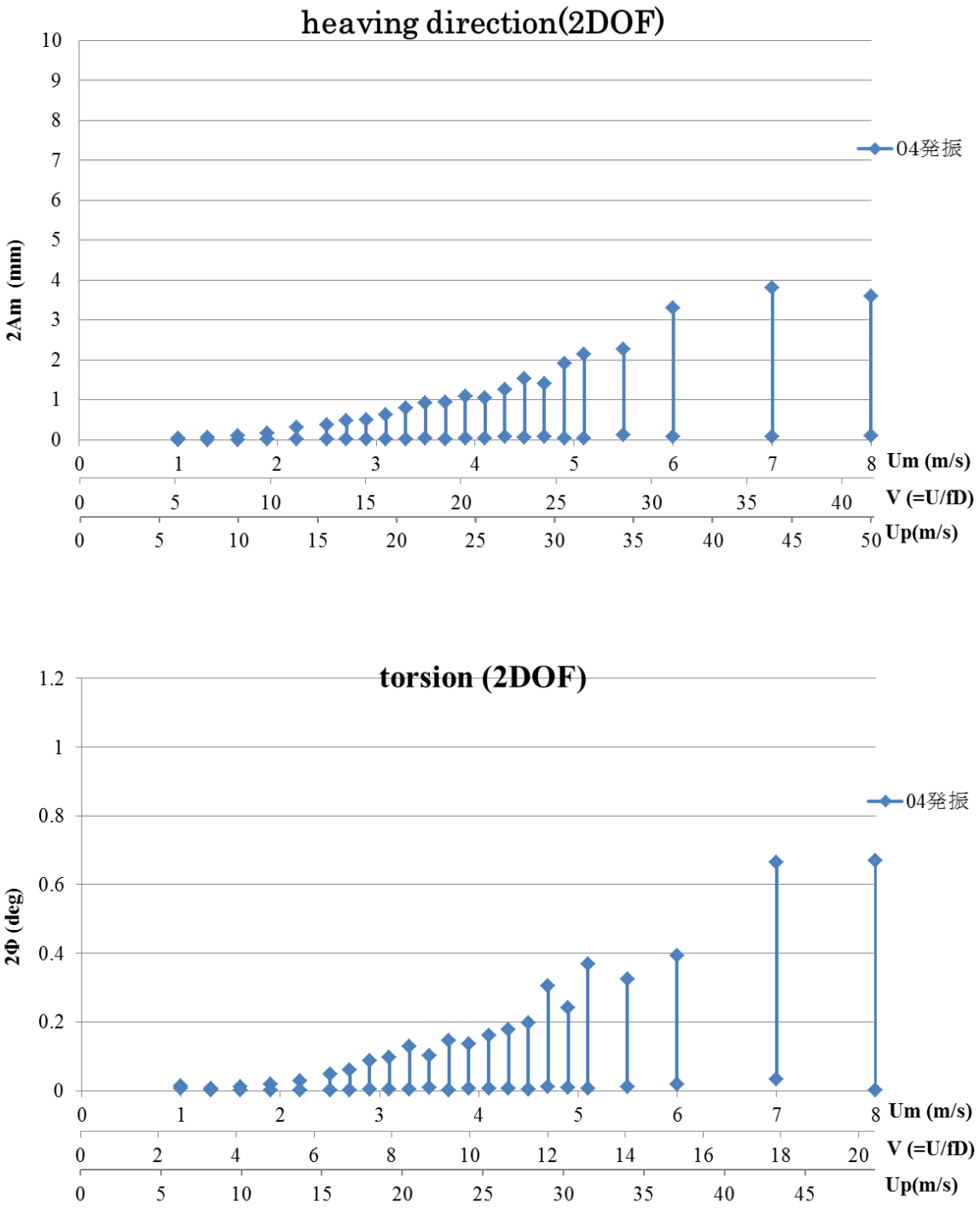

Fig. 6.4.18 Heaving and torsional response (AC, incidence angle = -3 [deg], in turbulent flow) (Stable response amplitude was measured after providing relevant initial disturbance to the model.)

6.3. Aerodynamic response of elastic tower model (scale ratio 1/120)

Aerodynamic response of the tower was tested in wind tunnel using fully elastic tower model of 1/120 scale ratio.

The target stage for wind tunnel test was chosen to be the same as those for the main girder test:

For the under construction stage, the following 2 stages were focused:

- Before the lowest cable being installed and just after the first segment of the main girder was installed. (Heaving 1 DOF, This condition was abbreviated as UC1, hereafter.)
- Just before the last segment of the main girder in the main span is installed. (Heaving and torsional 2 DOF, UC2)

For after completion stage, the following modes combination was set to the model:

- (Heaving and torsional 2 DOF, AC)

In the following tables, the wind direction along cable plane (i.e. along bridge axis) is denoted as x-direction, while the wind direction normal to cable plane is denoted as y-direction. In addition, yawing angle 0º refers to the angle when the wind is along the bridge axis, and 90º refers to the angle when the wind blows along the lateral direction of the bridge. For the cases of 'Under construction 1 (UC1)', the yawing angle 0º and 180º is defined as shown in Fig. 6.3.1 (a) and (b), respectively.

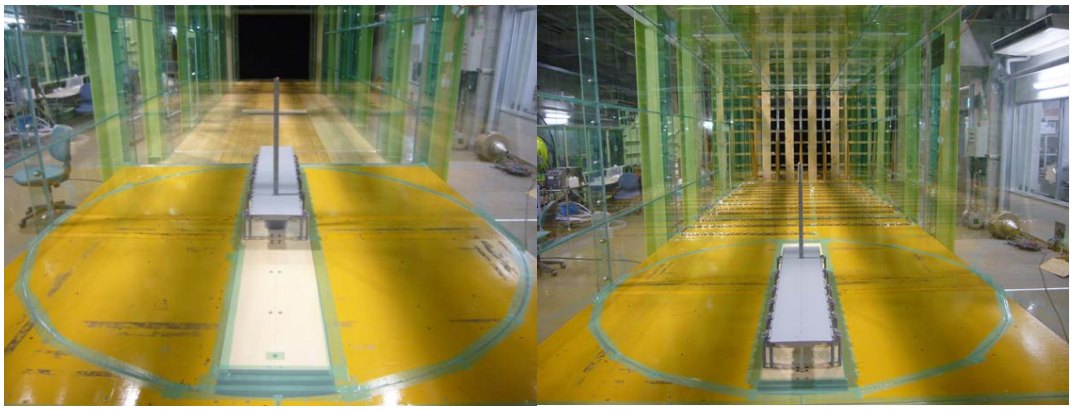

(a) Yawing angle 0º (b) Yawing angle 180º

Fig. 6.3.1 Definition of yawing angle for cases of under construction 1 (UC1)
(Wind comes from the back to the model side.)

6.3.1 Under construction 1 (UC1, Before the lowest cable being installed) (Original tower configuration)

During the under construction stage of UC1, the tower stands alone without any cables. In this situation, the aerodynamic sensitivity of the tower will be higher than those in the other 2 stages.

In the condition of smooth flow, y-direction (normal to cable plane) VIV was observed for yawing angle 0º and 5º (wind comes along bridge axis), while x-direction (along cable plane) VIV was observed for yawing angles 80º, 85º and 90º (wind comes normal to bridge axis). The y-direction galloping occurred for yawing angle 5º, while the x-direction galloping was observed for yawing angles 80º and 90º. The results are summarized in Table 6.3.1. The response of each case is shown in Fig 6.3.2-Fig. 6.3.9

Table 6.3.1 Under construction 1 (UC1, Original tower configuration (without aerodynamic device))

Flow condition	Yawing angle [deg]	Vortex-induced vibration	Galloping	Corresponding figure
Smooth	0	× in y-direction (16.5m/s~18.6m/s)	o	Fig.6.3.2
	5	× in y-direction (16.5m/s~18.6m/s)	× in y-direction (60.0m/s~)	Fig.6.3.3
	22.5	o	o	Fig.6.3.4
	45	o	o	Fig.6.3.5
	67.5	o	o	Fig.6.3.6
	80	× in x-direction (14.2m/s~22.3m/s)	× in x-direction (58.7m/s~)	Fig.6.3.7
	85	× in x-direction (14.2m/s~20.3m/s)	o	Fig.6.3.8
	90	× in x-direction (16.2m/s~22.3m/s)	× in x-direction (43.6m/s~)	Fig.6.3.9

“o” : The corresponding response was not observed.

“×” : The corresponding response occurred.

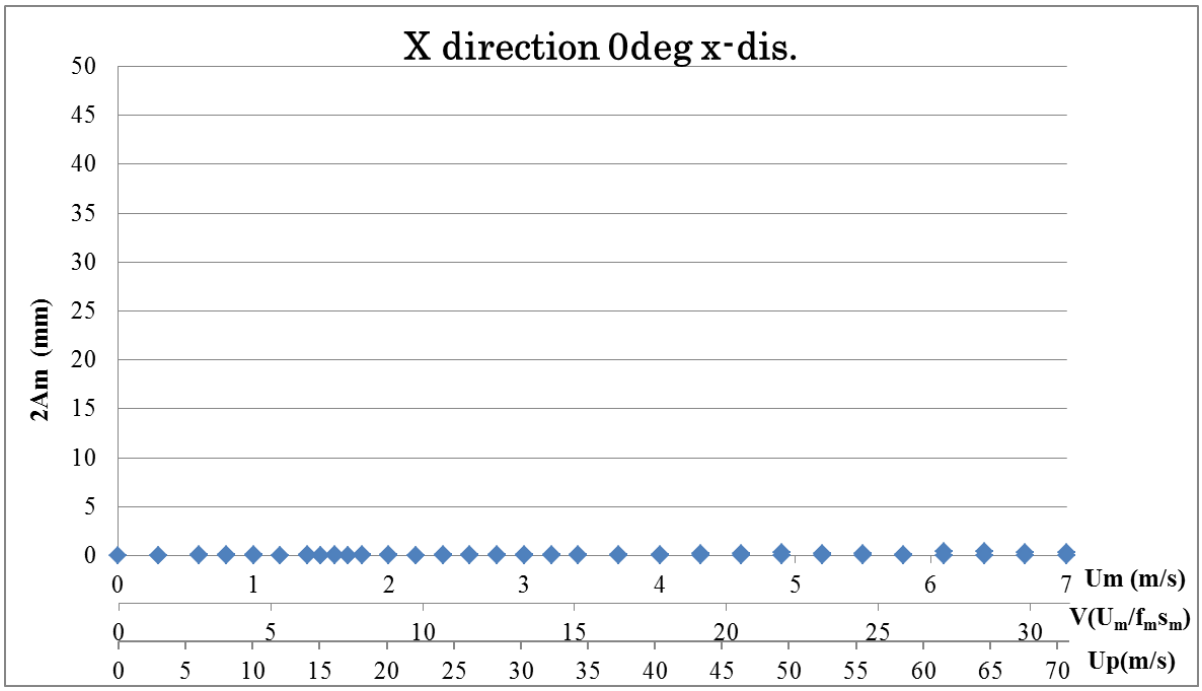

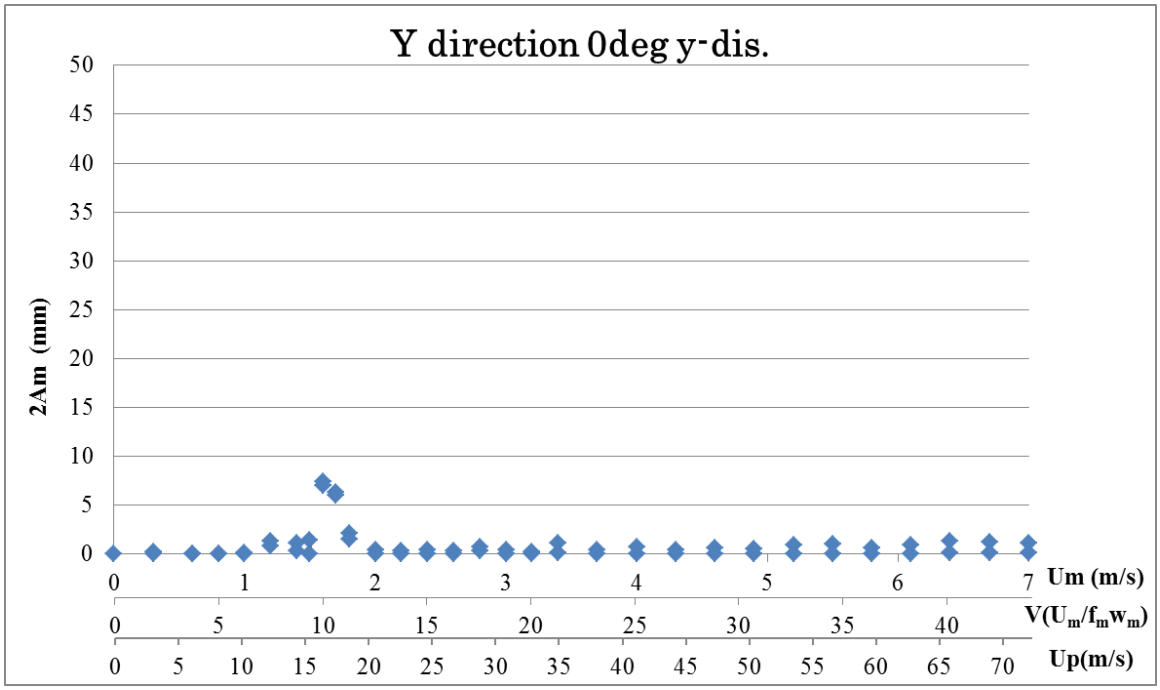

Fig. 6.3.2 Vibration response along (x-direction) and normal to cable plane (y-direction) (UC1, Original tower configuration (without aerodynamic device), Wind direction = 0 [deg.] (along bridge axis), in smooth flow) (Stable response amplitude was measured after providing relevant initial disturbance to the model.)

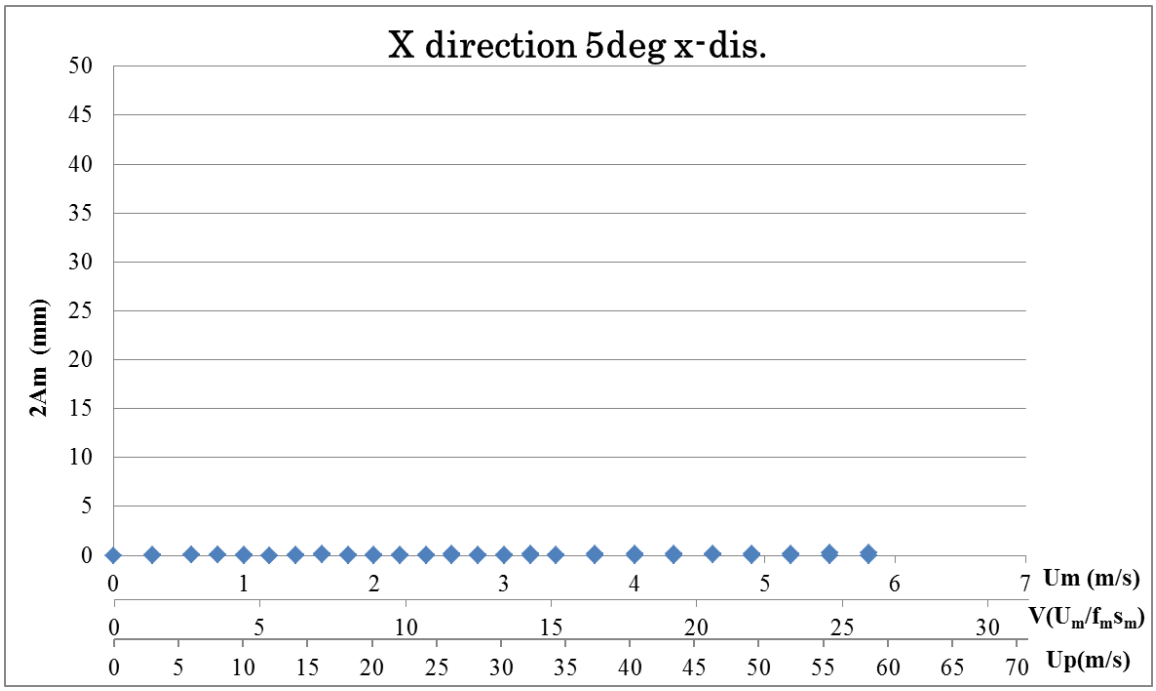

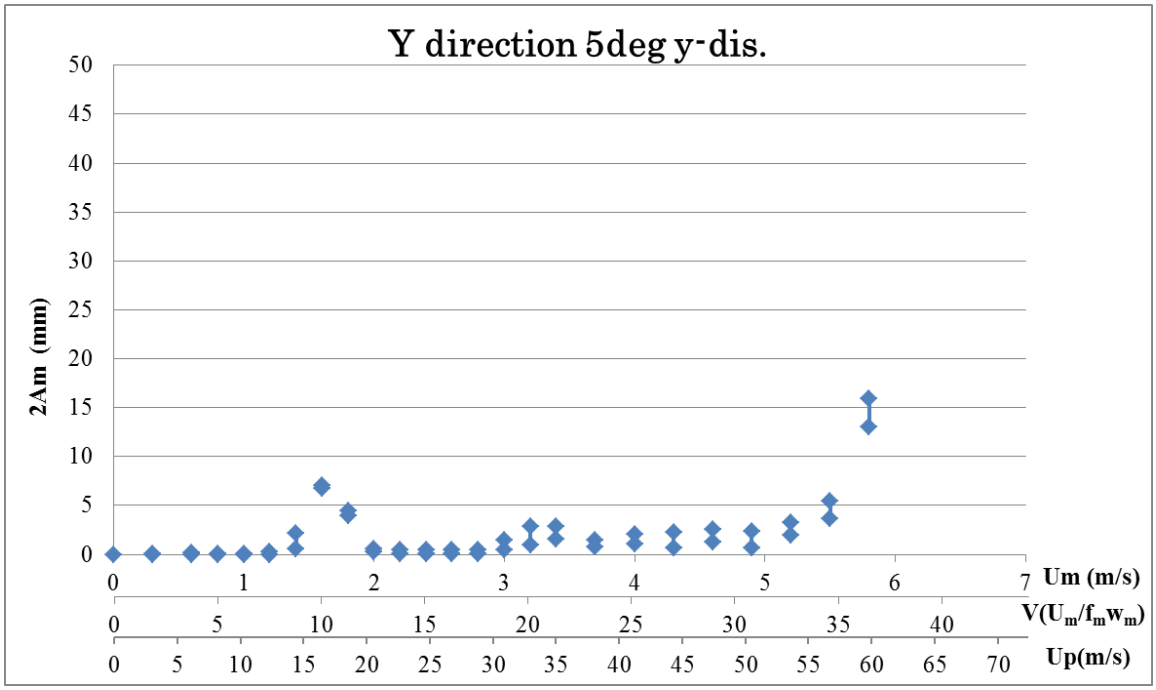

Fig. 6.3.3 Vibration response along (x-direction) and normal to cable plane (y-direction) (UC1, Original tower configuration (without aerodynamic device), Wind direction = 5 [deg.], in smooth flow) (Stable response amplitude was measured after providing relevant initial disturbance to the model.)

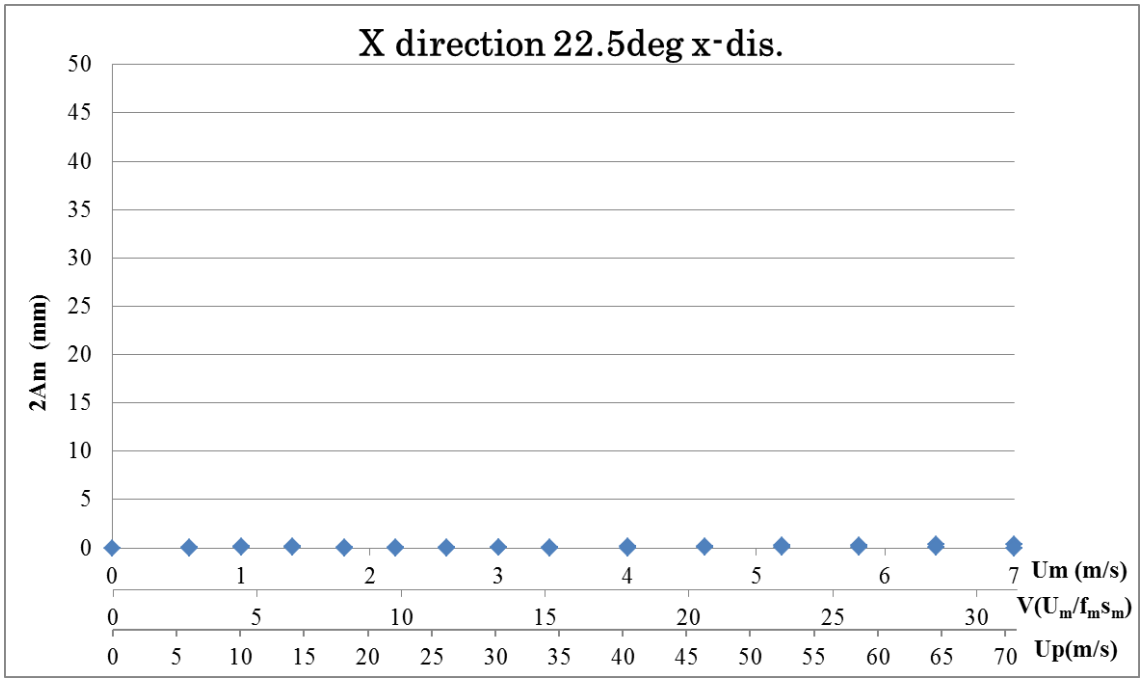

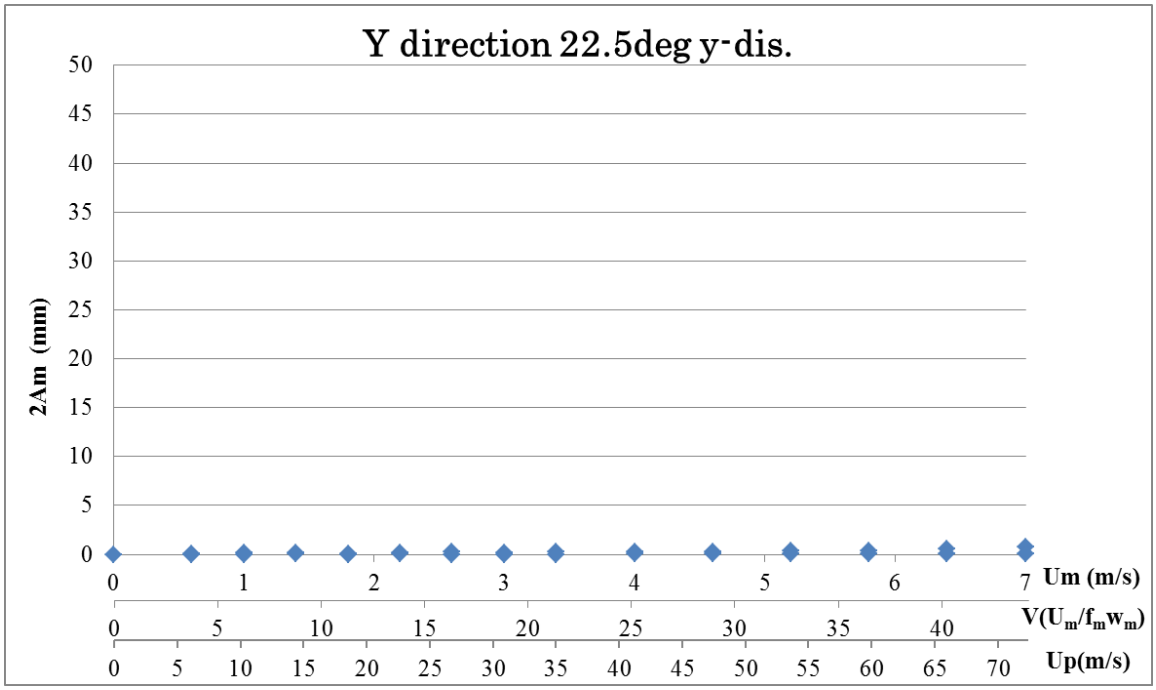

Fig. 6.3.4 Vibration response along (x-direction) and normal to cable plane (y-direction) (UC1, Original tower configuration (without aerodynamic device), Wind direction = 22.5 [deg.], in smooth flow) (Stable response amplitude was measured after providing relevant initial disturbance to the model.)

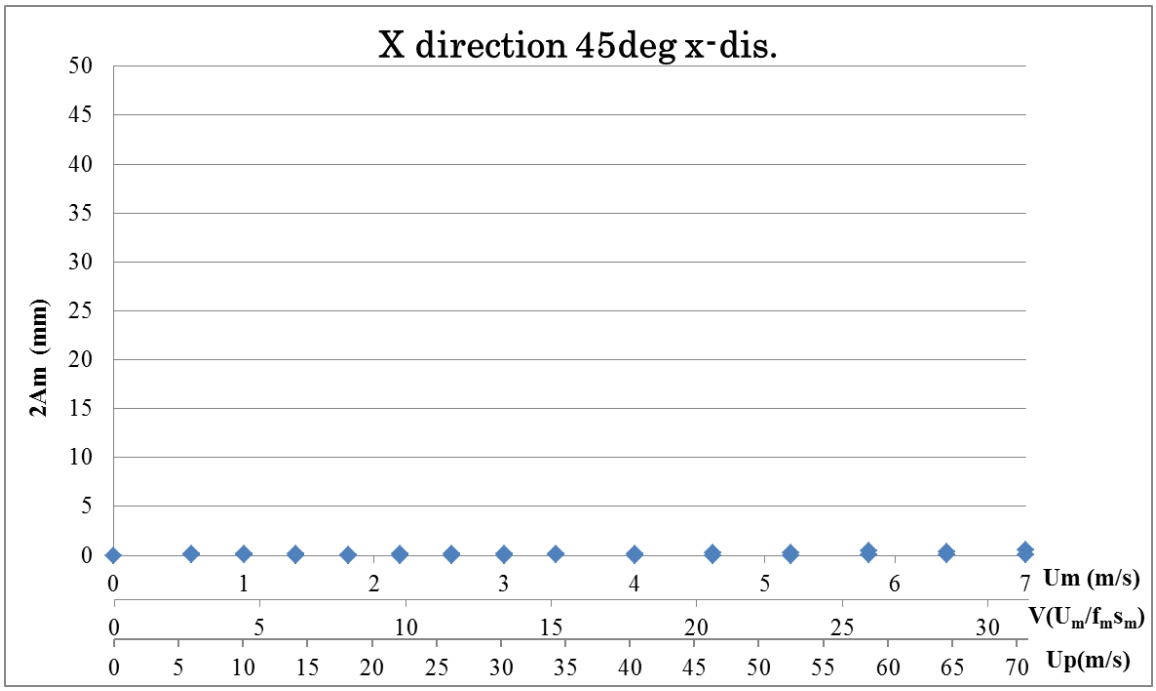

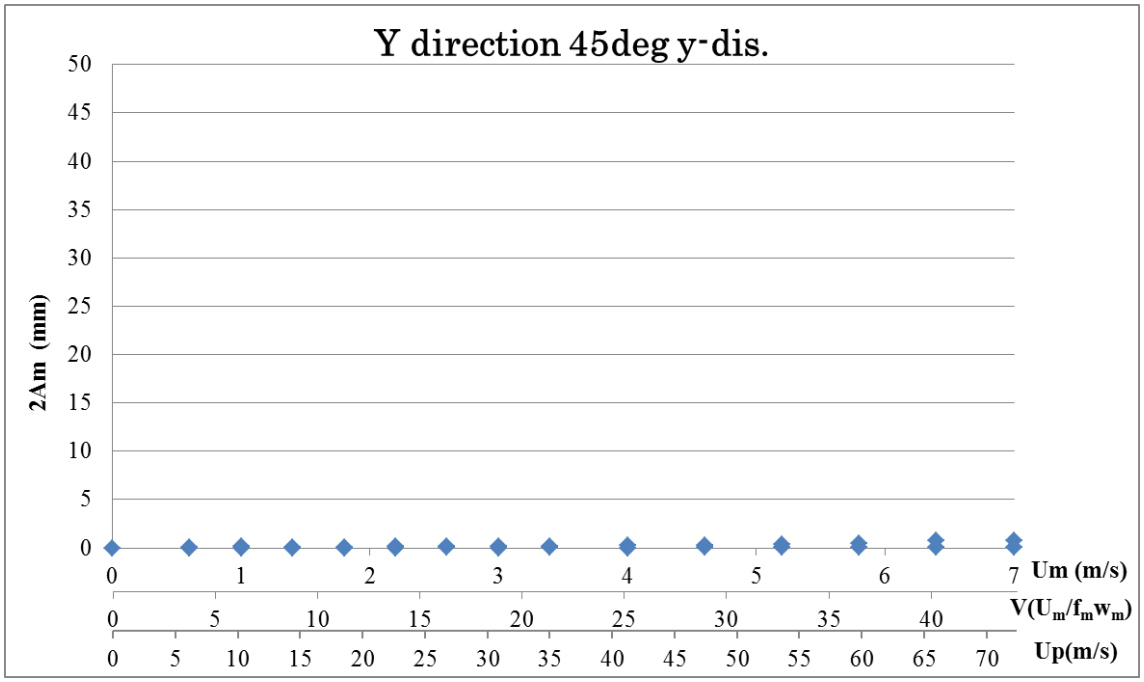

Fig. 6.3.5 Vibration response along (x-direction) and normal to cable plane (y-direction) (UC1, Original tower configuration (without aerodynamic device), Wind direction = 45 [deg.], in smooth flow) (Stable response amplitude was measured after providing relevant initial disturbance to the model.)

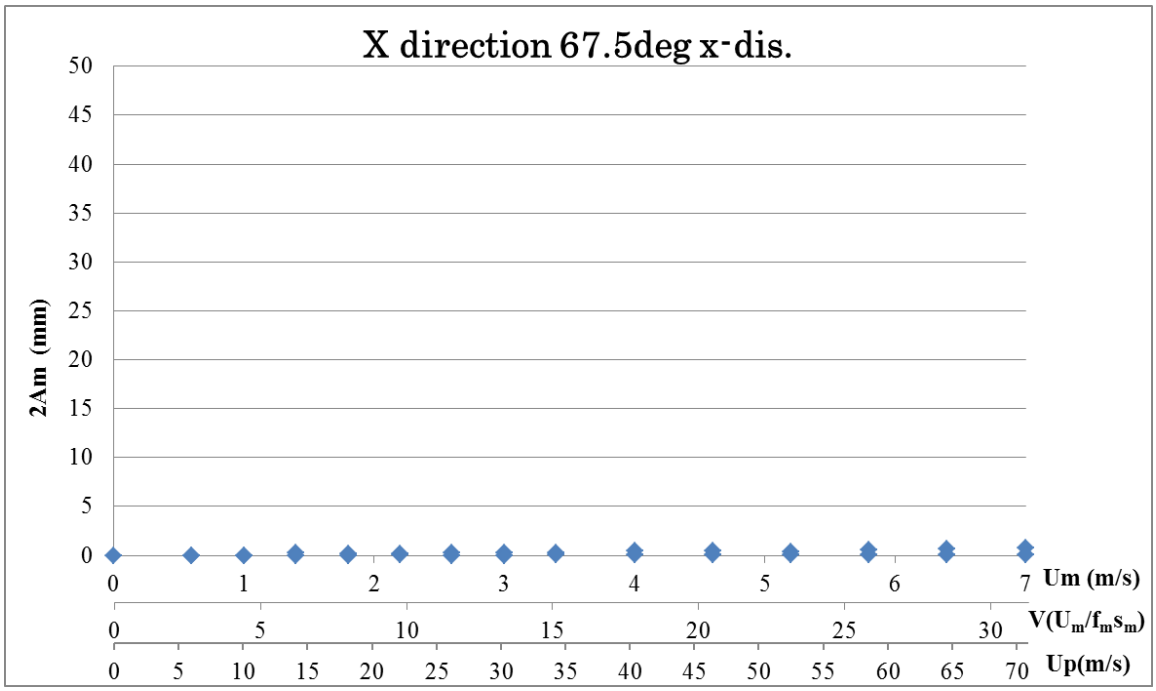

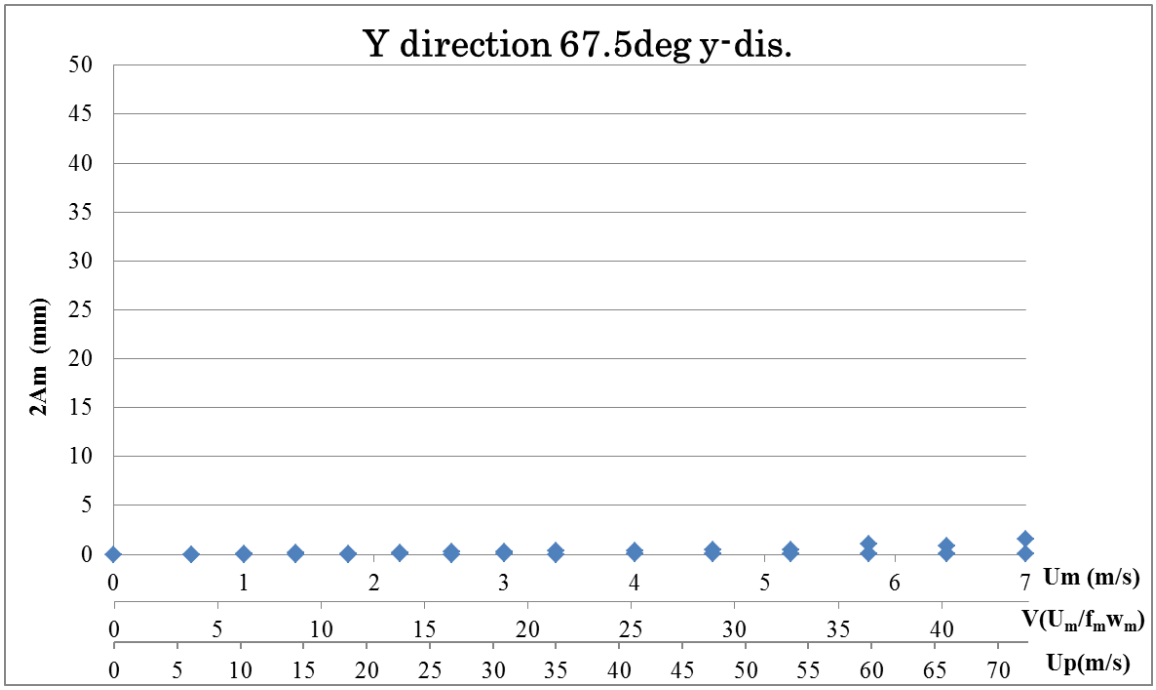

Fig. 6.3.6 Vibration response along (x-direction) and normal to cable plane (y-direction) (UC1, Original tower configuration (without aerodynamic device), Wind direction = 67.5 [deg.], in smooth flow) (Stable response amplitude was measured after providing relevant initial disturbance to the model.)

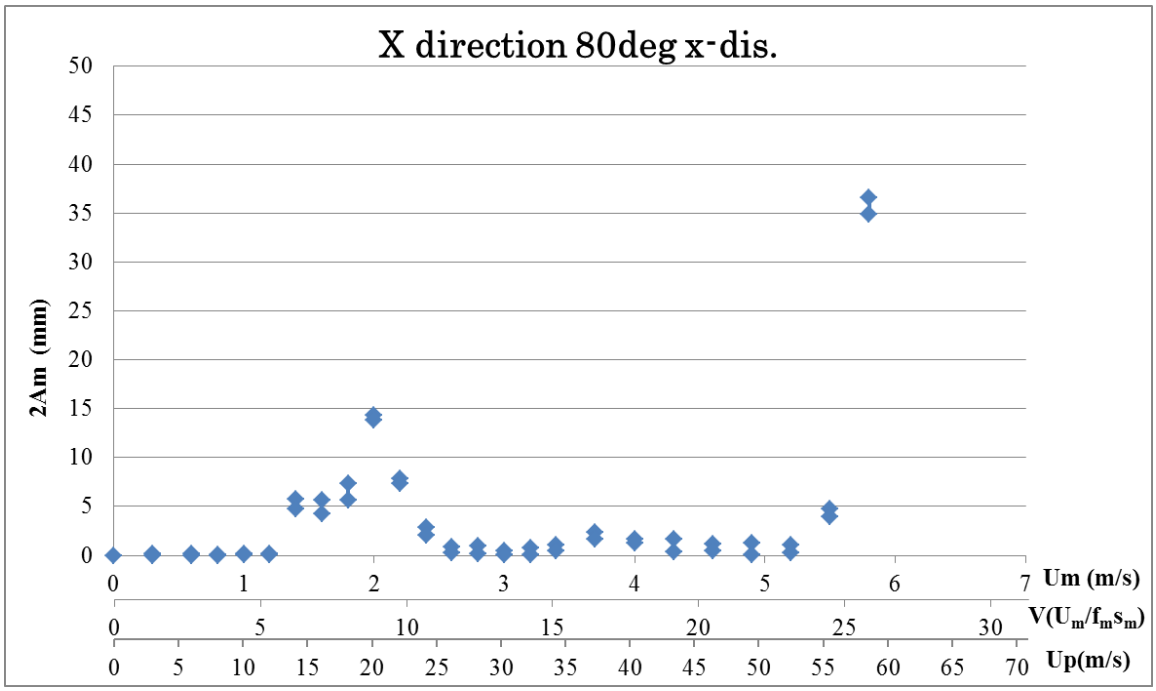

Fig. 6.3.7 Vibration response along cable plane (x-direction)
(UC1, Original tower configuration (without aerodynamic device), Wind direction = 80 [deg.], in smooth flow) (Stable response amplitude was measured after providing relevant initial disturbance to the model.)

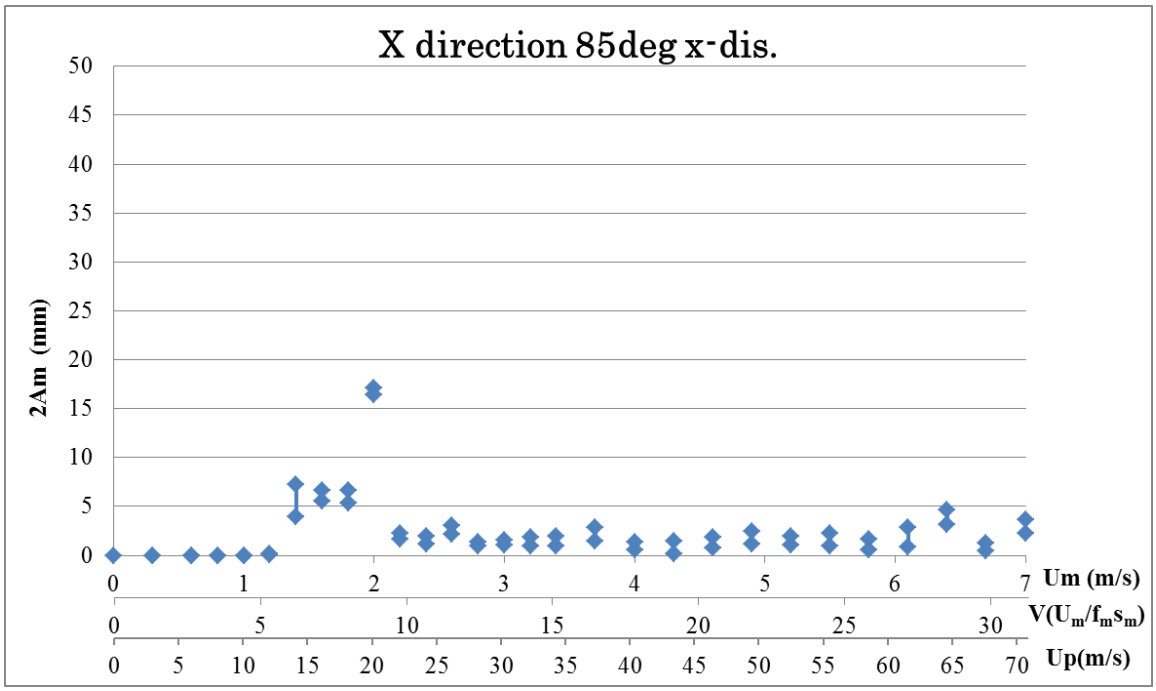

Fig. 6.3.8 Vibration response along cable plane (x-direction)

(UC1, Original tower configuration (without aerodynamic device), Wind direction = 85 [deg.], in smooth flow) (Stable response amplitude was measured after providing relevant initial disturbance to the model.)

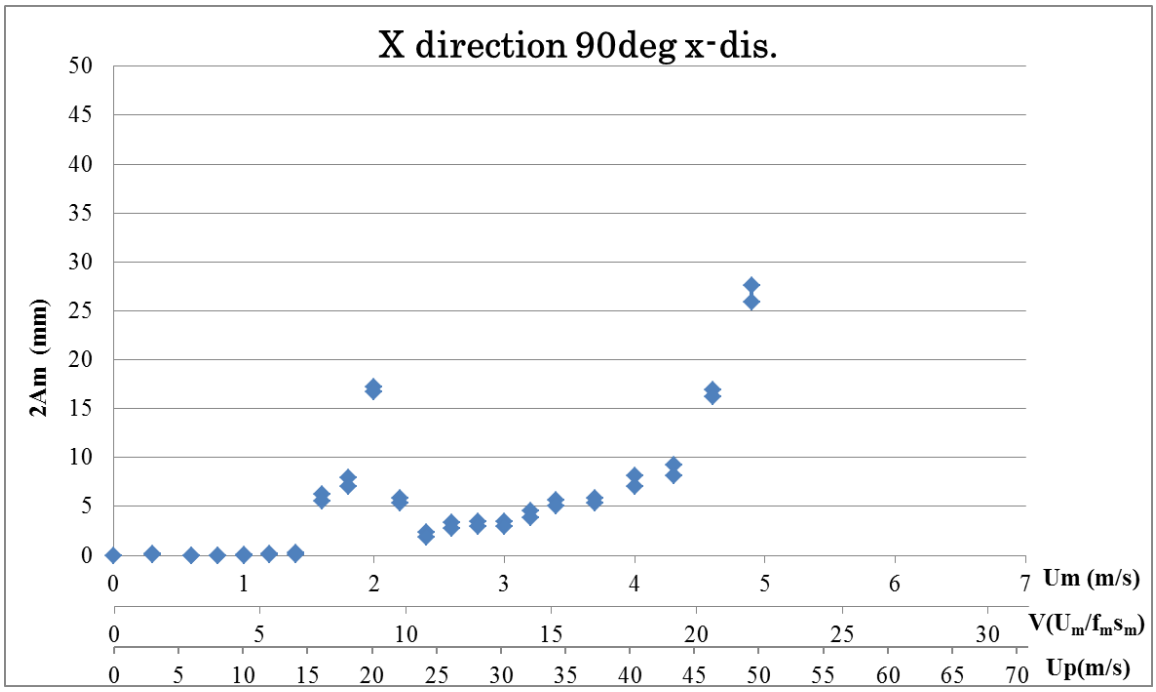

Fig. 6.3.9 Vibration response along cable plane (x-direction)

(UC1, Original tower configuration (without aerodynamic device), Wind direction = 90 [deg.] (normal to bridge axis), in smooth flow) (Stable response amplitude was measured after providing relevant initial disturbance to the model.)

6.3.2 Under construction 1 (UC1, Before the lowest cable being installed) (With L-shaped aerodynamic device, length: 91.7mm)

For UC1, countermeasure to stabilize the aerodynamic vibration, VIV and Galloping should be discussed, since these vibration were observed in smooth flow condition as described in previous section, 6.3.1. The L-shaped aerodynamic device as shown in Fig.6.3.10 was proposed and its stabilizing effect was tested in wind tunnel by attaching the device near the edge of the tower cross section on the front and rear surface near the top of the tower model.

In the condition of smooth flow, y-direction VIV was observed for yawing angle 0º, and x-direction VIV was observed for yawing angle 90º. In the condition of turbulence, no VIV and galloping were observed. The results are summarized in Table 6.3.2. The response of each case is shown in Fig 6.3.11-Fig. 6.4.50.

Table 6.3.2 Under construction 1 (UC1, With L-shaped aerodynamic device)
(Length of aerodynamic device: 91.7mm (= 11.0m for real bridge) from the top of the tower))

Flow condition	Yawing angle [deg]	Vortex-induced vibration	Galloping	Corresponding figure
Smooth	0	× in y-direction (12.6m/s~14.7m/s)	o	Fig.6.3.11
	90	× in x-direction (18.5m/s~20.6m/s)	o	Fig.6.3.12
Turbulent	80	o	o	Fig.6.3.13
	85	o	o	Fig.6.3.14
	90	o	o	Fig.6.3.15
	180	o	o	Fig.6.3.16

“o” : The corresponding response was not observed.

“×” : The corresponding response occurred.

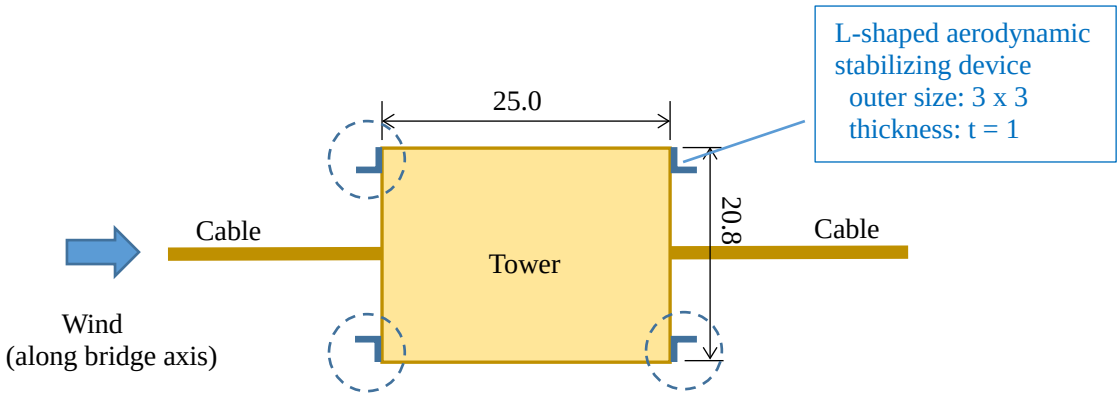

(a) For wind along bridge axis

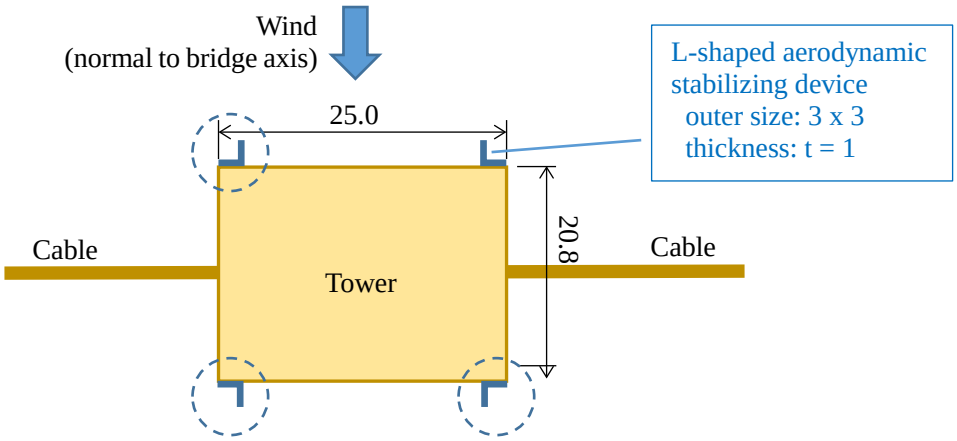

(b) For wind normal to bridge axis

Fig.6.3.10 L-shaped aerodynamic device (Model scale ratio: 1/120, unit: in mm)

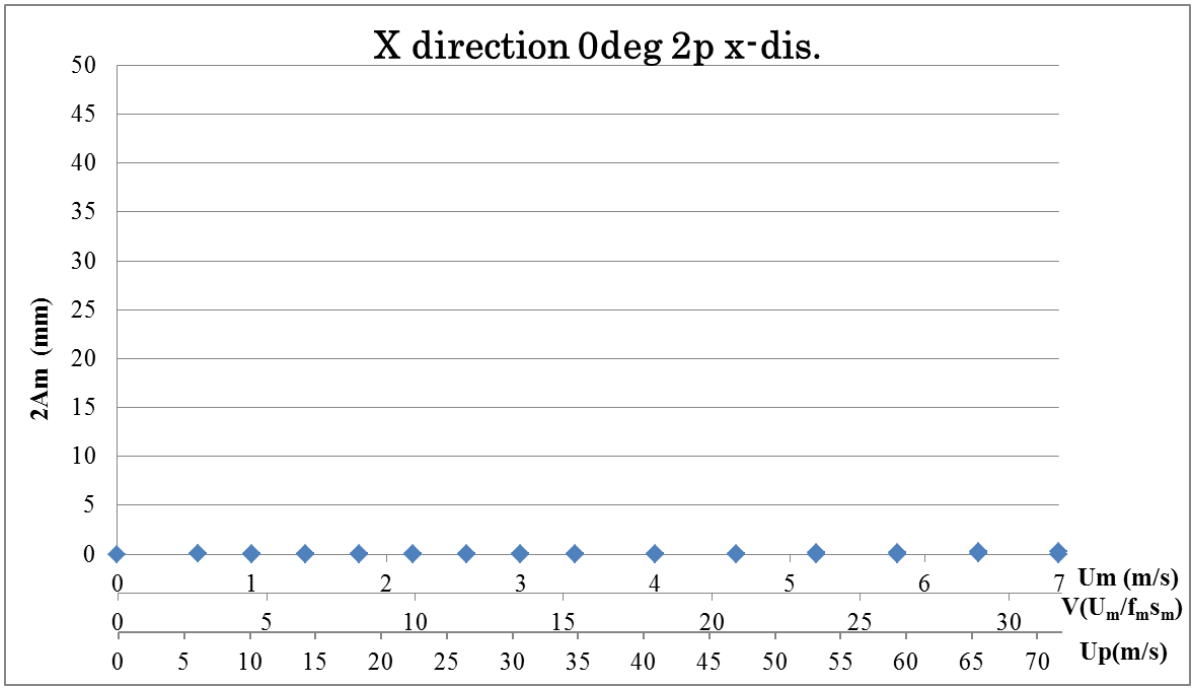

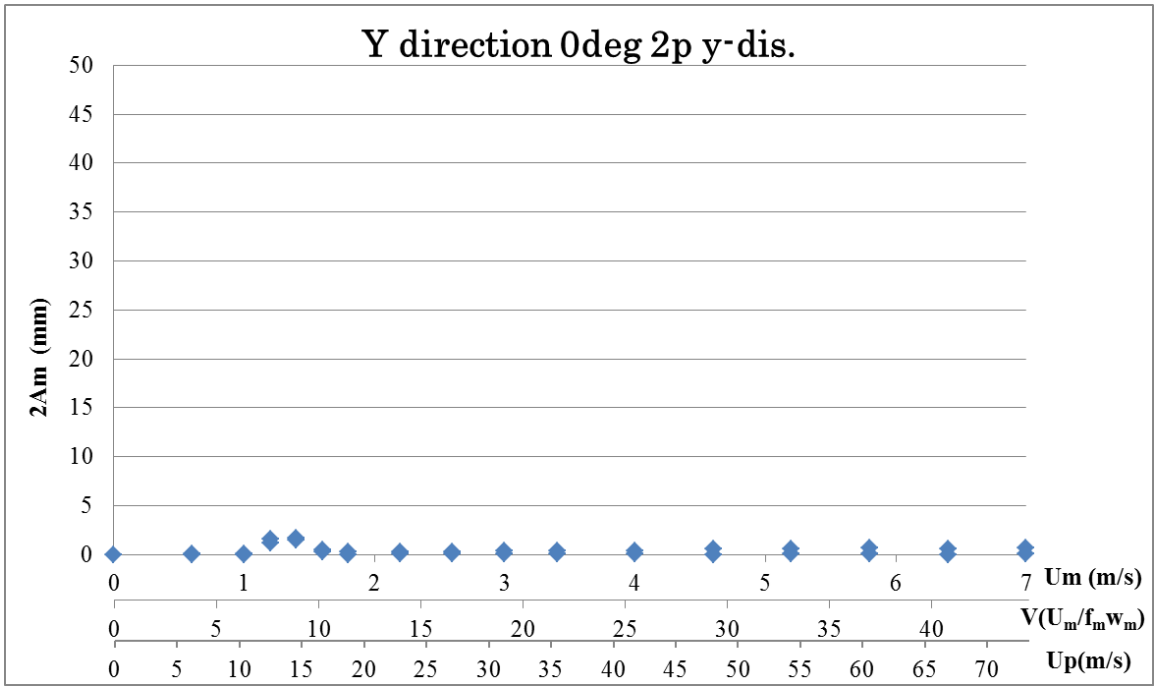

Fig. 6.3.11 Vibration response along (x-direction) and normal to cable plane (y-direction) (UC1, With L-shaped aerodynamic device (Length of aerodynamic device: 91.7mm (= 11.0m for real bridge) from the top of the tower), Wind direction = 0 [deg.] (along bridge axis), in smooth flow) (Stable response amplitude was measured after providing relevant initial disturbance to the model.)

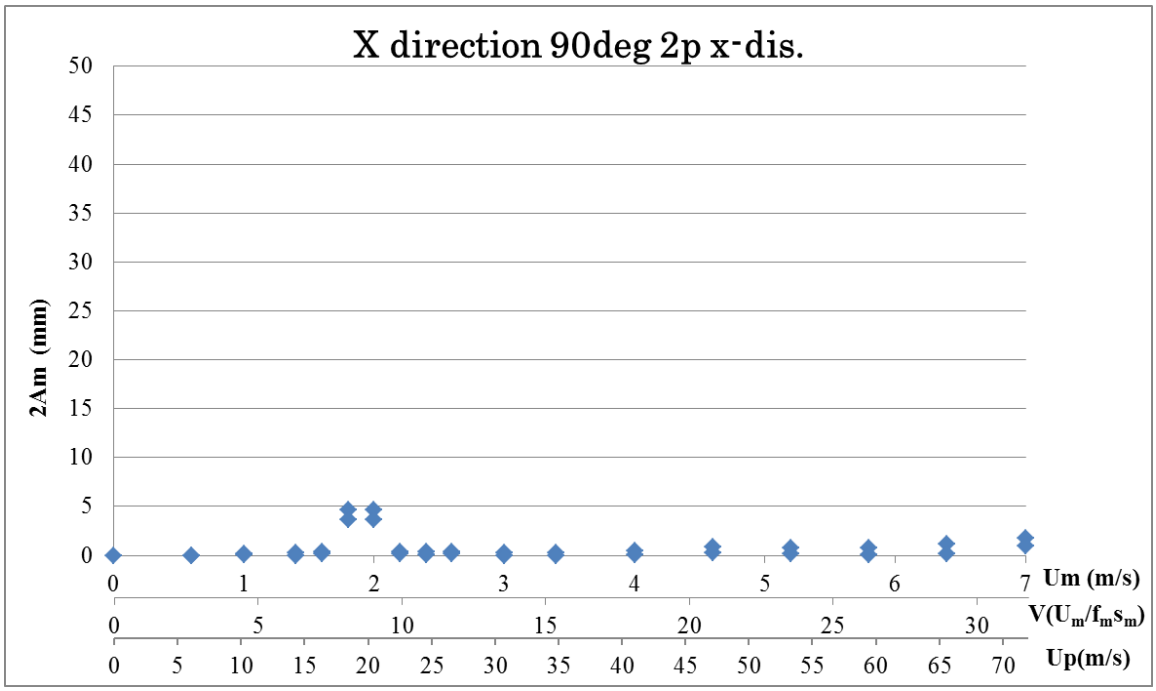

Fig. 6.3.12 Vibration response along cable plane (x-direction)

(UC1, With L-shaped aerodynamic device (Length of aerodynamic device: 91.7mm (= 11.0m for real bridge) from the top of the tower), Wind direction = 90 [deg.] (normal to bridge axis), in smooth flow) (Stable response amplitude was measured after providing relevant initial disturbance to the model.)

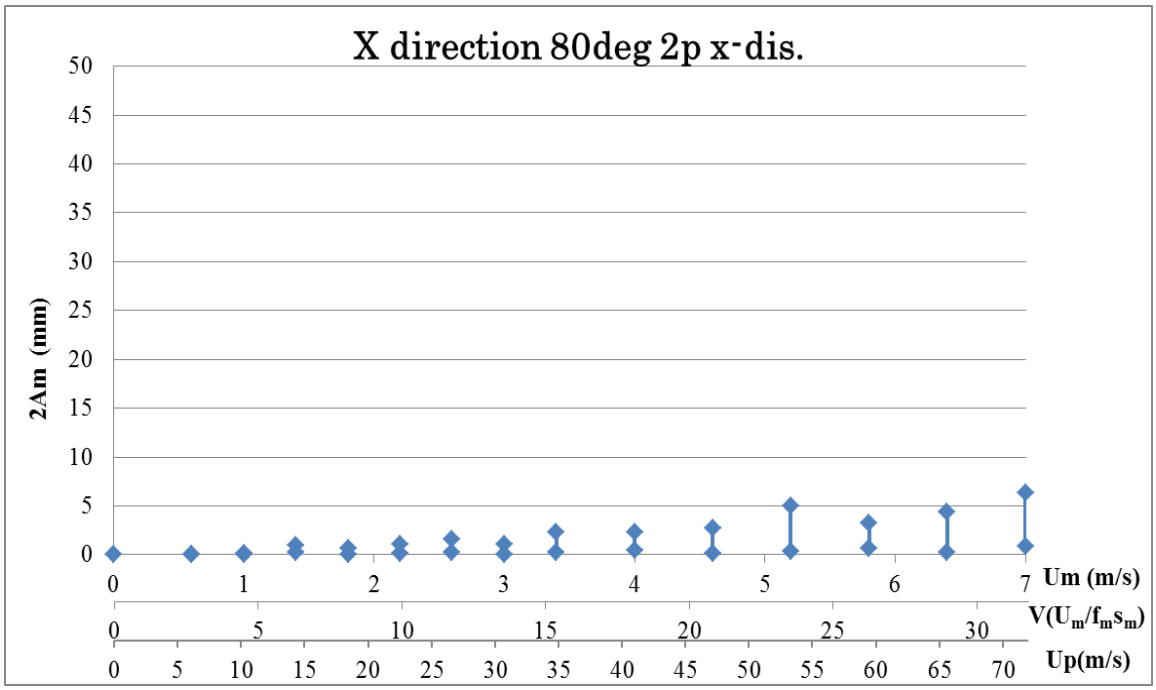

Fig. 6.3.13 Vibration response along cable plane (x-direction)

(UC1, With L-shaped aerodynamic device (Length of aerodynamic device: 91.7mm (= 11.0m for real bridge) from the top of the tower), Wind direction = 80 [deg.], in turbulent flow) (Stable response amplitude was measured after providing relevant initial disturbance to the model.)

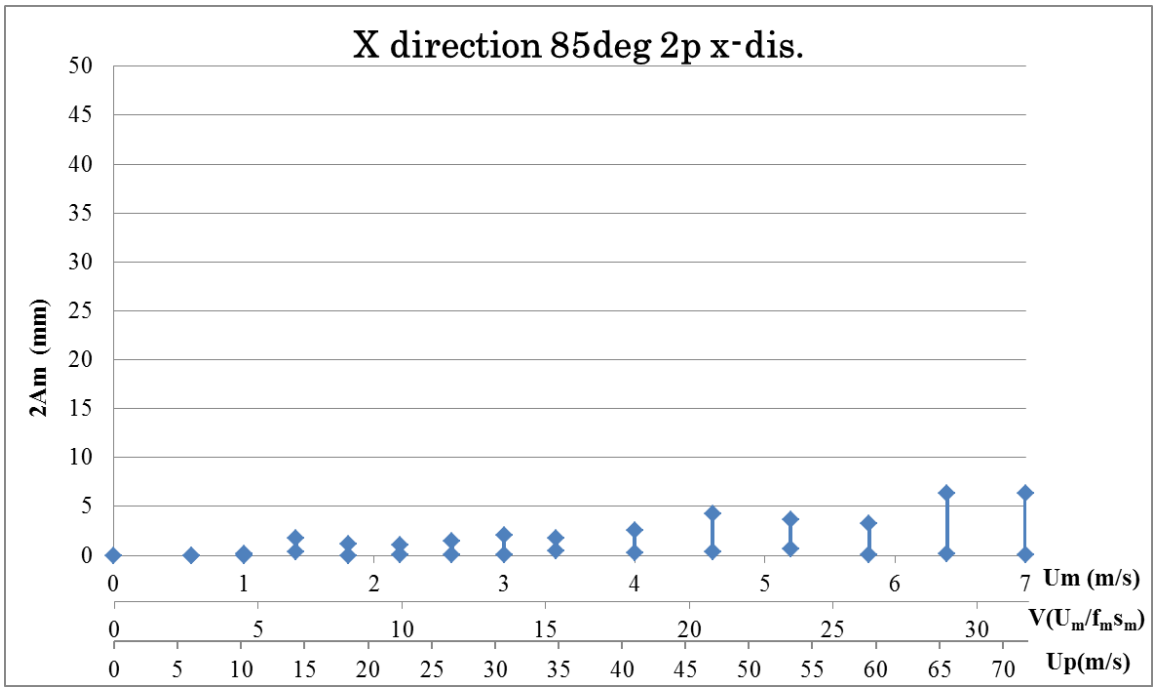

Fig. 6.3.14 Vibration response along cable plane (x-direction)

(UC1, With L-shaped aerodynamic device (Length of aerodynamic device: 91.7mm (= 11.0m for real bridge) from the top of the tower), Wind direction = 85 [deg.], in turbulent flow) (Stable response amplitude was measured after providing relevant initial disturbance to the model.)

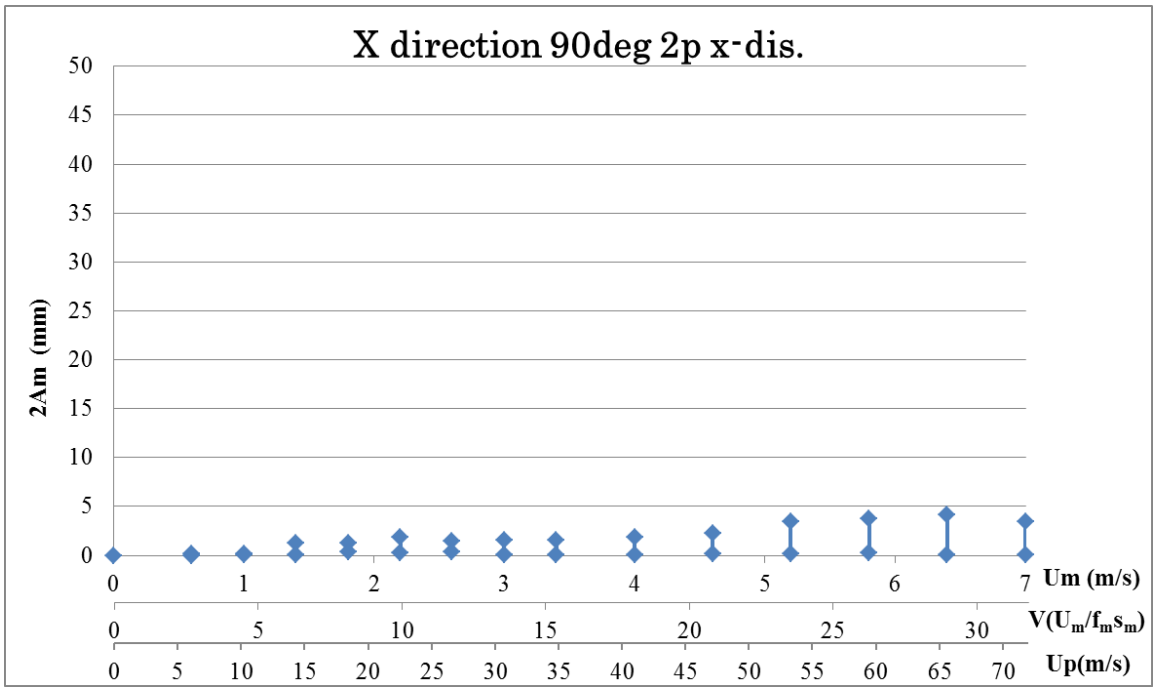

Fig. 6.3.15 Vibration response along cable plane (x-direction)

(UC1, With L-shaped aerodynamic device (Length of aerodynamic device: 91.7mm (= 11.0m for real bridge) from the top of the tower), Wind direction = 90 [deg.] (normal to bridge axis), in turbulent flow) (Stable response amplitude was measured after providing relevant initial disturbance to the model.)

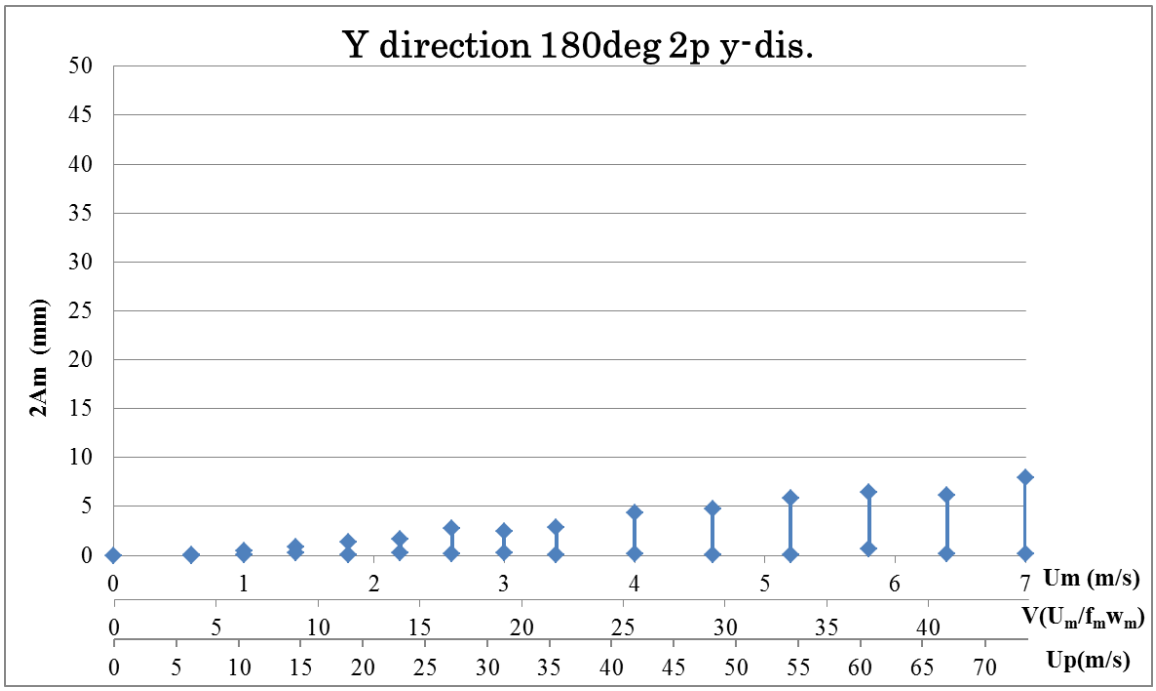

Fig. 6.3.16 Vibration response normal to cable plane (y-direction)
(UC1, With L-shaped aerodynamic device (Length of aerodynamic device: 91.7mm (= 11.0m for real bridge) from the top of the tower), Wind direction = 180 [deg.] (along bridge axis), in turbulent flow) (Stable response amplitude was measured after providing relevant initial disturbance to the model.)

6.3.3 Under construction 2 (UC2, Before the last girder segment being installed) (With L-shaped aerodynamic device, length: 91.7mm)

Aerodynamic vibration response of the tower was tested for the under construction stage UC2, in which the aerodynamic device was attached with the length of 91.7mm (= 11.0m for real bridge) expecting its stabilizing effect to the wind along bridge axis (see Fig. 6.3.10).

While the y-direction VIV was observed in smooth flow for yawing angle 0º, no vibration was observed in turbulent flow condition for yawing angle 0º and5 º. The results are summarized in Table 6.3.3. The response of each case is shown in Fig 6.3.17-Fig. 6.3.20.

Table 6.3.3 Under construction 2 (UC2, With L-shaped aerodynamic device)
(Length of aerodynamic device: 91.7mm (= 11.0m for real bridge) from the top of the tower))

Flow condition	Yawing angle [deg]	Vortex-induced vibration	Galloping	Corresponding figure
Smooth	0	× in y-direction (11.1m/s~29.5m/s) (34.2m/s~34.2m/s)	o	Fig.6.3.17
	5	o	o	Fig.6.3.18
Turbulent	0	o	o	Fig.6.3.19
	5	o	o	Fig.6.3.20

“o” : The corresponding response was not observed.

“×” : The corresponding response occurred.

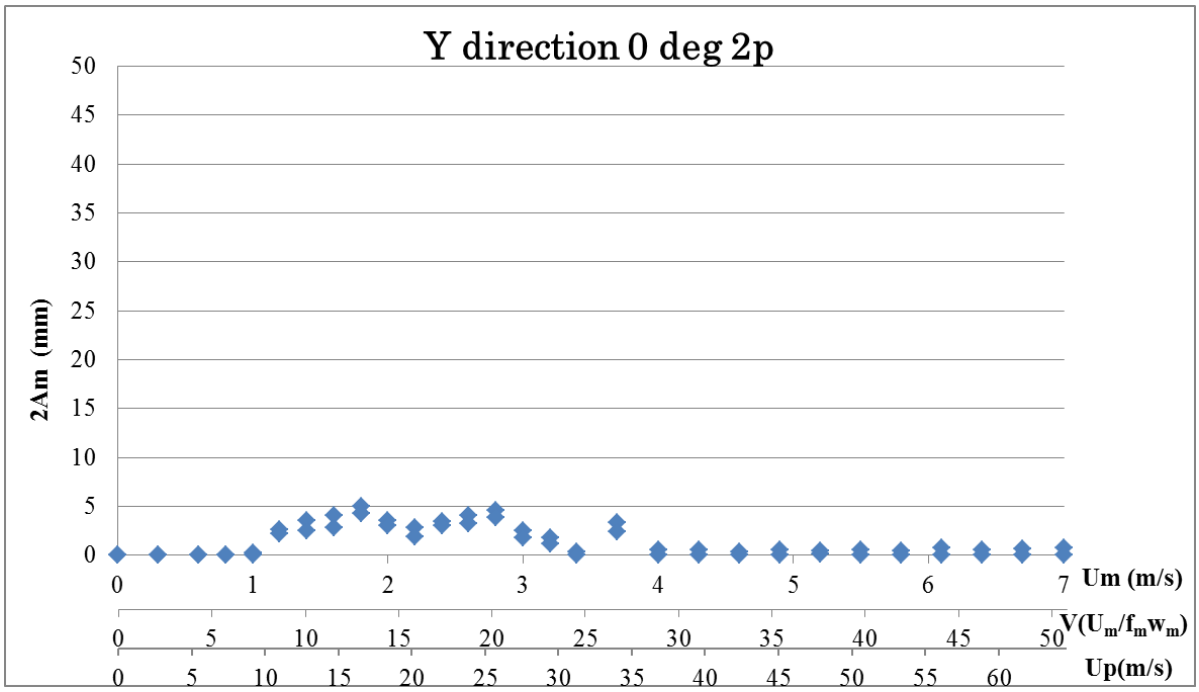

Fig. 6.3.17 Vibration response normal to cable plane (y-direction)
(UC2, With L-shaped aerodynamic device (Length of aerodynamic device: 91.7mm (= 11.0m for real bridge) from the top of the tower), Wind direction = 0 [deg.] (along bridge axis), in smooth flow) (Stable response amplitude was measured after providing relevant initial disturbance to the model.)

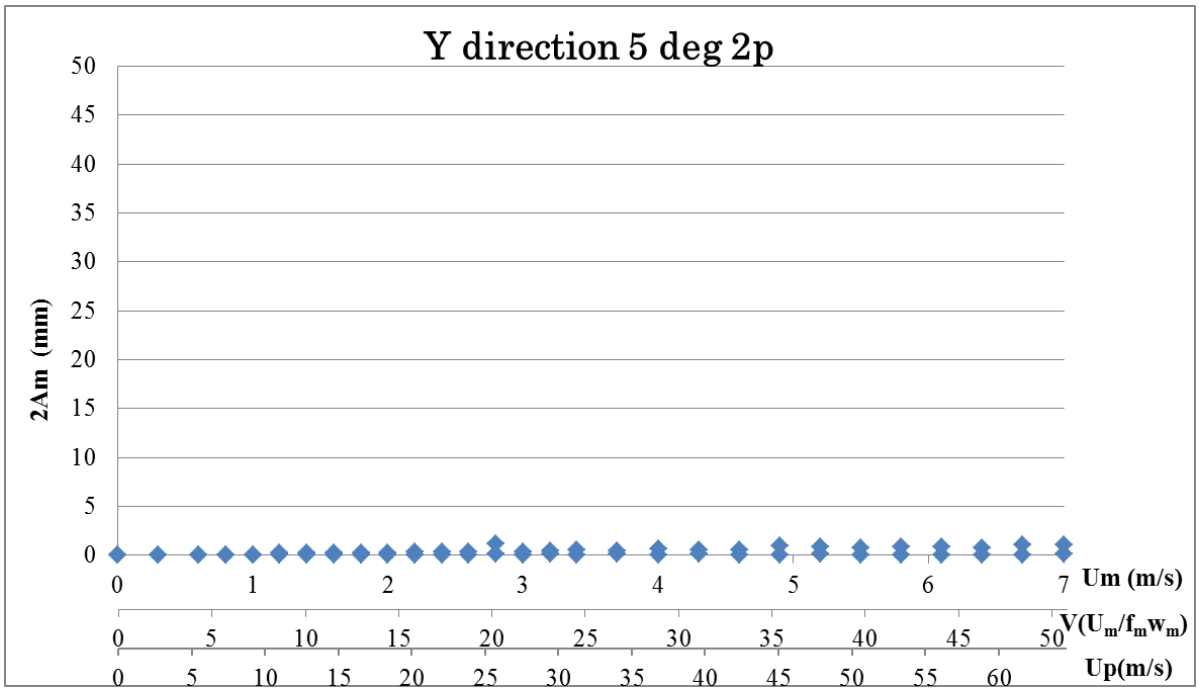

Fig. 6.3.18 Vibration response normal to cable plane (y-direction)
(UC2, With L-shaped aerodynamic device (Length of aerodynamic device: 91.7mm (= 11.0m for real bridge) from the top of the tower), Wind direction = 5 [deg.], in smooth flow) (Stable response amplitude was measured after providing relevant initial disturbance to the model.)

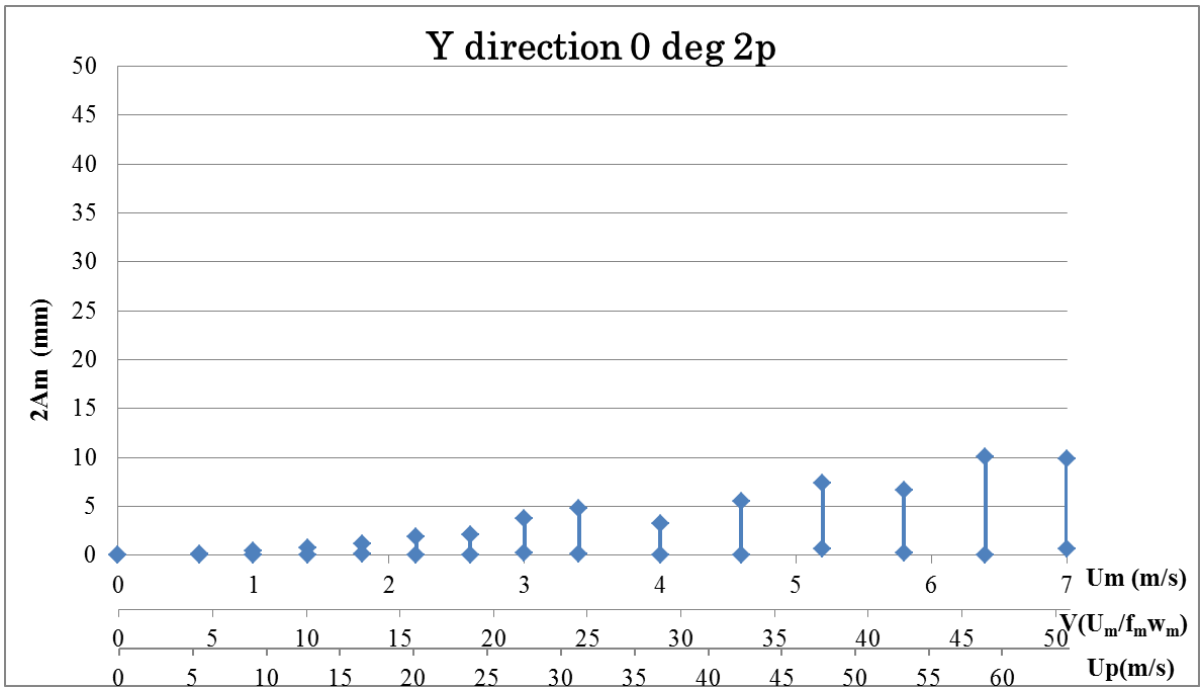

Fig. 6.3.19 Vibration response normal to cable plane (y-direction)
(UC2, With L-shaped aerodynamic device (Length of aerodynamic device: 91.7mm (= 11.0m for real bridge) from the top of the tower), Wind direction = 0 [deg.] (along bridge axis), in turbulent flow) (Stable response amplitude was measured after providing relevant initial disturbance to the model.)

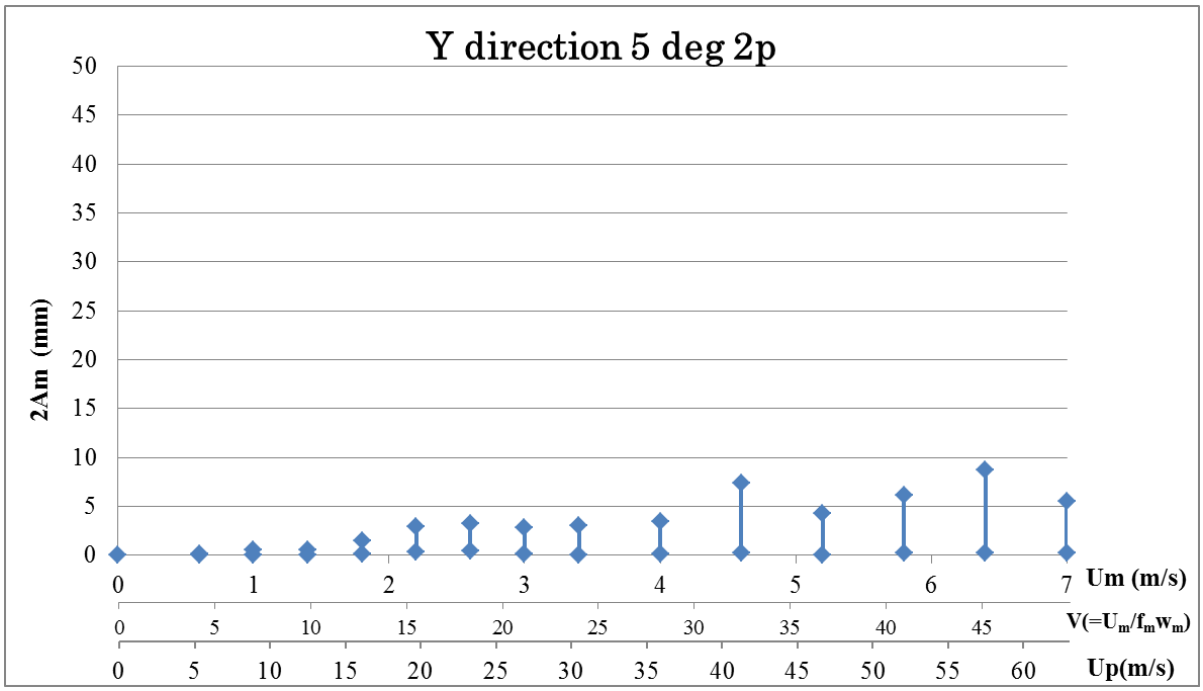

Fig. 6.3.20 Vibration response normal to cable plane (y-direction)
(UC2, With L-shaped aerodynamic device (Length of aerodynamic device: 91.7mm (= 11.0m for real bridge) from the top of the tower), Wind direction = 5 [deg.], in turbulent flow) (Stable response amplitude was measured after providing relevant initial disturbance to the model.)

6.3.4 After Completion (AC) (Original tower configuration)

In the condition of smooth flow, y-direction VIV was observed for yawing angles 0º and 5º. Besides, y-direction galloping occurred for yawing angel 5º. In the condition of turbulence, both of y-direction VIV and y-direction galloping were observed for yawing angle 0º. The results are summarized in Table 6.3.4. The response of each case is shown in Fig 6.3.21-Fig. 6.3.34.

Table 6.3.4 After completion (AC, Original tower configuration)

Flow condition	Yawing angle [deg]	Vortex-induced vibration	Galloping	Corresponding figure
Smooth	0	× in y-direction (10.7m/s~30.4m/s)	o	Fig.6.3.21
	5	× in y-direction (10.7m/s~19.7m/s)	× in y-direction (28.6m/s~)	Fig.6.3.22
	10	o	o	Fig.6.3.23
	22.5	o	o	Fig.6.3.24
	45	o	o	Fig.6.3.25
	67.5	o	o	Fig.6.3.26
	90	o	o	Fig.6.3.27
Turbulent	0	× in y-direction (17.9m/s~19.7m/s)	× in y-direction (23.3m/s~)	Fig.6.3.28
	5	o	o	Fig.6.3.29
	10	o	o	Fig.6.3.30
	22.5	o	o	Fig.6.3.31
	45	o	o	Fig.6.3.32
	67.5	o	o	Fig.6.3.33
	90	o	o	Fig.6.3.34

“o” : The corresponding response was not observed.

“×” : The corresponding response occurred.

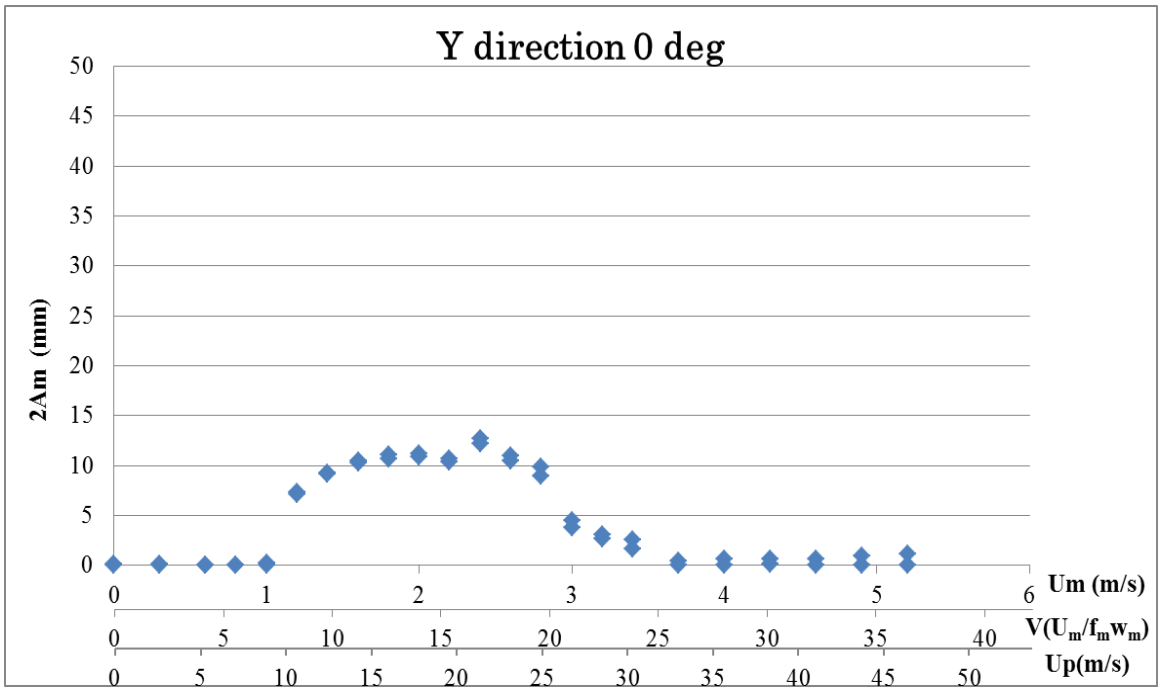

Fig. 6.3.21 Vibration response normal to cable plane (y-direction)

(AC, Original tower configuration, Wind direction = 0 [deg.] (along bridge axis), in smooth flow)

(Stable response amplitude was measured after providing relevant initial disturbance to the model.)

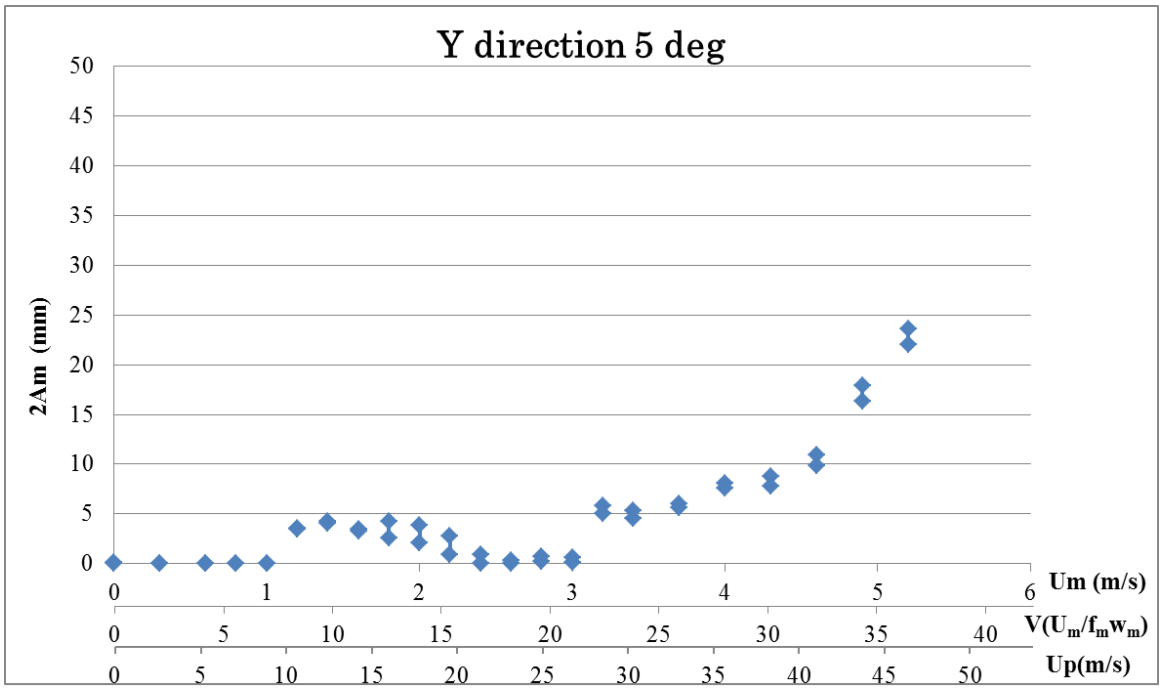

Fig. 6.3.22 Vibration response normal to cable plane (y-direction)
(AC, Original tower configuration, Wind direction = 5 [deg.], in smooth flow) (Stable response amplitude was measured after providing relevant initial disturbance to the model.)

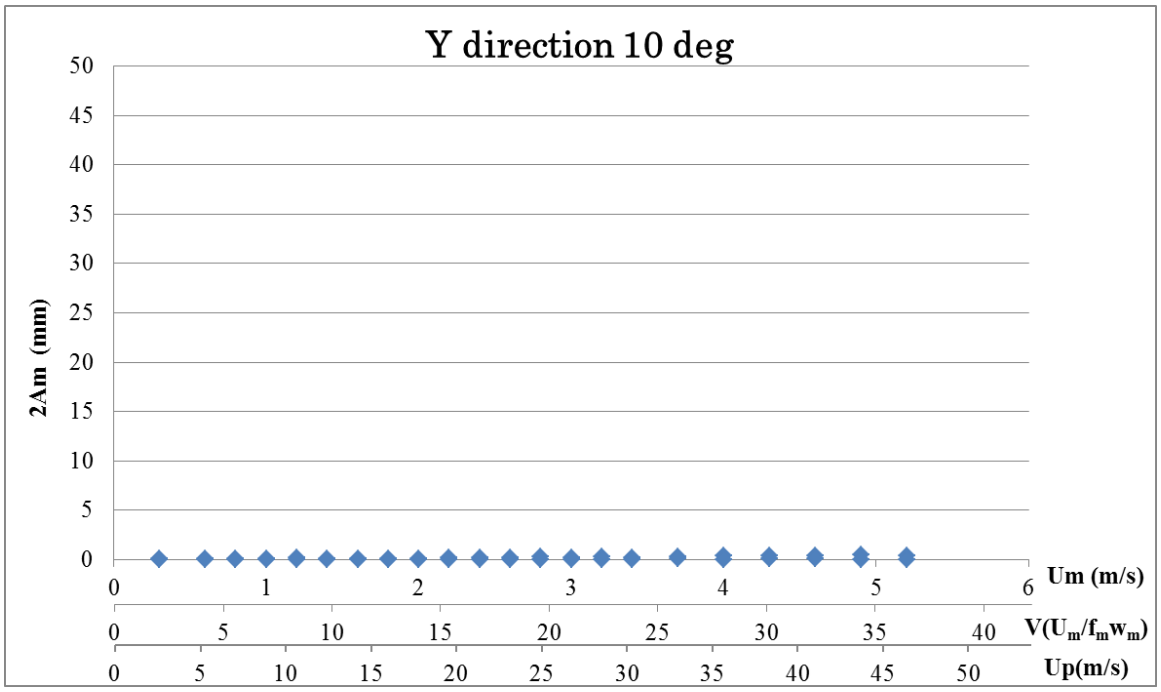

Fig. 6.3.23 Vibration response normal to cable plane (y-direction)
(AC, Original tower configuration, Wind direction = 10 [deg.], in smooth flow) (Stable response amplitude was measured after providing relevant initial disturbance to the model.)

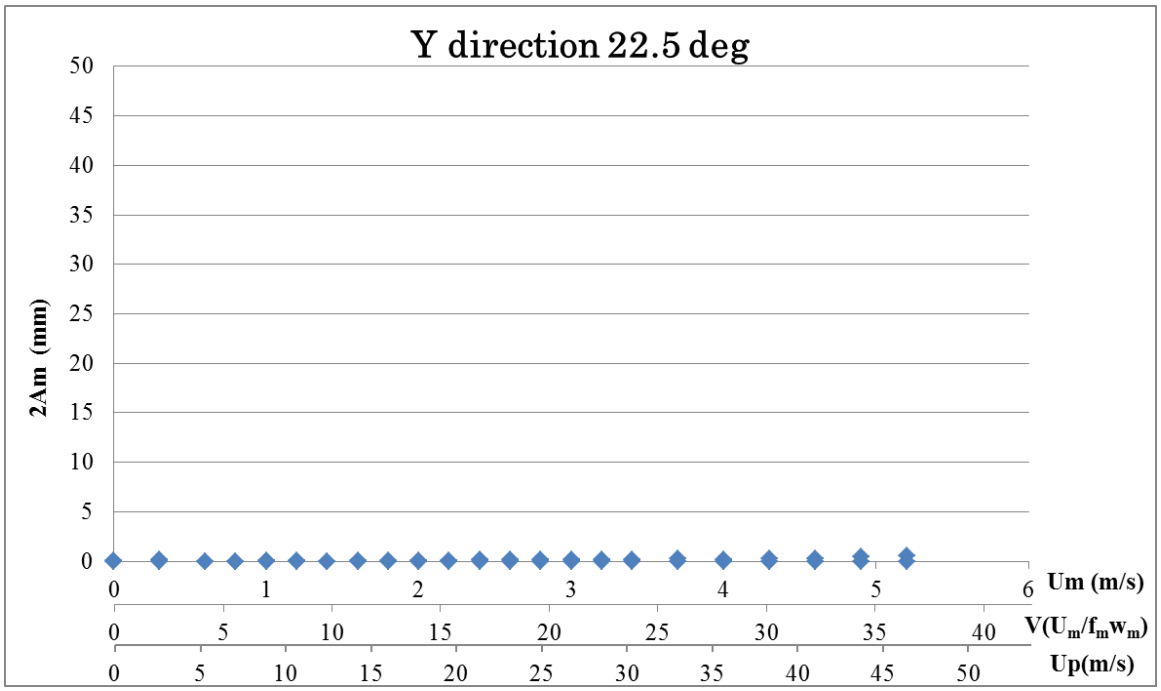

Fig. 6.3.24 Vibration response normal to cable plane (y-direction)
(AC, Original tower configuration, Wind direction = 22.5 [deg.], in smooth flow) (Stable response amplitude was measured after providing relevant initial disturbance to the model.)

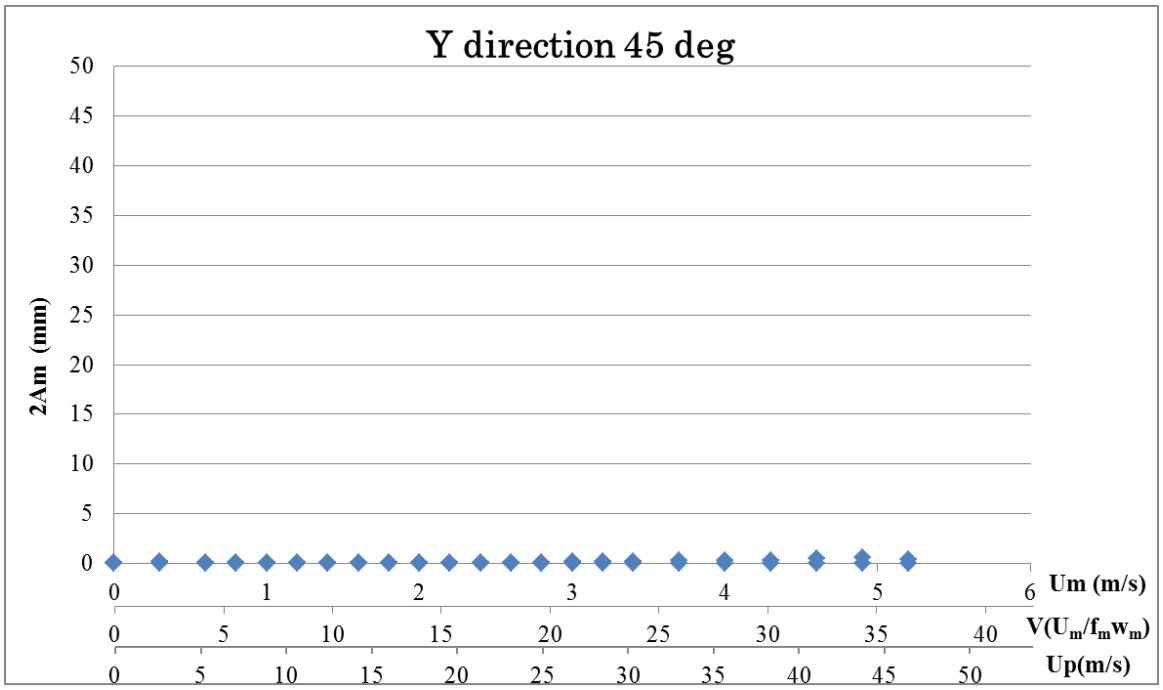

Fig. 6.3.25 Vibration response normal to cable plane (y-direction)
(AC, Original tower configuration, Wind direction = 45 [deg.], in smooth flow) (Stable response amplitude was measured after providing relevant initial disturbance to the model.)

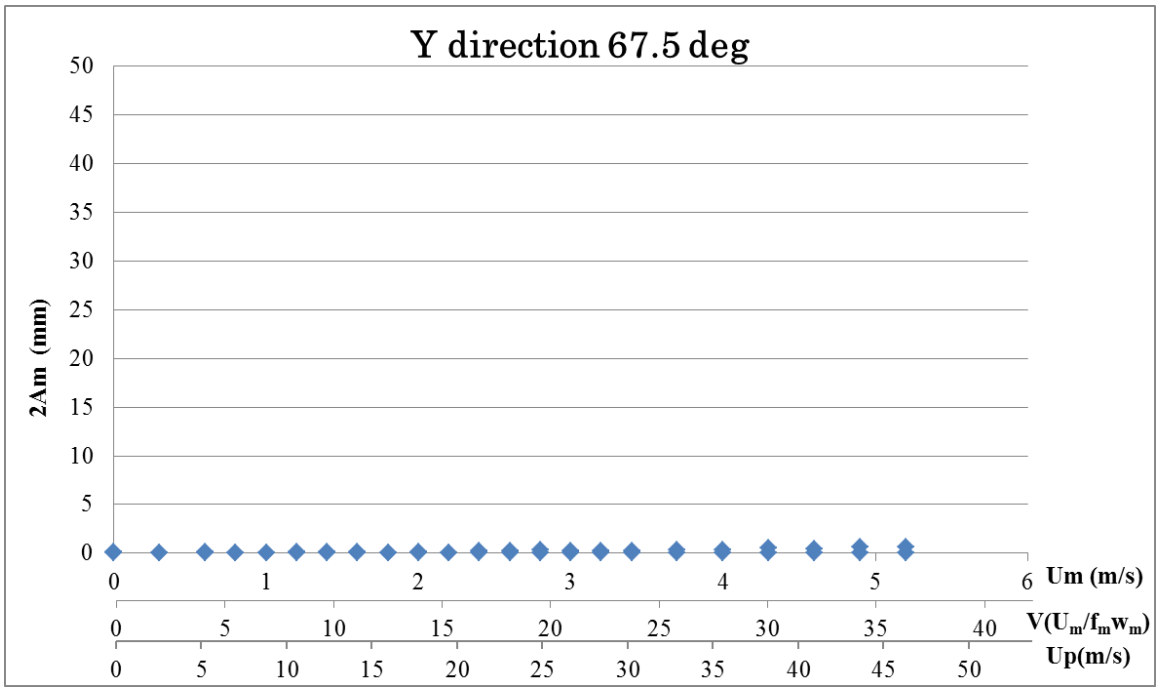

Fig. 6.3.26 Vibration response normal to cable plane (y-direction)
(AC, Original tower configuration, Wind direction = 67.5 [deg.], in smooth flow) (Stable response amplitude was measured after providing relevant initial disturbance to the model.)

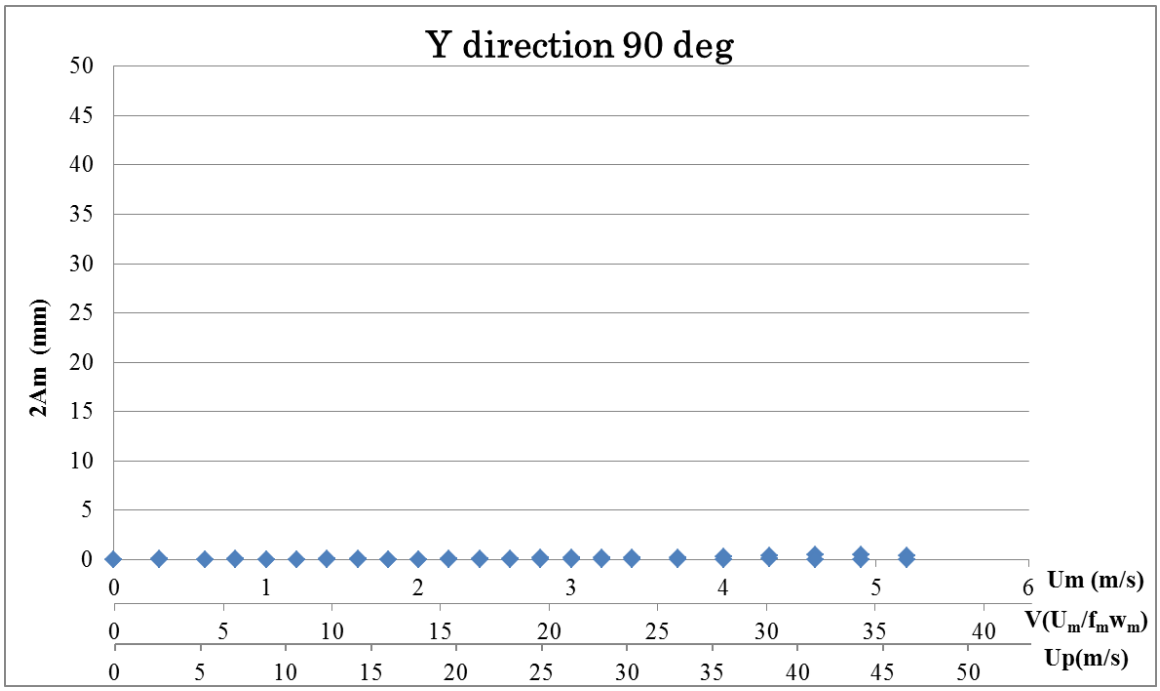

Fig. 6.3.27 Vibration response normal to cable plane (y-direction)
(AC, Original tower configuration, Wind direction = 90 [deg.] (normal to bridge axis), in smooth flow) (Stable response amplitude was measured after providing relevant initial disturbance to the model.)

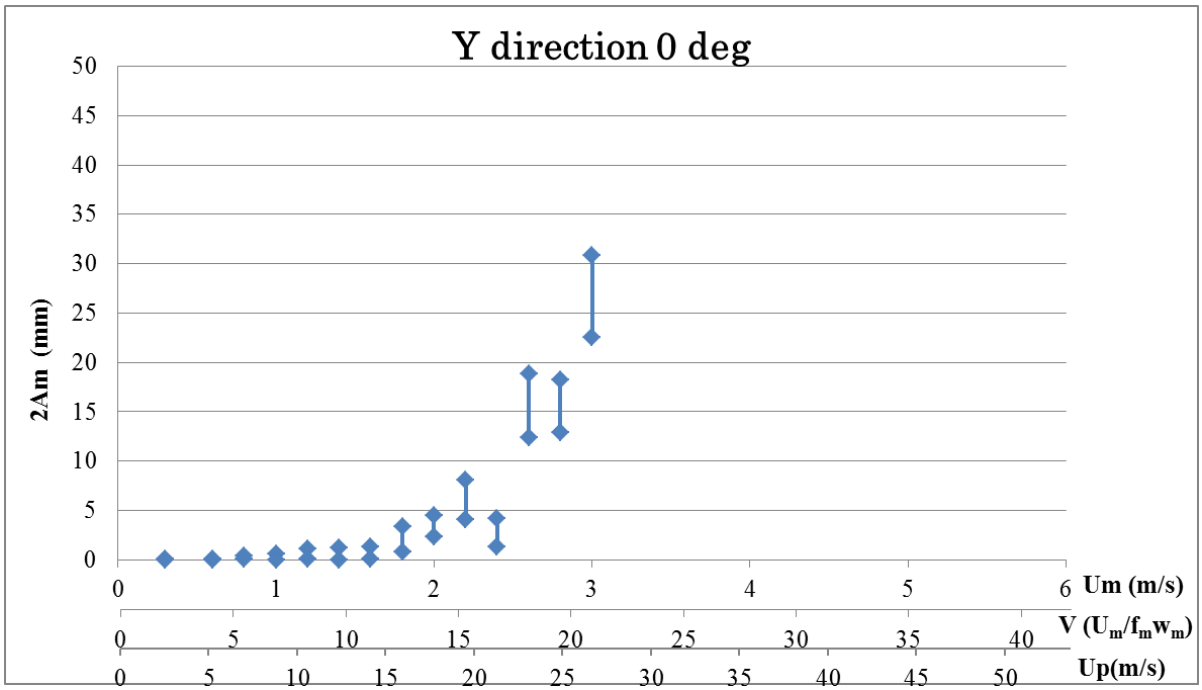

Fig. 6.3.28 Vibration response normal to cable plane (y-direction)

(AC, Original tower configuration, Wind direction = 0 [deg.] (along bridge axis), in turbulent flow)

(Stable response amplitude was measured after providing relevant initial disturbance to the model.)

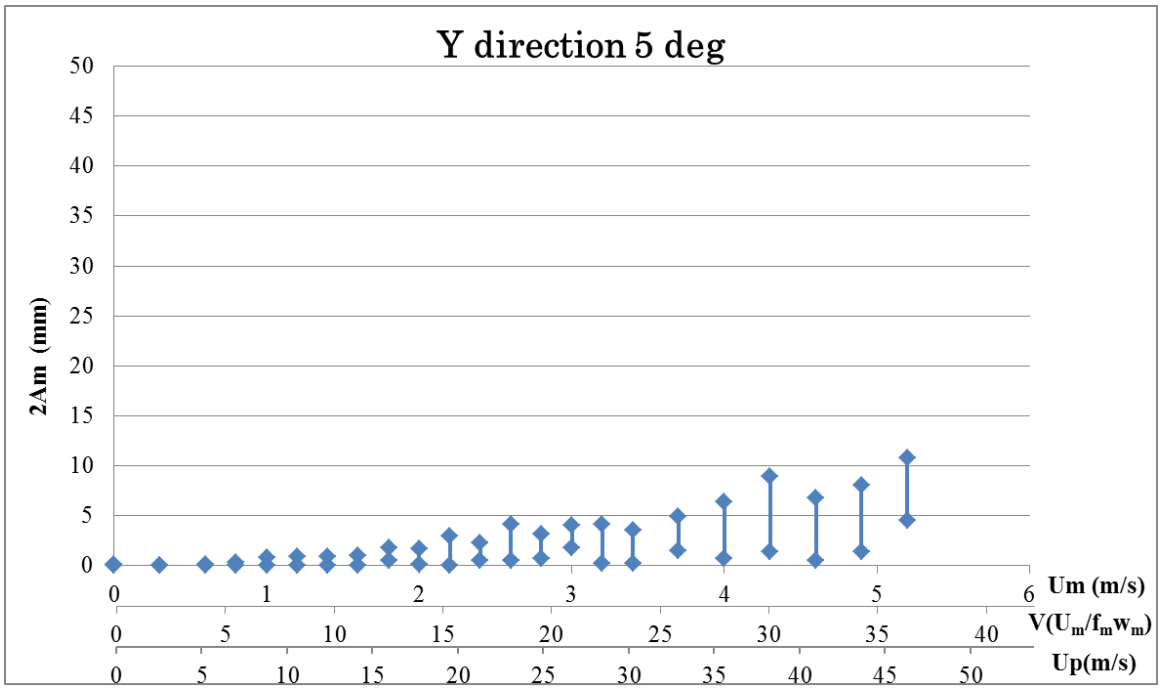

Fig. 6.3.29 Vibration response normal to cable plane (y-direction)
(AC, Original tower configuration, Wind direction = 5 [deg.], in turbulent flow) (Stable response amplitude was measured after providing relevant initial disturbance to the model.)

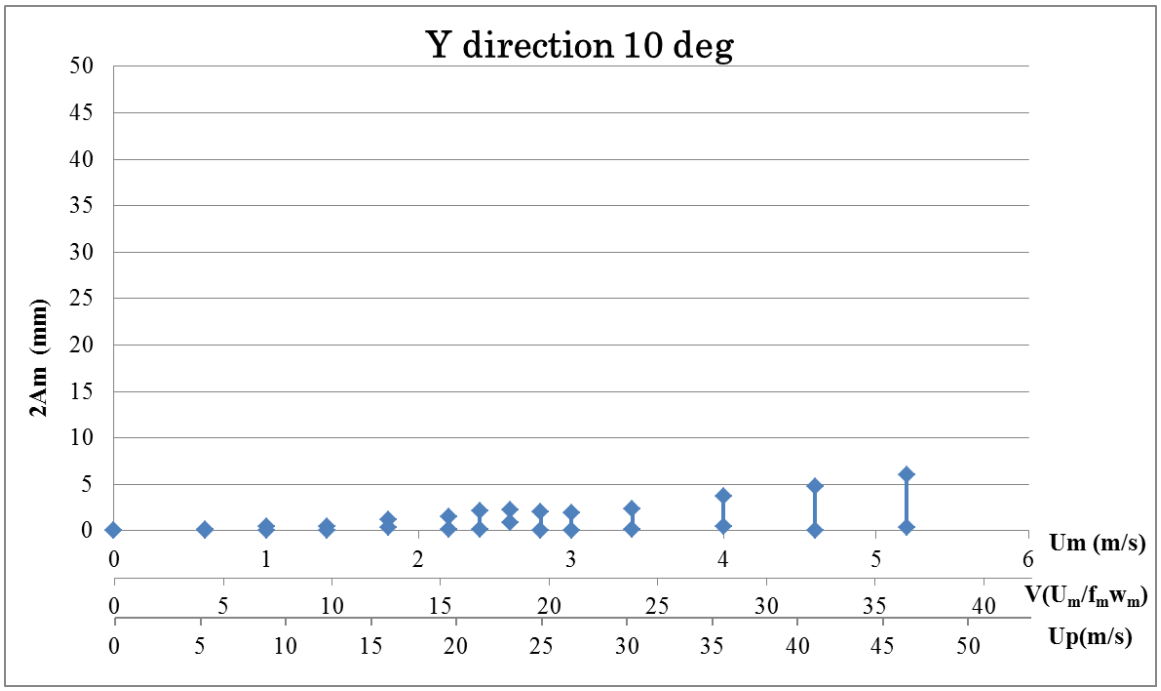

Fig. 6.3.30 Vibration response normal to cable plane (y-direction)
(AC, Original tower configuration, Wind direction = 10 [deg.], in turbulent flow) (Stable response amplitude was measured after providing relevant initial disturbance to the model.)

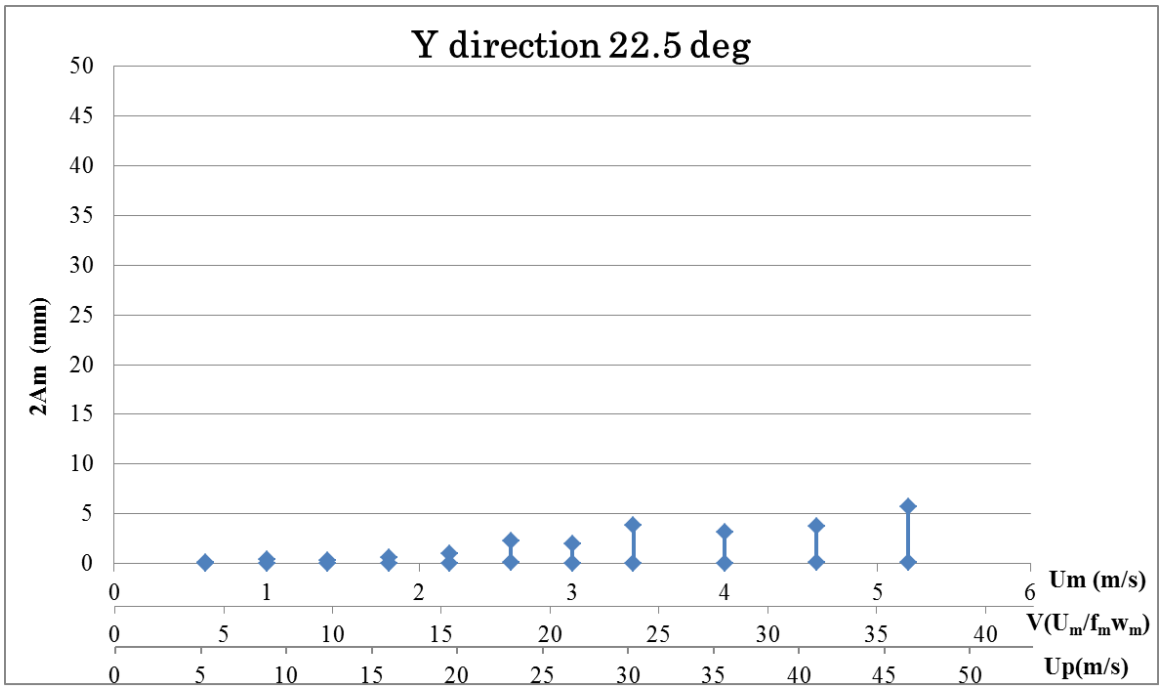

Fig. 6.3.31 Vibration response normal to cable plane (y-direction)

(AC, Original tower configuration, Wind direction = 22.5 [deg.], in turbulent flow) (Stable response amplitude was measured after providing relevant initial disturbance to the model.)

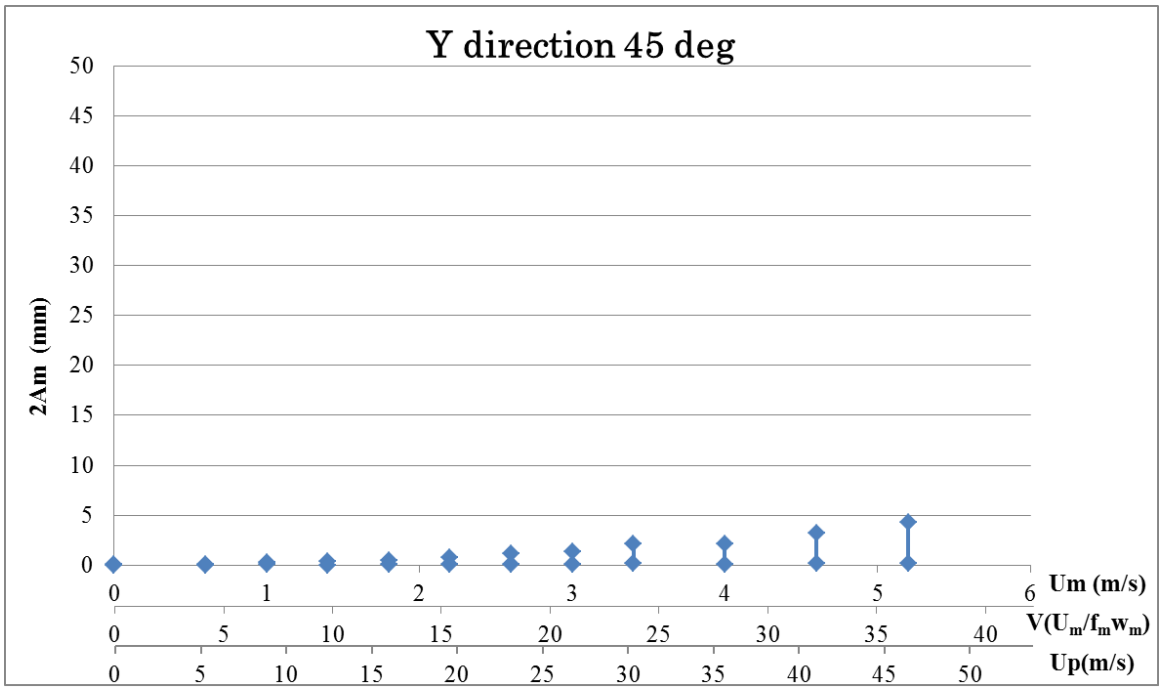

Fig. 6.3.32 Vibration response normal to cable plane (y-direction)
(AC, Original tower configuration, Wind direction = 45 [deg.], in turbulent flow) (Stable response amplitude was measured after providing relevant initial disturbance to the model.)

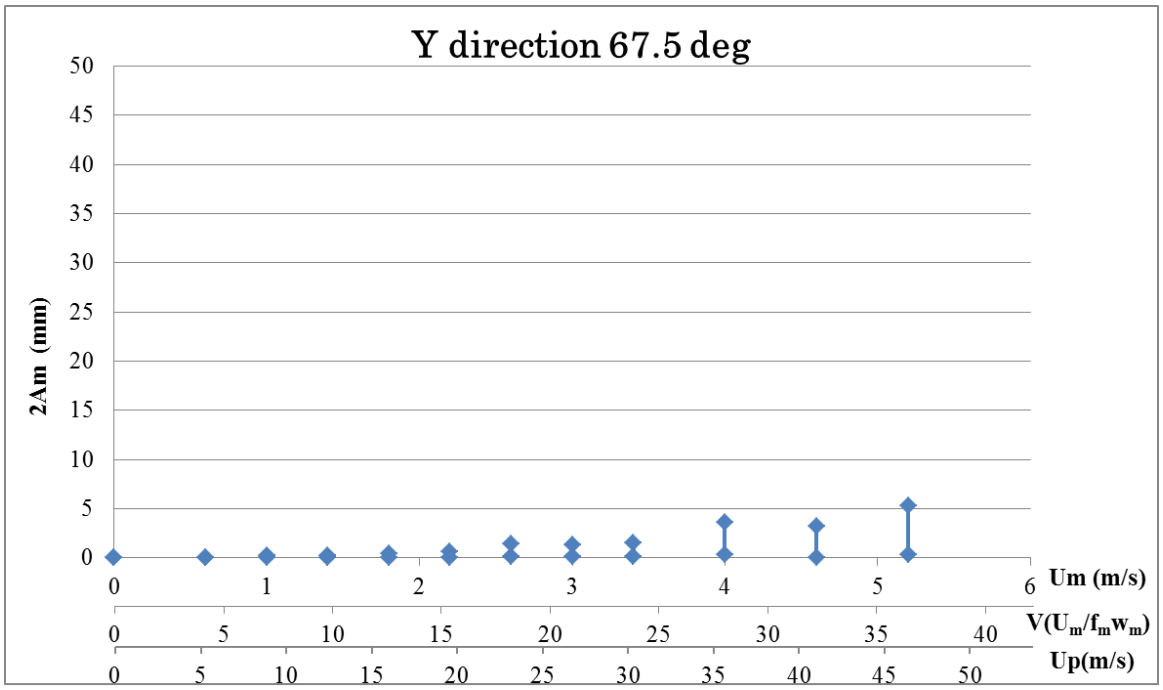

Fig. 6.3.33 Vibration response normal to cable plane (y-direction)

(AC, Original tower configuration, Wind direction = 67.5 [deg.], in turbulent flow) (Stable response amplitude was measured after providing relevant initial disturbance to the model.)

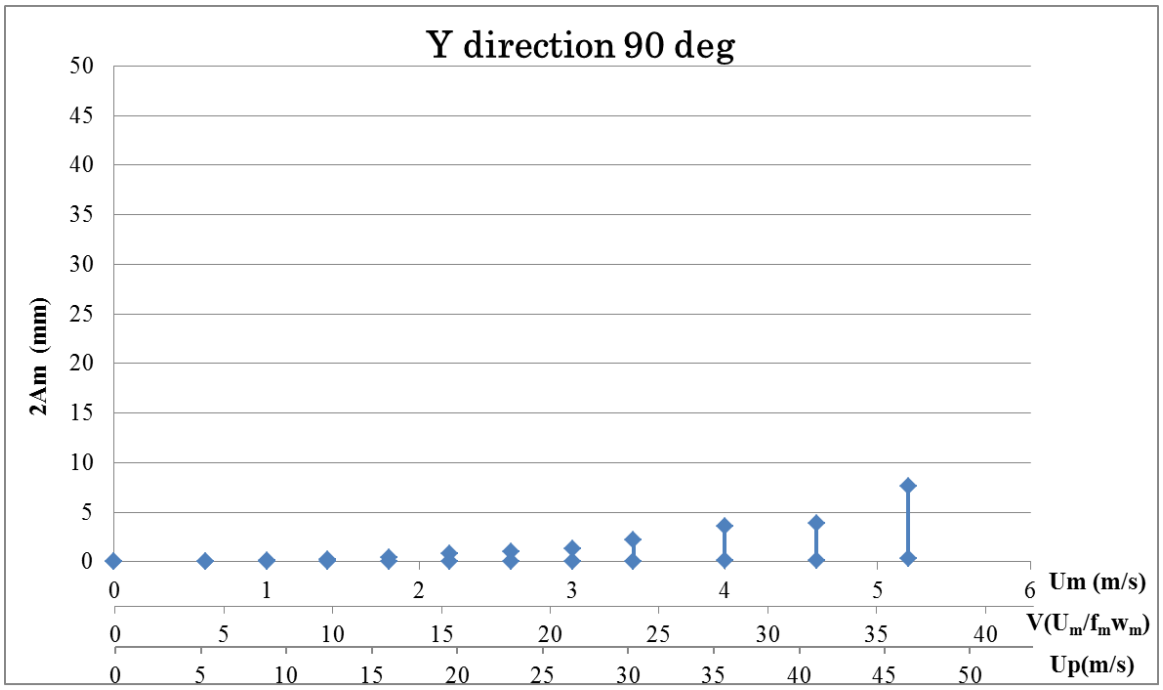

Fig. 6.3.34 Vibration response normal to cable plane (y-direction)
(AC, Original tower configuration, Wind direction = 90 [deg.] (normal to bridge axis), in turbulent flow) (Stable response amplitude was measured after providing relevant initial disturbance to the model.)

6.3.5 After completion (AC, with L-shaped aerodynamic device)
(With L-shaped aerodynamic device, length: 91.7mm)

The response was tested with the aerodynamic device attached (with the length of 91.7mm). The y-direction VIV was observed in smooth flow with yawing angle 0º. No galloping occurred in both of the smooth flow and turbulence. The results are summarized in Table 6.3.5. The response of each case is shown in Fig 6.3.35-Fig. 6.3.38.

Table 6.3.5 After completion (AC, With L-shaped aerodynamic device)
(Length of aerodynamic device: 91.7mm (= 11.0m for real bridge) from the top of the tower))

Flow condition	Yawing angle [deg]	Vortex-induced vibration	Galloping	Corresponding figure
Smooth	0	× in y-direction (22.1m/s~25.8m/s)	o	Fig.6.3.35
	5	o	o	Fig.6.3.36
Turbulent	0	o	o	Fig.6.3.37
	5	o	o	Fig.6.3.38

"o" : The corresponding response was not observed.

"×" : The corresponding response occurred.

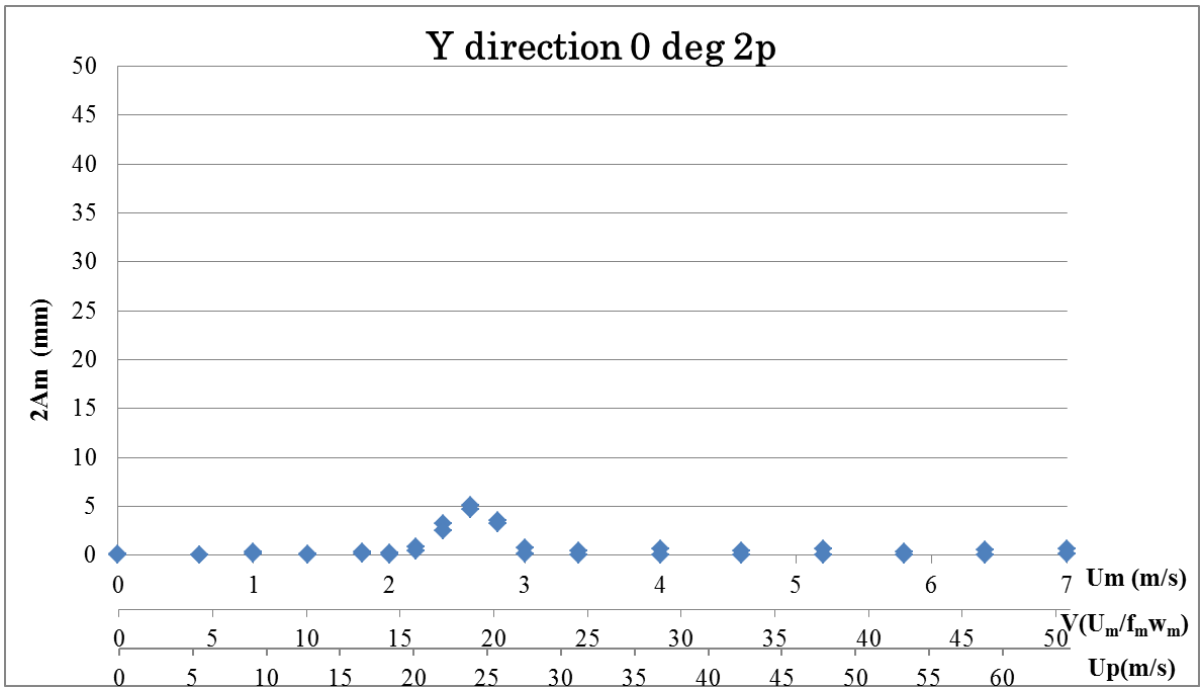

Fig. 6.3.35 Vibration response normal to cable plane (y-direction)

(AC, With L-shaped aerodynamic device (Length of aerodynamic device: 91.7mm (= 11.0m for real bridge) from the top of the tower), Wind direction = 0 [deg.] (along bridge axis), in smooth flow)

(Stable response amplitude was measured after providing relevant initial disturbance to the model.)

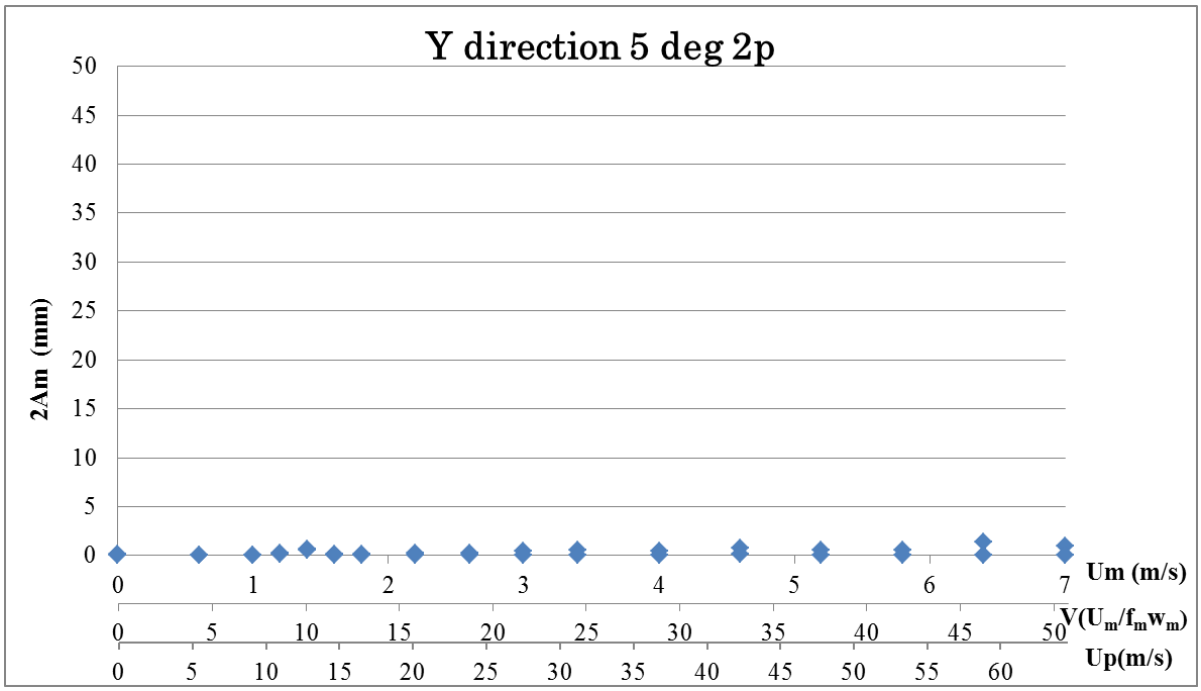

Fig. 6.3.36 Vibration response normal to cable plane (y-direction)

(AC, With L-shaped aerodynamic device (Length of aerodynamic device: 91.7mm (= 11.0m for real bridge) from the top of the tower), Wind direction = 5 [deg.], in smooth flow) (Stable response amplitude was measured after providing relevant initial disturbance to the model.)

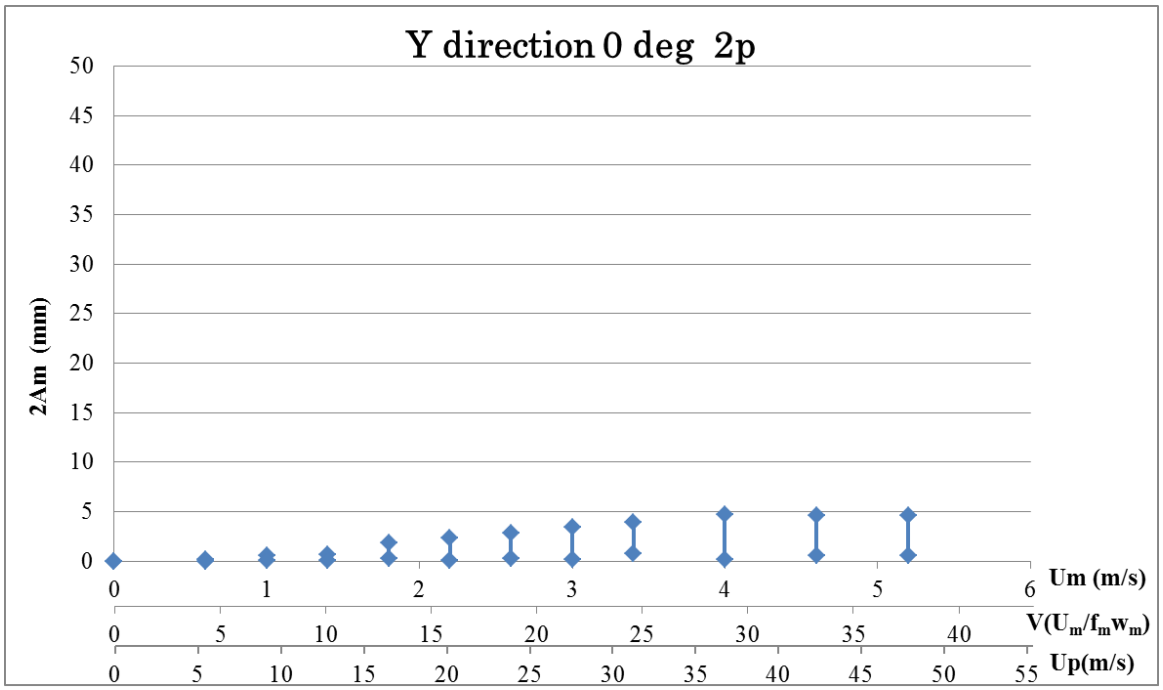

Fig. 6.3.37 Vibration response normal to cable plane (y-direction)
(AC, With L-shaped aerodynamic device (Length of aerodynamic device: 91.7mm (= 11.0m for real bridge) from the top of the tower), Wind direction = 0 [deg.] (along bridge axis), in turbulent flow)
(Stable response amplitude was measured after providing relevant initial disturbance to the model.)

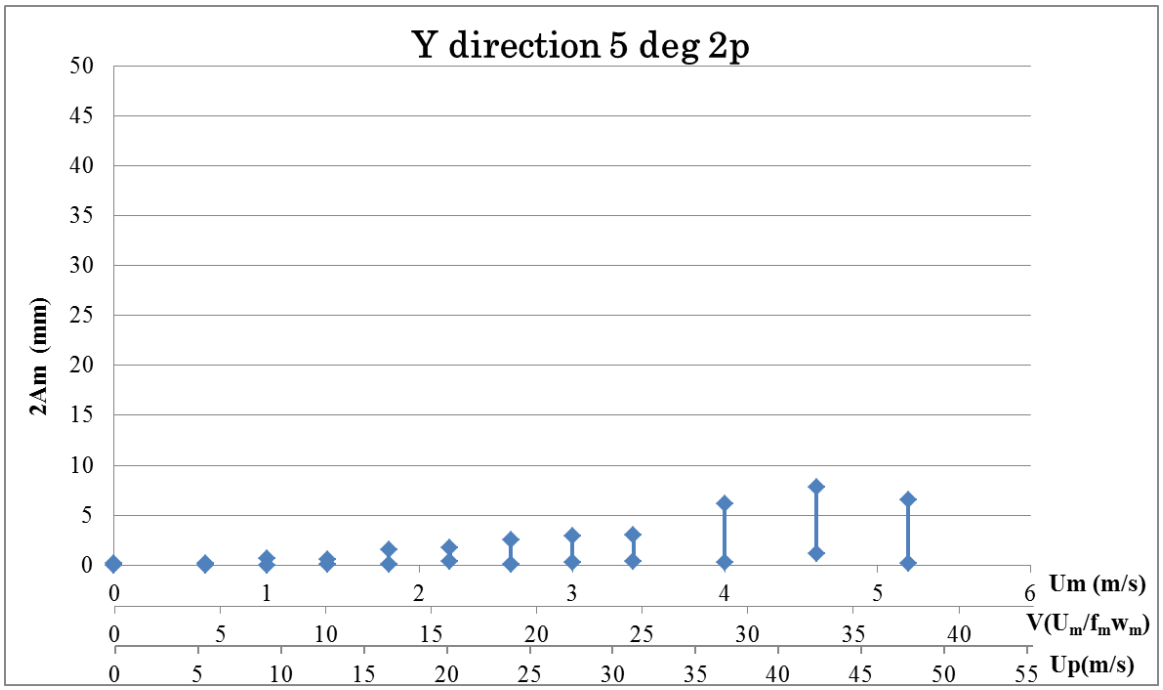

Fig. 6.3.38 Vibration response normal to cable plane (y-direction)

(AC, With L-shaped aerodynamic device (Length of aerodynamic device: 91.7mm (= 11.0m for real bridge) from the top of the tower), Wind direction = 5 [deg.], in turbulent flow) (Stable response amplitude was measured after providing relevant initial disturbance to the model.)

6.3.6 Determination of the length of aerodynamic device

The length of the aerodynamic device was determined based on the tower response with yawing angles 0º and 5º, in both of smooth and turbulent flow conditions. As shown in Table 6.3.4, galloping occurred in the case of smooth flow with yawing angle 5º as well as the case of turbulence with yawing angle 0º for the original configuration. It was confirmed that the aerodynamic device with the length of 91.7mm could suppress the galloping for both cases.

On the other hand, the length of the aerodynamic device should be as small as possible and have enough stabilizing performance. Therefore, aerodynamic devices with different length of 41.7mm (= 5.0m for real bridge), 141.7mm (17.0m) , 191.7mm (23.0m) and 233.4mm (= 28.0m)) were attached to the top of the tower. The responses are shown in Fig. 6.3.39-Fig. 6.3.40 for the cases in smooth flow (Length of the device was fixed to 141.7 [mm].), and Fig. 6.3.41-Fig.6.3.48 for the cases in turbulence.

From these results, it indicates that the length of 3 pieces is an optimal choice by taking the fact that VIV was measured in 141.7mm of the installed length in smooth flow and 0[deg] yawing angle. And this response was stabilized in turbulent flow condition. With the aerodynamic device applied, the galloping was enough suppressed as shown in Table 6.3.6.

Table 6.3.6 After completion (AC, With L-shaped aerodynamic device)

Flow condition	Yawing angle [deg]	Length of aerodynamic device [mm]	Vortex-induced vibration	Galloping	Corresponding figure
Smooth	0	141.7	× in y-direction (15.0m/s~40.0m/s)	o	Fig.6.3.39
	5	141.7	o	o	Fig.6.3.40
Turbulent	0	41.7	o	o	Fig.6.3.41
		141.7	o	o	Fig.6.3.42
		191.7	o	o	Fig.6.3.43
		233.4	o	o	Fig.6.3.44
	5	41.7	o	o	Fig.6.3.45
		141.7	o	o	Fig.6.3.46
		191.7	o	o	Fig.6.3.47
		233.4	o	o	Fig.6.3.48

“o” : The corresponding response was not observed.

“×” : The corresponding response occurred.

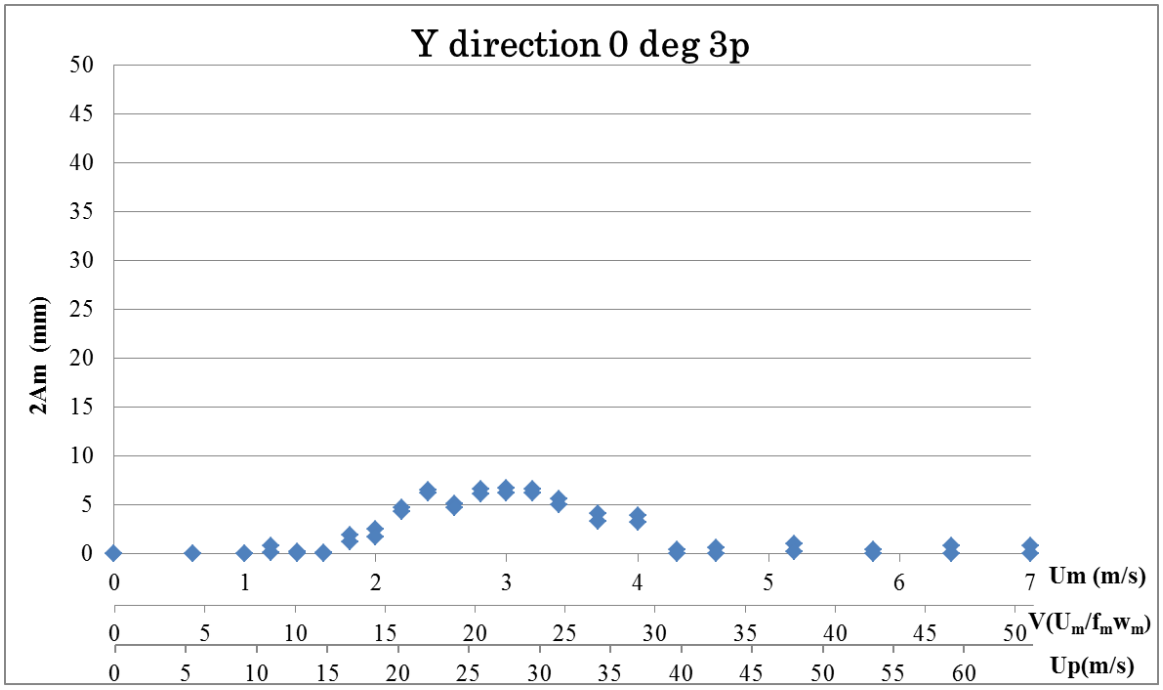

Fig. 6.3.39 Vibration response normal to cable plane (y-direction)
(AC, With L-shaped aerodynamic device (Length of aerodynamic device: 141.7mm (= 17.0m for real bridge) from the top of the tower), Wind direction = 0 [deg.] (along bridge axis), in smooth flow) (Stable response amplitude was measured after providing relevant initial disturbance to the model.)

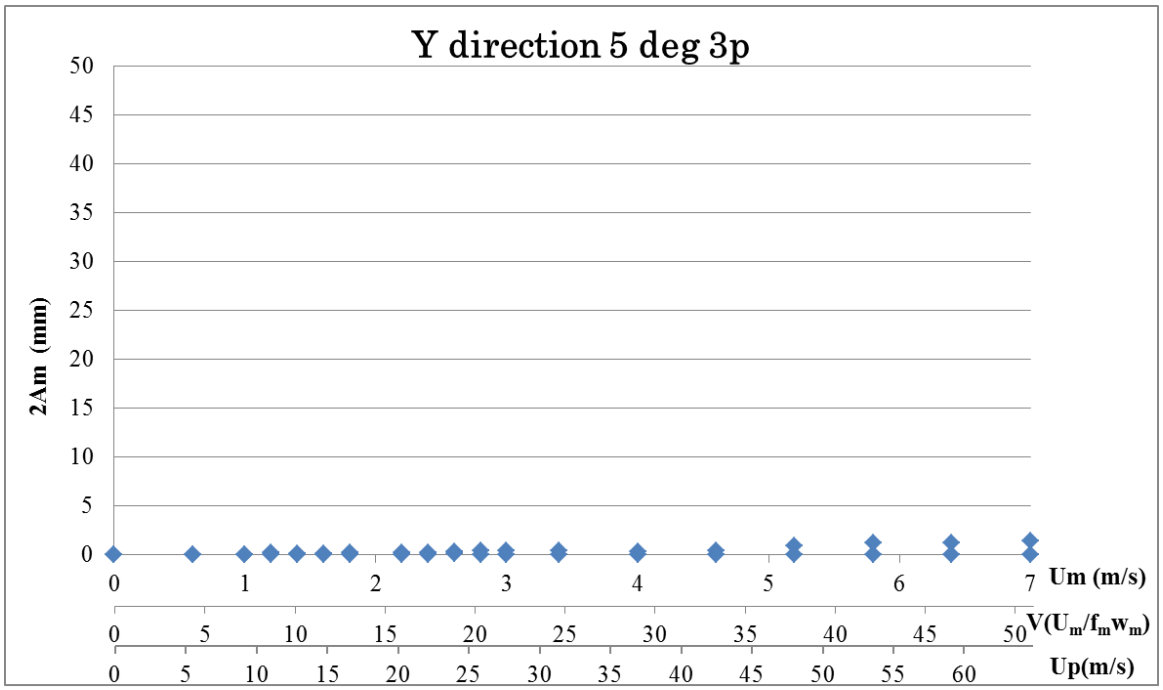

Fig. 6.3.40 Vibration response normal to cable plane (y-direction)
(AC, With L-shaped aerodynamic device (Length of aerodynamic device: 141.7mm (= 17.0m for real bridge) from the top of the tower), Wind direction = 5 [deg.], in smooth flow) (Stable response amplitude was measured after providing relevant initial disturbance to the model.)

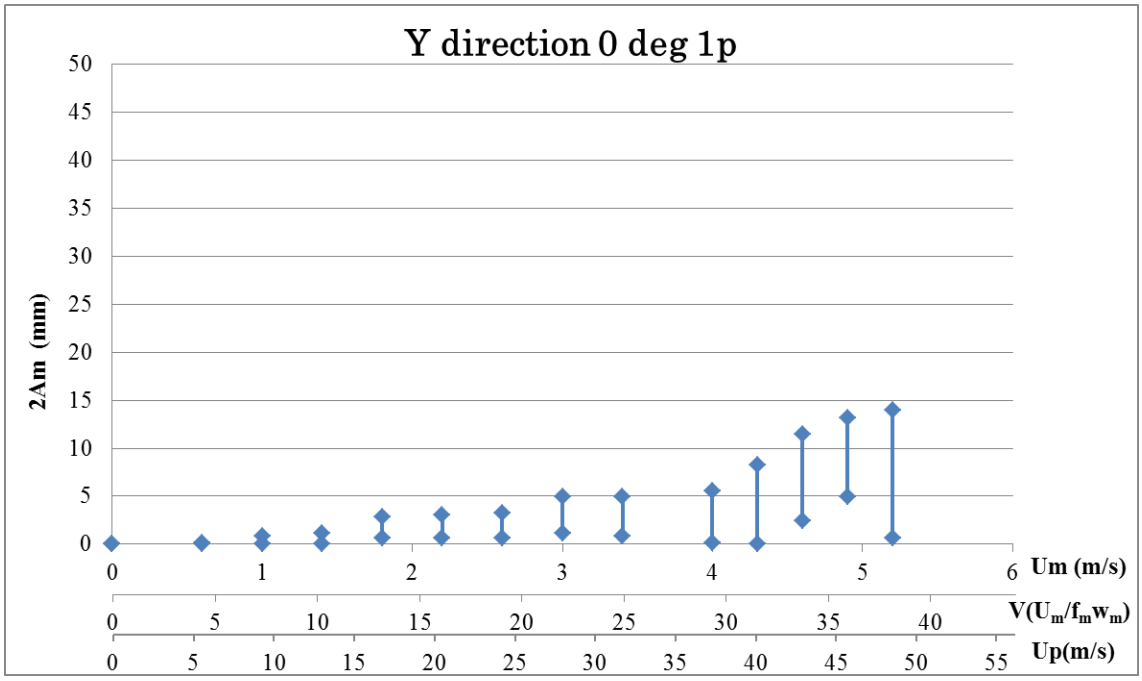

Fig. 6.3.41 Vibration response normal to cable plane (y-direction)
(AC, With L-shaped aerodynamic device (Length of aerodynamic device: 41.7mm (= 5.0m for real bridge) from the top of the tower), Wind direction = 0 [deg.] (along bridge axis), in turbulent flow)
(Stable response amplitude was measured after providing relevant initial disturbance to the model.)

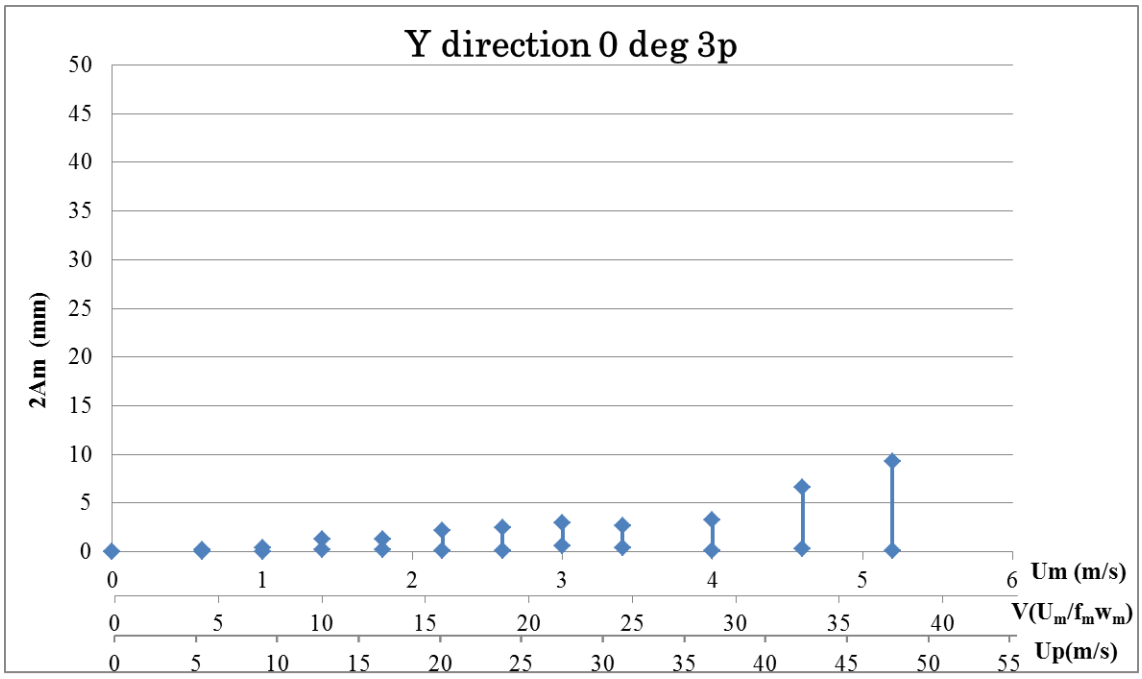

Fig. 6.3.42 Vibration response normal to cable plane (y-direction)
(AC, With L-shaped aerodynamic device (Length of aerodynamic device: 141.7mm (= 17.0m for real bridge) from the top of the tower), Wind direction = 0 [deg.] (along bridge axis), in turbulent flow) (Stable response amplitude was measured after providing relevant initial disturbance to the model.)

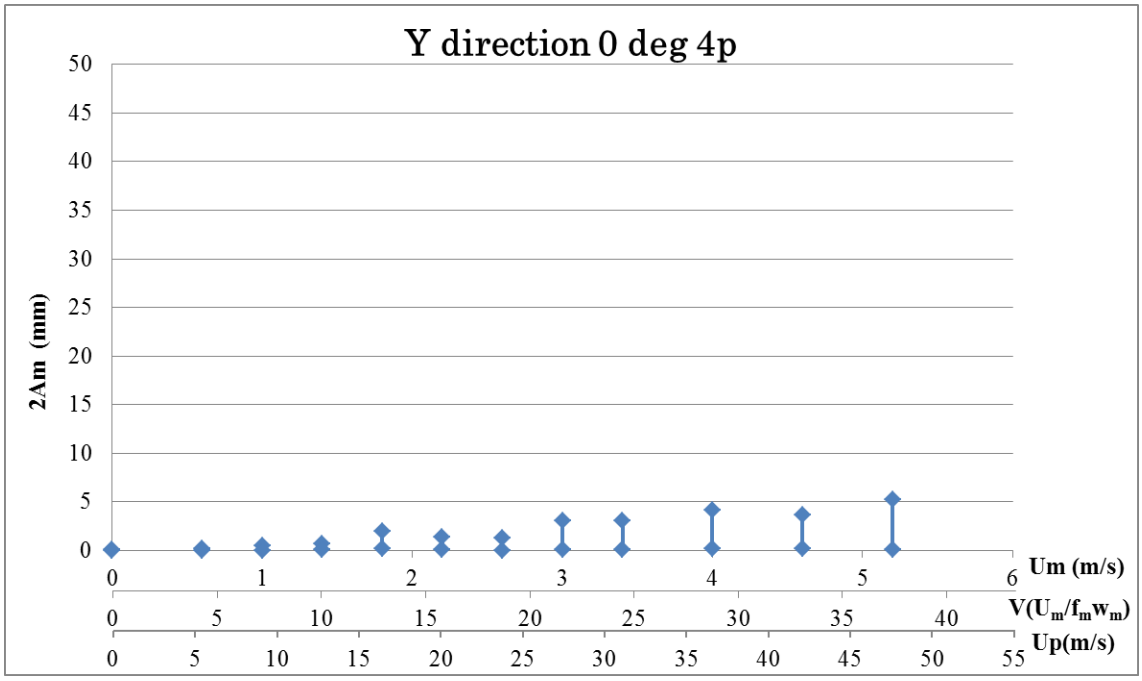

Fig. 6.3.43 Vibration response normal to cable plane (y-direction)
(AC, With L-shaped aerodynamic device (Length of aerodynamic device: 191.7mm (= 23.0m for real bridge) from the top of the tower), Wind direction = 0 [deg.] (along bridge axis), in turbulent flow) (Stable response amplitude was measured after providing relevant initial disturbance to the model.)

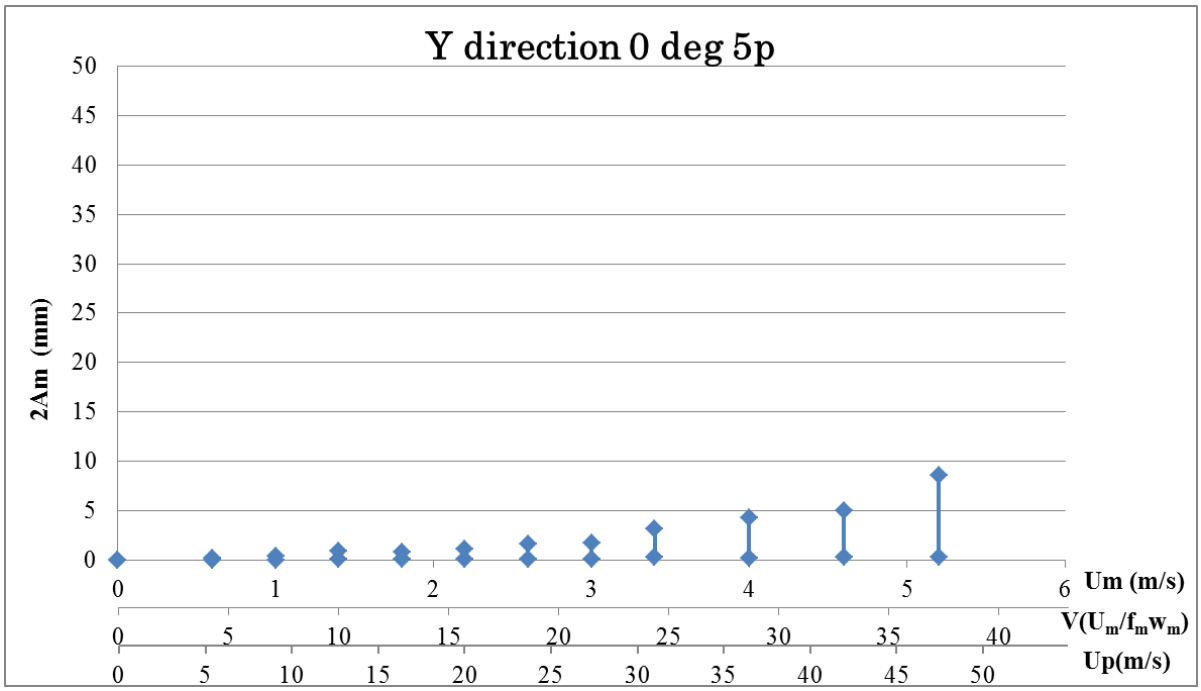

Fig. 6.3.44 Vibration response normal to cable plane (y-direction)
(AC, With L-shaped aerodynamic device (Length of aerodynamic device: 233.4mm (= 28.0m for real bridge) from the top of the tower), Wind direction = 0 [deg.] (along bridge axis), in turbulent flow) (Stable response amplitude was measured after providing relevant initial disturbance to the model.)

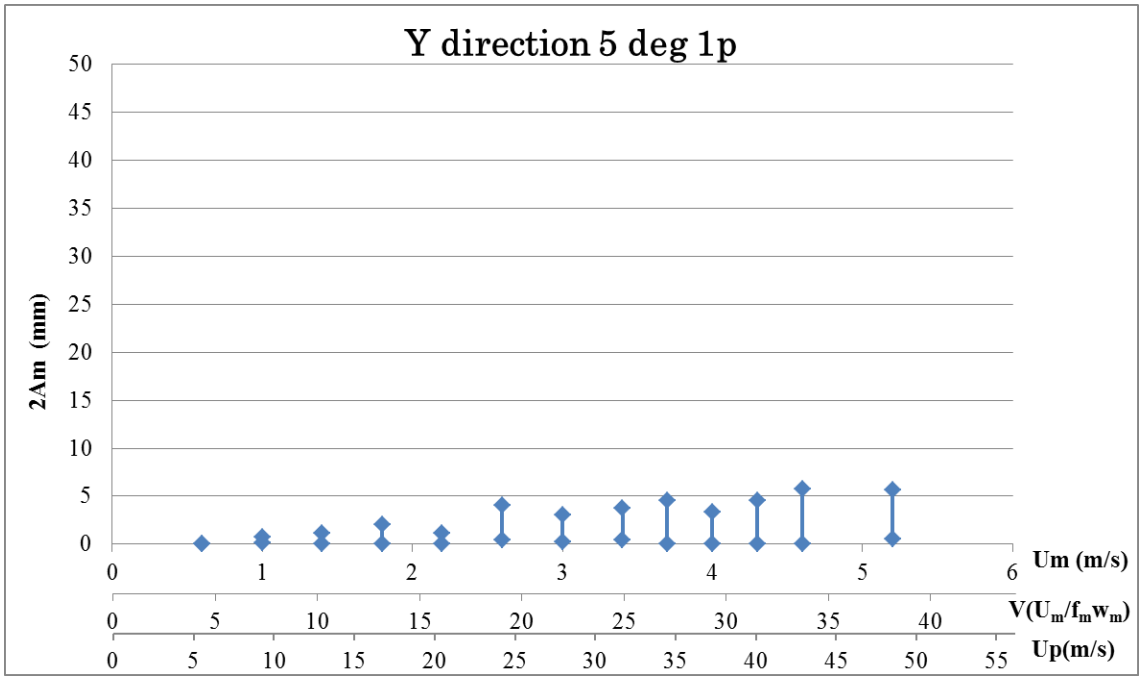

Fig. 6.3.45 Vibration response normal to cable plane (y-direction)
(AC, With L-shaped aerodynamic device (Length of aerodynamic device: 41.7mm (= 5.0m for real bridge) from the top of the tower), Wind direction = 5 [deg.], in turbulent flow) (Stable response amplitude was measured after providing relevant initial disturbance to the model.)

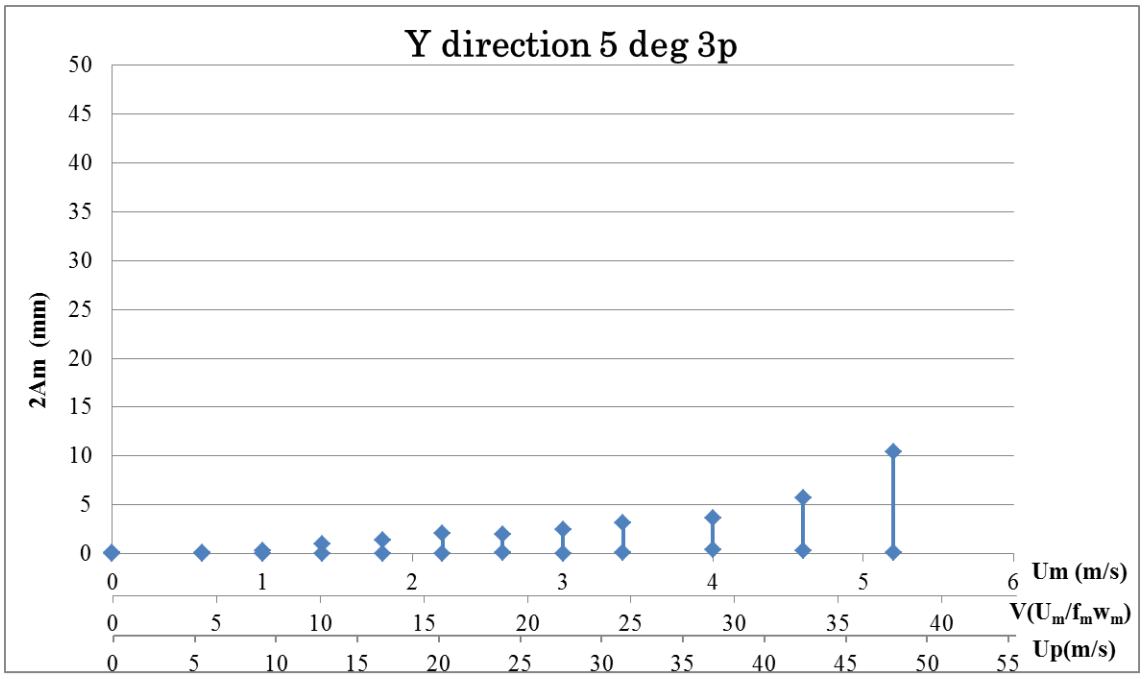

Fig. 6.3.46 Vibration response normal to cable plane (y-direction)

(AC, With L-shaped aerodynamic device (Length of aerodynamic device: 141.7mm (= 17.0m for real bridge) from the top of the tower), Wind direction = 5 [deg.], in turbulent flow) (Stable response amplitude was measured after providing relevant initial disturbance to the model.)

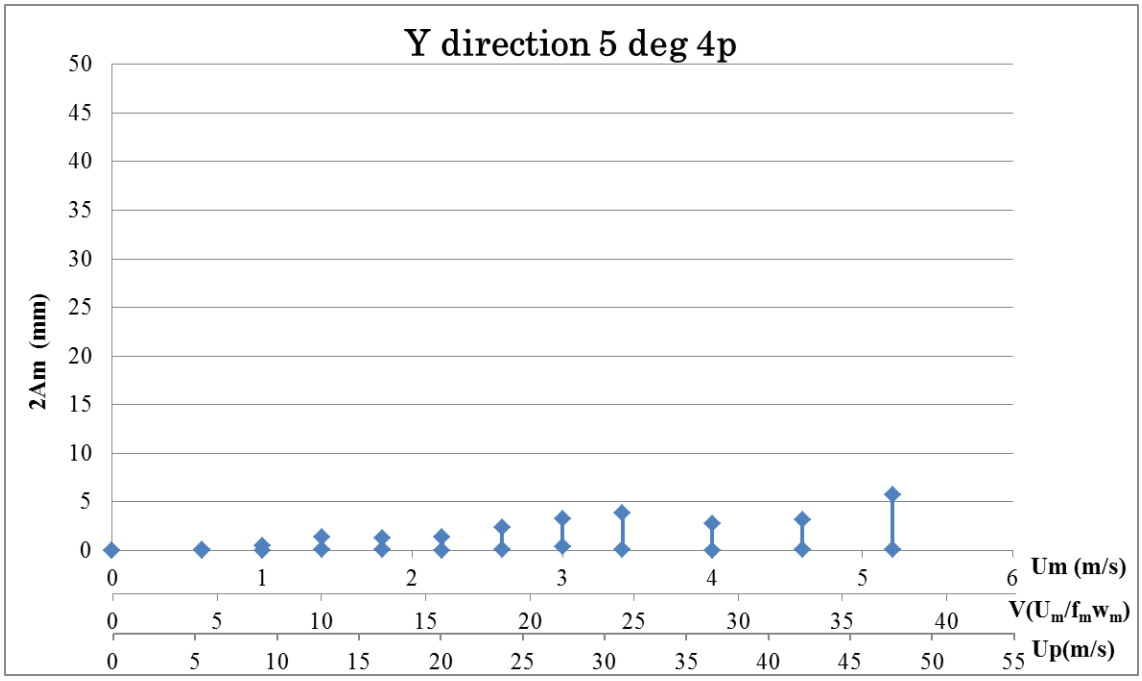

Fig. 6.3.47 Vibration response normal to cable plane (y-direction)

(AC, With L-shaped aerodynamic device (Length of aerodynamic device: 191.7mm (= 23.0m for real bridge) from the top of the tower), Wind direction = 5 [deg.], in turbulent flow) (Stable response amplitude was measured after providing relevant initial disturbance to the model.)

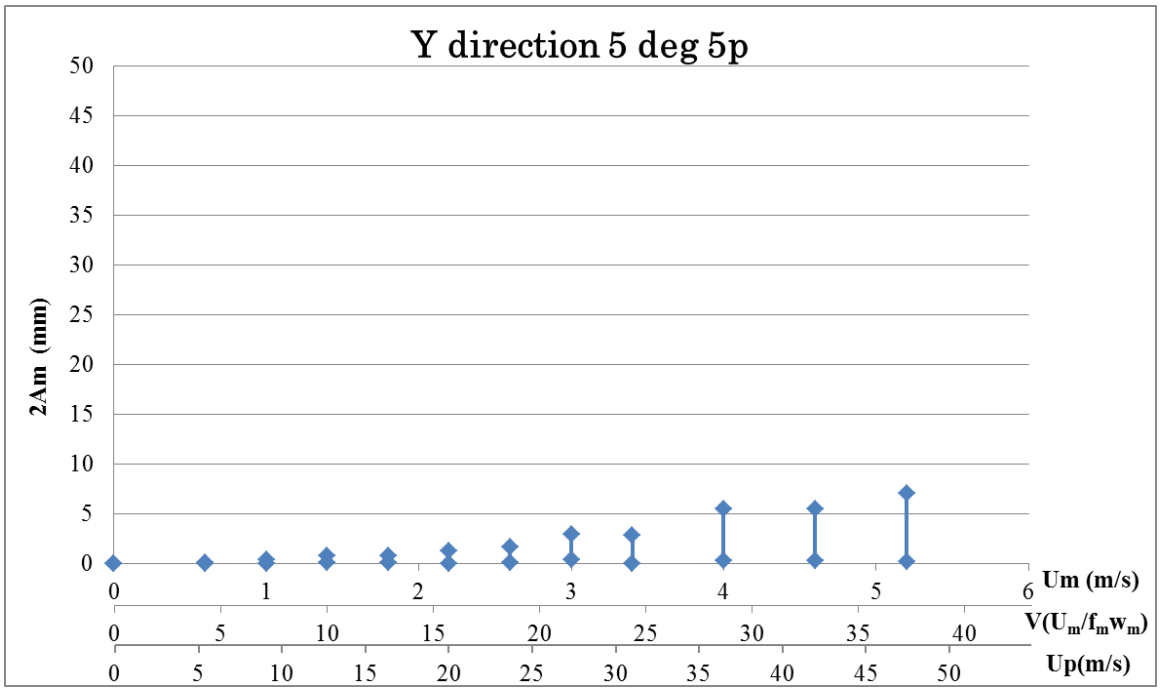

Fig. 6.3.48 Vibration response normal to cable plane (y-direction)
(AC, With L-shaped aerodynamic device (Length of aerodynamic device: 233.4mm (= 28.0m for real bridge) from the top of the tower), Wind direction = 5 [deg.], in turbulent flow) (Stable response amplitude was measured after providing relevant initial disturbance to the model.)

6.4 Aerodynamic derivatives

For a body moving in heaving/torsional 2DOF under the approaching wind speed *U*, the motion-induced lift force and pitching moment is expressed as:

$$\begin{aligned} L &= \frac{1}{2}\rho(2b)U^2\left\{kH_1^*\frac{\dot{\eta}}{U}+kH_2^*\frac{b\dot{\phi}}{U}+k^2H_3^*\phi+k^2H_4^*\frac{\eta}{b}\right\} \\ M &= \frac{1}{2}\rho(2b^2)U^2\left\{kA_1^*\frac{\dot{\eta}}{U}+kA_2^*\frac{b\dot{\phi}}{U}+k^2A_3^*\phi+k^2A_4^*\frac{\eta}{b}\right\} \end{aligned} \tag{6.4.1}$$

Where, *b*: half chord length [m] (*b*=*B*/2), η: heaving displacement [m] (positive downward), ϕ: torsional displacement [rad] (positive nose-up), *k*: reduced frequency ($k = b\omega/U$), ω: circular frequency of the motion, H_i^*, A_i^*, $(i=1,\cdots,4)$: aerodynamic derivatives.

If the given harmonic motion is heaving, $\eta = \eta_0 \sin\omega t$, the lift force L and the pitching moment M are described as follows after subtracting the inertia force from the signal:

$$L = L_{\eta 0}\sin(\omega t - \Psi_{L\eta}), \quad M = M_{\eta 0}\sin(\omega t - \Psi_{M\eta}) \tag{6.4.2}$$

Where, η_0: heaving amplitude, , $L_{\eta 0}$: amplitude of lift force, $M_{\eta 0}$: amplitude of pitching moment, $\Psi_{L\eta}$: phase lag of L from η, $\Psi_{M\eta}$: phase lag of M from η.

Then, eq. (7.3.1) is expressed as follows:

$$\begin{aligned} L &= \frac{1}{2}\rho(2b)U^2\left\{kH_1^*\frac{\dot{\eta}}{U}+k^2H_4^*\frac{\eta}{b}\right\} \\ M &= \frac{1}{2}\rho(2b^2)U^2\left\{kA_1^*\frac{\dot{\eta}}{U}+k^2A_4^*\frac{\eta}{b}\right\} \end{aligned} \tag{6.4.3}$$

And the aerodynamic derivatives are obtained by eqs. (7.3.2) and (7.3.3) as:

$$H_1^* = -\frac{L_{\eta 0}\sin\Psi_{L\eta}}{\rho b^2\omega^2\eta_0}, \quad H_4^* = \frac{L_{\eta 0}\cos\Psi_{L\eta}}{\rho b^2\omega^2\eta_0}, \quad A_1^* = -\frac{M_{\eta 0}\sin\Psi_{L\eta}}{\rho b^3\omega^2\eta_0}, \quad A_4^* = \frac{M_{\eta 0}\cos\Psi_{L\eta}}{\rho b^3\omega^2\eta_0} \tag{6.4.4}$$

Similarly, if the given harmonic motion is torsional, $\phi = \phi_0 \sin \omega t$, the lift force L and the pitching moment M are described as follows after subtracting the inertia force from the signal:

$$L = L_{\phi 0} \sin\left(\omega t - \Psi_{L\phi}\right), \quad M = M_{\phi 0} \sin\left(\omega t - \Psi_{M\phi}\right) \tag{6.4.5}$$

Where, η_0 : heaving amplitude, , $L_{\phi 0}$: amplitude of lift force, $M_{\phi 0}$: amplitude of pitching moment, $\Psi_{L\phi}$: phase lag of L from ϕ, $\Psi_{M\phi}$: phase lag of M from ϕ,.

And the aerodynamic derivatives are obtained as:

$$H_2^* = -\frac{L_{\phi 0} \sin \Psi_{L\phi}}{\rho b^3 \omega^2 \phi_0}, \quad H_3^* = \frac{L_{\phi 0} \cos \Psi_{L\phi}}{\rho b^3 \omega^2 \phi_0}, \quad A_2^* = -\frac{M_{\phi 0} \sin \Psi_{M\phi}}{\rho b^4 \omega^2 \phi_0}, \quad A_3^* = \frac{L_{\phi 0} \cos \Psi M_{M\phi}}{\rho b^4 \omega^2 \phi_0} \tag{6.4.6}$$

The result is shown in Fig.6.4.1 to Fig.6.4. .

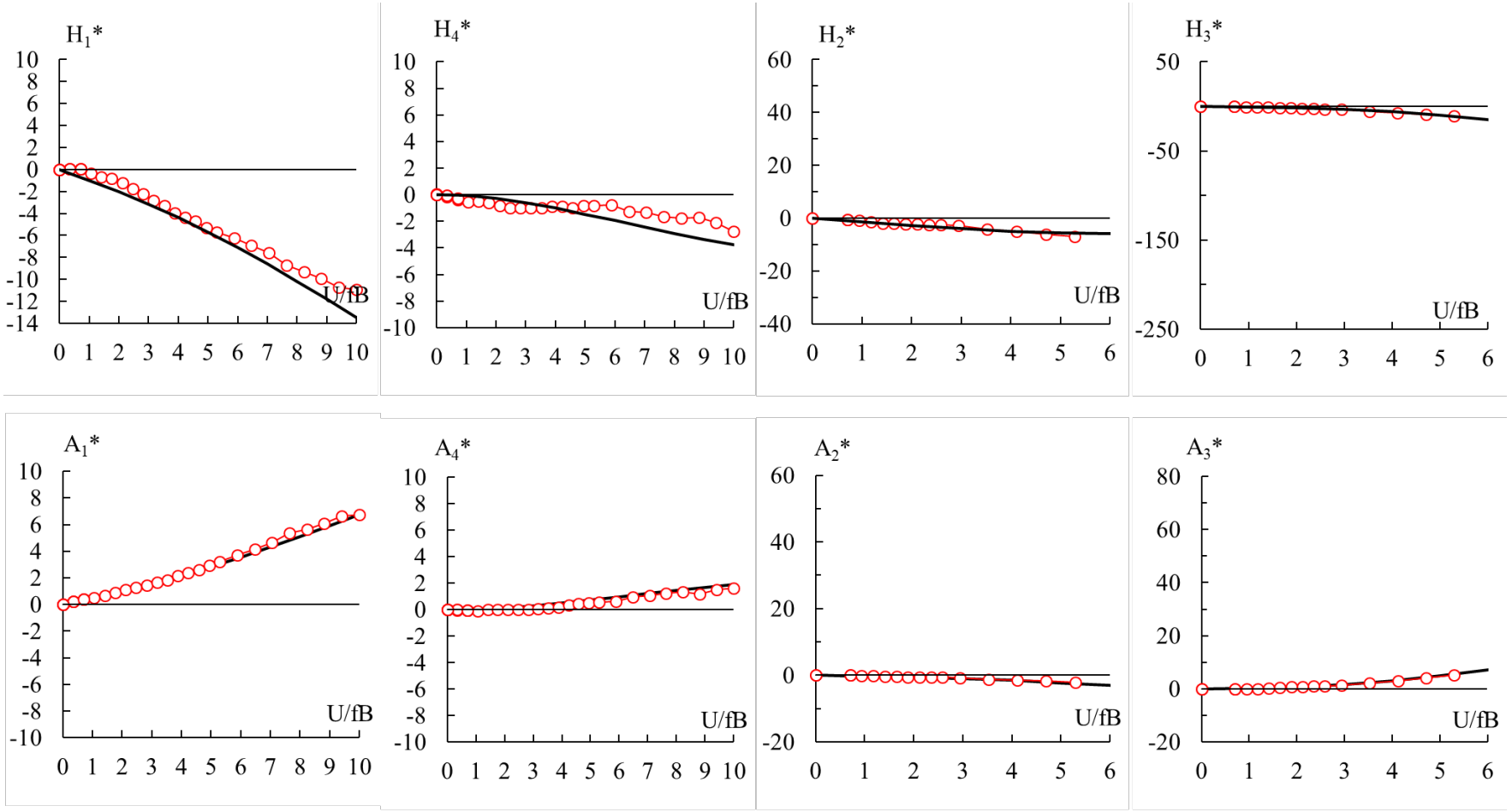

Fig.6.4.1 Aerodynamic derivatives (under construction stage, in smooth flow, incidence angle = 0 [deg.])

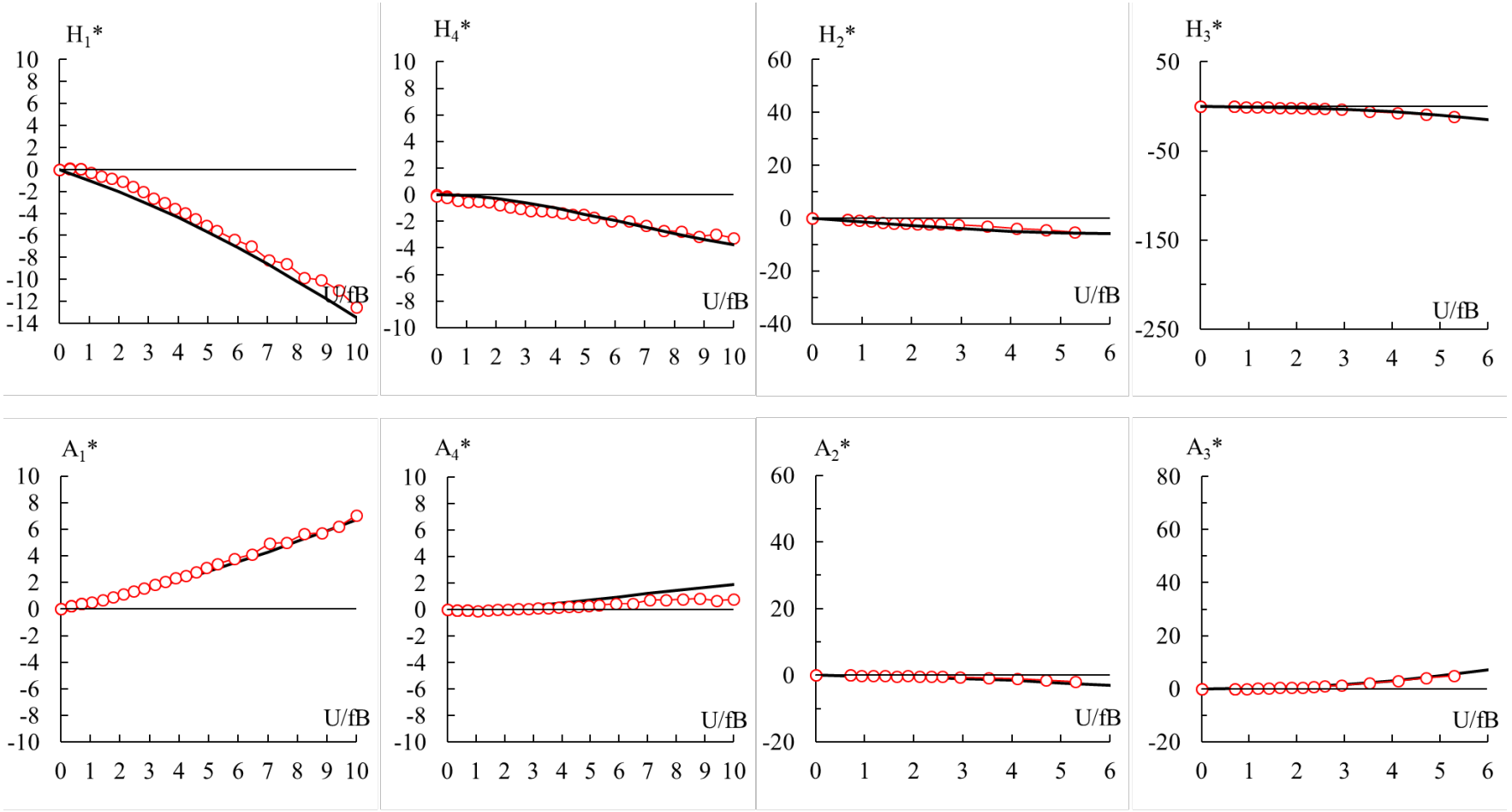

Fig.6.4.2 Aerodynamic derivatives (under construction stage, in smooth flow, incidence angle = +3 [deg.])

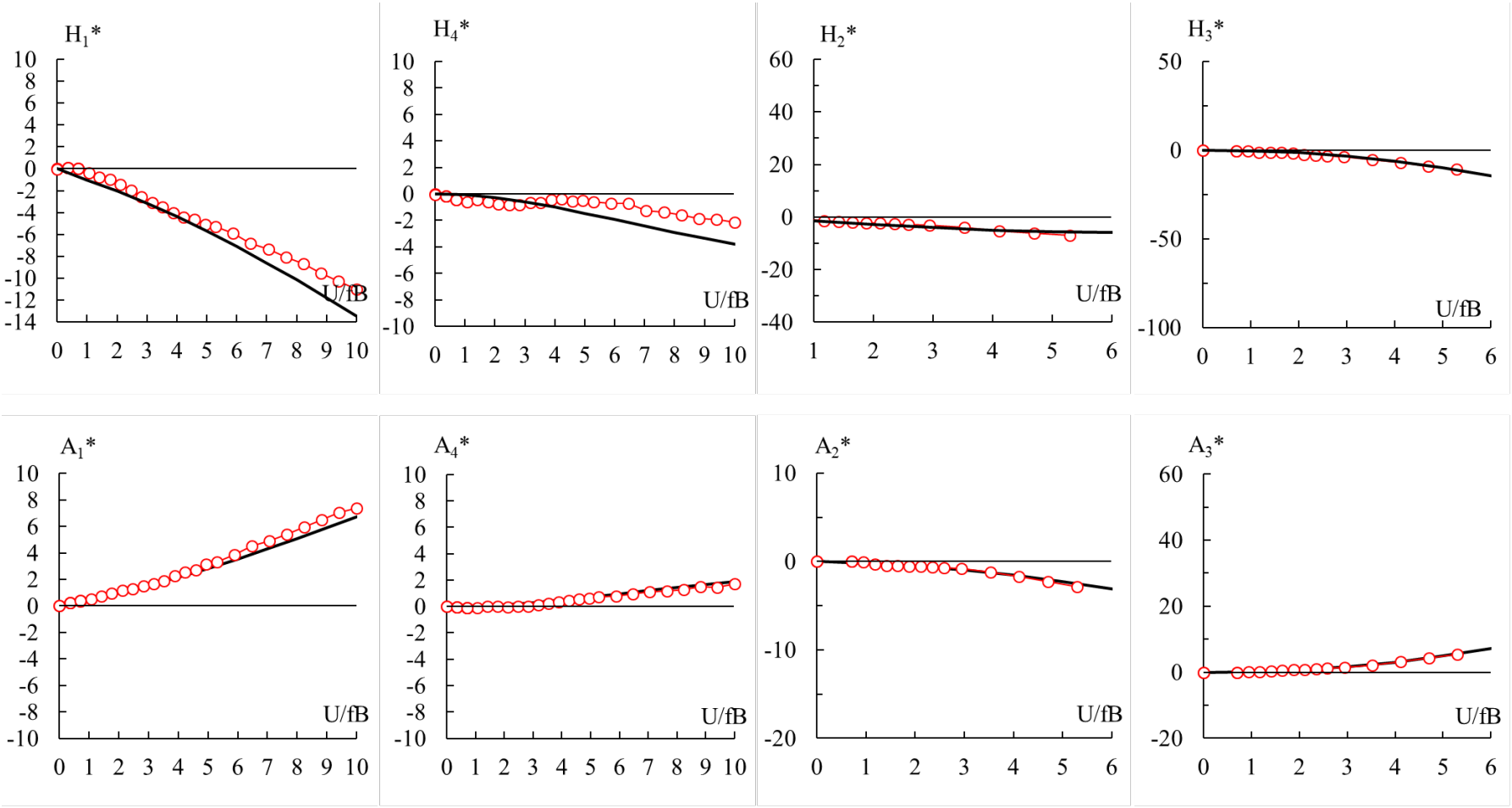

Fig.6.4.3 Aerodynamic derivatives (under construction stage, in smooth flow, incidence angle = -3 [deg.])

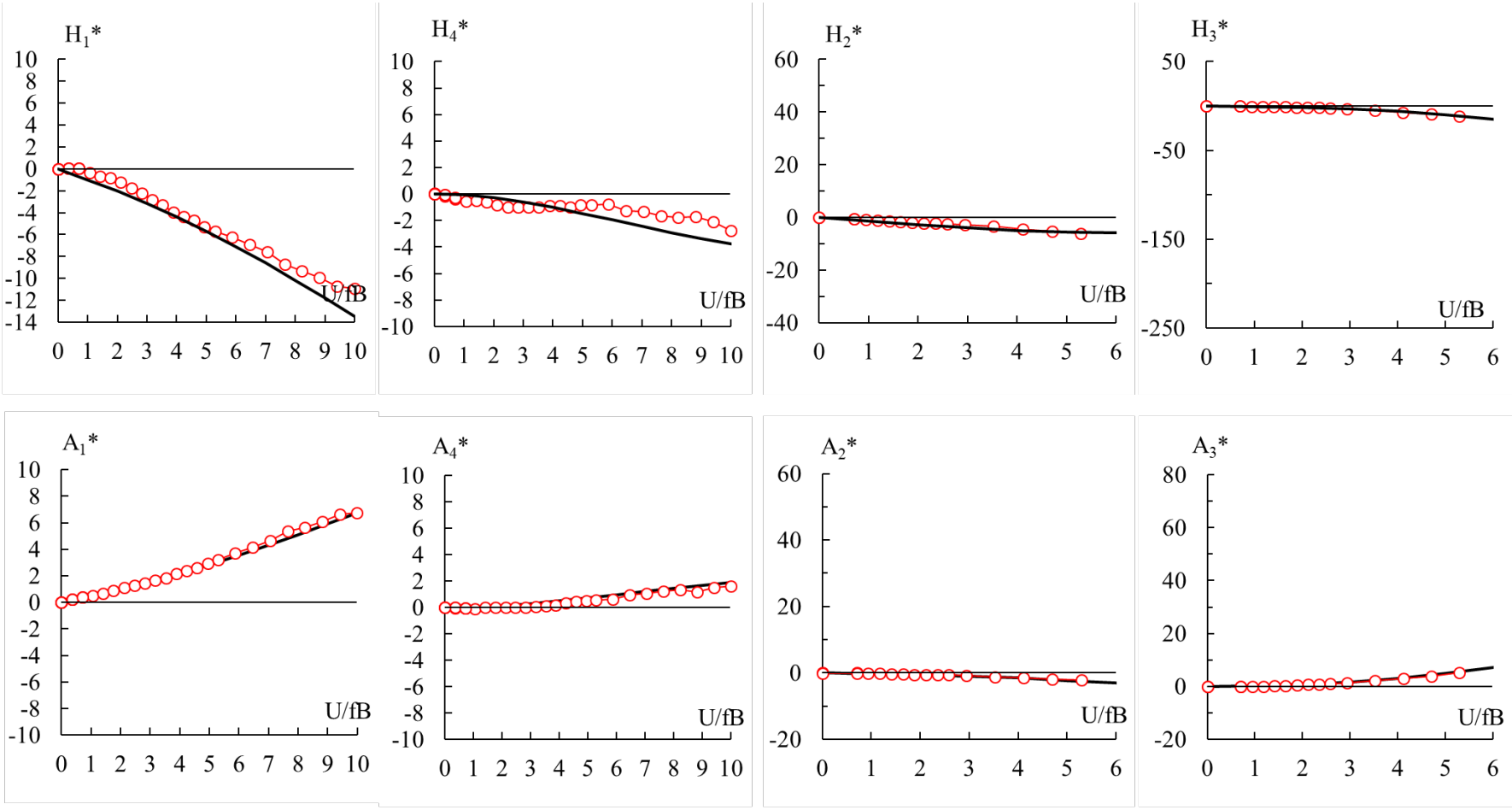

Fig.6.4.4 Aerodynamic derivatives (under construction stage, in turbulent flow, incidence angle = 0 [deg.])

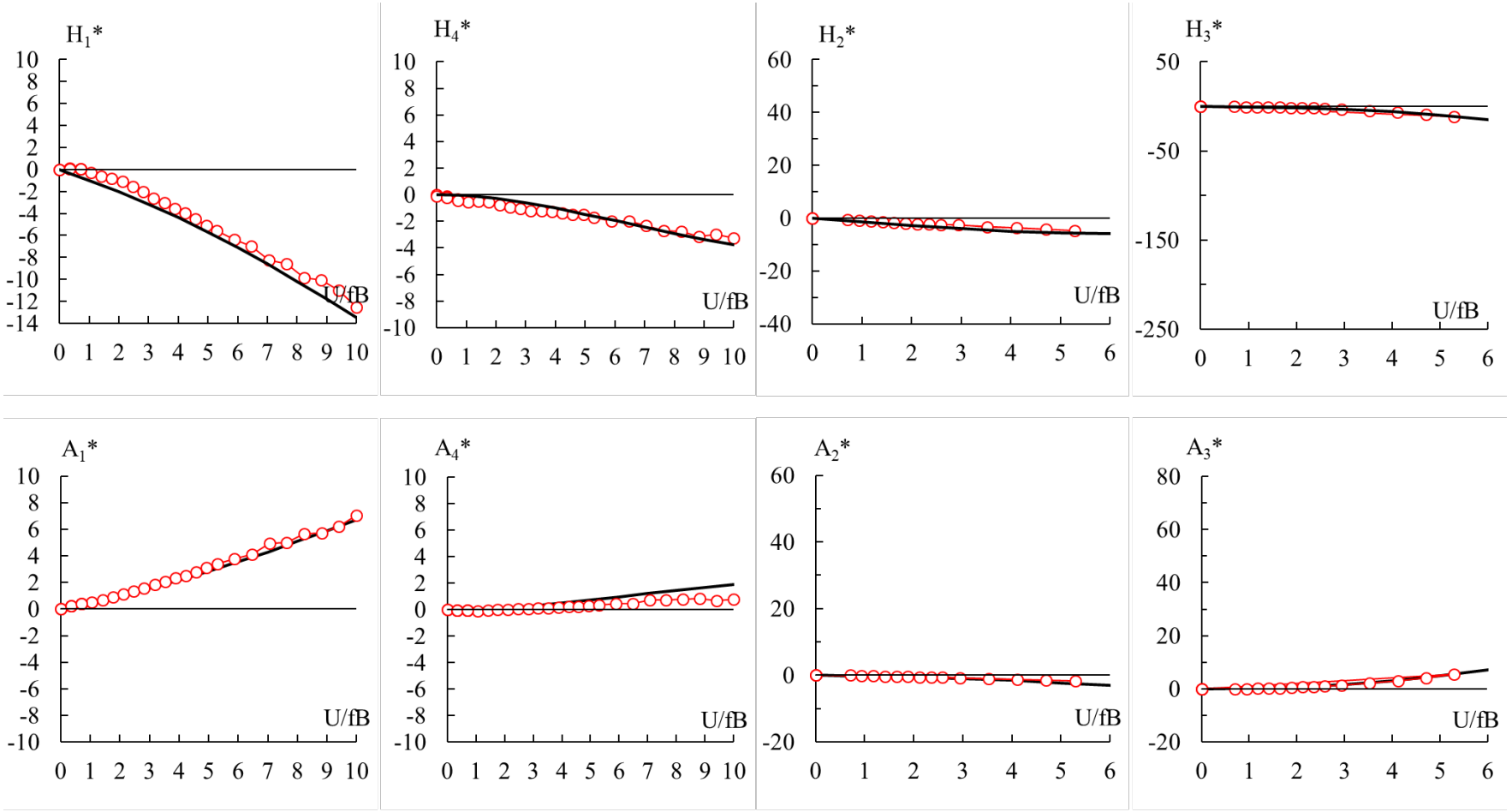

Fig.6.4.5 Aerodynamic derivatives (under construction stage, in turbulent flow, incidence angle = +3 [deg.])

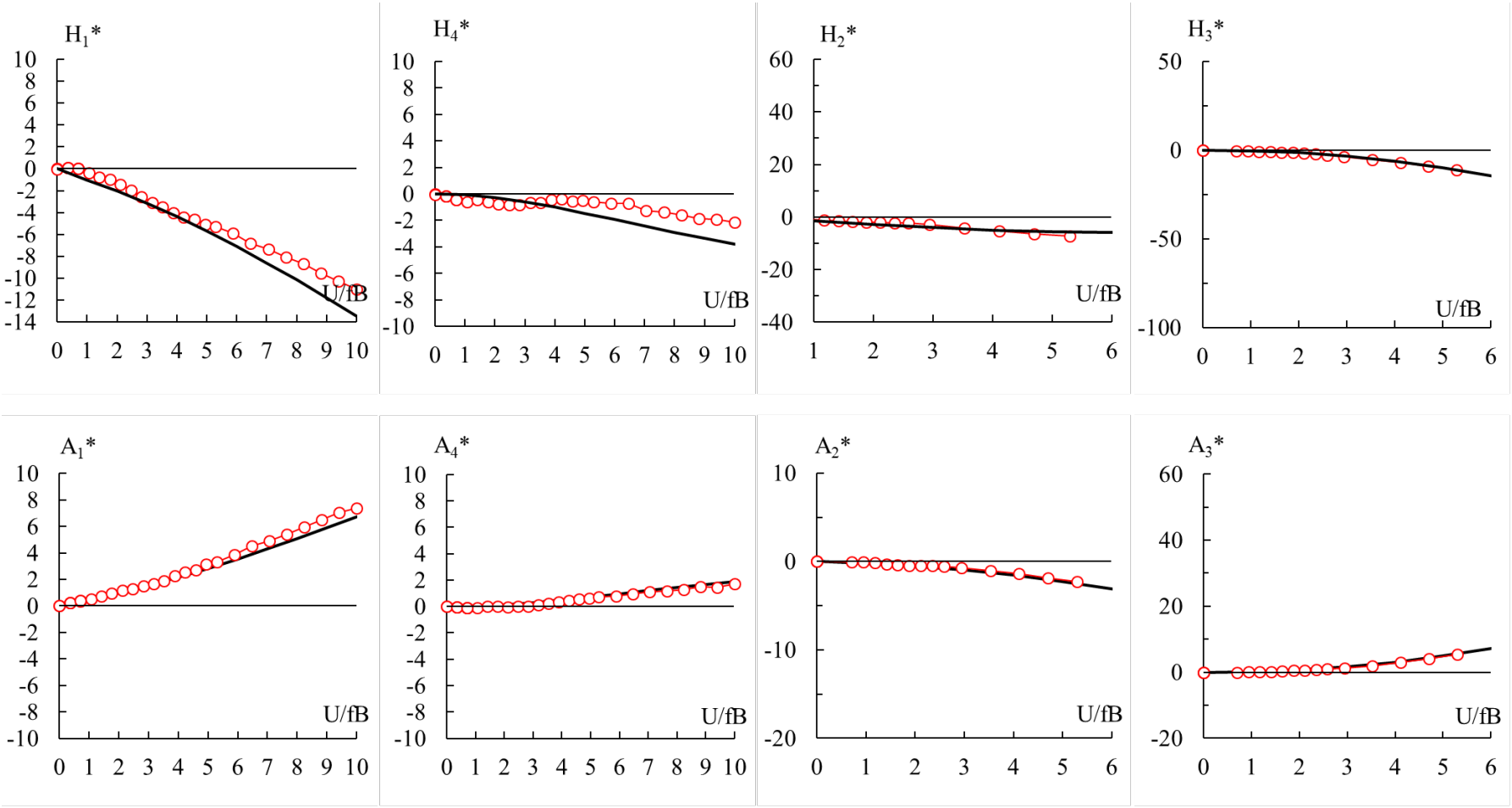

Fig.6.4.6 Aerodynamic derivatives (under construction stage, in turbulent flow, incidence angle = -3 [deg.])

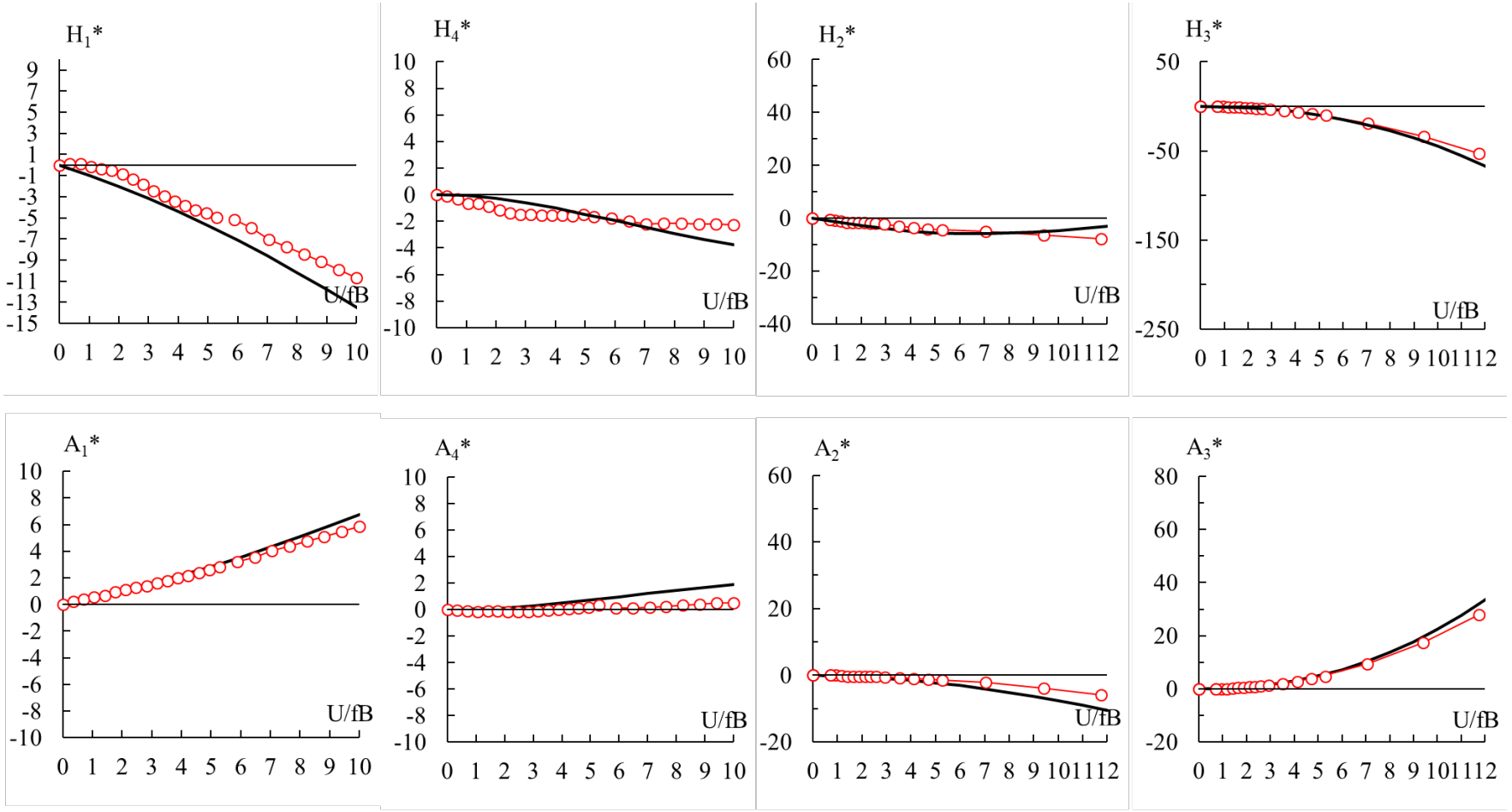

Fig.6.4.7 Aerodynamic derivatives (after completion stage, in smooth flow, incidence angle = 0 [deg.])

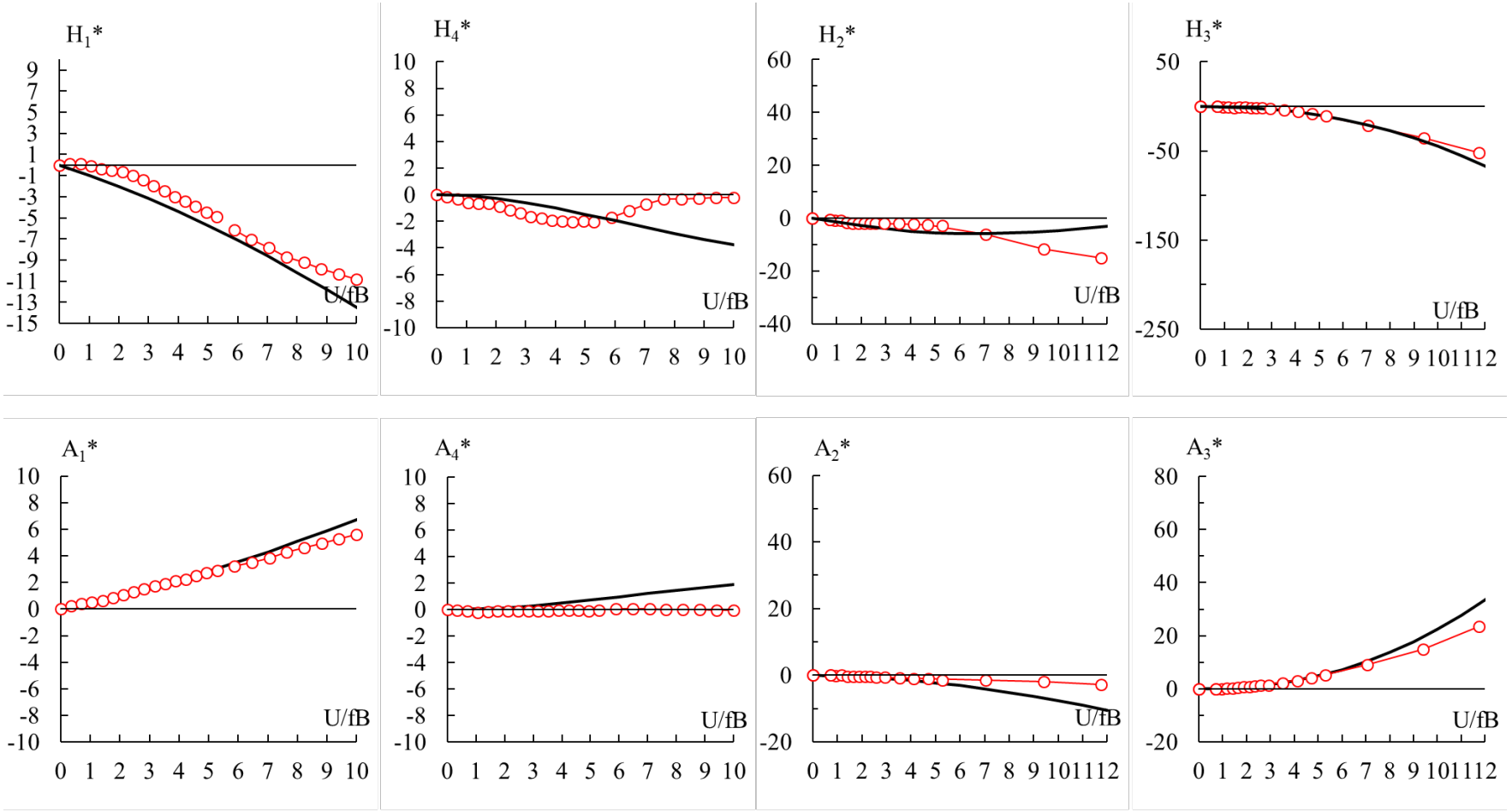

Fig.6.4.8 Aerodynamic derivatives (after completion stage, in smooth flow, incidence angle = +3 [deg.])

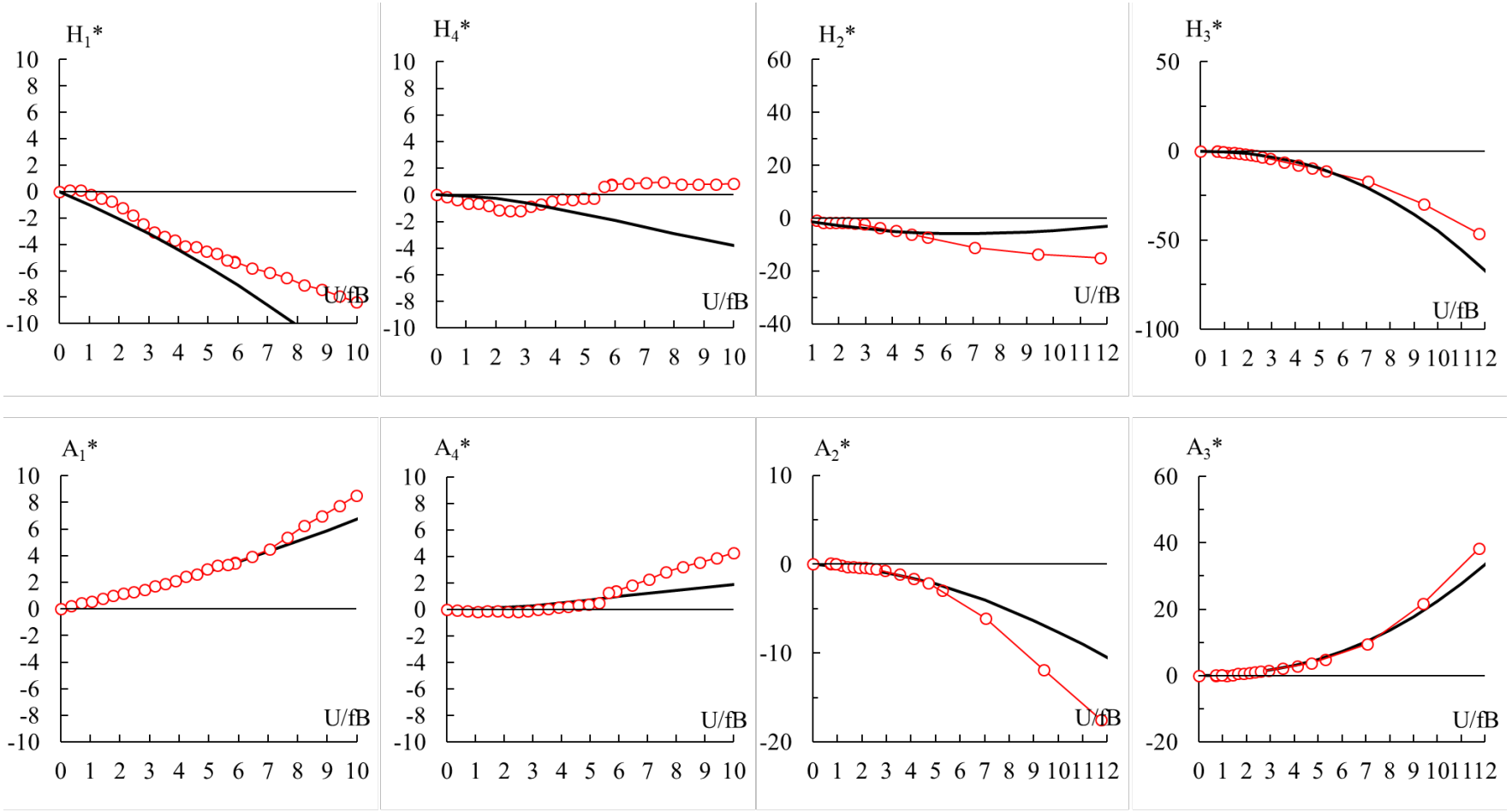

Fig.6.4.9 Aerodynamic derivatives (after completion stage, in smooth flow, incidence angle = -3 [deg.])

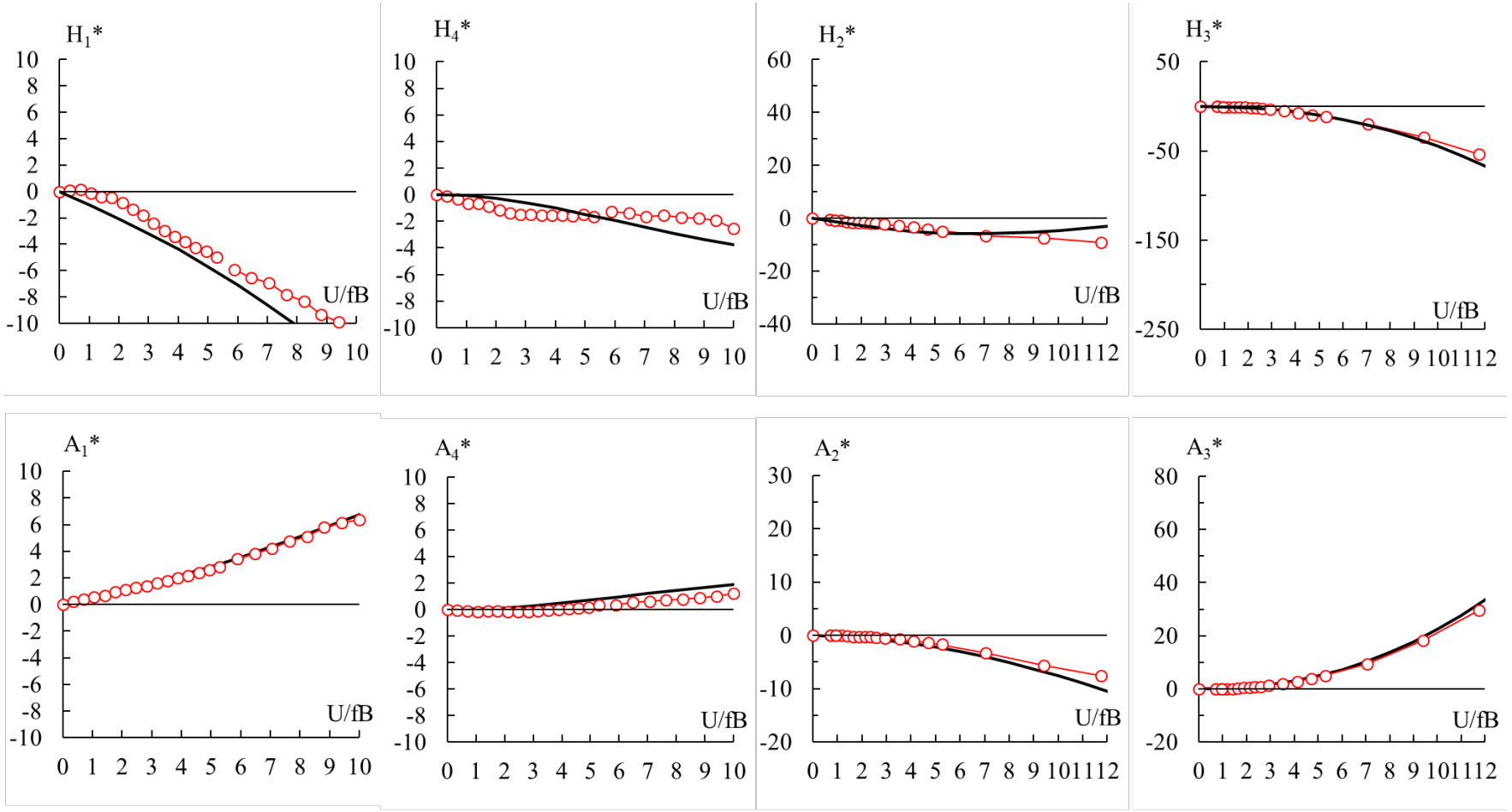

Fig.6.4.10 Aerodynamic derivatives (after completion stage, in turbulent flow, incidence angle = 0 [deg.])

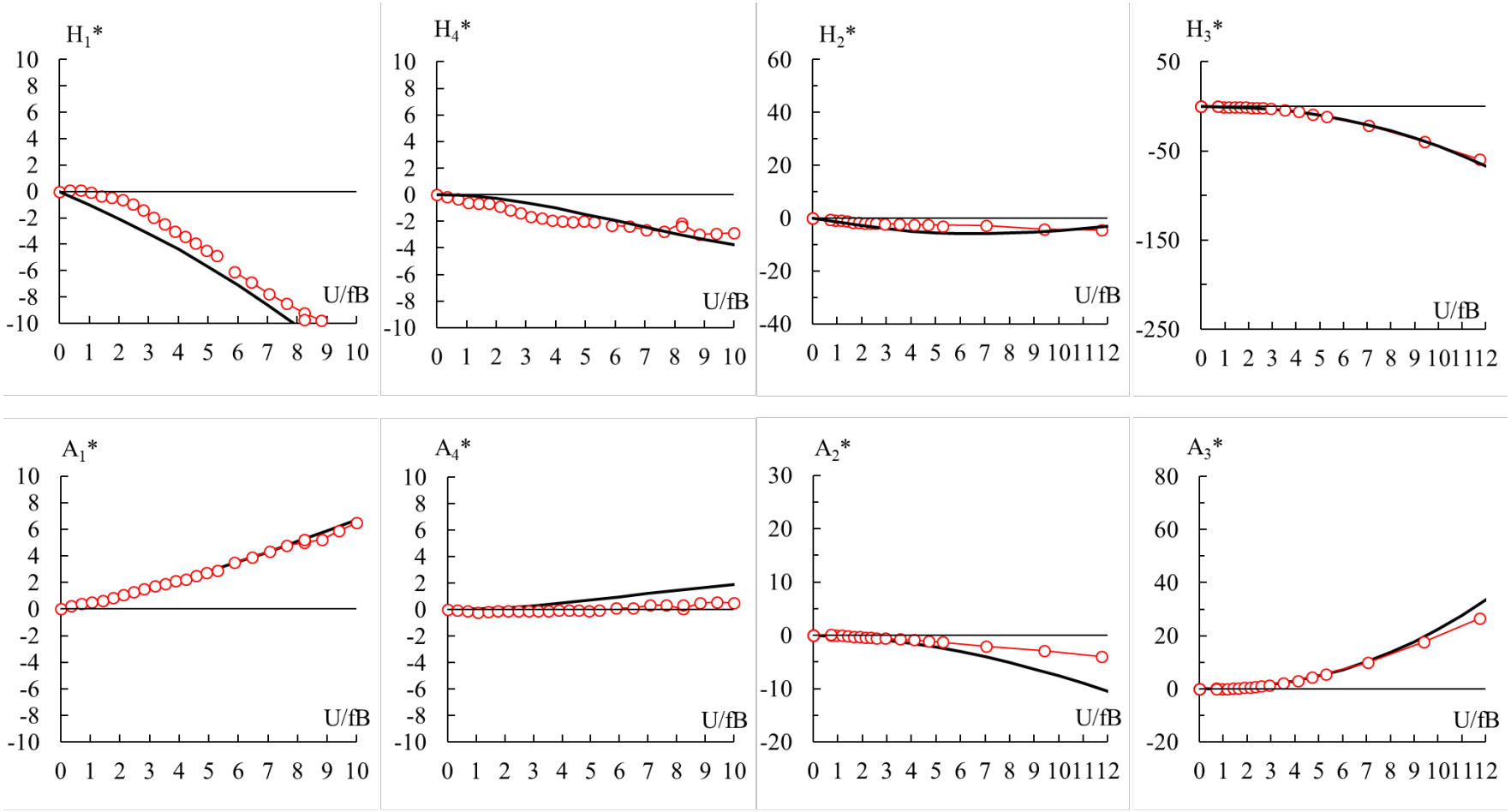

Fig.6.4.11 Aerodynamic derivatives (after completion stage, in turbulent flow, incidence angle = +3 [deg.])

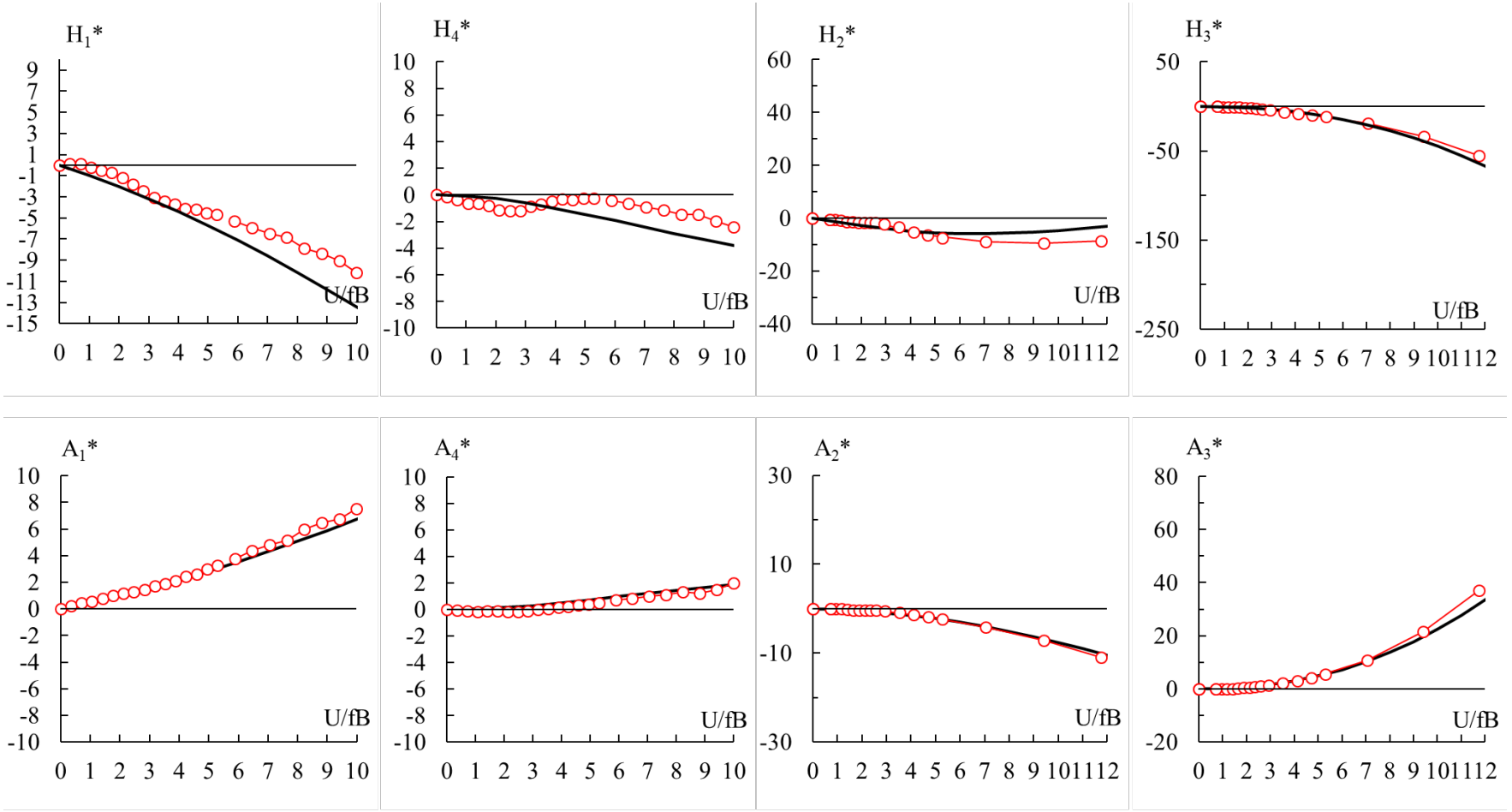

Fig.6.4.12 Aerodynamic derivatives (after completion stage, in turbulent flow, incidence angle = -3 [deg.])

6.5 Aero-static force components

The definition of each aerodynamic force coefficient is as follows:

Drag force coefficient:

$$C_D = \frac{drag \quad force}{\frac{1}{2}\rho U^2 DL} \tag{6.5.1}$$

Lift force coefficient:

$$C_L = \frac{lift \quad force}{\frac{1}{2}\rho U^2 BL} \tag{6.5.2}$$

Pitching moment:

$$C_M = \frac{pitching \quad moment}{\frac{1}{2}\rho U^2 B^2 L} \tag{6.5.3}$$

Where, *drag force*, *lift force* and *pitching moment*: force component on the section model measured in wind tunnel test (unit [N] for drag and lift forces, [kgm] for pitching moment),

C_D: drag force coefficient, C_L: lift force coefficient, C_M: pitching moment coefficient,

ρ: air density [kg/m^3], *U*: wind velocity [m/s], *D*: deck height (*D*=0.0311 [m]), *B*: deck width (*B*=0.3344 [m]), *L*: span length of the section model (L=900 [mm]).

The results are shown in Fig.6.5.1 to

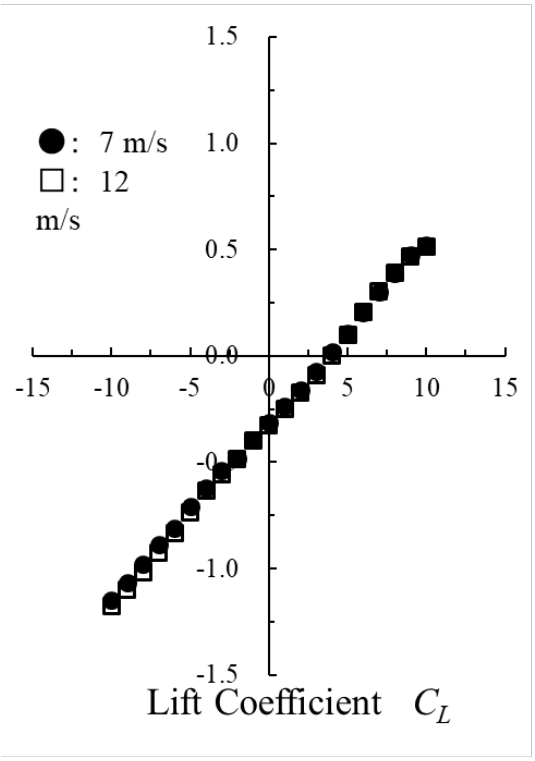

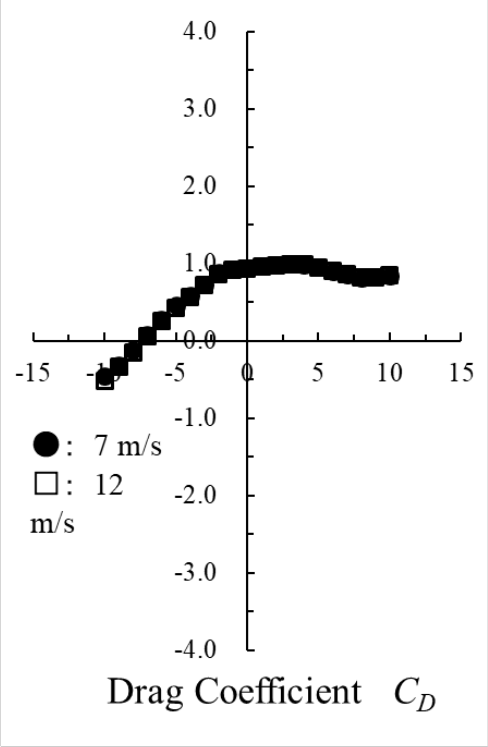

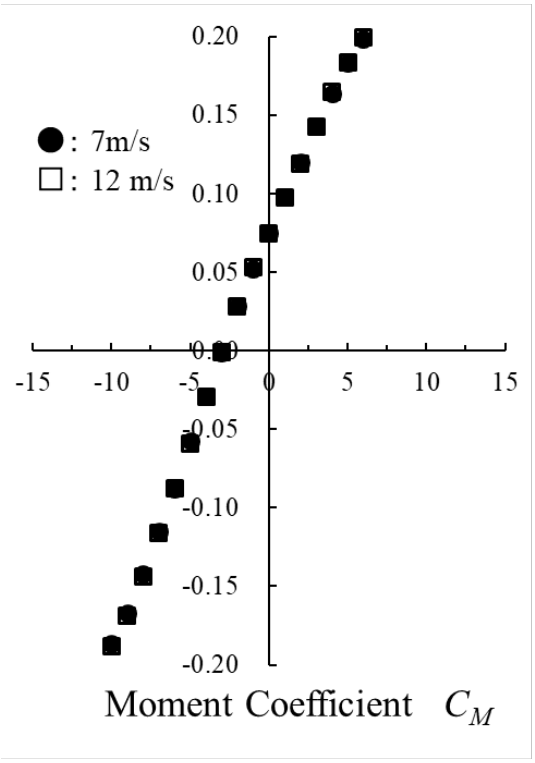

Fig.6.5.1 Aero-static force components (under construction stage, in smooth flow)

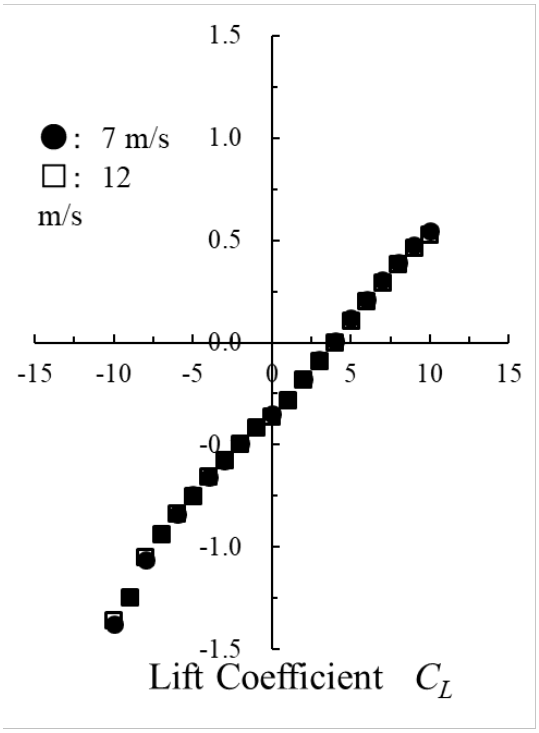

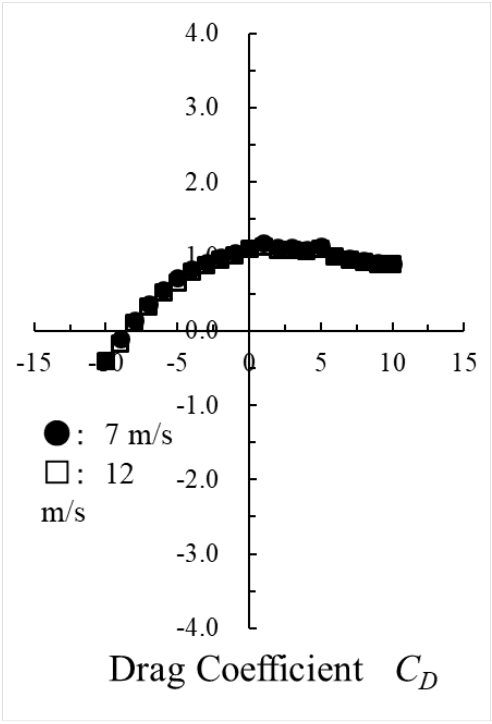

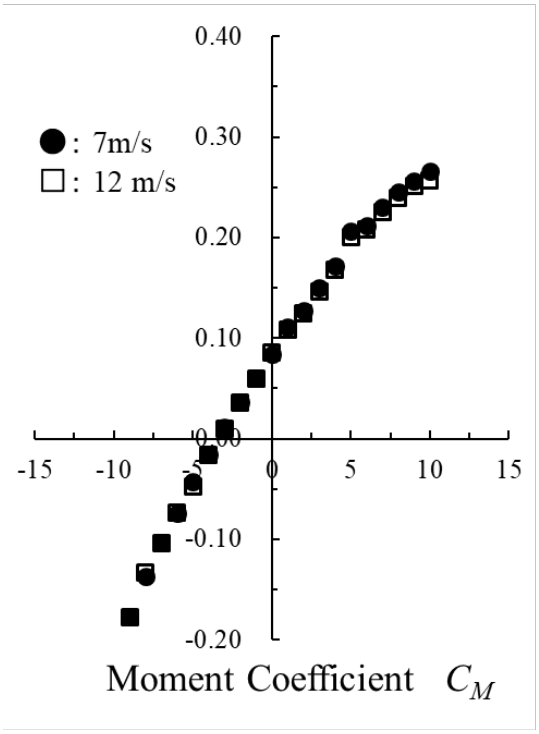

Fig.6.5.2 Aero-static force components (under construction stage, in turbulent flow)

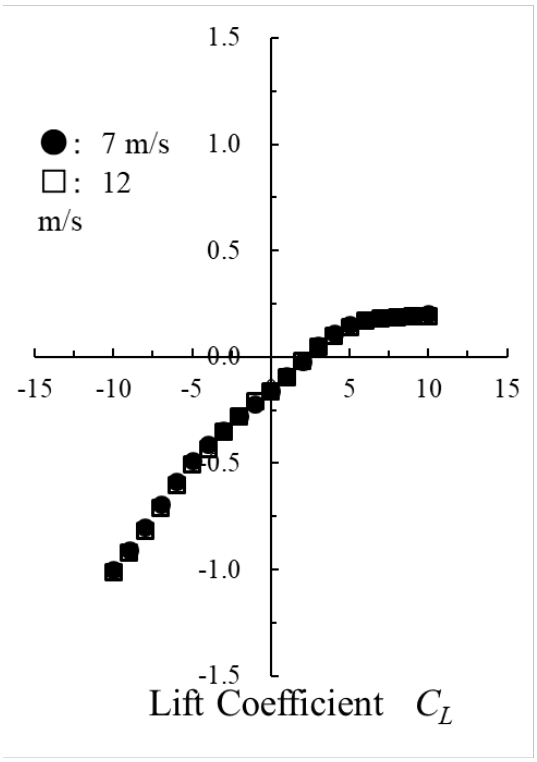

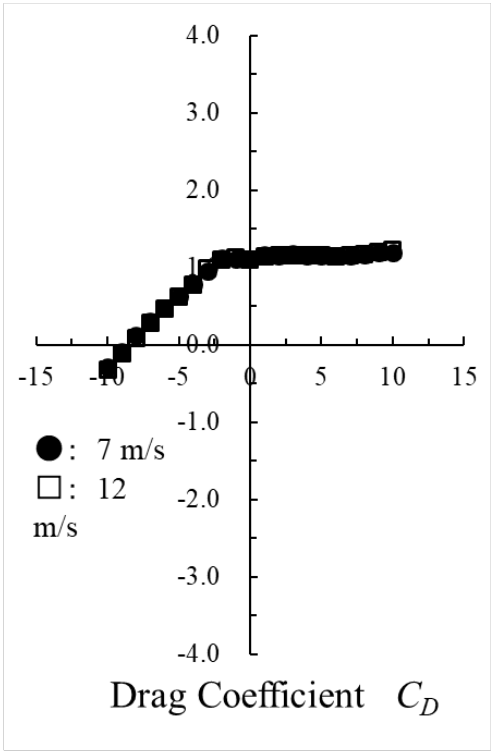

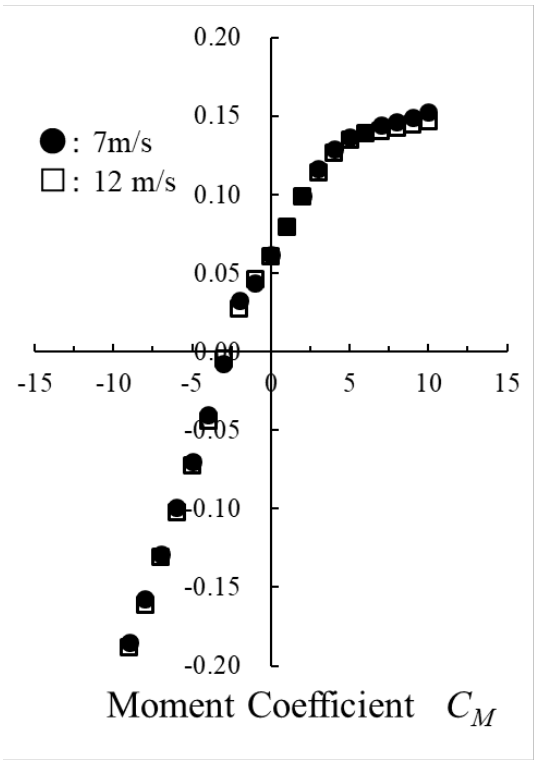

Fig.6.5.3 Aero-static force components (after completion stage, in smooth flow)

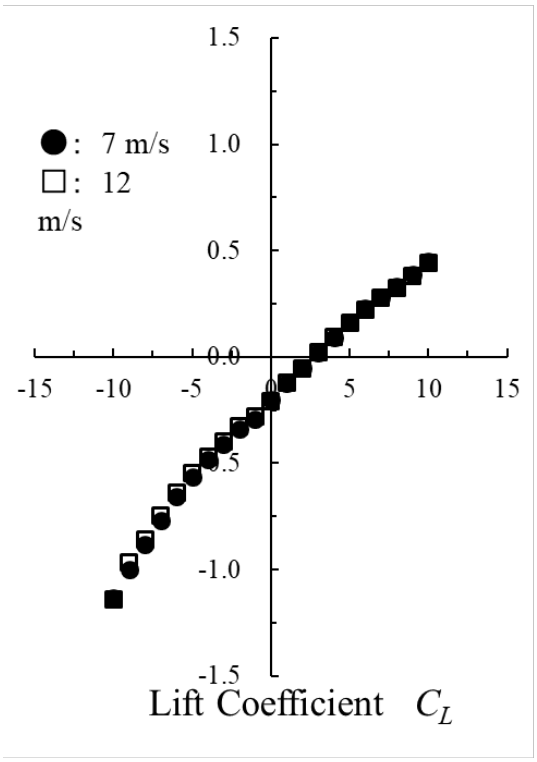

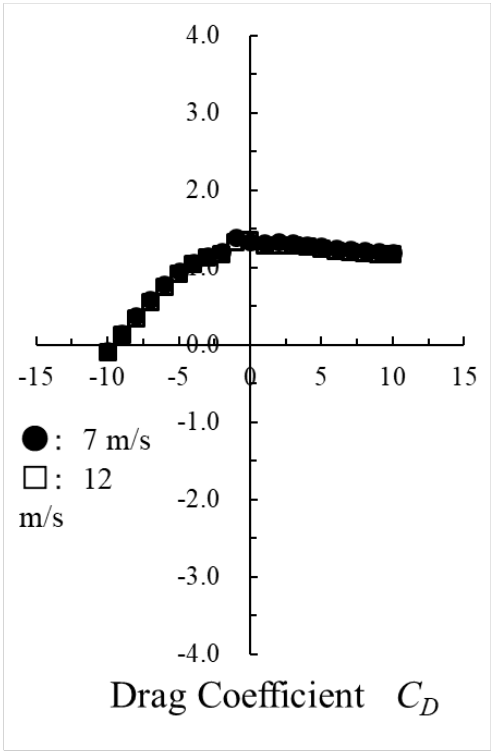

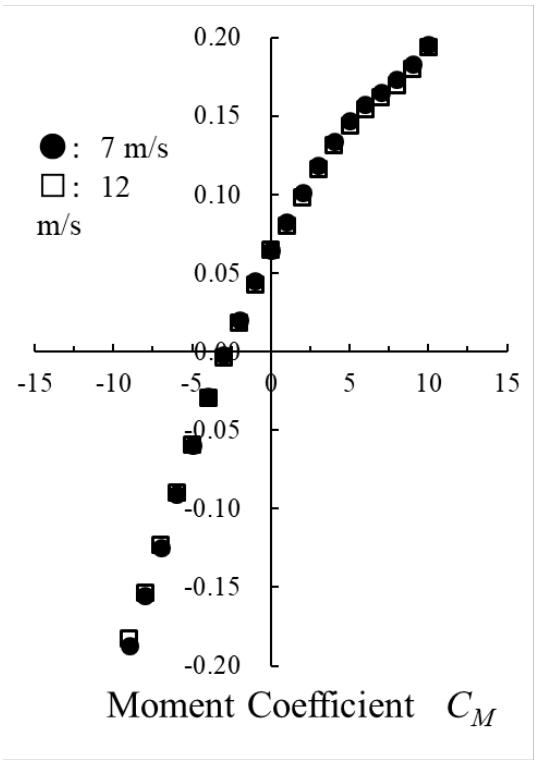

Fig.6.5.4 Aero-static force components (after completion stage, in turbulent flow)

7. Statistical analysis of wind speed record

Wind speed record near the bridge site is to be analysed in order to evaluate wind speed for a given return period. In the analysis, extreme value of the maximum wind speed in any observation period, for example yearly, monthly and daily maximum wind speed, is assumed to follow Gumbel distribution as shown in the following:

The non-exceeding probability of yearly maximum value of 10-minutes mean wind speed x is described as:

$$\Pr\left[x_{\max}\big|_{year} < x^*\right] = \left\{P(x^*)\right\}^N \tag{7.1}$$

where, $x_{\max}\big|_{year}$: yearly maximum of x, $P(x)$: non-exceeding probability of the wind speed x that is observed with a certain interval (Probability density function of $P(x)$, $p(x) = \dfrac{dP(x)}{dx}$, is sometimes called as mother distribution.), N: number of observation in a year (If the interval is one hour, N=24*365=8760.).

According to the extreme value theory, the non-exceeding probability function of the extrema $\Pr\left[x_{\max}\big|_{year} < x^*\right]$ (the maxima ($x_{\max}\big|_{year}$ in eq.(7.1) and the minima) is classified only into the following three types depending on the functional type of the upper tail of $P(x)$ for the mother distribution. It should be noted that these three types are not dependent on the functional shapes of mother distribution $P(x)$ themselves, but on those upper tail only.

Fischer-Tippet type I (Gumbel distribution):

$$\Pr\left[x_{\max}\big|_{year} < x^*\right] = \exp\left[-\exp\left\{a\left(x_{\max}\big|_{year} - b\right)\right\}\right] \equiv F_I\left(x_{\max}\big|_{year}\right) \tag{7.2}$$

The upper tail is expressed as:

$$P(x) = 1 - \exp\left\{-g(x)\right\} \tag{7.3}$$

Fischer-Tippet type II (Frechet distribution):

$$\Pr\left[x_{\max}\big|_{year} < x^*\right] = \exp\left\{-\left(\frac{u}{x_{\max}\big|_{year}}\right)^k\right\} \equiv F_{II}\left(x_{\max}\big|_{year}\right) \tag{7.4}$$

$$P(x) = 1 - \beta\left(\frac{1}{x}\right)^k \tag{7.5}$$

Fischer-Tippet type III dist. For the minima (Weibull distribution):

$$\Pr\left[x_{\min}\big|_{year} < x^*\right] = 1 - \exp\left\{-\left(\frac{x_{\min}\big|_{year} - \varepsilon}{u - \varepsilon}\right)^k\right\} \equiv F_{III}\left(x_{\min}\big|_{year}\right) \qquad \left(x_{\min}\big|_{year} \geq \varepsilon\right) \tag{7.6}$$

$$P(x) = \alpha(x - \varepsilon)^k \qquad \text{(lower tail)} \tag{7.7}$$

where, u: mode, k: shape parameter.

As for the mother distribution of x, that is $p(x)$, the probability distribution of 10 minutes mean wind speed is well described by the Weibull distribution:

Exceeding probability:

$$P(x) = \exp\left\{-\left(\frac{x}{c}\right)^k\right\} \tag{7.8}$$

Probability density function:

$$p(x) = \frac{d}{dx}\{1 - P(x)\} \tag{7.9}$$

where, c: scale parameter [m/s], k: shape parameter.

In general, he non-exceeding probability of the extrema (yearly maximum) of the 10 minutes mean wind speed in Japan is well expressed by the Gumbel distribution as shown in eq.(7.2).

The parameters a and b are determined by the following formula:

$$a = \frac{\pi}{\sqrt{6}\sigma_x} = \frac{1}{0.780\sigma_x} \tag{7.10}$$

$$b = \bar{x} - 0.450\sigma_x \tag{7.11}$$

where, σ_x: standard deviation of x, $\bar{x}$: average of x.

The expected maximum wind speed for a given return period R is determined as follows:

By taking logarithm of times to both sides in eq.(7.2),

$$\ln\left[-\ln\left\{\Pr\left[x_{\max}\big|_{year} < x^*\right]\right\}\right] = -a\left[x_{\max}\big|_{year} - b\right] \tag{7.12}$$

The value of $\Pr\left[x_{\max}\big|_{year} < x^*\right]$ is related to R as shown below:

$$R = \left\{1 - \Pr\left[x_{\max}\big|_{year}\right] < x^*\right\}^{-1} \tag{7.13}$$

The wind speed record used in the analysis is at the Yangon International Airport (May, 2014 to April, 2016, 10 minutes mean in every 10 minutes) and at the Power plant in Thilawa (August, 2015 to May, 2016, Daily maximum and hourly maximum).

Fig. 7.1 to Fig.7.3 show the results at the Yangon International Airport. Hourly, daily and monthly maximum wind speed were evaluated by the raw data. The data obtained was recorded from November, 2011 to May, 2016. However, those from January to September, 2013 were lacked. Fig. 7.4 and Fig.7.5 show the results at the Power plant in Thilawa. Daily and weekly maximum speed were used for the analysis. The evaluated wind speed of 100 year return period is in the range of 17.2 to 19.6 [m/s] for Yangon, while 19.9 [m/s] for Thilawa. Both values are much lower than the design wind speed of the bridge, 30 [m/s]. It should be noted that the data length used in this discussion is rather short, which means that the data might lack strong and rare wind speed events due to cyclone or other meteorological phenomena.

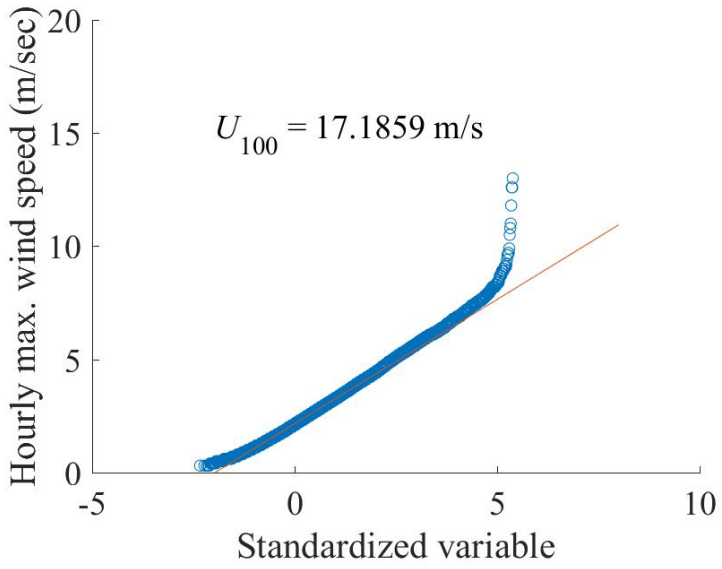

Fig.7.1 Expected maximum wind speed for the return period of 100 year based on hourly maximum speed at the Yangon International Airport (May, 2014 to April, 2016, 10 minutes mean in every 10 minutes).

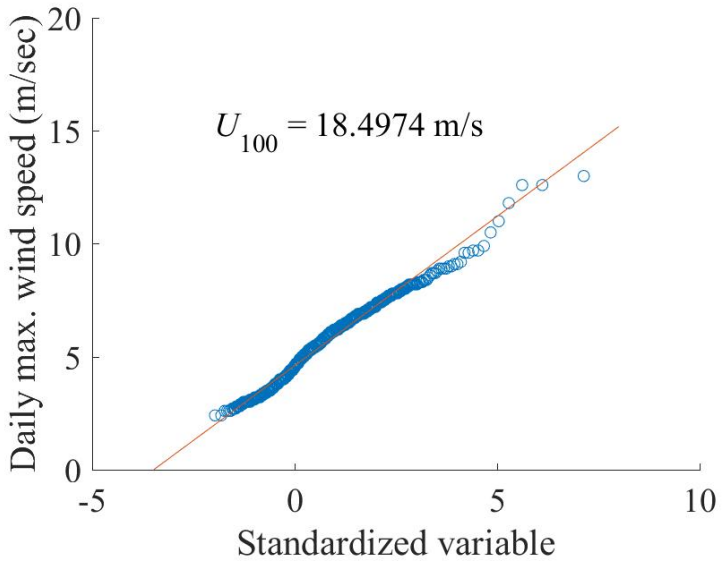

Fig.7.2 Expected maximum wind speed for the return period of 100 year based on daily maximum speed at the Yangon International Airport (May, 2014 to April, 2016, 10 minutes mean in every 10 minutes).

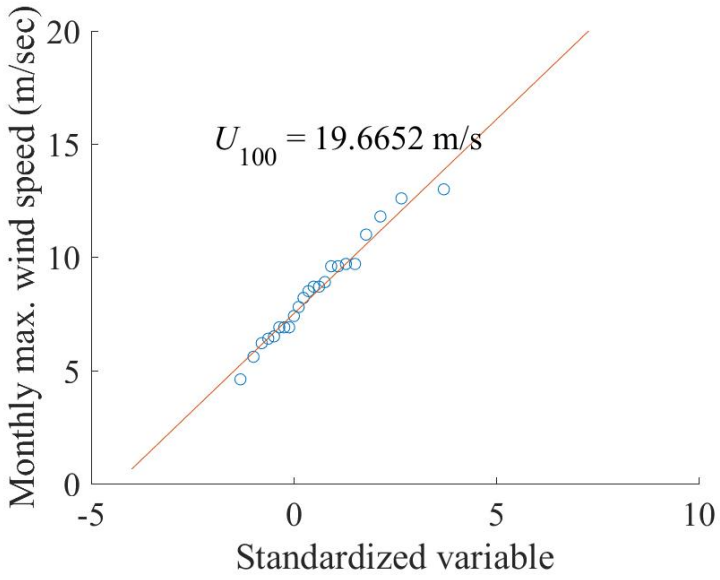

Fig.7.3 Expected maximum wind speed for the return period of 100 year based on monthly maximum speed at the Yangon International Airport (May, 2014 to April, 2016, 10 minutes mean in every 10 minutes)

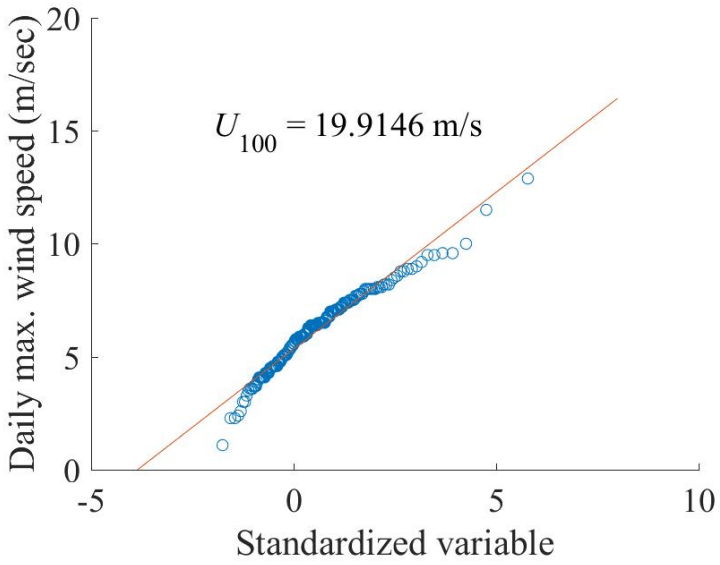

Fig.7.4 Expected maximum wind speed for the return period of 100 year based on daily maximum speed at the Power plant in Thilawa (August, 2015 to May, 2016, Daily maximum and hourly maximum).

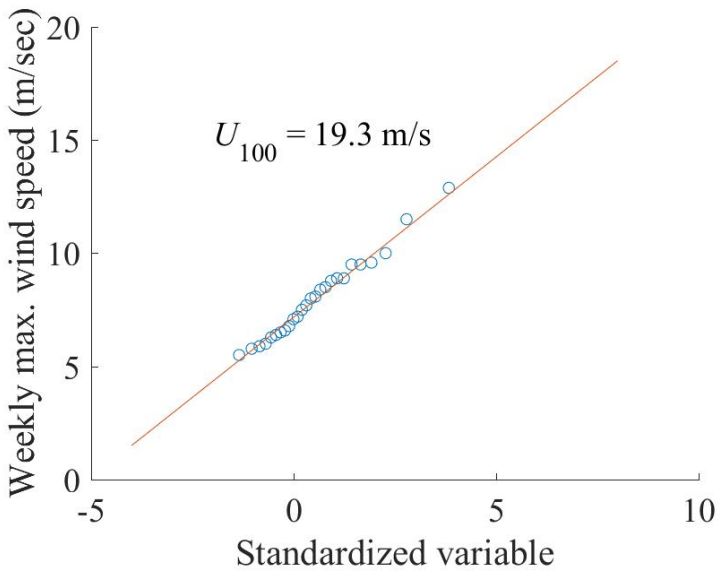

Fig.7.5 Expected maximum wind speed for the return period of 100 year based on weekly maximum speed at the Power plant in Thilawa (August, 2015 to May, 2016, Daily maximum and hourly maximum).

8. Recommendations to cable vibration

The cable of the bridge may suffer from aerodynamic vibration such as rain wind induced vibration. According to the Wind resistant design handbook [1], cables are estimated to be stable for wind if their Scruton number Sc ($Sc=2m\delta/\rho D^2$, m: mass of a cable per unit length, δ: logarithmic damping decrement, ρ: air density [kg/m^3] and D: cable diameter [m]) is 140 to 200, which corresponds to δ = about 0.02 to 0.03.

Cable vibration is one of the academic research subjects and there is still discussion on its generation mechanism and the effect of wind turbulence. Therefore, it should be conservative to recommend to install a rubber damper in order to achieve the above damping.

To install pedestals on the deck is recommended. This enables to install a conventional damper if cable vibration will become a major concern after completion.

9. Conclusion

9.1 Aerodynamic response of main girder and tower

Aerodynamic vibration response of the main girder and the tower of Bago Cable-stayed Bridge was examined by wind tunnel tests.

For the under construction stage, the following 2 stages were focused:

- Before the lowest cable being installed and just after the first segment of the main girder was installed. Heaving 1 DOF of the main girder dominates. The tower stands in isolated condition. Hence, both bending modes along/normal to cable plane may be possible. (Abbreviated as UC1)
- Just before the last segment of the main girder in the main span is installed. Heaving and torsional 2 DOF of the main girder dominates. Sine all cables are already installed, possible bending mode of the tower is normal to cable plane only. (UC2)

For after completion stage,

- Heaving and torsional 2 DOF of the main girder dominates. Sine all cables are already installed, possible bending mode of the tower is normal to cable plane only. (AC)

The aerodynamic response of the main girder shows stable characteristics for the above 2 under construction stages (UC1, UC2) in smooth and in turbulent flow conditions. Neither vortex-induced vibration (VIV) nor flutter was measured.

On the other hand, only vortex-induced vibration (VIV) of the main girder was measured in the after completion stage (AC) at about 15 to 25 [m/s] for real bridge under the vertical incidence of angle 0, +3 and -3[deg.] in smooth flow condition. In case of turbulent flow condition, neither VIV nor flutter was measured.

Therefore, the main girder possesses stability to aerodynamic vibration, if turbulent flow condition is taking into account.

Vortex-induced vibration and galloping were observed in the tower for its original configuration.

For UC1 in smooth flow, VIV of bending mode normal to the cable plane (in y-direction) occurs at 16 to 19 [m/s] under wind direction of 0 [deg.] and 5 [deg.] (almost in parallel to the bridge axis), while galloping occurs from 60 [m/s] under 5 [deg.]. VIV of bending mode in parallel to the cable plane (in x-direction) was also observed in smooth flow under 80, 85 and 90 [deg.] (almost normal to bridge axis) at 14 to 23 [m/s]. Galloping occurs from 58 [m/s] for 80 [deg.] and from 43 [m/s] for 90 [deg.].

For AC in smooth flow, VIV was measured in smooth flow at 10 to 31 [m/s] for 0 [deg.] and 10 to 20 [m/s] for 5 [deg.]. For 10, 22.5, 45, 67.5 and 90 [deg.], stability for VIV was confirmed. The occurrence of galloping was confirmed from 28 [m/s] for 5 [deg.], while no galloping for other cases with different wind direction. The VIV and galloping in turbulent flow condition remains only for 0 [deg.]. VIV was observed at 17 to 20 [m/s] and galloping occurred from 23 [m/s]. The tower was stable for other wind directions, 5, 10, 22.5, 45, 67.5 and 90 [deg.].

From these results, the occurrence of galloping for the wind direction along bridge axis should be main concern.

In order to suppress the galloping as mentioned above, the L-shaped aerodynamic device which is to be attached nearby the corner of the tower cross section was proposed.

For UC1 in smooth flow, the response characteristics were examined by installing the device along 11.0 [m] from the top of the tower. VIV was still observed at 12 to 15 [m/s] for 0 [deg.] and 18 to 21 [m/s] for 90 [deg.], although no galloping was measured for both measurement cases. The response in turbulent flow condition was examined for 80, 85, 90 and 180 [deg.]. The tower was stable for all of these wind direction conditions. (There is no big difference in the response for 0 [deg.] and 180 [deg.], since the flow around the top of tower can be almost identical and no significant influence by the upstream elongation length of the main girder. (see Fig.6.3.1))

For UC2 in smooth flow with the L-shaped device installed along 11.0 [m], VIV was measured at 11 to 32 and 34 [m/s] for 0 [deg.], whereas, stable for 5 [deg.]. The tower showed stable for 0 and 5 [deg.] in turbulent flow.

For AC in smooth flow with the L-shaped device installed along 11.0 [m], the tower was stable for 5 [deg.] but VIV occurred at 22 to 26 [m/s] for 0 [deg.]. No galloping was observed for both cases of wind direction. In turbulent flow, the tower was stable for 0 [deg.] and 5 [deg.].

Install length of the device was changed to 41.7 [mm] (= 5.0 [m] in real bridge), 141.7 [mm] (17.0 [m]), 191.7 [mm] (23.0 [m]) and 233.4 [mm] (28.0 [m]), respectively, in order to know its effect to stabilizing performance. Target wind direction was fixed to 0 [deg.] and 5 [deg.] only. In smooth flow, VIV was measured only for 0 [deg.] and the length of 141.7 [mm], while stable for 5 [deg.]. In turbulent flow, the tower showed stable response characteristics for all cases. No galloping was observed for all cases.

From these results, the response for 0 [deg.] with the length of the device 191.7 [mm] should be focused. This response was totally stabilized under turbulent flow condition. And the wind direction 0 [deg.] (along bridge axis) means the wind comes over the city of Yangon or the field in Thilawa. Moreover, this wind may be further disturbed by the existence of the cable in upstream

of the tower, From these reasons, the wind resistant characteristics of the tower shyld be estimated under turbulent flow condition rather than in smooth flow. It was confirmed that, in turbulent flow condition, the tower is stabilized by installing the device longer than 141.7 [mm] (17.0 [m]) from the top. Therefore, it is recommended to install the device over 17.0 [m] from the top of the tower.

9.2 Statistical analysis of wind speed record

The expected recurrence wind speed in Yangon and Thilawa was analyzed in order to discuss the design wind speed for the bridge.

The wind speed data recorded at Yangon International Airport and at Power plant in Thilawa were used to the analysis. Record period was from May, 2014 to April, 2016 for Yangon and from August, 2015 to May, 2016 for Thilawa. Hourly, daily and monthly maximum wind speed data for Yangon were used and the daily maximum for Thilawa. The expected wind speed of 100 year return period was evaluated by fitting these data to Gumbel distribution.

As a result, the evaluated wind speed of 100 year return period was in the range of 17.2 to 19.6 [m/s] for Yangon, while 19.9 [m/s] for Thilawa. Both values are much lower than the design wind speed of the bridge, 30 [m/s]. It should be noted that the data length used in this discussion were rather short, which means that the data might lack strong and rare wind speed events due to cyclone or other meteorological phenomena.

9.3 Recommendation to cable vibration

The cable of the bridge may suffer from aerodynamic vibration such as rain wind induced vibration. According to the Wind resistant design handbook [1], cables are estimated to be stable for wind if their Scruton number Sc ($Sc=2m\delta/\rho D^2$, m: mass of a cable per unit length, δ: logarithmic damping decrement, ρ: air density [kg/m^3] and D: cable diameter [m]) is 140 to 200, which corresponds to δ = about 0.02 to 0.03.

Cable vibration is one of the academic research subjects and there is still discussion on its generation mechanism and the effect of wind turbulence. Therefore, it should be conservative to recommend to install a rubber damper in order to achieve the above damping.

To install pedestals on the deck is recommended. This enables to install a conventional damper if cable vibration will become a major concern after completion.